THE SURFACE IMPEDANCE

OF

SUPERCONDUCTING NIOBIUM

G. A. Wilkinson

Royal Society Mond Laboratory

and

Jesus College

Thesis submitted in partial fulfilment of the requirements

for the degree of Doctor of Philosophy

at the

University of Cambridge

1969

' I saw my lady weep ,

And sorrow proud to be advanced so ... '

(Dowland)

ABSTRACT

Measurements are reported of the surface impedance of niobium at 10 Gc./s. Anomalies have been found in the behaviour of both the normal and superconducting states. The normal state exhibits deviations from the predictions of the Reuter-Sondheimer theory which are believed to be associated with anisotropic scattering of the electrons, possibly combined with effects of Fermi surface anisotropy. The superconducting state measurements are compared with a detailed computation of the Mattis and Bardeen integrals for the London limit; discrepancies are found which become more extreme in the purest specimens and are tentatively attributed to the effects of the second energy gap in niobium.

Data have also been obtained for the magnetic field dependence of the surface impedance in the Meissner-, mixed-, and surface superconducting- regimes , and are related to the current theories of such behaviour.

ACKNOWLEDGMENTS:

This dissertation contains an account of work undertaken by the author during the three and a half years since October 1965 in the Mond Laboratory. Saving the first review chapter, the work described is essentially original except where specific acknowledgment is given, and in that chapter much of the comment made is believed to be novel; it will in any case usually be apparent what is derivative and what not. However, the author is the first to realise his indebtedness to many members of the laboratory for a continual fund of help and inspiration, and his sincerest thanks are due to his supervisor Dr. J. K. Waldram for time, patience, and encouragement unfailingly given. It is a pleasure also to acknowledge helpful discussions with Professors Pippard and Hopfield, Dr. V. Heine, and many others.

Invaluable technical assistance has been given by Messrs. Sadler and Booth with an occasionally exasperating cryostat, and help over sample preparation by Mr. T. Brown. Finally, thanks are due to Mrs. M. R. Brown for typing the manuscript, and to S.R.C. and A.E.R.E. Harwell for financial support during the time of this work.

No part of this dissertation is to be submitted to any other university.

G. A. Wilkinson.

July 1969

CONTENTS:

CHAPTER 1 - INTRODUCTION

Of the two elements known to be London superconductors in their pure state, namely Vanadium and niobium, the latter has received a great deal of attention recently both experimentally and theoretically, and some interest attaches to whether its behaviour conforms to that predicted by the B.C.S. theory (1). In this introductory chapter we discuss some of the pertinent information obtained to date, and the modifications to the simple B.C.S. theory which have been put forward in explanation.

1. ENERGY GAPS:

A: TEMPERATURE-DEPENDENCE:

Several measurements have been made on niobium which have been interpreted as deriving from a non-B.C.S. temperature dependence of the energy gap, being in some cases quite bizarre. In fig. (1) are shown three examples:

1. Maxfield & McLean (2) - penetration depth measurements at 4 Mc/s. and 80 Mc/s.
2. French (3) - magnetisation measurements of H_{c2}.

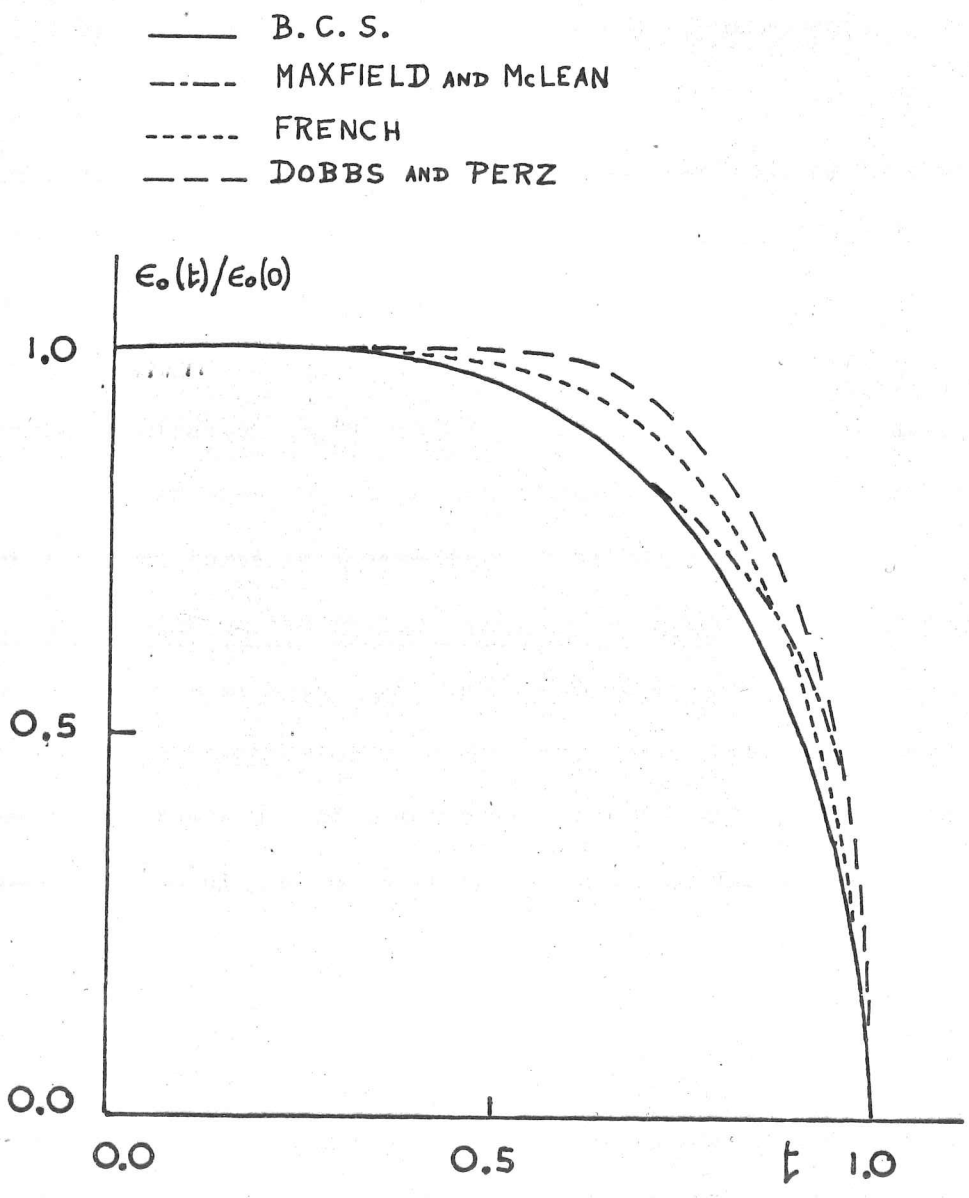
B. C. S.
MAXFIELD AND McLEAN
FRENCH
DOBBS AND PERZ
$\epsilon_0(t)/\epsilon_0(0)$
1.0
0.5
0.0
0.0
0.5
t
1.0

FIG. 1.

3. Dobbs and Perz (4) - longitudinal ultrasonic absorption at 1280 Mc/s.

The degree of consistency is scarcely high, and one feels that this point deserves comment. Determinations 1 and 2 rely on the rather indirect inversion procedure described by Waldram (5) in which the non-B.C.S. temperature dependence of the London penetration depth $\lambda L(t)$ is interpreted as a rescaling of the energy gap $\epsilon_0(t)$, since in the B.C.S. theory the London parameter is formally independent of the actual form of ϵ_0, depending only on the ratio $\epsilon_0(t)/kT$. Provided one accepts this procedure as being reasonable for niobium, the results of Maxfield and McLean appear to have been rather well analysed apart from their use of a value of $\kappa = 0.96\,\lambda_L/\xi_0$ which would seem to be about 20% too high on the basis of the most recent magnetisation measurements; the value of this quantity enters into the calculation of the London penetration depth $\lambda L(t)$ from the penetration depth actually measured $\lambda(t)$ via the non-local corrections given by the B.C.S. theory. We shall discuss later in Chapter 4 in more detail what effect this may have on their results.

On the other hand, the magnetisation determination 2 seems to us to be distinctly more dubious since it would appear that the deduction of $\lambda(t)$ from the measured values of upper critical field $H_{c2}(t)$ is based on a Ginzburg-Landau argument which takes no proper account of non-locality. Again, this point is discussed further in Chapter 3.

Determination 3 is only one of a number of determinations from ultrasonic attenuation all of which seem to have given idiosyncratic and curiously inconsistent results. For example, the results at low (ql) of Levy et al. (6), Weber (7), and Ikushima et al. (8) all show deviations from B.C.S. behaviour, which are, however, much slighter than that claimed by Dobbs & Perz. More significant deviations, still at low (ql), have been observed by Tsuda et al. (9) and by Tsuda & Suzuki (10) in niobium, and the latter authors suggest the effects of small angle phonon scattering as being a possible cause of the decreased attenuation near Tc compared with the B.C.S. prediction. Similar peculiarities have been noted in lead by Deaton (11) and in tin by Phillips (12); he ascribes this to the effect of phonon scattering on the basis that at low (ql) inelastic 'oblique' scattering of quasi-particles by phonons across the Fermi surface

is sufficiently destructive to the attenuation to explain the observed results - a process inoperative in the normal state because the coherence factors cancel. This is because the dissipative stress carried by a quasi particle is, according to Kadanoff & Pippard (13):

$$\hbar v D$$

v being the quasi-particle velocity, and D the deformation parameter. This reverses sign at the Fermi surface, and thus a small angle scattering is sufficient to cause relaxation of the stress resulting in a decreased attenuation; such a process is destructive to all 'symmetric' perturbations of the superconducting distribution e.g. thermal conductivity, but is ineffective for the 'antisymmetric' electrodynamic properties since the current carried is determined by the wave-vector $\underline{k}$ of the quasiparticle (Rickayzen - (14) and does not reverse in a small angle electron-hole scattering. Incidentally, if this interpretation is correct, it indicates that there is a real physical difference between the 'semiconductor' and 'excitation' pictures of the B.C.S. spectrum since in the former case states of similar velocities are adjacent in $\underline{k}$-space, whereas in the latter states of opposite velocities are adjacent and available for small angle scattering.

At any rate, we feel that the low (ql) measurements of ultrasonic attenuation in pure specimens are sufficiently difficult to interpret that any reliable deductions of energy-gap are impossible. As regards the one measurement claimed at high (ql), namely that of Dobbs & Perz, we shall present evidence in chapter 3 that their estimates of (ql) are probably seriously in error; a reanalysis of their results for the normal-state attenuation suggests that their mean free paths should be scaled down by a factor of at least 3 or even more if more conventional estimates of (pl) are used. This implies that the maximum value of (ql) which they used was probably about 2.4 or less, rather than 7.3 as they believed; this value is scarcely sufficient to take them into the high (ql) region (15) and may well explain why their observed gap anisotropy is noticeably less than that obtained in tunnelling measurements. Thus it would seem that there is still, as yet, no reliable measurement of ultrasonic attenuation at high (ql) where the determination of the energy gap should indeed be independent of the details of scattering. There is really a strong need for tunnelling measurements to be made of the temperature dependence of the energy gap, we feel, since all indirect measurements seem to be bedevilled by complications in niobium.

B ABSOLUTE VALUES:

In the following table, we give the results of recent determinations of the mean energy gap in niobium at absolute zero by various methods:

source	method	$\bar{\epsilon}_0(0)/\epsilon_{0\,B.C.S.}(0)$
MacVicar & Rose (16)	tunnelling	1.11
Townsend & Sutton (17)		1.09
Sung & Shen (18)	specific heat	1.05
Cappelletti (19)	infra-red absorption	1.08
Mendelssohn (20)	thermal conductivity	1.08
Dobbs & Perz (4)	ultrasonics	1.01
Maxfield & McLean (2)	surface impedance	1.00
Turneaure & Weissman (21)		1.06

We should point out that a fair degree of selection has been exercised in constructing the above list, and that rather wilder values have been reported from time to time; however it would appear that a consensus of opinion is that the mean gap is around

1.06 x B.C.S. value, this no doubt reflecting the strong-coupling nature of niobium (the figure is predicted to be 1.14 on the strong-coupling theory of Thouless (22)).

As regards anisotropy, we are most inclined to believe the results of MacVicar & Rose which agree qualitatively with those of Dobbs & Perz, but show a higher degree of anisotropy:

crystal orientation	<100>	<110>	<111>	<102>	<112>	<311>
$\epsilon_0(0)/\epsilon_{0\,B.C.S.}(0)$	1.02	1.11	1.14	1.11	1.10	1.15

A plot of this anisotropy is given in fig. (2).

ENERGY-GAP ANISOTROPY

(MAC VICAR AND ROSE)

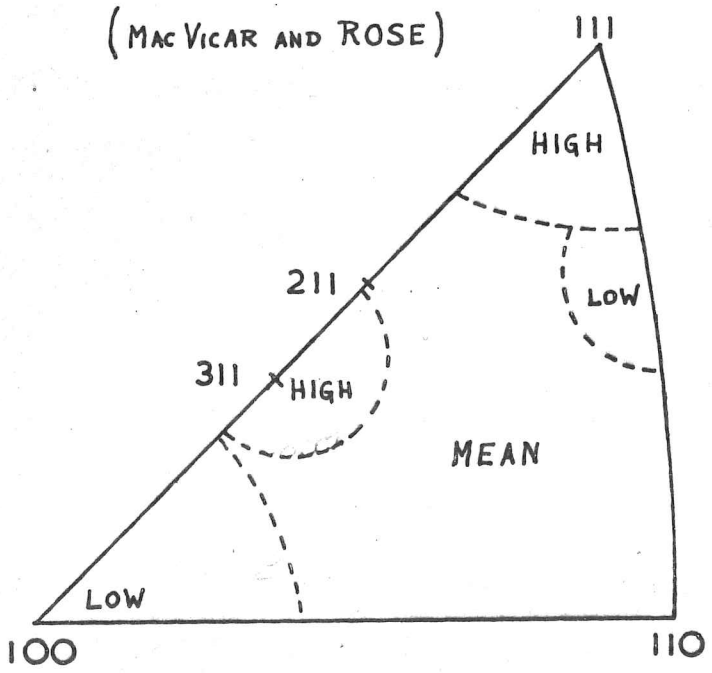

FIG. 2

2 TWO-BAND CHARACTER

There is an accumulating body of evidence that niobium is not well represented by the isotropic, single band, single energy gap model of B.C.S. and that this may well be so for other transition metal superconductors. The specific heat measurements of Shen et al. (23) strongly suggest the presence of two very different energy gaps; Sung and Shen (18) have analysed these data, and have shown that they can be represented on a simple 2 isotropic band model by:

$$C_{es} = \frac{N_d}{N_s+N_d} C_{es}^{d} + \frac{N_s}{N_s+N_d} C_{es}^{s}$$

where the two specific heats arise from energy gaps:

$$\epsilon_{od}(0) \simeq 1{\cdot}76\, k T_c \quad ; \quad \epsilon_{os}(0) \simeq 0{\cdot}16\, k T_c$$

and the relative densities of states of the s-and d- bands they estimate to be:

$$N_s/N_d \simeq 0{\cdot}015$$

This conclusion has since been supported by the tunnelling measurements of MacVicar & Rose (24) which shew structure in the tunnelling density of states at both $\frac{1}{5}$ th. and $\frac{1}{10}$ th. of the usual energy gap in specimens of R.R.R. $\sim$ 200 - 750. Also, the measurement of microwave absorption made by Tumeaure & Weissman (21) at

low temperatures shows a surface resistance below about 1.8°K. which is higher than that expected on the single gap model; this they interpret as being possibly due to a second energy gap, although here extraneous surface loss is the limiting experimental factor. An interesting feature of the results of Shen et al. is that this behaviour persists even down to resistance ratios ~ 24. This runs contrary to the conclusion of Garland (25) that all such effects would be washed out by impurity s-d scattering on an Anderson type of argument. It may well thus be that the sort of anisotropy measured by Dobbs & Perz (4), is essentially rather trivial in view of this giant anisotropy which is not washed out except in the most impure specimens.

Since the Fermi surface of niobium is highly anisotropic, the existence of a small gap on the s-like parts of it must indeed represent a rather violent anisotropy, and it is not totally clear how adequate an approximation a simple two-isotropic-band model will be; however, such a model is the best we have and was proposed originally by Suhl et al. (26) and extended by Kondo (27). It has been usefully elaborated in the case where:

$$N_s \ll N_d \quad ; \quad \epsilon_{os} \ll \epsilon_{od}$$

by Sung & Wong (28) to include the effects of non-magnetic impurity scattering and we show in fig. (3) their calculation of the

low temperatures shows a surface resistance below about 1.8°K. which is higher than that expected on the single gap model; this they interpret as being possibly due to a second energy gap, although here extraneous surface loss is the limiting experimental factor. An interesting feature of the results of Shen et al. is that this behaviour persists even down to resistance ratios ~ 24. This runs contrary to the conclusion of Garland (25) that all such effects would be washed out by impurity s-d scattering on an Anderson type of argument. It may well thus be that the sort of anisotropy measured by Dobbs & Perz (4), is essentially rather trivial in view of this giant anisotropy which is not washed out except in the most impure specimens.

Since the Fermi surface of niobium is highly anisotropic, the existence of a small gap on the s-like parts of it must indeed represent a rather violent anisotropy, and it is not totally clear how adequate an approximation a simple two-isotropic-band model will be; however, such a model is the best we have and was proposed originally by Suhl et al. (26) and extended by Kondo (27). It has been usefully elaborated in the case where:

$$N_s \ll N_d \quad ; \quad \epsilon_{os} \ll \epsilon_{od}$$

by Sung & Wong (28) to include the effects of non-magnetic impurity scattering and we show in fig. (3) their calculation of the

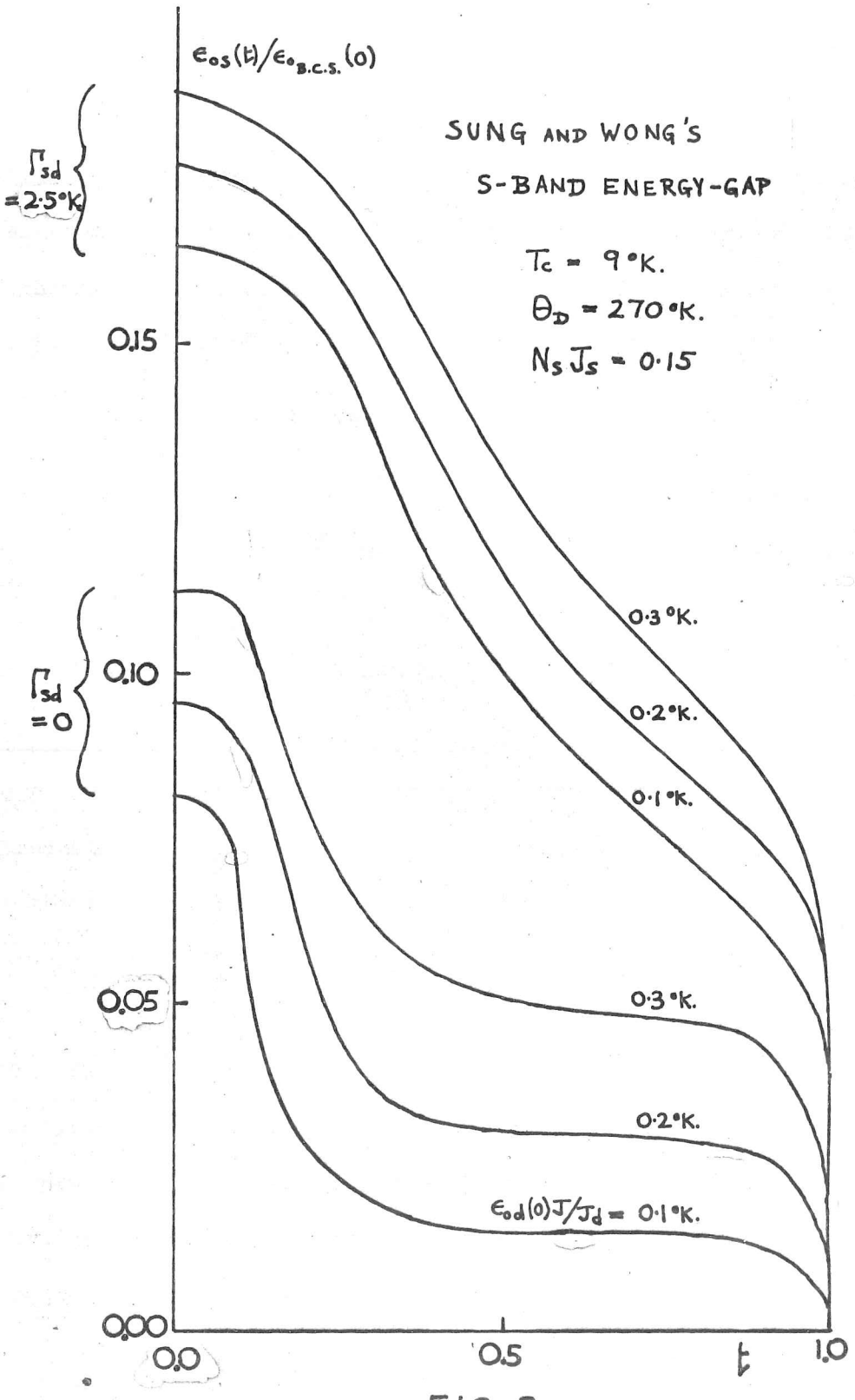
$\epsilon_{os}(t)/\epsilon_{o_{B.C.S.}}(0)$
SUNG AND WONG'S
S-BAND ENERGY-GAP
T_c = 9°K.
Θ_D = 270°K.
$N_s J_s$ = 0·15
Γ_{sd} = 2·5°K
Γ_{sd} = 0
0·3°K.
0·2°K.
0·1°K.
0·3°K.
0·2°K.
$\epsilon_{od}(0) J/J_d$ = 0·1°K.
0.15
0.10
0.05
0.00
0.0
0.5
1.0
t

FIG. 3

temperature dependence of $\epsilon_{os}(T)$ for various coupling parameters J and s-d scattering amplitudes Γ_{sd} . These parameters arise in the two-band model as follows; the single band Hamiltonian of B.C.S. becomes modified to:

$$\mathcal{H} = \sum_{k,\sigma} \epsilon_{ks} s_{k\sigma}^{\dagger} s_{k\sigma} + \sum_{k,\sigma} \epsilon_{kd} d_{k\sigma}^{\dagger} d_{k\sigma}$$

$$+ J_s \sum_{k,k'} s_{k\uparrow}^{\dagger} s_{-k\downarrow}^{\dagger} s_{-k'\downarrow} s_{k'\uparrow} + J_d \sum_{k,k'} d_{k\uparrow}^{\dagger} d_{-k\downarrow}^{\dagger} d_{-k'\downarrow} d_{k'\uparrow}$$

$$+ J \sum_{kk'} \left(s_{k\uparrow}^{\dagger} s_{-k\downarrow}^{\dagger} d_{-k'\downarrow} d_{k'\uparrow} + d_{k\uparrow}^{\dagger} d_{-k\downarrow}^{\dagger} s_{-k'\downarrow} s_{k'\uparrow} \right)$$

where the last term is the interband pairing interaction and represents the fundamental difference from the single band model; the scattering amplitudes are defined by:

$$\mathcal{H}_{imp.} = n_i (V_s + V_d)$$

$$\Gamma_s = \pi n_i N_s \overline{V_s^2} \; ; \; \Gamma_d = \pi n_i N_d \overline{V_d^2} \; ; \begin{cases} \Gamma_{ds} = \pi n_i N_s \overline{V_d V_s} \\ \Gamma_{sd} = \pi n_i \overline{N_d V_d V_s} \end{cases}$$

where ni is the impurity density and the V's. are the scattering potentials of the Born approximation. The gap parameters $\epsilon_{os,d}$ are then solved for self-consistently from coupled equations of the B.C.S. sort with which we shall not bore the reader by writing down, but refer him to the literature; for finite coupling J, both

gaps have non-B.C.S. temperature dependences in general. This sort of calculation shows how critically dependent upon the coupling parameters is the temperature dependence of the small gap and therefore the related superconducting properties. Sung and Wong's calculation of the impurity dependence of the electronic specific heat predicts a low-temperature variation:

$$C_{es} \sim \exp.\left(-\left[G_{os}(T) + \Gamma_{sd}\right]/kT\right)$$

which is not in accordance with the results of Shen et al. who saw the same shape of temperature dependence in specimens of resistance ratios 24 and 110, though they point out that for the impure sample the lattice specific heat is dominant and difficult to subtract out. A theory of the specific heat jump at Tc for pure 2-band superconductors has been formulated by Soda & Wada (29) and shows a reduction over the B.C.S. prediction ; it thus cannot explain the anomalously large jump seen in niobium by Leupold and Boorse (30) namely :

$$\frac{C_S - C_N}{\gamma T_c} = 1.87 \quad (\text{c.f. } 1.43 - \text{B.C.S.})$$

this being more likely attributable to the effects of strong-coupling.

ELECTRODYNAMICS:

Radhakrishan (31) has put forward a calculation of the penetration depth to be expected in a two-band superconductor, and applied this to a reinterpretation of that measured in niobium by Maxfield and McLean who explained their results on the basis of a non-B.C.S. energy gap. In this calculation, he takes the energy gaps and densities of states which Sung and Shen deduce from the specific heat data and is left with two free parameters - the effective masses of the s- and d- bands - which he fits to give $\frac{d\lambda_L}{dy}\Big|_{y=1}$ and $\frac{d\lambda_L}{dy}\Big|_{y=\infty}$; this yields:

$$m_s^* = 1.9\ m \quad ; \quad m_d^* = 70\ m.$$

Unfortunately, as we later point out in Chapter 2, he apppears to have fitted in error not the experimental results of Maxfield & McLean, but their calculation of the London penetration depth which would be given by the temperature dependence of the energy gap deduced by Dobbs & Perz., so that the above figures probably cannot be taken very seriously. It is also not transparently clear that the approximations which he uses in calculating $\frac{d\lambda_L}{dy}\Big|_{y=1}$ are correct since he uses expressions correct sufficiently near to T = 0 and the value he fits is actually at y = 1.02 which

corresponds to 4.2°K; this is a distinctly high temperature as regards the s- energy gap.

Fuller discussions of the two-band modifications to the Mattis and Bardeen theory have been given by Geylikman et al. (32); (——) for pure superconductors in which, as a consequence of different values of $\lambda_L(0)/\xi_0$ for each band, the London-Pippard character of the superconductor becomes temperature dependent. As we shall see later, the s-band in niobium is probably much more Pippard-like than the d-band. What they say seems to indicate that the electromagnetic response may be rather more Pippard-like in the regime intermediate between T = 0 and Tc, being more London-like at the extremes. They indicate that such a temperature dependence has been seen in pure Tl by Makharov and Tereshina, but we are unable to find any subsequent publication of these results to date.

Sung and Wong also develop the theory of the electromagnetic response, and point out that their calculation shows that the effect of increasing impurity should raise the threshold for electromagnetic absorption since the s-gap becomes larger until, in the Anderson limit, the two gaps merge completely. However,

the impurity levels at which this should occur still seem to be in question in view of the specific heat data. In this connection, we should note that the frequency at which we are working, namely 10Gc./s., is about 1½% of the d-gap frequency $2\epsilon_{od}(0)/\hbar$, and is therefore about 15% of the s-gap frequency at T = 0; one may well not have to go to very high temperatures before one is in the gap-jumping region for this band therefore, and in Chapter 4 we shall examine this possibility in the interpretation of our results.

We should perhaps point out that, in common with other forms of gap anisotropy, a full calculation of the electromagnetic response of a two-band superconductor with wide angle scattering should include the effect of transitions involving interband scattering; this would give rise to an energy-dependent mean free path in the superconducting state, as discussed by Phillips (12) for the energy-gap anisotropy in tin, via the coherence factors - for this reason, at low temperatures the s-band quasi particles just above the gap edge could be very long-lived. This is a nicety which has not been included in the calculations mentioned, and probably with good reason at this stage of development.

In passing, we may note that it is rather unlikely that the curious temperature-dependence of the energy gap seen in niobium by the ultrasonic measurements of Dobbs & Perz can be explained on the basis of the two-band model. Falko (33) has derived the intuitively obvious result that the longitudinal ultrasonic attenuation in a two-band superconductor is given, for $ql \gg 1$, by that for the individual energy gaps weighted according to Fermi surface area S:

$$\frac{\alpha_s}{\alpha_N} = 2\,\frac{S_s}{S_s+S_d}\,f(\epsilon_{os}) + 2\,\frac{S_d}{S_s+S_d}\,f(\epsilon_{od})$$

In this case, where there is no supercurrent screening by the d-gap of the loss produced by the s-gap, unlike the transverse electromagnetic response, since their measurements appear to extend down only to $t = 0.3$ one might argue that their estimate of their residual losses could be in error to the extent of the loss still occurring in the s-gap. Now they found that near Tc:

$$B \equiv \frac{\epsilon_o^2/\epsilon_o^2(0)}{1-t} = 4{\cdot}8 \quad (\text{c.f. } 3{\cdot}03 - \text{B.C.S.})$$

and it is easy to show that the slope of the attenuation curve in the 2-band model near Tc is given by:

$$\frac{d}{dt}\left(\frac{\alpha_s}{\alpha_N}\right) = \frac{1}{4}\left[\frac{S_s}{S_s+S_d}\,B_s\,\frac{\epsilon_{os}}{kT_c} + \frac{S_d}{S_s+S_d}\,B_d\,\frac{\epsilon_{od}}{kT_c}\right](1-t)^{-1}$$

which will be, if anything, rather smaller than that predicted

by B.C.S. if the d-gap is B.C.S.-like. So that even if we bring the normalised gradient down only to the B.C.S. value, this would require a residual loss:

$$\frac{\alpha_{res.}}{\alpha_N} = -\left(\sqrt{\frac{4{\cdot}8}{3{\cdot}03}}\right)^{-1} + 1 = 0{\cdot}20$$

which seems most unlikely in view of our estimate that the s-band constitutes about 6% of the total Fermi surface area (see Chapter 3).

CRITICAL FIELDS:

Radhakrishanan(34) has calculated the thermodynamic critical field Hc resulting from the model of Suhl et al., and obtains the results:

$$\begin{cases} H_c^2(0) = N_d \epsilon_{od}^2(0) + N_s \epsilon_{os}^2(0) \\ \left.\frac{dH_c}{dT}\right|_{T_c} = 2\sqrt{\frac{\pi N_d}{a}}\, k_B \, \frac{1 + \frac{N_s}{N_d}\theta_c^2}{\sqrt{1 + \frac{N_s}{N_d}\theta_c^4}} \end{cases}$$

where: $a = \frac{7\zeta(3)}{8\pi^2}$, $\theta_c = -\frac{\epsilon_{od}(0)}{\epsilon_{os}(0)} \frac{N_d}{N_s} \frac{\log.(\epsilon_{od}(0)/1{\cdot}76 k T_c)}{\log.(\epsilon_{os}(0)/1{\cdot}76 k T_c)}$

and calculates for niobium :

$$\begin{cases} H_c(0) = 1970 \text{ G.} \\ \left.\frac{dH_c}{dT}\right|_{T_c} = -384 \text{ G.}^\circ\text{K.}^{-1} \end{cases}$$

He quotes for comparison the results of Brown et al. (35):

$$H_c(0) = 2000\ G. \ ; \ \left.\frac{dH_c}{dT}\right|_{T_c} = -453\ G.^{\circ}K.^{-1}$$

We note, however, that the latter was an early measurement (they quote Tc as $8.7^{\circ}K.$!), and that the recent results of French:

$$H_c(0) = 1980\ G. \ ; \ \left.\frac{dH_c}{dT}\right|_{T_c} = -396\ G.^{\circ}K.^{-1}$$

would agree much better. He deduces values for the interaction parameters as follows:

$$\begin{cases} J_s = 3{\cdot}1 \times 10^{-34} \text{ erg. cm.}^{-3} \\ J_d = 4{\cdot}3 \times 10^{-36} \\ J = -3{\cdot}1 \times 10^{-37} \end{cases}$$

$$N_s J_s = 0{\cdot}30 \ ; \ N_d J_d = 0{\cdot}28$$

the intraband interaction being repulsive.

Several authors have discussed the two-band formulation of the Ginzburg Landau equations, and have related this to the determination of the nucleation fields H_{c1} and H_{c2} - namely: Tilley (36), Kon (37), Geylikman et al. (38), Moskalenko (39), and Chow (40). These calculations have shown that:

$$\left.\frac{H_{c3}}{H_{c2}}\right|_{T_c} = 1{\cdot}69$$

as in the single band model, and that for pure 2-band superconductors, the symmetry of the Abrikosov flux-line structure depends on the relative sizes of κ_s and κ_d . As the superconductor is made increasingly impure, its type II characteristics become identical to those of the single band case with an effective κ , Tc, Hc essentially dependent on the two-band properties, however. As regards the temperature dependence of H_{c2}, Chow shows that the effect of impurity s-d scattering is to depress H_{c2} in the range between the transition temperatures which the two bands would have in the absence of the interband interaction, and to enhance it at the lowest temperatures - this even if the s-band is Pippard-like. No detailed application of these results to the interpretation of experimental data seems to have been made yet, however.

COLLECTIVE EXCITATIONS:

Leggett (41) makes the interesting conjecture that, unlike a single-band superconductor, a two-band superconductor is capable of supporting a collective excitation between the bands equivalent to Josephson tunnelling in k-space. This analogy arises from the

coupled equations for the gap-parameters given by Suhl et al; Leggett argues that each gap-parameter has associated with it a certain quantum mechanical phase and occupation number, and that a sort of Josephson tunnelling between the bands is provoked by the interband coupling J which is analogous to the tunnelling Hamiltonian. The resulting oscillation is to be regarded as a fairly low-lying excitation of the system, and Leggett estimates its characteristic frequency to be significantly below the two particle gap-jumping threshold:

$$\omega_0 \simeq 0{\cdot}6 \times \frac{2\epsilon_{0s}}{\hbar} \qquad \text{for niobium}$$

He states that, in principle, the excitation should give rise to absorption in the transverse electromagnetic response, but that the coupling is probably impracticably low; he speculates that the effect might be discernible in ultrasonic absorption, however. We note, again, that this frequency is not incomparable with our measuring frequency of 10Gc/s.

3. STRONG-COUPLING:

The original theory of B.C.S. was worked out for conditions of weak coupling where the size of the interaction parameter is small, that is for $(T_c/\theta_D) \ll 1$. For niobium, $(T_c/\theta_D) \sim (9.25/277) \sim 0.034$, and the approximations of the weak-coupling theory begin to break down.

Under these conditions, it is possible to define a complex gap parameter and quasiparticle energy which are both functions of energy:

$$\epsilon_k(E) = Z(E)\sqrt{E^2 - \Delta^2(E)}$$

Z being a renormalisation factor for the bare wave-functions arising from the electron-phonon and electron-electron interactions; this gives a renormalisation of the Fermi-velocity in the normal state:

$$v_F^* = v_F / Z(0)$$

and a corresponding enhancement of the electronic specific heat — Prange & Kadanoff (42); Prange & Sachs (43)

$$\gamma^* = Z(0)\,\frac{k_B^2 S}{12\pi\hbar v_F} \quad ; \quad S \text{ - Fermi-surface area.}$$

Δ and Z are determined from self-consistent integral equations

of the form:

$$\begin{cases} \Delta(E) = \dfrac{1}{Z(E)} \int dE' \, \mathrm{Re}\left\{ \dfrac{\Delta(E')}{\sqrt{E'^2 - \Delta^2(E')}} \right\} K_+(E,E') \\ [1 - Z(E)]E = \int dE' \, \mathrm{Re}.\left\{ \dfrac{E'}{\sqrt{E'^2 - \Delta^2(E')}} \right\} K_-(E,E') \end{cases}$$

where: $K^{\pm}$ are kernels representing the electron-phonon interaction. The quantity:

$$N(E) = \mathrm{Re}.\left\{ \frac{E}{\sqrt{E^2 - \Delta^2(E)}} \right\}$$

represents the effective density of states for tunnelling (44) while: $\Gamma(E) = \mathrm{Im}.(\epsilon_k) = \mathrm{Im}.\left(Z(E)\sqrt{E^2 - \Delta^2(E)} \right)$

represents the effect of quasi-particle damping.

McMillan (45) develops an empirical method of estimation of Z(0) from the experimental value of (T_c/θ_D) in which:

$$Z(0) = 1 + \frac{1.04 + \mu^* \log.(\theta_D / 1.45 T_c)}{(1 - 0.62\mu^*) \log.(\theta_D / 1.45 T_c) - 1.04}$$

where μ^* is the pseudopotential for the Coulomb interaction parameter, and which he takes to be 0.13 in his calculations for the polyvalent transition metals. For Nb, he estimates:

$$Z(0) = 1.82$$

which would give considerable enhancement of the electronic specific heat.

ELECTROMAGNETIC PROPERTIES:

The modifications to the weak-field electromagnetic response in the weak-coupling limit given by the theory of Mattis and Bardeen (46) expected on the basis of strong-coupling have been discussed by Nam (47). In the Pippard Limit, he obtains for the response kernel:

$$\frac{K}{4\pi}(q\to\infty,\omega) = \frac{3}{4\pi}\pi i\omega\left[q v_F \Lambda(0)\right]^{-1}\left(\frac{\sigma_S}{\sigma_N}\right)$$

where: $\Lambda^{-1}(0) = \dfrac{e^2 S v_F}{12\hbar\pi^3}$; S- Fermi surface area

$$\frac{\sigma_S}{\sigma_N} = \frac{\sigma_1}{\sigma_N} - i\frac{\sigma_2}{\sigma_N}$$

$$\begin{cases} \dfrac{\sigma_1}{\sigma_N} = \dfrac{2}{\hbar\omega}\displaystyle\int_{\epsilon_g}^{\infty} dE\left[f(E)-f(E+\hbar\omega)\right] g_1(1,2) + \frac{1}{\hbar\omega}\int_{\epsilon_g-\hbar\omega}^{-\epsilon_g} dE\left[1-2f(E+\hbar\omega)\right] g_1(1,2) \\ \dfrac{\sigma_2}{\sigma_N} = \dfrac{1}{\hbar\omega}\displaystyle\int_{\epsilon_g-\hbar\omega,-\epsilon_g}^{\epsilon_g} dE\left[1-2f(E+\hbar\omega)\right] g_2(1,2) + \frac{1}{\hbar\omega}\int_{\epsilon_g}^{\infty} dE\left\{\left[1-2f(E+\hbar\omega)\right] g_2(1,2) + \left[1-2f(E)\right] g_2(2,1)\right\} \end{cases}$$

the coherence factors being given by:

$$\begin{cases} g_1(1,2) = \mathrm{Re}.[N(1)]\,\mathrm{Re}.[N(2)] + \mathrm{Re}[P(1)]\,\mathrm{Re}.[P(2)] \\ g_2(1,2) = \mathrm{Im}.[N(1)]\,\mathrm{Re}.[N(2)] + \mathrm{Im}.[P(1)]\,\mathrm{Re}.[P(2)] \end{cases}$$

where N, and P are complex densities of states and paired states

respectively:

$$\begin{cases} N(E) = E / \sqrt{E^2 - \Delta^2(E)} \\ P(E) = \Delta(E) / \sqrt{E^2 - \Delta^2(E)} \end{cases}$$

These expressions reduce to those of Mattis & Bardeen in the weak coupling limit: $\Delta(E) = \epsilon_0$ the second integral in σ_2 then vanishing by symmetry. ϵ_g is interpreted as the effective energy gap in the sense of being the energy where the density of states: Re (N(E)) first becomes non-zero. Nam, and Shaw & Swihart (105) have calculated the infra-red absorption of lead from these expressions with some success. It is unfortunate that Nam does not seem to state explicitly whether the Fermi velocity (and London parameter) are the renormalised values in these expressions. Of course in this Pippard limit it is in fact irrelevant since the renormalisation would cancel out anyway; this is to be expected physically on an anomalous-skin-effect-type argument - the width of the effective zone being inversely proportional to the current-carrying capacity of the quasiparticles. Such a result for the normal state has been demonstrated by Nakajima and Watabe (48) for the extreme anomalous limit, and also for the D.C. conductivity; in the former case (σ/l) is simply related to the area S of Fermi surface by the usual accelerative arguments: $\frac{\sigma}{l} = \frac{e^2 S}{12\pi^3 \hbar}$

and in the latter case it is shown that l , and therefore σ , is independent of renormalisation because the relaxation time is enhanced by the same factor $Z(0)$ as the Fermi velocity is depressed.

In the London limit, however, these renormalisation effects would seem not to cancel out; Nam shows that the supercurrent response in this limit is:

$$\frac{k}{4\pi}\,(q=0,\,\omega=0) = \Lambda^{-1}(0) \sum_n 2\pi \frac{k_B T}{Z_n} \frac{\Delta_n^2}{\left[(2n+1)^2\pi^2 k_B^2 T^2 + \Delta_n^2\right]^{3/2}}$$

This leads to the usual B.C.S. expression for the London parameter in the weak-coupling limit ($\Delta n = \epsilon_0$, $Zn = 1$), namely:

$$\frac{k}{4\pi}\,(q=0,\omega=0) = \frac{\Lambda(T)}{\Lambda(0)} = \epsilon_0^2 \int_0^\infty \frac{d\epsilon}{\epsilon^2}\left[\frac{1-2f(\epsilon_0)}{\epsilon_0} - \frac{1-2f(E)}{E}\right]$$

Now if we assume that we can extract the qualitative behaviour of Nam's expression by setting $\Delta n \sim \epsilon_0$, $Zn \sim Z(0)$ (at any rate at low T), then this would indicate a renormalisation of the London parameter:

$$\Lambda^*(0) = Z(0)\,\Lambda(0)$$

and if we are correct in our interpretation of his $\Lambda(0)$ as being

free of any renormalisation effects, then:

$$\Lambda^{*-1}(0) \sim Z^{-1}(0)\, S_{v_F} = S_{v_F}{}^{*}$$

which is what we would expect physically. The only point which causes one slight doubt is that in the second of his two papers where he calculates the infra-red absorptivity of lead he quotes a formula for the coherence length (which may only be intended as approximate):

$$\xi_0 = \frac{\hbar v_F}{\pi \epsilon_0(0)}$$

in which, presumably, he means the unrenormalised v_F. This may simply be a matter of definition. However, a more reasonable definition of a coherence length is:

$$\xi_0 = \frac{\hbar v_F{}^{*}}{\pi \epsilon_0(0)}$$

there being some indication that such a coherence length is that determining the thickness-dependence of the periodicity of the Tomasch effect in lead (McMillan (49); Tomasch (50); Rowell & McMillan (51), McMillan and Anderson (52)), though the results of the latter authors give a value nearer to the free-band value v_F than to the value deduced from the anomalous skin effect (for lead McMillan estimates $Z(0) = 2.12$); this they attribute to Fermi surface anisotropy in that their lead films might well have had preferred crystal orientation. Thus although we should perhaps not be too glib over regarding the

effects of renormalisation as being completely settled, it would appear that the Faber & Pippard formula:

$$v_F = \frac{\pi^2 k_B^2}{e^2 \gamma(pl)}$$

ought to be validly reinterpreted with $\gamma \rightarrow \gamma^* =$ experimental value and $v_F \rightarrow v_F^*$ – this being the value appropriate to determining the minimum distance over which the order parameter can change. Of course, the question of how this is related to the purported measurements of ξ_0 from magnetisation measurements is open to some doubt and to date there have been no published measurements of ξ_0 from the Tomasch effect in niobium, unfortunately. Most deductions from magnetisation results rely on the non-local B.C.S. relation for the penetration depth λ in terms of λL and ξ_0, and until a detailed calculation of Nam's formulae is made one cannot know how important will be the strong-coupling corrections. As we have seen, the use of the weak-coupling relation is equivalent to a renormalisation of λL, ξ_0, and vF which renormalises the London limit ($q \rightarrow o$) and the Pippard limit ($q \rightarrow \infty$) in what appears to be an approximately correct fashion and assumes that the region of intermediate ($q\ \xi_0$) scales as in the weak-coupling case; it remains to be seen how adequate this is.

CRITICAL FIELDS:

The measurements by Finnemore et al. (53) and French (3) of the thermodynamic critical field Hc of niobium have shown that it deviates by less than 1% from the empirical form:

$$H_c = H_c(0)\,(1-t^2)$$

and thus, in common with other strong coupling superconductors like Hg, Pb, and Ta, lies above the weak-coupling B.C.S. prediction. At low temperatures, this theory predicts relationships to the normal state electronic specific heat:

$$\begin{cases} \epsilon_0(0) = H_c(0)\sqrt{\dfrac{\pi k_B^2}{6\gamma}} \\ H_c^2 = H_c^2(0) - 4\pi\gamma T^2 \end{cases}$$

and the value of γ so calculated by these two authors, namely $8.0\ \text{mJ. mole}^{-1}\ ^\circ\text{K}^{-2}$ is in good agreement with the experimental value of $7.8\ \text{mJ. mole}^{-1}\ ^\circ\text{K}^{-2}$ — Leupold & Boorse (30); van der Hoeven & Keesom (54), but the high-temperature jump in specific heat as calculated from:

$$C_S - C_N = \frac{T_c}{4\pi}\left(\frac{dH_c}{dT}\right)^2\Big|_{T_c}$$

is about 11% higher than the experimental value. It is interesting to note that if the inversion procedure described by Finnemore & Mapother (55) were used to determine the energy-gap $\epsilon_0(t)$ from the measured critical field on the basis of the weak-coupling B.C.S.

expression which is solely a function of (ϵ_o /kT), then, as they found even for Hg, the energy gap resulting deviates only very slightly from the B.C.S. form. Such a determination, unlike ultrasonic or surface impedance measurements, should be free of the complications of scattering, at any rate in the single band model. Theoretical treatments of the thermodynamics of strong-coupling superconductors have been given by Wada (56) and Bardeen & Stephen (57) based on the Eliashberg formulation, and have been successfully applied to the calculation of Hc for lead by Swihart et. al. (58). Such a calculation has not yet been made for niobium.

A rather different approach to the thermodynamics of strong-coupling superconductors has been developed by Sheahen (59) on an empirical basis in which the thermodynamic properties are related by pseudo-weak-coupling expressions containing an effective interaction parameter NV* which is allowed to be temperature dependent. This idea has since been shown by Rothwarf (60) to follow from the Eliashberg theory, and is proposed as an explanation for the empirical relation given by Toxen (61):

$$\frac{d\left(\frac{H_c}{H_d(0)}\right)}{dt} = \frac{\epsilon_o(0)}{kT_c}$$

which was known to be the case in the weak-coupling limit, but not otherwise. According to French, this gives a gap value of 1.06 x B.C.S. for niobium.

The effect of strong-coupling on the nucleation fields H_{c2} and H_{c3} has been discussed by Eilenberger & Ambegaokar (62), Werthamer & McMillan (63), and Yorke & Bardasis (64). Werthamer & McMillan undertook a numerical computation for niobium, but do not give the detailed results, being content with the statement that the temperature dependence deduced was identical (to within 2%) of the weak-coupling prediction; however, they assert that the scale of H_{c2} is substantially renormalised by the electron-phonon interaction, again without giving precise details. Eilenberger and Ambegaokar derive the following result for the strong-coupling correction near Tc:

$$\frac{H_{c2}}{H_{c2\,B.C.S.}} = \left(2\,\frac{\epsilon_0'^2}{\epsilon_{0\,B.C.S.}^2} - \frac{H_c^2}{H_{c\,B.C.S.}^2}\,\frac{\epsilon_{0\,B.C.S.}^2}{\epsilon_0^2} \right)$$

and make statements about the renormalisations which appear to support ours. They attempt to fit $\left.\frac{dH_{c2}}{dT}\right|_{T_c}$ for lead on this basis using the specific heat and Fermi-surface data, but obtain a value 20% lower than that measured. A similar discrepancy is noted by Yorke & Bardasis. A puzzling feature of the latter's paper is that the strong-coupling Ginzburg-Landau theory which they obtain

(equation 18) appears to contain a $\sqrt{Z}$ renormalisation of the effective Ginzburg-Landau coherence length for fluctuations rather than the Z which we expect. Both Eilenberger & Ambegsokar and Yorke & Bardasis agree that the ratio:

$$\left.\frac{H_{c3}}{H_{c2}}\right|_{T_c} = 1.695$$

as in the weak-coupling limit.

Generally, it would seem that the strong-coupling corrections envisaged here are inadequate to explain the large deviation of the temperature dependence of H_{c2} from the weak-coupling predictions of Hohenberg & Werthamer (65) observed experimentally by Finnemore et al. (53), French (3) and others; a combination of Fermi surface anisotropy and non-locality seems a more likely candidate.

4. SURFACE IMPEDANCE

The theory of the transverse electromagnetic response of isotropic, weak-coupling, single-band superconductors has been given by Mattis & Bardeen (46); an extensive computation of the response has been made by Waldram for a wide range of temperatures and frequencies in the cases where a simple description in terms of a conductivity relative to the normal state (σ_S/σ_N) is applicable i.e. in the extreme Pippard limit where the skin depth $\delta \ll \xi_0, l$ and in the extreme dirty limit $l \ll \xi_0, \delta$ where we have respectively:

$$\frac{Z_S}{Z_N} = \left(\frac{\sigma_S}{\sigma_N}\right)^{-1/3} \quad \text{&} \quad \frac{Z_S}{Z_N} = \left(\frac{\sigma_S}{\sigma_N}\right)^{-1/2}$$

The extent to which these limits are of use in practice depends on the particular metal under investigation, and exactly what its London-Pippard character is. Miller (66) has made the full calculation for pure tin and aluminium taking proper account of the actual degree of non-locality obtaining in each case, as has Ginsberg for alloys of lead (67). When we first undertook to make such a calculation for niobium, the results of Turneaure & Weissman (21) had not been published; they give a rather limited calculation of the surface impedance at a few temperatures and for a single value of mean free path only - we compare our

computation with theirs later. Yet more recently (Feb. 1969), a more general set of tabulated surface resistances due to Halbritter (68) has come to our attention; these give values of surface resistance at temperature intervals $\delta t = 0.1$ in the frequency range $10^{-3} < \hbar\omega/\epsilon_0(t) < 10^{-1}$ for values of $\kappa_L = \lambda_L(0)/\xi_0$ in the range $0.009 < \kappa_L < 0.8$ and for five values of mean free path $\frac{2}{\pi}\frac{l}{\xi_0}\cdot\frac{\epsilon_0(t)}{\epsilon_0(0)}$ ranging down to 1. No values of reactance are given, however, and we feel that our own working program has some advantages in obtaining both resistance and reactance at conveniently close temperature intervals for any desired form of the energy gap; it is also convenient to be able to adjust the normal and supercurrent scalings separately both via the values of κ_L and via the values of mean free path.

As discussed by Miller, it is convenient to express the results of Mattis & Bardeen in terms of the response to each Fourier component of the field penetrating the surface of the superconductor:

$$\underline{J}(q) = -\frac{1}{4\pi} K(q)\, \underline{A}(q)$$

The Fourier transform of this equation gives rises to a convolution which represents the Mattis & Bardeen version of the Pippard type of non-local integral response in real space:

$$\underline{J}(\underline{r}) = -\frac{3}{\hbar v_F \Lambda(0)} \int d\underline{r}' \; \frac{\underline{R}\,[\underline{R}\cdot\underline{A}(\underline{r}')]}{R^4}\; e^{-R/l}\; I(\omega, R, T)$$

where the square brackets denote the retarded value,

$\underline{R} = \underline{r}' - \underline{r}$, and I is the Mattis and Bardeen kernel:

$$I(\omega,R,T) = -\pi i \int_{\epsilon_0-\hbar\omega}^{\epsilon_0} [1-2f(E+\hbar\omega)][g(E)\cos\alpha\epsilon_2 - i\sin\alpha\epsilon_2]\exp i\alpha\epsilon_1\, dE$$

$$-\pi i \int_{\epsilon_0}^{\infty} \Big\{ [1-2f(E+\hbar\omega)][g(E)\cos\alpha\epsilon_2 - i\sin\alpha\epsilon_2]\exp i\alpha\epsilon_1$$

$$- [1-2f(E)][g(E)\cos\alpha\epsilon_1 + i\sin\alpha\epsilon_1]\exp -i\alpha\epsilon_2 \Big\}\, dE$$

The one-particle energies are:

$$\epsilon_1 = \mathrm{sign}(E+\epsilon_0)\sqrt{E^2-\epsilon_0^2} \qquad \text{and} \qquad \epsilon_2 = \sqrt{(E+\hbar\omega)^2-\epsilon_0^2}$$

the coherence factor is: $g(E) = (E^2 + \hbar\omega E + \epsilon_0^2)/\epsilon_1\epsilon_2$

and: $\alpha = R/\hbar v_F$

We then obtain the response kernel as the Fourier transform of I:

$$K(q) = -\frac{3}{\hbar v_F \Lambda(0)} \int_0^{\infty} dR \int_{-1}^{+1} du\,(1-u^2)\exp\left(iqRu - \frac{R}{l}\right) I(\omega,R,T)$$

the integral over θ being the angular integration around the

(spherical) Fermi surface. This angular integral can be done analytically, and yields:

$$K(q_\parallel) = \frac{12\pi i}{\hbar v_F q_\parallel \Lambda(0)} \left\{ \int_0^\infty R(x)\,dx \int_{\epsilon_0-\hbar\omega}^{\epsilon_0} \left[1-2f(E+\hbar\omega)\right]\left[g(E)\cos\alpha\epsilon_2 - i\sin\alpha\epsilon_2\right] \times \right.$$

$$\exp.\left(i\alpha\epsilon_1 - \frac{R}{L}\right) dE$$

$$+ \int_0^\infty R(x)\,dx \int_{\epsilon_0}^\infty \left\{ \left[1-2f(E+\hbar\omega)\right]\left[g(E)\cos\alpha\epsilon_2 - i\sin\alpha\epsilon_2\right] \exp.\left(+i\alpha\epsilon_1 - \frac{R}{L}\right) \right.$$

$$\left. \left. - \left[1-2f(E)\right]\left[g(E)\cos\alpha\epsilon_1 + i\sin\alpha\epsilon_1\right] \exp.\left(-i\alpha\epsilon_2 - \frac{R}{L}\right) \right\} dE \right\}$$

where the Bessel function R is:

$$R(x) = x^{-2}\left[x^{-1}\sin.x - \cos.x\right] \qquad \text{and} \qquad x = q_\parallel R .$$

The spatial integrals over x may be done analytically using the lemmas

$$\int_0^\infty dx\, R(x)\,\sin.ax\,\exp.-bx$$

$$= \tfrac{1}{2}a + \tfrac{1}{8}\left(1-a^2+b^2\right)\log.\left[\frac{1+\left(\frac{a+1}{b}\right)^2}{1+\left(\frac{a-1}{b}\right)^2}\right] - \tfrac{1}{2}ab\left[\tan.^{-1}\left(\frac{a+1}{b}\right) - \tan.^{-1}\left(\frac{a-1}{b}\right)\right]$$

and:

$$\int_0^\infty dx\, R(x)\,\cos.ax\,\exp.-bx$$

$$= -\tfrac{1}{2}b + \tfrac{1}{4}ab\,\log.\left[\frac{1+\left(\frac{a+1}{b}\right)^2}{1+\left(\frac{a-1}{b}\right)^2}\right] + \tfrac{1}{4}\left(1-a^2+b^2\right)\left[\tan.^{-1}\left(\frac{a+1}{b}\right) - \tan.^{-1}\left(\frac{a-1}{b}\right)\right]$$

(spherical) Fermi surface. This angular integral can be done analytically, and yields:

$$K(q) = \frac{12\pi i}{\hbar v_F q \, \Lambda(0)} \left\{ \int_0^\infty R(x)\,dx \int_{\epsilon_0 - \hbar\omega}^{\epsilon_0} \left[1 - 2f(E+\hbar\omega)\right]\left[g(E)\cos\alpha\epsilon_2 - i\sin\alpha\epsilon_2\right] \times \right.$$

$$\exp.\left(i\alpha\epsilon_1 - \frac{R}{L}\right) dE$$

$$+ \int_0^\infty R(x)\,dx \int_{\epsilon_0}^\infty \left\{ \left[1 - 2f(E+\hbar\omega)\right]\left[g(E)\cos\alpha\epsilon_2 - i\sin\alpha\epsilon_2\right] \exp.\left(+i\alpha\epsilon_1 - \frac{R}{L}\right) \right.$$

$$\left. \left. - \left[1 - 2f(E)\right]\left[g(E)\cos\alpha\epsilon_1 + i\sin\alpha\epsilon_1\right] \exp.\left(-i\alpha\epsilon_2 - \frac{R}{L}\right) \right\} dE \right\}$$

where the Bessel function R is:

$$R(x) = x^{-2}\left[x^{-1}\sin.x - \cos.x\right] \qquad \text{and} \qquad x = qR.$$

The spatial integrals over x may be done analytically using the lemmas

$$\int_0^\infty dx\, R(x)\, \sin.ax\, \exp.-bx$$

$$= \tfrac{1}{2}a + \tfrac{1}{8}\left(1 - a^2 + b^2\right) \log.\left[\frac{1 + \left(\frac{a+1}{b}\right)^2}{1 + \left(\frac{a-1}{b}\right)^2}\right] - \tfrac{1}{2}ab\left[\tan.^{-1}\left(\frac{a+1}{b}\right) - \tan.^{-1}\left(\frac{a-1}{b}\right)\right]$$

and:

$$\int_0^\infty dx\, R(x)\, \cos.ax\, \exp.-bx$$

$$= -\tfrac{1}{2}b + \tfrac{1}{4}ab \log.\left[\frac{1 + \left(\frac{a+1}{b}\right)^2}{1 + \left(\frac{a-1}{b}\right)^2}\right] + \tfrac{1}{4}\left(1 - a^2 + b^2\right)\left[\tan.^{-1}\left(\frac{a+1}{b}\right) - \tan.^{-1}\left(\frac{a-1}{b}\right)\right]$$

which in the pure limit b = o reduce to:

$$\int_0^\infty dx\ R(x)\ \sin.ax = \frac{1}{4}\left[2a + (1-a^2)\ \log.\left|\frac{1+a}{1-a}\right|\right]$$

and:

$$\int_0^\infty dx\ R(x)\ \cos.ax = \begin{cases} \frac{\pi}{4}(1-a^2) & \text{for } |a|<1 \\ 0 & \text{for } |a|>1 \end{cases}$$

$|a| = 1$ corresponds to the critical value of q for surf-riding of the quasi-particles on the incident field. It is convenient to adopt the following dimensionless notation at this stage:

$$k_L \equiv \frac{\lambda_L(0)}{\xi_0} \qquad r \equiv \frac{R}{\xi_0} \qquad l \equiv \frac{l}{\xi_0} \qquad k \equiv q\xi_0 \qquad E \equiv \frac{E}{\epsilon_0(t)} \qquad W \equiv \frac{\hbar\omega}{\epsilon_0(t)}$$

and then :

$$\begin{cases} \epsilon_1 = \text{sign.}\,(1+E)\ \sqrt{E^2-1} \\ \epsilon_2 = \sqrt{(E+W)^2-1} \\ \epsilon_1' = \sqrt{1-E^2} \\ \epsilon_\pm = \epsilon_1 \pm \epsilon_2 \\ g(E) = (E^2+WE+1)/\epsilon_1\epsilon_2 \\ h(E) = (E^2+WE+1)/\epsilon_1'\epsilon_2 \\ f(E) = (1+\exp.\frac{E}{t})^{-1} \\ x = kr \end{cases}$$

Then the response kernel may be split into real and imaginary parts as follows, corresponding respectively to the super- and normal- currents(neglecting retardation):

$$K_1 \equiv Re(K) = \frac{3}{\pi} k_L^{-2} k^{-1} \frac{\epsilon_0(t)}{\epsilon_0(0)} \int_0^\infty dx\, R(x)\, x$$

$$\left\{ \int_{1-W,-1}^{1} dE \left[1-2f(E+W)\right]\left[h(E) \cos.\left(\frac{x}{\pi k}\frac{\epsilon_0(t)}{\epsilon_0(0)}\epsilon_2\right) + \sin.\left(\frac{x}{\pi k}\frac{\epsilon_0(t)}{\epsilon_0(0)}\epsilon_2\right)\right] \exp.\left(-x\left(\frac{\frac{\epsilon_0(t)}{\epsilon_0(0)}\epsilon_1 + \frac{1}{kL}}{\pi k}\right)\right)\right.$$

$$- \int_1^\infty dE \left(\left[1-f(E)-f(E+W)\right]\left[g(E)-1\right] \sin.\left(\frac{x}{\pi k}\frac{\epsilon_0(t)}{\epsilon_0(0)}\epsilon_+\right) + \left[f(E)-f(E+W)\right]\left[g(E)+1\right] x \right.$$

$$\left. \sin.\left(\frac{x}{\pi k}\frac{\epsilon_0(t)}{\epsilon_0(0)}\epsilon_-\right)\right) \exp.-\frac{x}{kL}$$

$$\left. - \frac{1}{2} \int_{-1,1-W}^{-1} dE \left[1-2f(E+W)\right] \left(\left[g(E)-1\right] \sin.\left(\frac{x}{\pi k}\frac{\epsilon_0(t)}{\epsilon_0(0)}\epsilon_+\right) + \left[g(E)+1\right] \sin.\left(\frac{x}{\pi k}\frac{\epsilon_0(t)}{\epsilon_0(0)}\epsilon_-\right)\right) \exp.-\frac{x}{kL} \right\}$$

and:

$$K_2 \equiv Im.(K) = \frac{3}{\pi} k_L^{-2} k^{-1} \frac{\epsilon_0(t)}{\epsilon_0(0)} \int_0^\infty dx\, R(x)\, x$$

$$\left\{ \int_1^\infty dE \left[f(E)-f(E+W)\right] \left(\left[g(E)-1\right] \cos.\left(\frac{x}{\pi k}\frac{\epsilon_0(t)}{\epsilon_0(0)}\epsilon_+\right) + \left[g(E)+1\right] \cos.\left(\frac{x}{\pi k}\frac{\epsilon_0(t)}{\epsilon_0(0)}\epsilon_-\right) \exp.-\frac{x}{kL} \right.\right.$$

$$\left. \left. + \frac{1}{2} \int_{-1,1-W}^{-1} dE \left[1-2f(E+W)\right] \left(\left[g(E)-1\right] \cos.\left(\frac{x}{\pi k}\frac{\epsilon_0(t)}{\epsilon_0(0)}\epsilon_+\right) + \left[g(E)+1\right] \cos.\left(\frac{x}{\pi k}\frac{\epsilon_0(t)}{\epsilon_0(0)}\epsilon_-\right)\right) \exp.-\frac{x}{kL} \right\}$$

where the 2nd alternative in the lower limits only arises in the gap-jumping regime $W > 2$. These are the kernels which we have evaluated numerically for niobium, and we show some examples in fig. (4). It is useful to keep in mind the following simple limiting forms for the pure limit (reverting back to dimensional notation temporarily):

$$\begin{cases} \lim_{q\to 0} \; K_2 = 0 \quad ; \quad \lim_{q\to 0} \; K_1 = \lambda_L^{-2}(0) \; - \text{London limit} \\ \lim_{q\to\infty} \; K = \dfrac{3}{4q\xi_0}\dfrac{\hbar\omega}{\epsilon_0(0)}\, i\,\dfrac{\sigma_S}{\sigma_N} \; - \text{Pippard limit} \end{cases}$$

The problem of calculating the skin depth from the computed kernel then reduces to a second numerical integration of the form (in dimensionless notation):

p = o (diffuse surface scattering):

$$\frac{\delta}{\lambda_L(0)} = \frac{\pi}{k_L}\, i \left\{ \int_0^\infty dk \, \log\left[1 + k^{-2} K(k)\right] \right. = \frac{\pi}{k_L}\, \frac{I_1 + i I_2}{I_1^2 + I_2^2}$$

where:

$$\begin{cases} I_1 = \displaystyle\int_0^\infty dk \, \tan^{-1}\left(\frac{k^{-2} K_2}{1 + k^{-2} K_1} \right) \\ I_2 = \tfrac{1}{2} \displaystyle\int_0^\infty dk \, \log\left[(1 + k^{-2} K_1)^2 + (k^{-2} K_2)^2 \right] \end{cases}$$

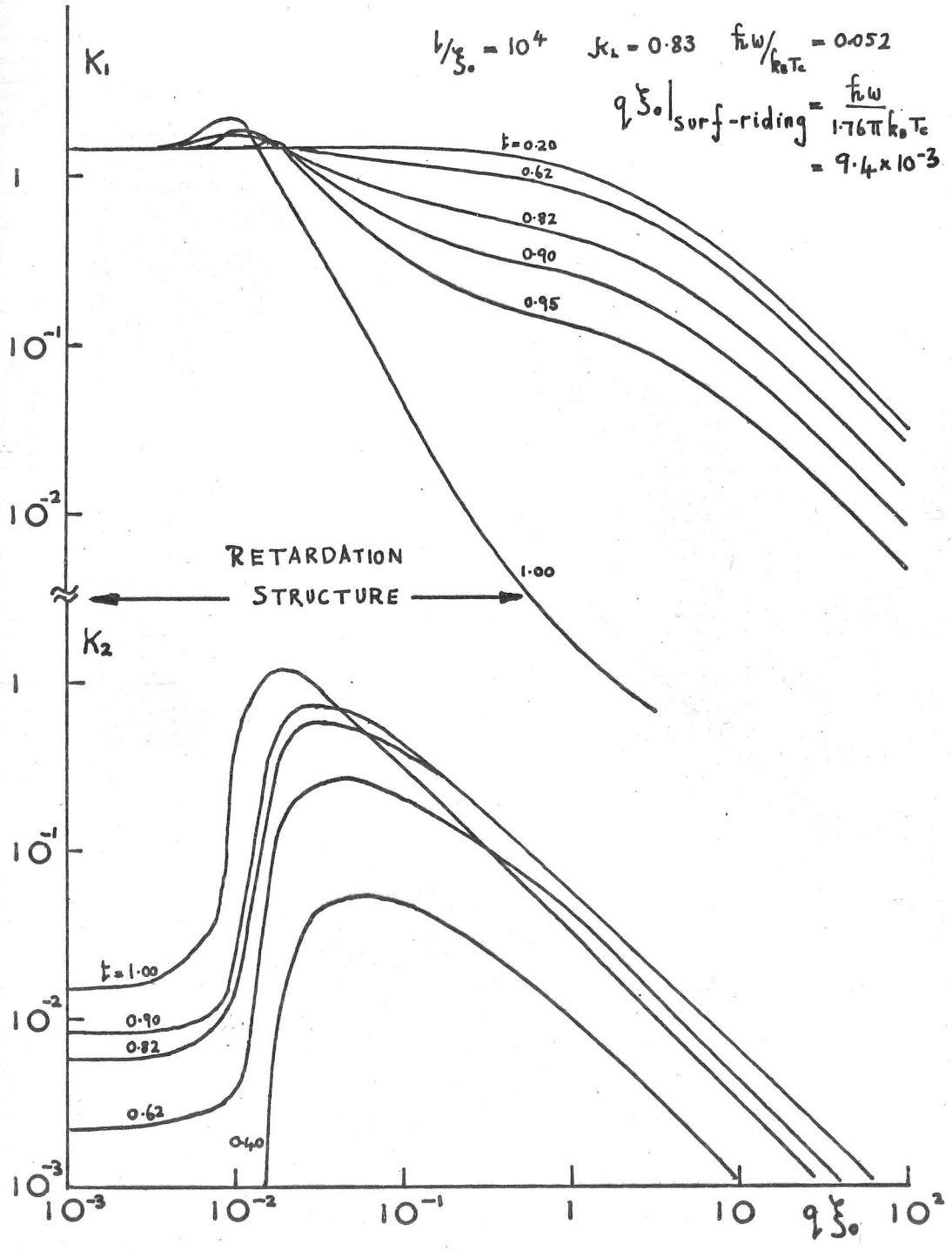
K_1
$l/\xi_0 = 10^4$ $\kappa_L = 0.83$ $\hbar\omega/k_B T_c = 0.052$
$q\xi_0|_{surf\text{-}riding} = \frac{\hbar\omega}{1.76\pi k_B T_c} = 9.4\times10^{-3}$
t=0.20
0.62
0.82
0.90
0.95
1.00
RETARDATION STRUCTURE
K_2
t=1.00
0.90
0.82
0.62
0.40
1
10^{-1}
10^{-2}
10^{-3}
10^{-3} 10^{-2} 10^{-1} 1 10 $q\xi_0$ 10^2

FIG. 4 (a)

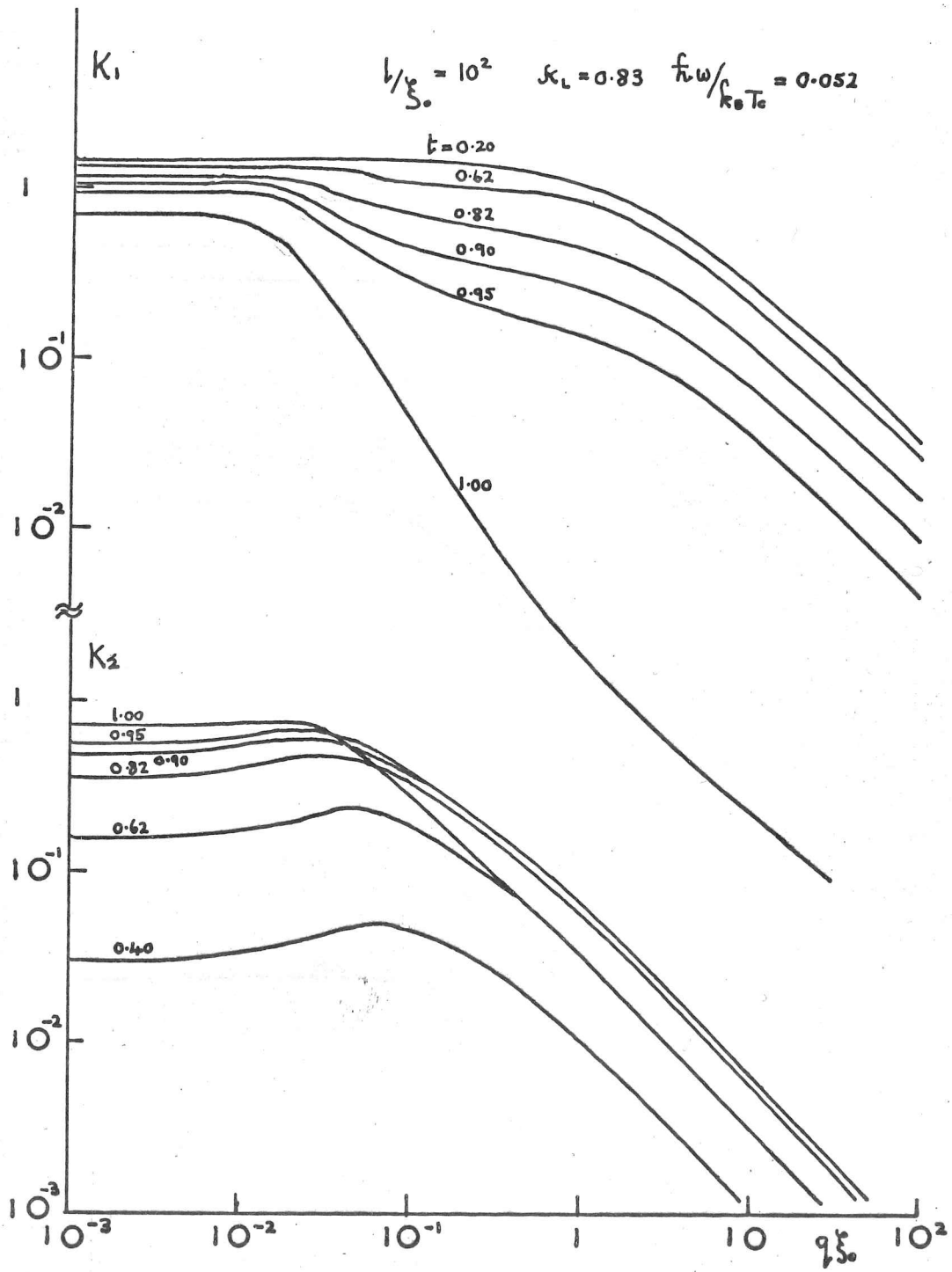
K1
$l/\xi_0 = 10^2$
$\kappa_L = 0.83$
$\hbar\omega/k_B T_c = 0.052$
t=0.20
0.62
0.82
0.90
0.95
1.00
1
10^{-1}
10^{-2}
K2
1.00
0.95
0.82
0.90
0.62
0.40
10^{-3}
10^{-3}
10^{-2}
10^{-1}
1
10
$q\xi_0$
10^2

FIG. 4(b)

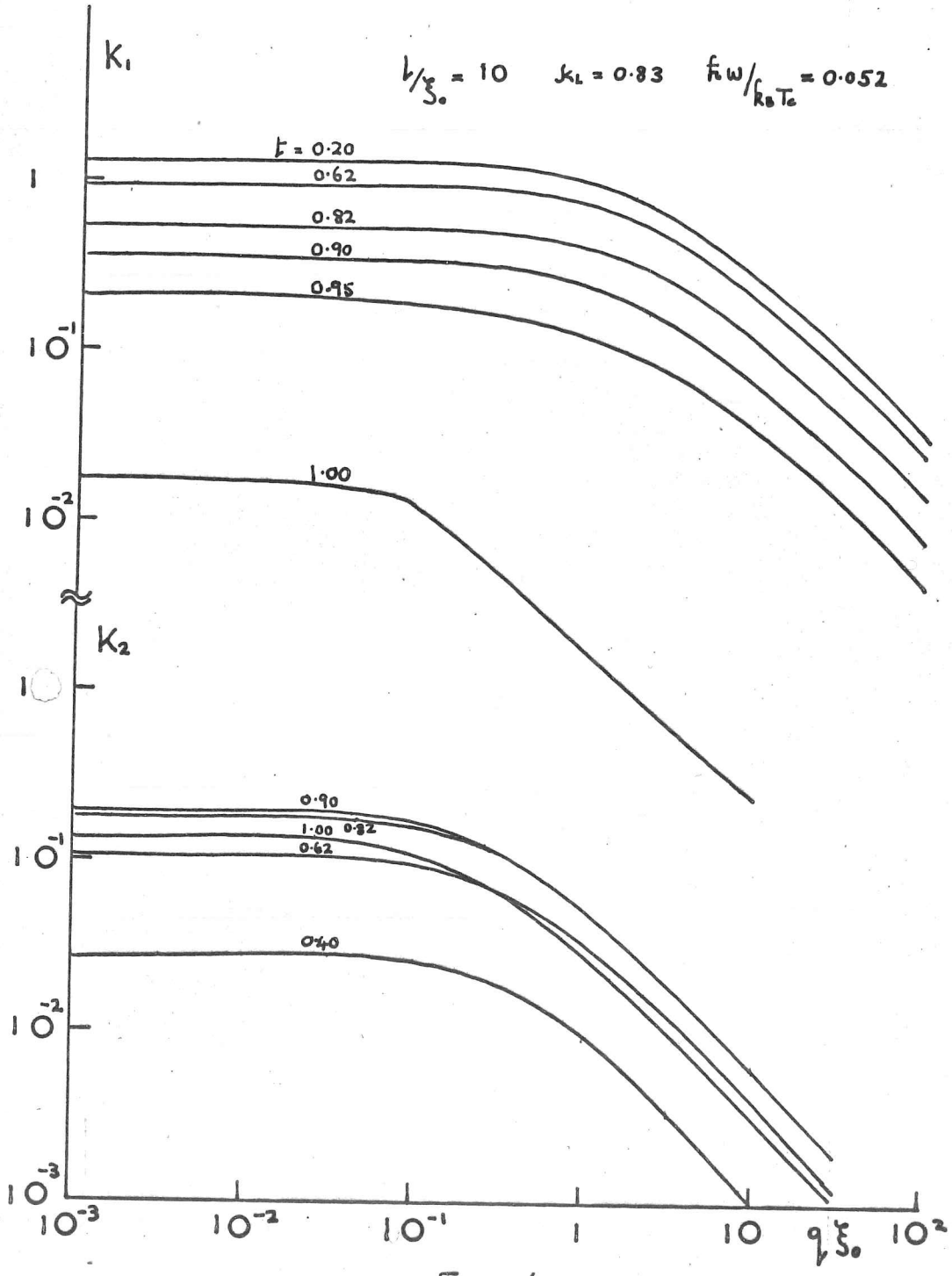
K1
l/ξ0 = 10
κL = 0.83
ħω/kBTc = 0.052
t = 0.20
0.62
0.82
0.90
0.95
1.00
K2
0.90
1.00 0.82
0.62
0.40
1
10⁻¹
10⁻²
10⁻³
10⁻³
10⁻²
10⁻¹
1
10
q ξ0
10²

FIG. 4 (c)

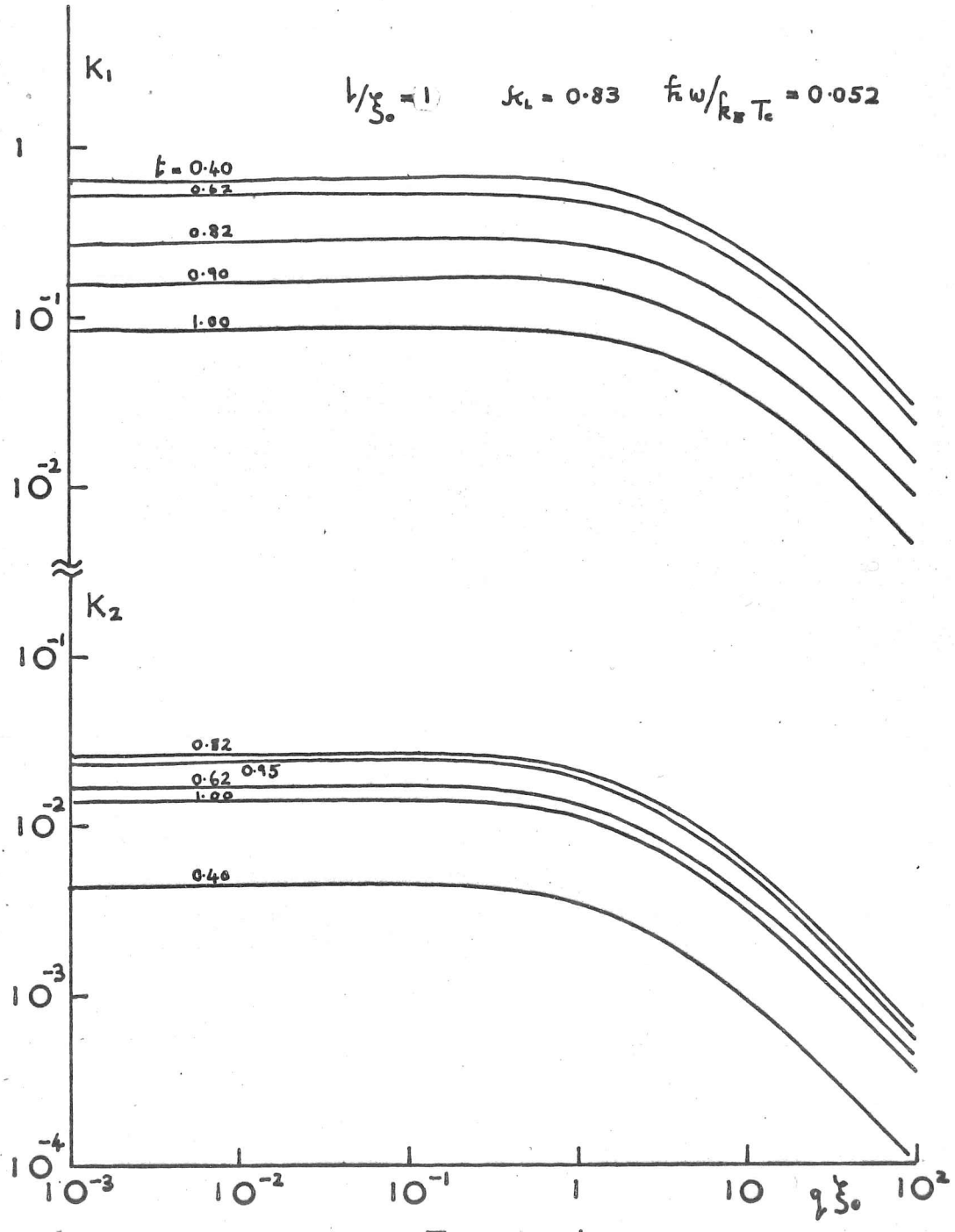
K1
l/ξ0 = 1
κL = 0.83
ħω/kB Tc = 0.052
1
10-1
10-2
t = 0.40
0.62
0.82
0.90
1.00
K2
10-1
10-2
10-3
10-4
0.82
0.62
0.95
1.00
0.40
10-3
10-2
10-1
1
10
q ξ0
10²

FIG. 4 (d)

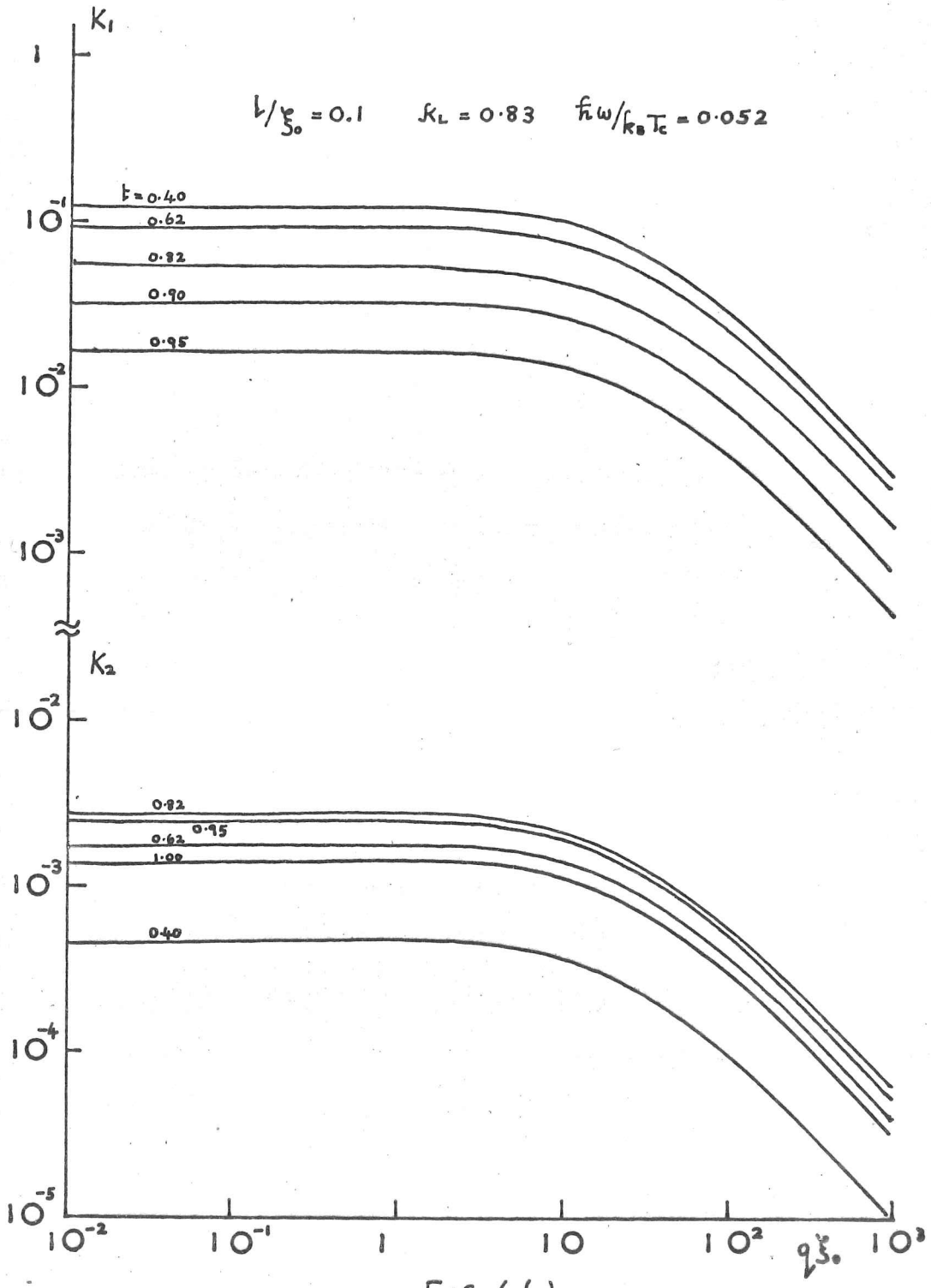
K1
1
$l/\xi_0 = 0.1$ $\kappa_L = 0.83$ $\hbar\omega/k_B T_c = 0.052$
t = 0.40
0.62
0.82
0.90
0.95
10^{-1}
10^{-2}
10^{-3}
K2
10^{-2}
0.82
0.95
0.62
1.00
10^{-3}
0.40
10^{-4}
10^{-5}
10^{-2}
10^{-1}
1
10
10^2
$q\xi_0$
10^3

FIG. 4(e)

p = 1 (specular surface scattering):

$$\frac{\delta}{\lambda_L(0)} = \frac{2}{\pi k_L} i \left\{ \int_0^\infty dk \left[k^2 + K(k) \right]^{-1} \right\}$$

$$= \frac{2}{\pi k_L} \int_0^\infty dk \, \frac{K_2}{(k^2+K_1)^2 + K_2^2} + \frac{2i}{\pi k_L} \int_0^\infty dk \, \frac{(k^2+K_1)}{(k^2+K_1)^2 + K_2^2}$$

It is found that to obtain sufficient accuracy, the calculation of a single pair of resistance and reactance values takes about 17 seconds computation time on average.

We have made rather extensive checks that the program written for this computation gives good values for the normal state impedance; it appears to be correct to 1 or 2% in the classical, extreme anomalous, and intermediate regions, and also in the extreme retardation and classical retardation regions. Further, in fig. (5) we show a comparison of our computation of resistance and reactance of niobium with the values given by Turneaure & Weissmann (21) which appears to have been carried out for the following reduced parameters:

$$k_L = 0.847 \,, \quad \frac{l}{\xi_0} = 24.3 \,, \quad \frac{\hbar\omega}{kT_c} = 0.0581 \,, \quad \epsilon_0 = 1.05 \, \epsilon_{0\,B.C.S.}$$

The agreement is seen to be excellent. We have also checked that

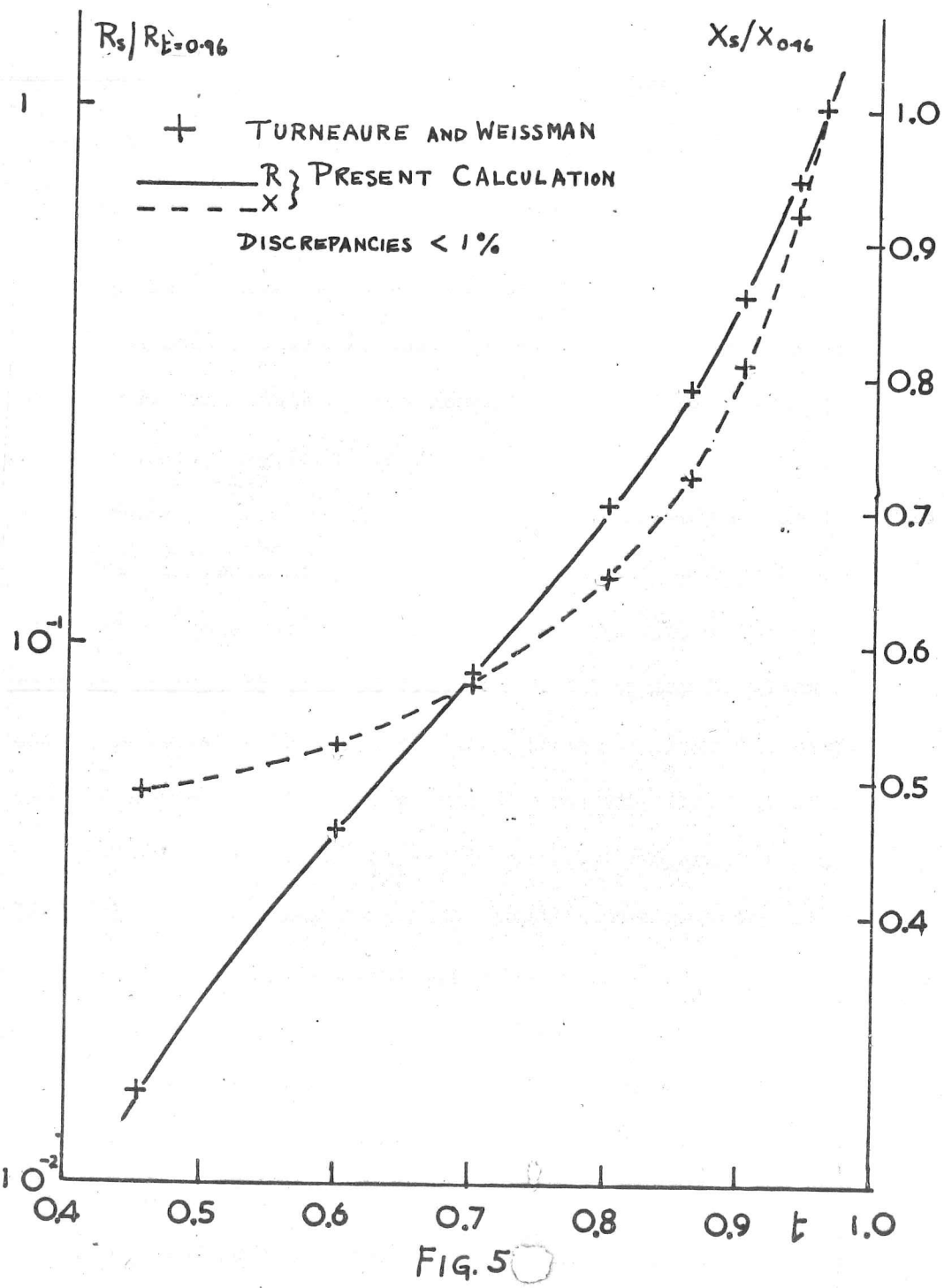
$R_s/R_{t=0.96}$
$X_s/X_{0.96}$
1
10^{-1}
10^{-2}
+ TURNEAURE AND WEISSMAN
R } PRESENT CALCULATION
X
DISCREPANCIES < 1%
1.0
0.9
0.8
0.7
0.6
0.5
0.4
0.4
0.5
0.6
0.7
0.8
0.9
t
1.0

FIG. 5

the limiting values of the kernel give good figures for the temperature dependence of the London parameter, and for the Mattis & Bardeen conductivities σ_S/σ_N .

An interesting general feature of this calculation in the clean London limit is that the surface resistance in the superconducting state at low temperatures is higher for specular surface scattering than for diffuse, in contrast to the normal state where $\frac{\delta_1|_{p=1}}{\delta_1|_{p=0}} = \frac{8}{9}$ in the extreme anomalous limit, and therefore in contrast to the behaviour in the extreme Pippard limit where this ratio is maintained at all temperatures; we show an example of this in fig. (6). This may be given a simple physical interpretation as follows; unlike the extreme anomalous limit in the normal metal where the field penetrates with oscillating spatial phase, in the low temperature London limit where the normal current is small compared with the super-current the field penetrates approximately as e^{-z/λ_L} . This means that an electron on the effective zone on being reflected at the surface continues to pick up energy from the field on its way back into the metal, and the absorption is higher than it would be in the case of diffuse scattering. Of course, if the field penetration were exactly exponential, one can show that

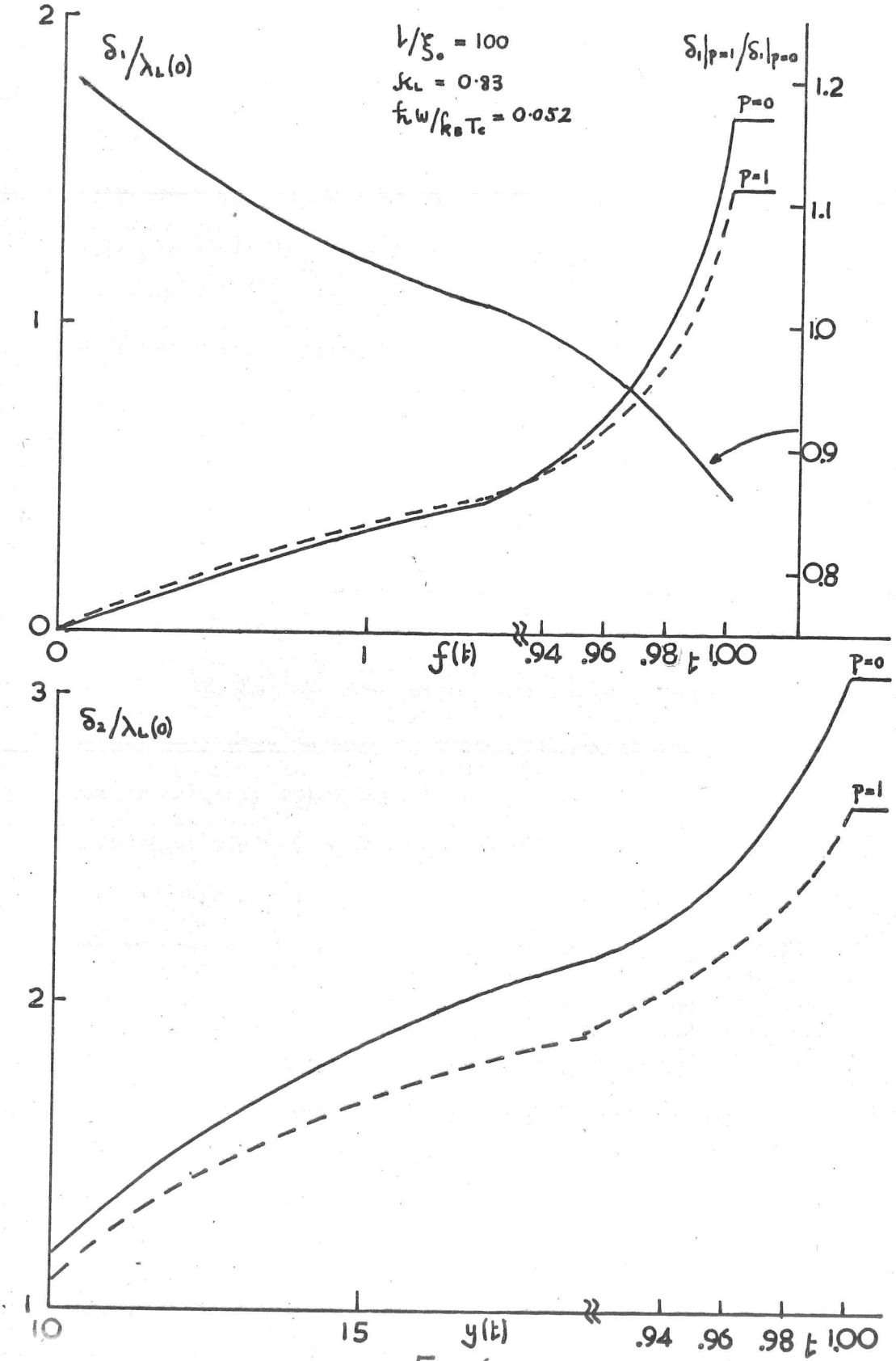
$\delta_1/\lambda_L(0)$
$l/\xi_0 = 100$
$\kappa_L = 0.83$
$\hbar\omega/k_B T_c = 0.052$
$\delta_1|_{p=1}/\delta_1|_{p=0}$
p=0
p=1
1.2
1.1
1.0
0.9
0.8
2
1
0
0
1
f(t)
.94
.96
.98
t
1.00
$\delta_2/\lambda_L(0)$
3
2
1
10
15
y(t)
.94
.96
.98
t
1.00
p=0
p=1

FIG. 6

the momentum acquired by the electron in this process would be infinite in fact; what prevents this divergence in practice is the effect of retardation giving a temporal change in the phase of the accelerating field, and the fact that at sufficiently large depths within the metal the supercurrent and normal current must become comparable thus altering the spatial phase variation of the field.

If we be allowed to speculate, it would seem that in the clean London limit of an anisotropic superconductor there is a possibility that the low temperature surface resistance could be anomalously high on this account; if one envisages the admittedly rather unlikely situation of a superconductor with a fairly sharp energy gap minimum in one particular cross-section of its Fermi surface then for a crystal surface cut parallel to this section, the effective zone for the normal current will lie around this band. At sufficiently low temperatures, the thermally excited quasi-particles will lie in this region only, and an inelastic scattering would seem to be the only process capable of destroying the current, unlike the situation for ultrasonic attenuation. Under such conditions, the surface scattering, which is elastic but not necessarily momentum-conserving, might conceivably become enforcedly specular giving rise to an increased absorption.

ANISOTROPY OF FERMI-SURFACE & ENERGY GAP:

Nam's calculation (47) shows that the isotropic expression for the response kernel can be modified to include the effects of anisotropy as follows:

$$J_i = -\sum_j \frac{K_{ij}}{4\pi} A_j \quad ; \quad K_{ij}(q) = \frac{e^2}{\pi^2} \int \frac{ds}{|v|} v_i v_j \, I$$

where I is the Fourier transform with respect to R of:

$$I_{\omega,R,T} = -\pi i \int_{\epsilon_0 - \hbar\omega}^{\epsilon_0} \left[1 - 2f(E+\hbar\omega)\right] \{I\} \, e^{-R/l} \, dE$$

$$- \pi i \int_{\epsilon_0}^{\infty} \left\{ \left[1-2f(E+\hbar\omega)\right]\{I\} - \left[1-2f(E)\right]\{II\} \right\} e^{-R/l} \, dE$$

where:

$$\begin{cases} \{I\} = \left[g_{+-}(1,2)+1\right] \exp.\left[i\alpha(\epsilon_1-\epsilon_2)\right] + \left[g_{++}(1,2)-1\right] \exp.\left[i\alpha(\epsilon_1+\epsilon_2)\right] \\ \{II\} = \left[g_{+-}(1,2)+1\right] \exp.\left[i\alpha(\epsilon_1-\epsilon_2)\right] + \left[g_{--}(1,2)-1\right] \exp.\left[i\alpha(\epsilon_1+\epsilon_2)\right] \end{cases}$$

where: $g_{\alpha\beta} = N_\alpha(1) N_\beta(2) + P_\alpha(1) P_\beta(2)$ are the coherence factors

and: $\begin{cases} N = E/\epsilon = E/\sqrt{E^2-\epsilon_0^2} \\ P = \epsilon_0/\epsilon = \epsilon_0/\sqrt{E^2-\epsilon_0^2} \end{cases}$

ϵ 1,2 are the single particle energies such that: $\epsilon_2 - \epsilon_1 = q \cdot \underline{v}$

and α or $\beta = \pm$ denotes which cut (upper or lower) of the complex

E-plane is to be used, thus determining the sign of the square roots. The effective mean free path is given by:

$$l^{-1} = \left(\Gamma(\underline{k}_1) + \Gamma(\underline{k}_2)\right)/|v| \quad ; \quad \underline{k}_2 - \underline{k}_1 = q$$

$\Gamma(\underline{k})$ being the relaxation rate for the state $\underline{k}$.

It is not clear to us that this is an adequate description of the scattering process in the presence of gap anisotropy; we note that in this formulation, as in that of Mattis & Bardeen, the states coupled are essentially very close together in $\underline{k}$-space and $\Gamma(\underline{k}_1) = \Gamma(\underline{k}_2)$ for all practical purposes involving a gradual variation in ϵ_0 around the Fermi surface, the effect of impurity being included as a blurring of the original eigenstates over a region $\sim l^{-1}$ in $\underline{k}$-space in Anderson fashion. (69). We believe a more correct formulation in the case where the mean free path is sufficiently long not to cause Anderson blurring of the gap anisotropy would be to make the perturbation calculation of the response from processes involving simultaneous photon absorption and impurity scattering. This would correspond to transitions between widely separated states on the Fermi surface for isotropic scattering. In this case we would expect a relaxation of the form:

$$\Gamma_s(E) = \left\{\Gamma_{NM} \int \frac{ds'}{v'} \frac{E}{\epsilon'}\left(1 - \frac{\epsilon_0\epsilon_0'}{E^2}\right) + \Gamma_{NM} \int \frac{ds'}{v'} \frac{E}{\epsilon'}\left(1 + \frac{\epsilon_0\epsilon_0'}{E^2}\right)\right\} \Big/ \int \frac{ds'}{v'}$$

for $\hbar\omega \ll \epsilon_0$, where $\Gamma_{NN,NM}$ are the relaxation rates for

non-magnetic and magnetic impurity scatterings respectively; the mean free path is thus energy and temperature dependent in the superconducting state, as discussed by Phillips (12). We have made no detailed attempt to assess the effect of this sort of modification on the calculation of the surface impedance, but would guess that no dramatic alteration will result in view of the insensitivity of the current carrying properties to oblique scattering as discussed earlier.

CHAPTER 2 - EXPERIMENTAL DETAILS

1. Specimens

Several single crystals of Nb of various orientations were supplied to the author by Prof. Vinen, Dr. C. Gough, Dr. M. MacVicar, and Metals Research Ltd., to whom his thanks are due. In addition, some crystals were grown in a zone-melting rig kindly loaned by Dr. MacVicar, and designed for use in a Varian ultra high vacuum system; resistance ratios ranging from 300 to 1200 were obtained.

The starting material was $\frac{1}{8}$" Nb rod supplied by Murex Ltd., a 6" length of which was supported in a vertical slide traverse passing through an electron gun and driven by a slow-speed electric motor capable of giving traverse times from 1 - 10 hrs. The procedure for growing the crystal was generally as follows; the rod was melted onto a seed crystal beneath it, and then degassed at just below the melting point in a slow 10 hour traverse at about 10^{-6} torr. The vacuum system was then baked out, and the rod given its first growth on a slow traverse at about 10^{-8} torr. After a further bake-out, sections of the crystal were regrown on a 1 hour traverse 2 or 3 times at 10^{-9} torr;

For the microwave measurements, the specimen was mounted on a thin silica holder, being supported at its centre by small polythene spacers held in place with a minimum of distrene cement. Resistance ratio measurements were subsequently made on each specimen using a conventional 4-terminal technique all specimens grown as described previously showing excellent D.C. transitions at Tc. The leads were attached to each specimen by silver paint; this produces contacts causing minimal damage to the crystal surface as compared with either soldering or spot-welding thus allowing later microwave measurements to be made if required, but suffers from the disadvantage that the lowest contact resistance obtainable at low temperatures by this method is about 0.1 Ω. This proved somewhat of a nuisance for the purer specimens, since it was found convenient to make the measurements of resistance ratio in situ in the microwave resonator where there existed already, of course, the facilities for heating up to 9^{o}K and for applying a large magnetic field; however, this meant that the specimen was only sitting in the exchange gas in the resonator, and not actually in liquid He, and even though firmly glued to an H.C. Cu insert in the waveguide the heating produced by the measuring current ($\sim$ 1Amp) had to be

corrected for, amounting to about 0.5°K at 9°K for a specimen of resistance ratio about 1000, and room temperature resistance about 1mΩ . The voltage across the specimen was fed into a Keithley nanovoltmeter, the output of which was read on a Solartron digital voltmeter; the current supply used was simply an accumulator and rheostat, since any mains-driven D.C. supply seemed to interact with the Keithley producing large spurious signals. Care had also to be taken in this regard over the presence of small leakage currents between any of the contacts before they actually reached the specimen; this seems to be particularly the case with silver-painted contacts where the contact resistance is of order 0.1Ω at best, and even a leakage of only 1MΩ between, say, a voltage and current contact area can produce a spurious voltage signal looking like a resistance of order 0.1μ . This,however, shows up as an apparent (perhaps even negative!) resistance in the superconducting state, and can easily be allowed for if not too large.

2 CRYOGENICS

The cryostat was of conventional metal design (fig. 7), being constructed by Oxford Instruments Ltd. The microwave resonator, which is described more fully later, was shielded by an H.C. copper conduction shield attached to the base of the helium vessel; weak thermal connection between the two was maintained by a thin copper wire thus enabling the resonator to be heated above 4.2°K. by a heater wound on the resonator. Temperature stablisation was achieved by feeding the heater from the amplified output of a Wheatstone bridge with an Allen Bradley 47 Ω . carbon resistor mounted on the resonator as one arm of the bridge; fine temperature control was then effected by means of setting a resistance box in the opposite arm. This arrangement produced a temperature stable to about 1m°K. over long periods.

The temperature was measured using a Cryocal germanium resistance thermometer calibrated between 4 and 20°K, the resistance being recorded by a digital voltmeter in a 4-terminal arrangement operating at about 20mV. and 100 μA. at 9°K. The current was supplied by a simple stabilised current supply

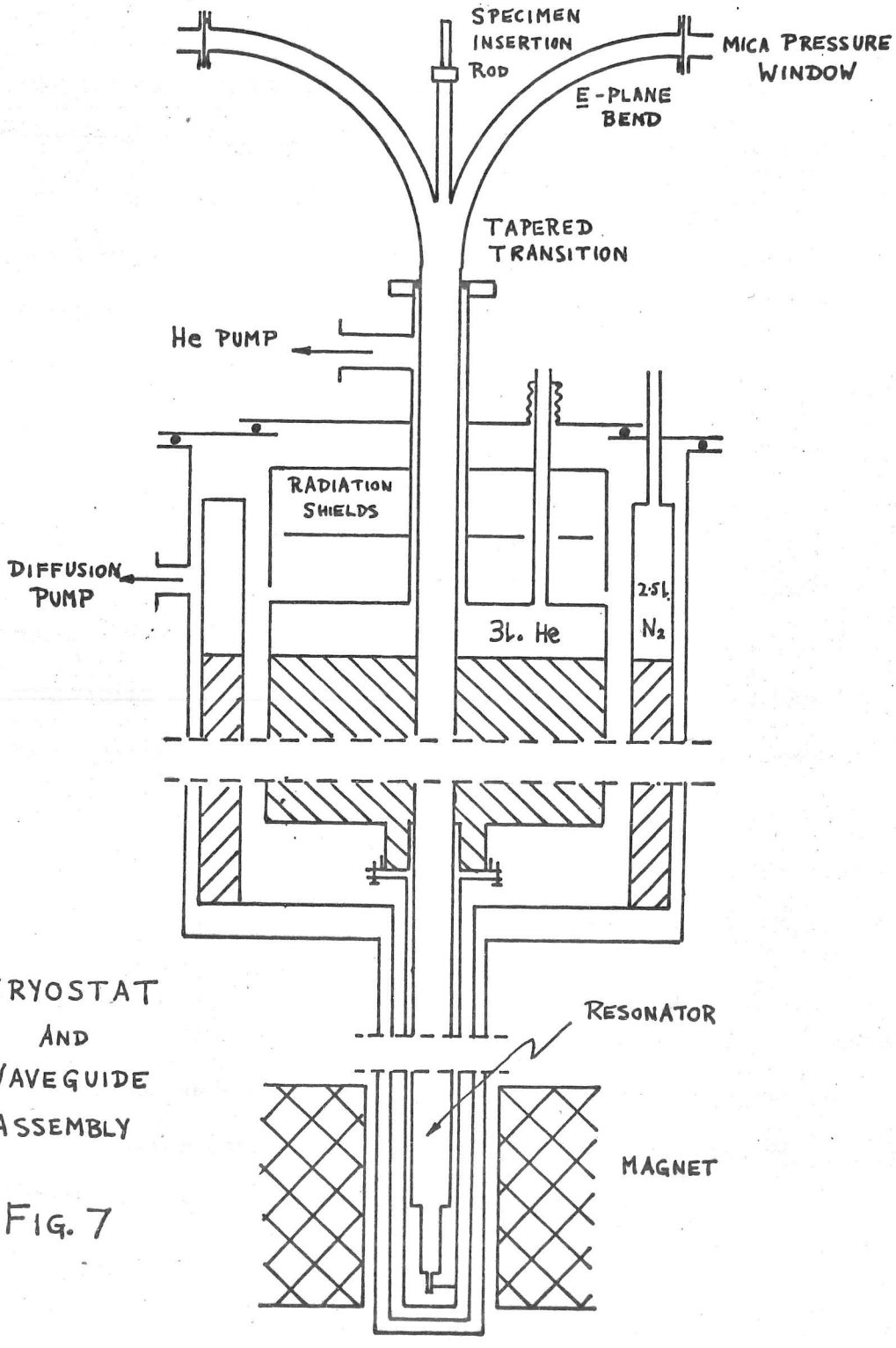

CRYOSTAT
AND
WAVEGUIDE
ASSEMBLY

FIG. 7

calibrated each run by measuring the voltage across a standard resistor in series with the thermometer. In this way, temperature intervals of 1-2 $m^{o}K.$ could be detected, the absolute accuracy of the calibration given by Cryocal being about 5 $m^{o}K.$, though better differentially.

3 Microwave Apparatus

The measurements of surface impedance were made using the by now classical design of Pippard resonator, comprising a coaxial cavity of which the central conductor is a half-wavelength crystal of niobium about 1 mm. diameter supported at it s centre by thin polythene spacers attached with distrene cement to a light silica frame capable of vertical movement to vary the coupling. The outer cylindrical can was of H.C. copper, and of 15 mm. internal diameter, and about 12Cm. total length; this provides about 45 dB of cut-off attenuation between the ends of the specimen and the ends of the resonator at 10 Gc/s. Power was coupled onto the ends of the specimen via the electric probes shewn (fig. 8).

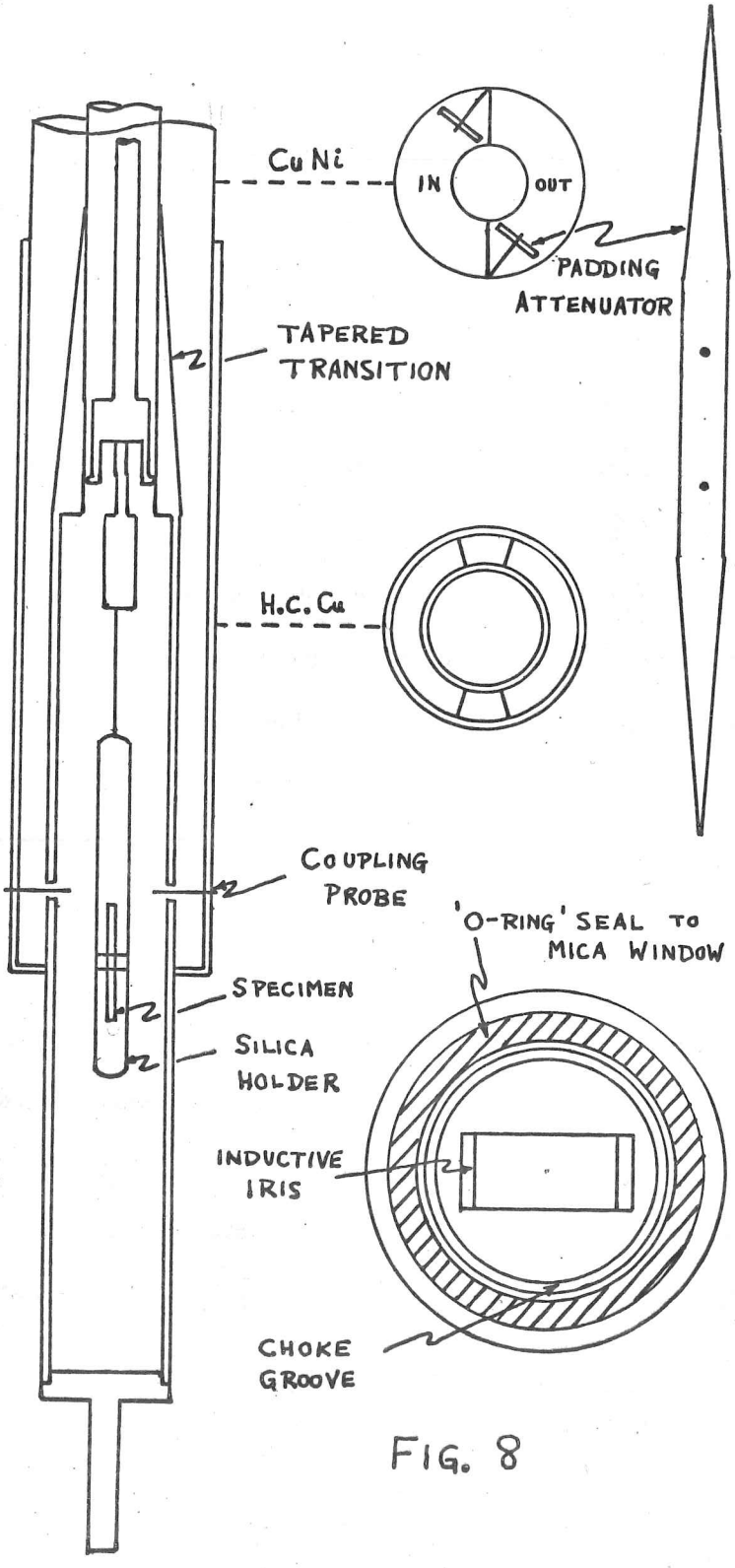
Cu Ni
IN
OUT
PADDING ATTENUATOR
TAPERED TRANSITION
H.C. Cu
COUPLING PROBE
'O-RING' SEAL TO MICA WINDOW
SPECIMEN
SILICA HOLDER
INDUCTIVE IRIS
CHOKE GROOVE

FIG. 8

In view of the necessity to take the input and output waveguides down the cylindrical tail of the cryostat into the narrow bore of the electromagnet, a rather unusual design of waveguide was adopted, having a septate cross-section (fig. 8) and capable of supporting evacuation despite its cryogenically necessary thin walls; with the dimensions shewn, this has a cut-off wavelength of 5.24 cm. in the H_{11} mode (Marcuvitz - Waveguide Handbook M.I.T. series - McGraw-Hill 1951 p. 79) and 2.76 cm. in the H_{21} (the next highest) so that only the lowest mode propagates. The waveguide was constructed from copper-nickel sheet and tubing and was soft-soldered together along most of its length except at the bottom near the resonator, where hard-solder was used to avoid the flux-trapping properties of superconducting solders. At its lower end, the waveguide was hard-soldered into an H.C. copper tapered transition constructed integrally with the resonator and necessitated by the fact that the resonator diameter for convenience of the coupling arrangements had to be made rather larger than that of the inner tube of the waveguide. As a consequence of the narrower gap thus produced

around the resonator, the thin fins of the septate waveguide were gradually widened into wedges as shewn in (fig. 8) to maintain the cut-off wavelength at 5.24 cm. and prevent the propagation of the H_{21} mode which could otherwise have occurred. The length of the tapered region was made equal to the guide-wavelength of 3.66 cm. at 10 Gc/s. to minimise reflexions.

At the top of the waveguide a further tapered transition to conventional rectangular X-band waveguide was constructed, with E-plane bends to bring the guides horizontal. Pressure sealing of the guides to enable their evacuation was achieved using 5 thou' thick discs of mica seating against an O-ring in a choke-flange at the end of each bend. This produced a V.S.W.R. of only about 1.1, but it was thought worthwhile to tune out the reflection with small inductive windows of thickness 0.6 mm and width 2.1 mm inserted immediately next to the mica sheet. (fig. 8).

It was thought desirable to measure the impedance of the finished waveguide to check on the importance of the reflections occurring at the tapered transitions, and at any other non-uniformities along its length. For this purpose, a choke-plunger

was constructed to slide in the section of the guide around the resonator, and the method of measurement for lossless 2-port networks described by Sucher and Fox - (Handbook of Microwave Measurements 3rd edition vol. 1 p. 254. Polytechnic Press, New York 1963) was used to obtain the value of 1.17 for the V.S.W.R. on matched load, which was considered reasonable in view of the complexity of the transitions.

The final item in the construction of the waveguide was the insertion of padding atten uators as close to the resonator as possible to minimise the effect of the reflexions in the guide. Some difficulty was had in finding attenuators suitable for use at low temperatures in regard to both temperature variation and thermal cycling. However, some precision metallised glass attenuators kindly provided by Decca Radar Ltd. proved satisfactory. These were ground to size with a 1 wavelength taper on each end (fig 8) , and each supported on 2 thin brass pins separated by $\frac{1}{2}$ wavelength, and inserted in the waveguide about 4cm. above the top of theresonator producing about 15 dB. of attenuation in both sides; unfortunately there was insufficient room to place them in the section of guide around the resonator, so that there was inevitably a reflexion

at the lower transition which might pull the resonator - however its frequency-dependence was estimated to be negligible (Appendix A).

The waveguide was then inserted into the cryostat, and soldered through the base of the helium can using a special bush fixed to the outside of the guide. The upper end emerged through the pumping-tube with a collar sliding in a well-greased O-ring seal to accommodate thermal contractions.

Microwave power was provided by an air-cooled E.M.I. 80 mW. plug-in klystron type R9696 with external cavity type 25182 and micrometer tuning, and feeding through a padding attenuator of 15dB (fig 8). Sensitive tuning of the klystron was achieved electronically using a simple potentiometer system, the electronic tuning rate in the $4^3/4$ mode being about 0.5 Mc/s V^{-1}. (fig. 9) and the resistance box setting having 1kc./s. at its smallest step. This apparently crude lash-up of power supplies was capable, at a given potentiometer setting, of a stability of about 1 - 2 kc/s. min^{-1}. and seemed more satisfactory in practice than the use of commercial stabilised klystron supplies.

KLYSTRON TUNING ARRANGEMENT

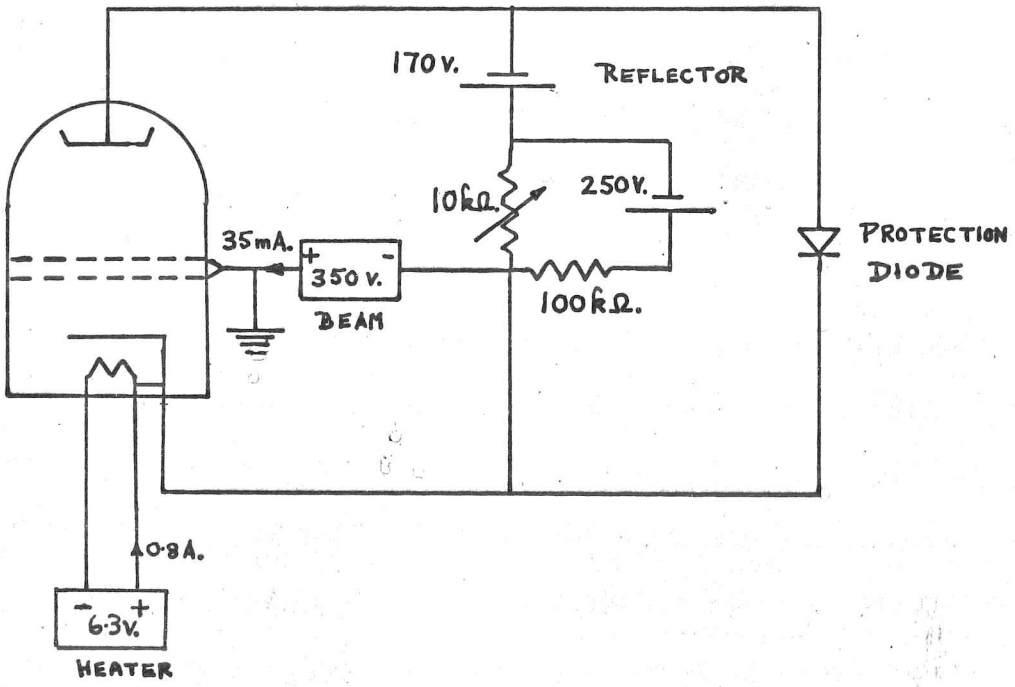

FIG. 9

The microwave signal was measured using a Sivers tunable 3-stub crystal detector feeding directly into a sensitive galvanometer, and operating at the μW. level where its response is accurately square law. Prior to each run, and particularly for the frequency-shift measurements, the detector was accurately tuned at the specimen freqency using a standing wave detector to V.S.W.R. better than 1.05; the detector had then a bandwidth of several tens of Mc/s., and the frequency dependence of its response never proved a difficulty in comparison with that of the klystron.

For each run, the electronic tuning of the klystron was calibrated absolutely against the microwave interferometer described by Pippard (J. Sci. Inst. 26 no. 9, 296 - 298) in 1 Mc/s steps for the measurements of bandwidth at nitrogen temperaturs, and in 100or 200kc/s. steps for the low temperature measurements. A typical tuning characteristic is shewn in Fig. 10 ; also, measurements of the output power of the klystron as a function of tuning were made in the case of the nitrogen bandwidth, since this is becoming comparable with the electronic tuning range of the klystron, and it was felt desirable to correct the measured bandwidth for this effect. The absolute

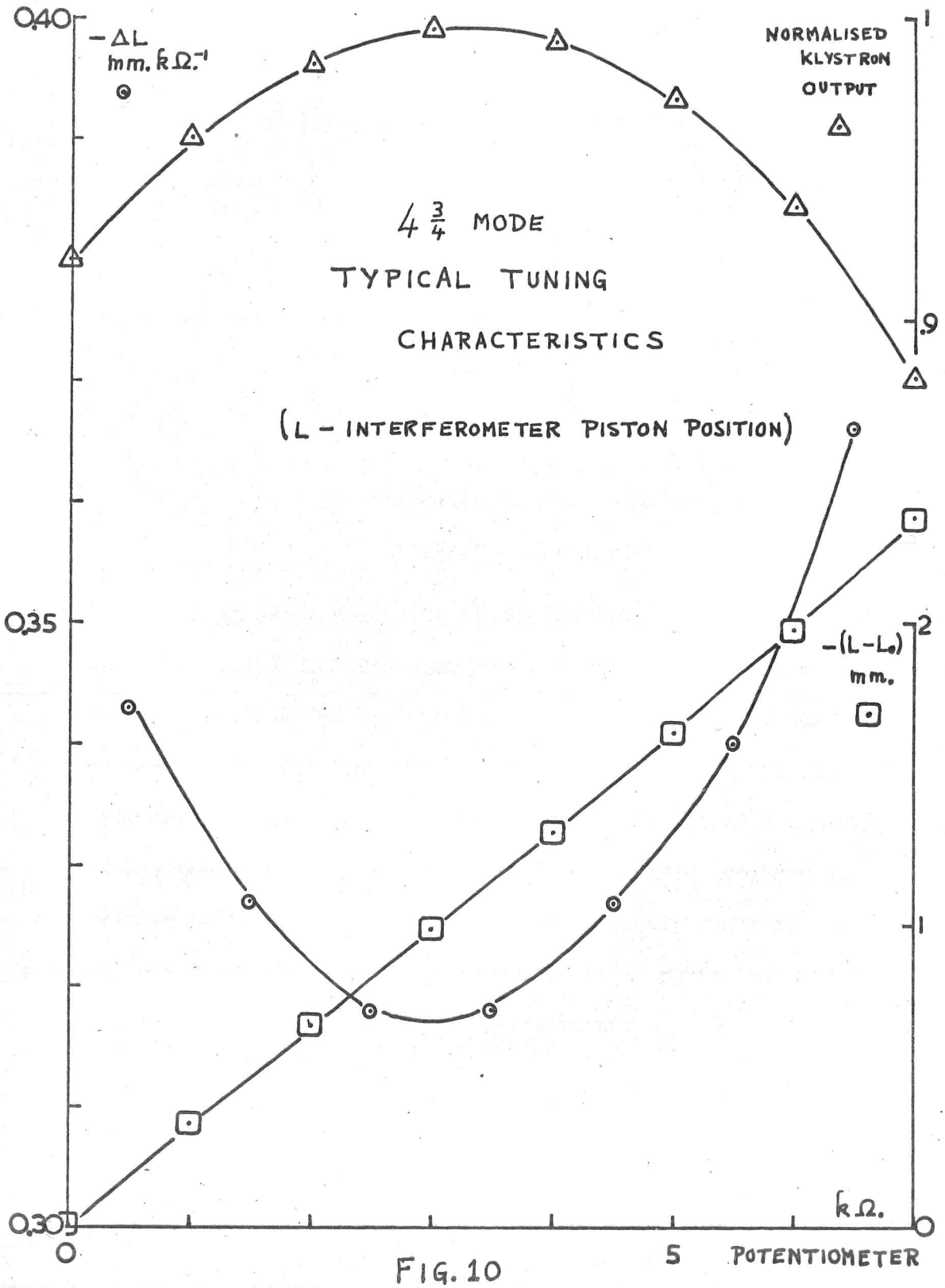
0.40
$-\Delta L$
mm. kΩ.$^{-1}$
NORMALISED
KLYSTRON
OUTPUT
1
.9
$4\frac{3}{4}$ MODE
TYPICAL TUNING
CHARACTERISTICS
(L - INTERFEROMETER PISTON POSITION)
0.35
$-(L-L_0)$
mm.
2
1
kΩ.
0.30
0
5
POTENTIOMETER

FIG. 10

calibration was then calculated from the formula:

$$\frac{d\nu}{dL} = -\frac{2.809}{\left(\frac{n}{100}\right)\left(\frac{\lambda_g/2}{20\text{ mm.}}\right)^3\left(\frac{\nu}{10\text{ Gc/s.}}\right)} \quad \text{Mc./s. mm.}^{-1} \text{ shift of piston}$$

$$= -3.2 \text{ Mc/s. mm.}^{-1} \text{ typically}$$

where: n = difference in length of the 2 arms of the interferometer expressed in half guide-wavelengths $\left(\frac{\lambda_g}{2}\right)$ = 110 typically

ν = absolute frequency (measured on a separate calibrated wavemeter)

The smallest shift resoluble on the micrometer-driven piston was about $0.2\frac{5}{}\mu$. corresponding to about 1.5 kc/s. Provided one accepts that the low temperature resonator constant is the same as that calculated from the measured nitrogen bandwidth where the skin depth is classical, the measurements are actually independent of any possible scaling errors in $\frac{d\nu}{dL}$ provided they are all related to the nitrogen bandwidth, and the only point of the calibration against the interferometer is to allow for the non-linearity of the tuning characteristic.

4 Microwave Measuring Procedure.

The technique used in the measurements was essentially that used by Waldram (5). The resonator constant for each specimen was determined from the measurement of nitrogen bandwidth, the experimental values being 20 - 30% higher than those calculated from the simple geometrical formula:

$$\gamma = Q_0 \delta = a \log_e \left(\frac{b}{a}\right)$$

This is believed to be due to the rather large end-correction for the resonator arising from its rather large internal diameter of 15 mm. ; typically, the specimen length was 11.6 mm. compared by $\lambda/2$ = 15.0 mm. It is difficult to make any very reliable estimate of the effect of this on the resonator constant, but an order of magnitude estimate shews that corrections in the range 20-30% are probably reasonable.

Measurements of the resonant frequency shifts were made in some cases by the application of a magnetic field to compare with the normal state, and in others by heating to just above

Tc; no significant differences in the temperature dependence of the shifts as measured by both these methods on a single specimen could be discerned, implying that the effects of thermal expansion on the resonant frequency can be ignored which would be supported by the high Debye temperatures of both niobium and copper. The advantage of temperature-switching in practice was to avoid the rather large spurious shift in klystron frequency produced by the effect of the stray field of the magnet on the klystron.

Corrections to the shifts for skewness were applied as discussed in Appendix B, and heating-corrections to the impedance as in Appendix C.

Tc; no significant differences in the temperature dependence of the shifts as measured by both these methods on a single specimen could be discerned, implying that the effects of thermal expansion on the resonant frequency can be ignored which would be supported by the high Debye temperatures of both niobium and copper. The advantage of temperature-switching in practice was to avoid the rather large spurious shift in klystron frequency produced by the effect of the stray field of the magnet on the klystron.

Corrections to the shifts for skewness were applied as discussed in Appendix B, and heating-corrections to the impedance as in Appendix C.

CHAPTER 3 - THE NORMAL STATE

We shall devote this chapter to a discussion of the measured surface resistance of niobium in the normal state, since the interpretation of the results is rather difficult, and has correspondingly made the analysis of the superconducting state somewhat uncertain.

In fig. (11) we present measurements, on specimens of various orientations and residual resistance, of surface resistance as a function of D.C. resistivity, being normalised to the value measured at nitrogen temperature; the error bar shews estimated experimental error limits. Also plotted are the parabola representing the classical skin effect:

$$\frac{R}{R_{N_2}} = \sqrt{\frac{\rho}{\rho_{N_2}}}$$

and the Reuter-Sondheimer curves for $(\rho l) = 5.0 \times 10^{-12} \Omega.\,\text{cm.}^2$

and: $3.3 \times 10^{-12} \Omega.\,\text{cm.}^2$

with diffuse surface-scattering, giving respectively: $\frac{R_\infty}{R_{N_2}} = 0.150$ and 0.130; $\delta_{1_{N_2}} \Big|_{\text{pure Nb}} = 4020$ Å. @ 10 Gc/s.

The measurements of surface resistance were obtained in the usual way from the bandwidth, the extraneous and coupling losses

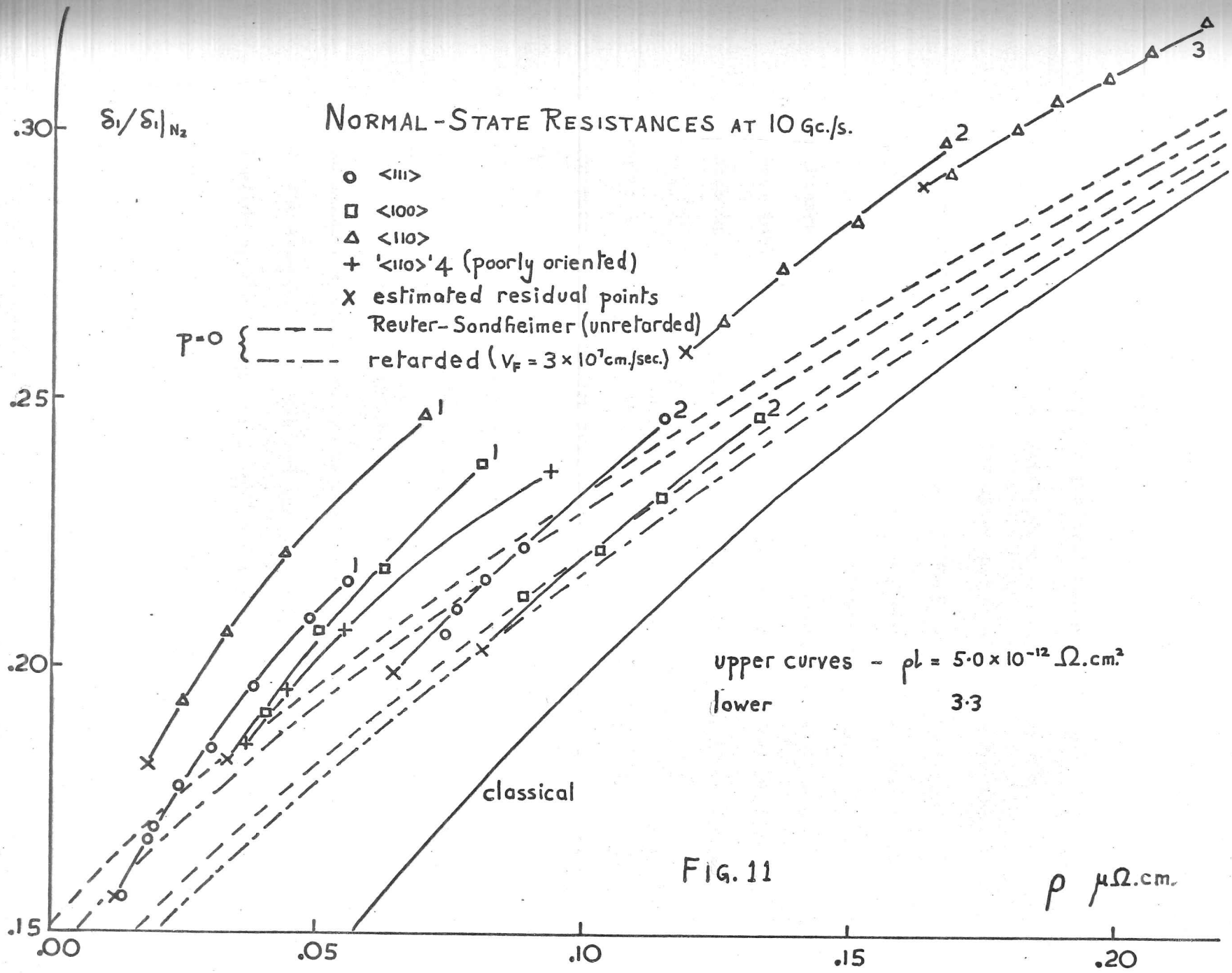
NORMAL-STATE RESISTANCES AT 10 Gc./s.
$\delta_1/\delta_1|_{N_2}$
.30
.25
.20
.15
.00
.05
.10
.15
.20
ρ μΩ.cm.
o <111>
□ <100>
△ <110>
+ '<110>'4 (poorly oriented)
X estimated residual points
p=0 { Reuter-Sondheimer (unretarded)
retarded ($V_F = 3 \times 10^7$ cm./sec.)
upper curves - $\rho l = 5{\cdot}0 \times 10^{-12}\ \Omega.cm.^2$
lower 3·3
classical
1
2
3

FIG. 11

being subtracted out using the residual bandwidth in the superconducting state; the temperature was varied from 9°K at the lower end to 20°K at the upper end of the curve for each specimen. Readings were not normally taken above 20°K. on account of the excessive boil-off of helium involved. The D.C. resistivities were those already measured for each specimen during the resistance ratio determinations in this temperature range, and we have included in fig (14) our results for the ideal resistivity of niobium as deduced from the measurements on our <111>1 specimen of resistance ratio 1180; also plotted for comparison are the results of White and Woods (Phil. Trans. 251, 273 - 302, '69) which show a rather higher resistance at low temperatures. However, in view of the fact that their purest specimen had a residual resistance ratio of only about 30, we may feel some confidence that our results are rather more reliable.

At any rate, to return to fig. (11), we see that there is by no means a good fit to the Reuter-Sondheimer theory. We see that, for example, the curve for the specimen <111>1 shows no indication as the temperature, and therefore ρ, is raised, of joining onto the curve for <111>2 ; and, indeed, there appears

to be a marked tendency for all the curves to be ascending with too large a slope to fit even the classical curve very well if one were to allow horizontal or vertical scalings or shifts as possible errors in the observations. There also seems to be some suggestion that the lower end of each curve, where the scattering is residual, falls fairly near to a reasonable Reuter-Sondheimer curve. In view of these peculiarities, measurements were made over a much wider temperature range up to 77°K. on specimen <111>1 , the results of which are shewn in fig. (12) where it may be seen that the rather large deviation from the classical curve persists even up to a temperature of around 40°K, when classical behaviour seems to prevail. Also plotted are some results for specimen <111>3 , which had R.R.R. = 15.38 and a bandwidth at T_c of about 1400 kc/s., obtained in the range 9 - 20°K. They are seen to fit the classical curve remarkably well, but are just beyond the region of interest.

In order to test for the possibility of systematic errors in the observations, it was thought desirable to make measurements with the existing apparatus on some other metal of known behaviour, and for this purpose a polycrystalline specimen of lead of resistance

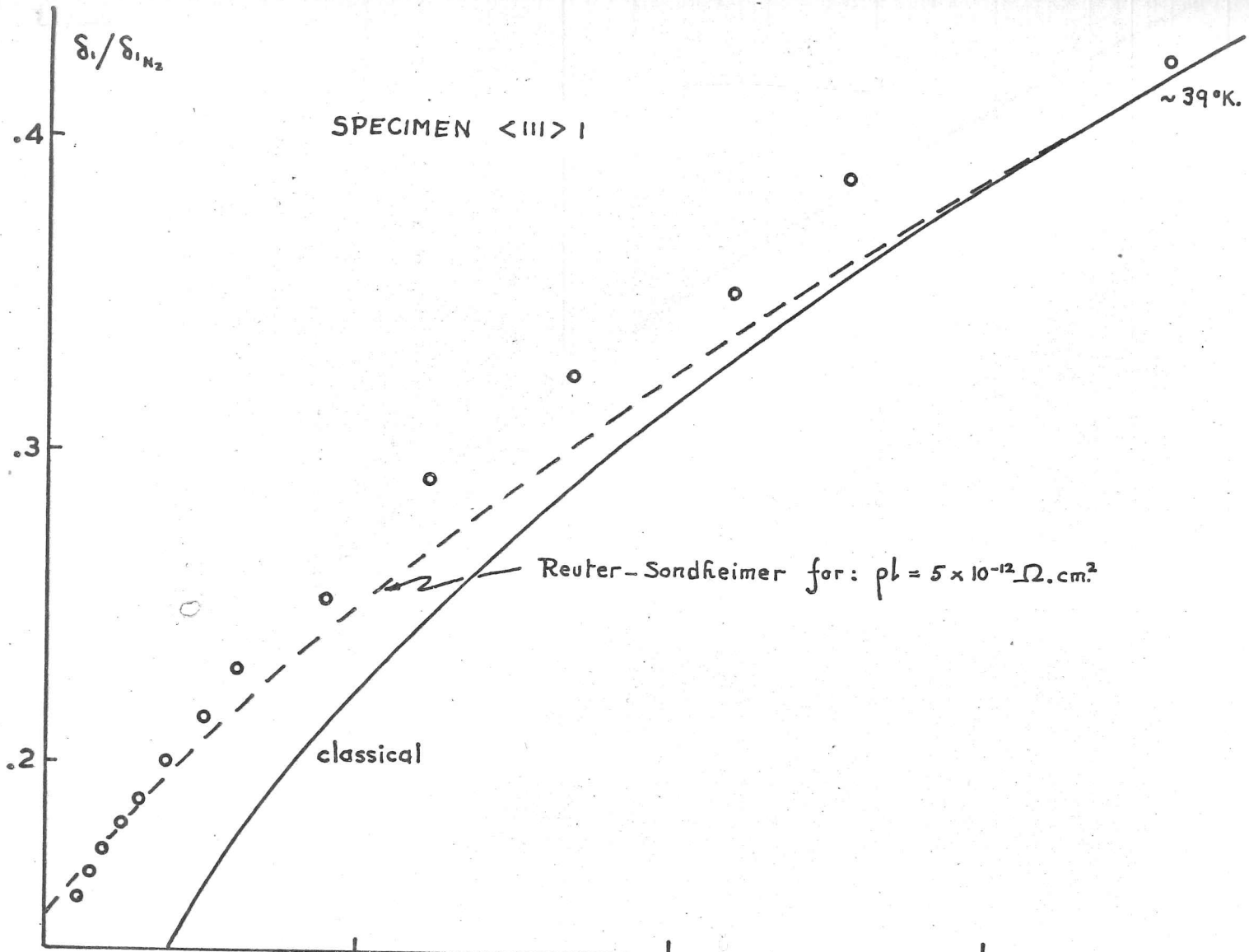
$\delta_\perp/\delta_{\perp N_2}$
SPECIMEN <111> I
~ 39°K.
.4
.3
.2
Reuter-Sondheimer for: $\rho l = 5 \times 10^{-12}\ \Omega.cm^2$
classical
.00
.05
.10
.15
ρ/ρ_{N_2}

FIG. 12(a)

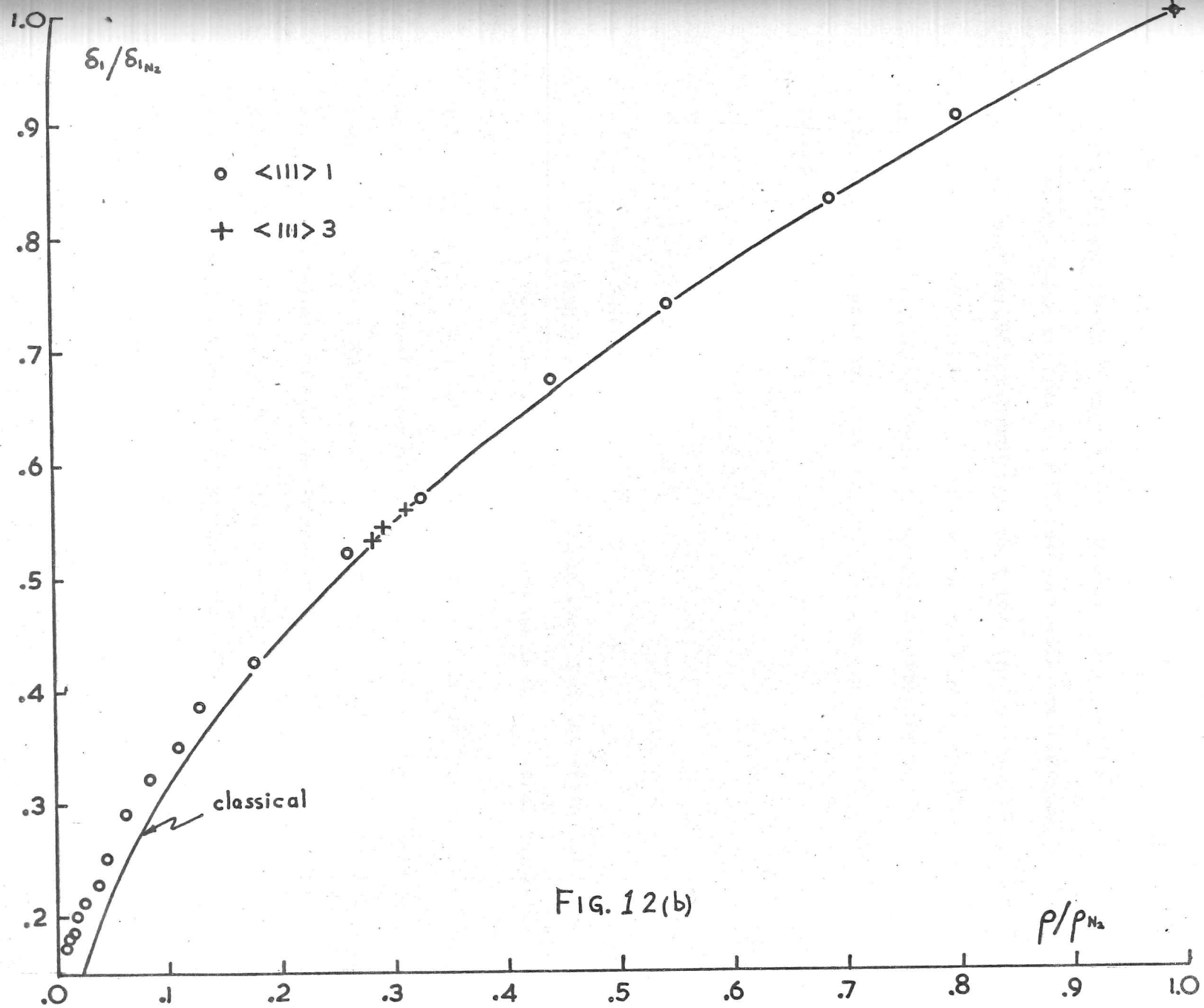
1.0
δ_1/δ_{1N_2}
.9
.8
.7
.6
.5
.4
.3
.2
o <111> 1
+ <111> 3
classical
.0
.1
.2
.3
.4
.5
.6
.7
.8
.9
1.0
ρ/ρ_{N_2}

FIG. 12(b)

ratio 3300 was kindly loaned by Dr. Waldram. The results so obtained are shewn in fig. (13), together with the classical parabola, and the Reuter-Sondheimer plot for: $(\rho l) = 10.6 \times 10^{-12} \Omega.cm.^2$ and frequency of 10Gc/s. Also plotted are Waldram's measurements at 3Gc/s. In fact, there seems to be some uncertainty in the literature regarding the value of (ρl) for lead, being variously quoted as:

	$10^{12}(\rho l)\ \Omega.cm.^2$	
(71) Chambers:	10.6	
(72) Aubrey:	8.9	
(73) Ashcroft:	7.1	-(calculated from Anderssen and Golds
(74) Hahn et al:	7.1	measurements of the Fermi surface).

These values give those of R_∞ / RN_2 indicated in the figure. It is seen that our results (which are uncorrected for the effects of retardation) give a value of R_∞ lying somewhere between Chamber's and Aubrey's values, though our points seem to tend slightly more rapidly towards the classical curve than does the Reuter-Sondheimer plot. We should perhaps add that the surface finish of the specimen was by no means as good to all appearances as that of the niobium specimens, and this may well explain why our value of R_∞ tends to agree with those of the earlier workers (Chambers and Aubrey).

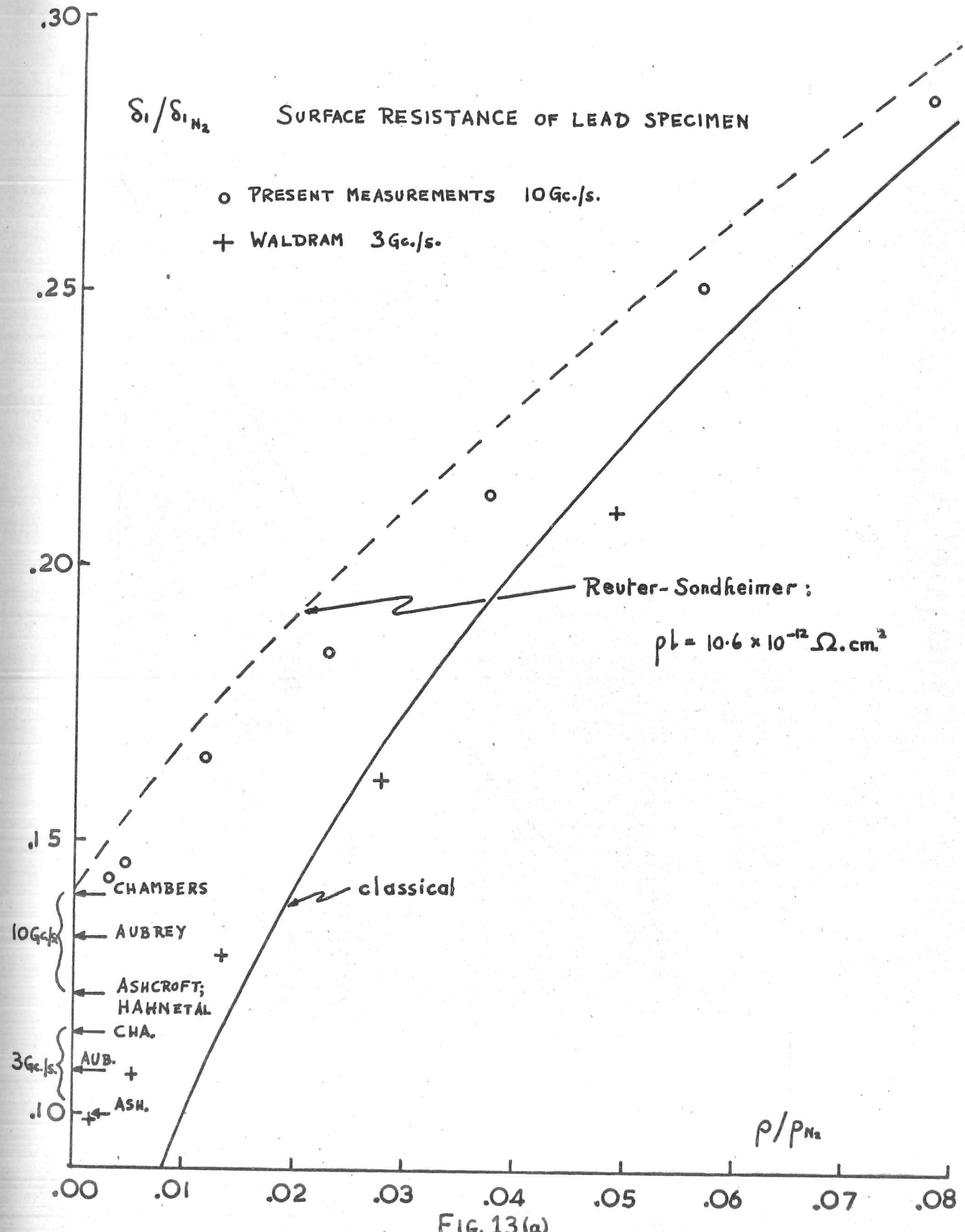
.30
.25
.20
.15
.10
$\delta_1/\delta_{1_{N_2}}$
SURFACE RESISTANCE OF LEAD SPECIMEN
o PRESENT MEASUREMENTS 10Gc./s.
+ WALDRAM 3Gc./s.
Reuter-Sondheimer :
$\rho l = 10.6 \times 10^{-12} \Omega.cm.^2$
classical
o CHAMBERS
10Gc/s
AUBREY
ASHCROFT;
HAHNETAL
3Gc./s.
CHA.
AUB.
ASH.
ρ/ρ_{N_2}
.00
.01
.02
.03
.04
.05
.06
.07
.08

FIG. 13(a)

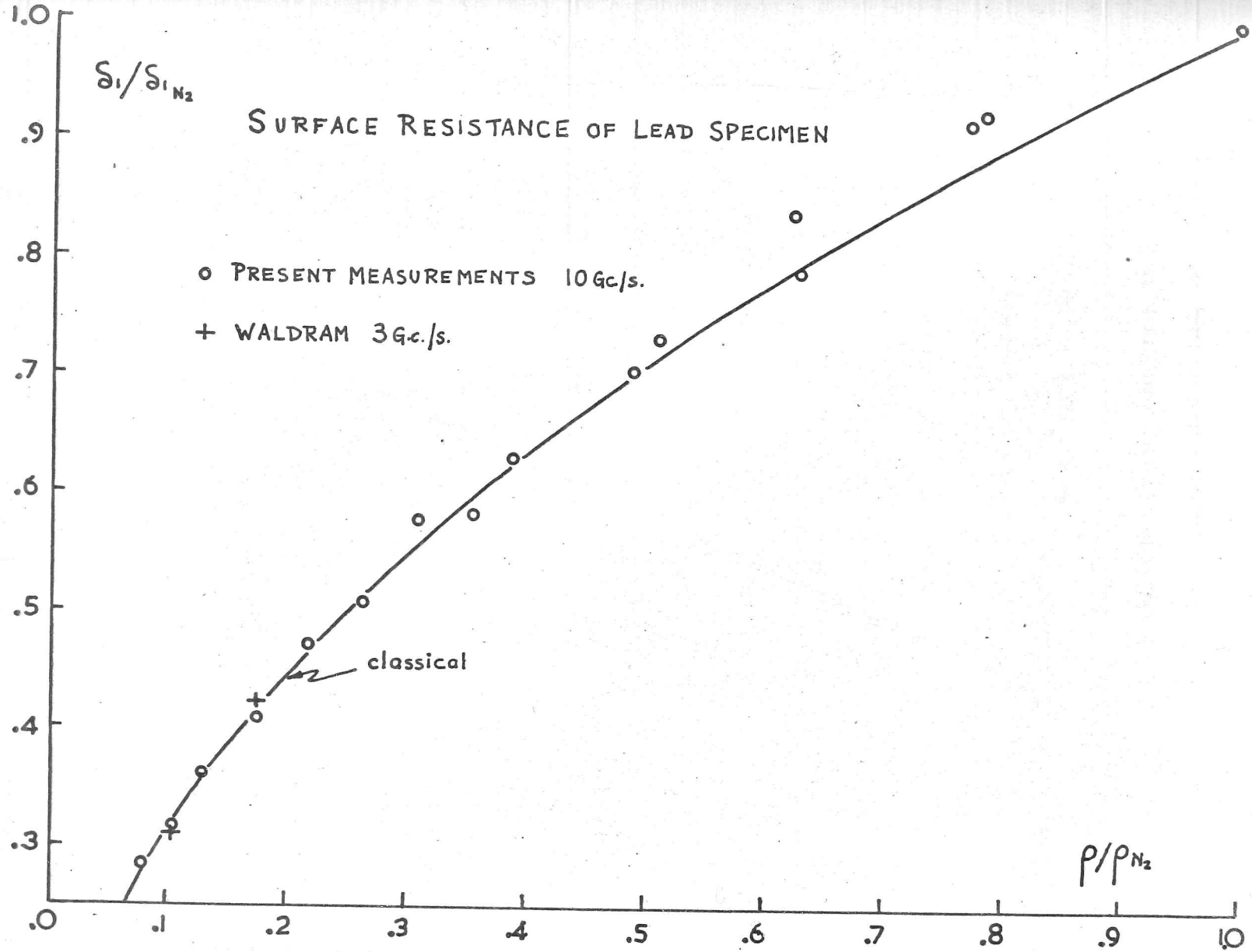
SURFACE RESISTANCE OF LEAD SPECIMEN
$\delta_1/\delta_{1_{N_2}}$
o PRESENT MEASUREMENTS 10 Gc/s.
+ WALDRAM 3 Gc./s.
classical
ρ/ρ_{N_2}
1.0
.9
.8
.7
.6
.5
.4
.3
.0
.1
.2
.3
.4
.5
.6
.7
.8
.9
1.0

FIG. 13(b).

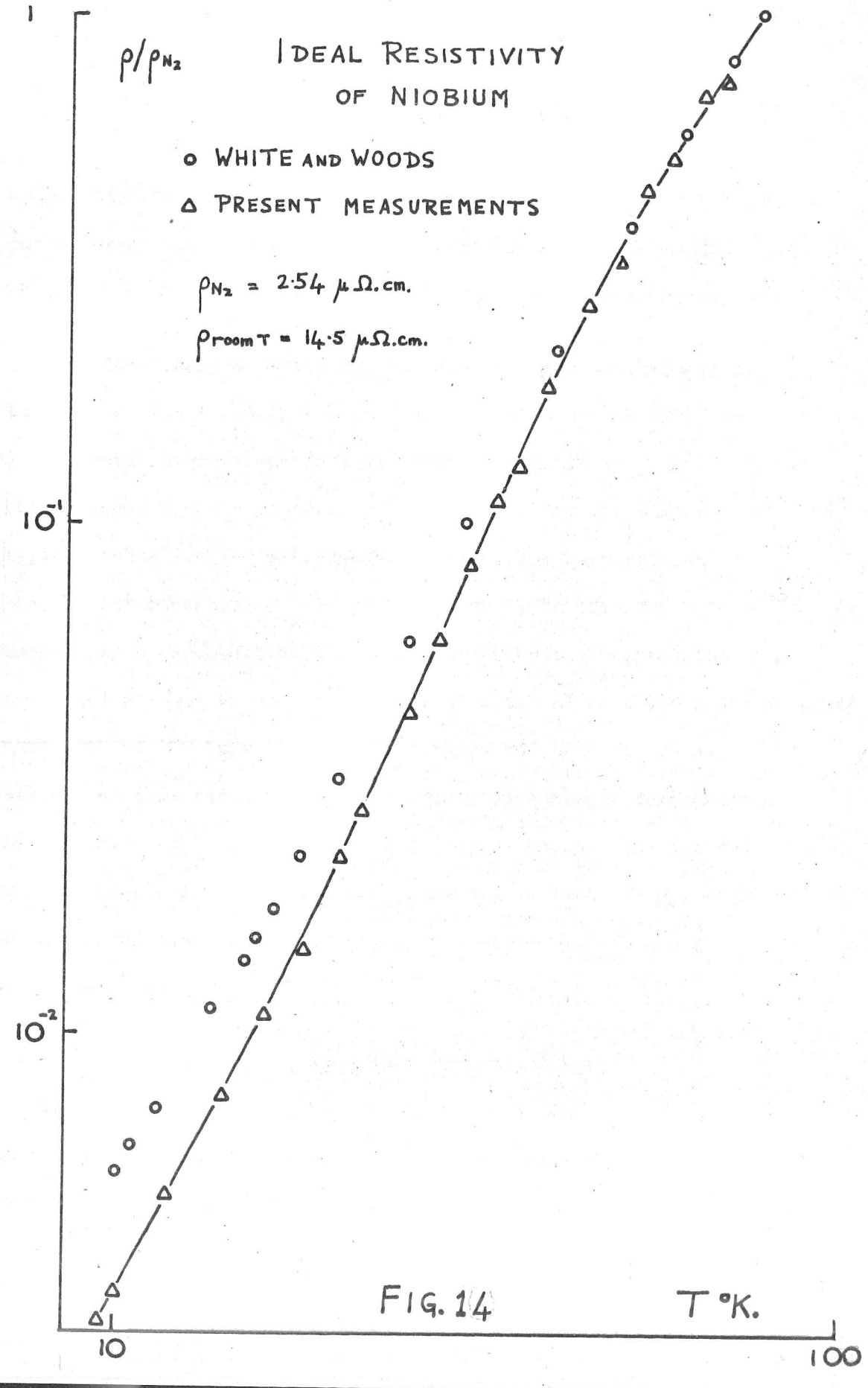
1
ρ/ρ_{N_2}
IDEAL RESISTIVITY
OF NIOBIUM
o WHITE AND WOODS
Δ PRESENT MEASUREMENTS
ρ_{N_2} = 2·54 μΩ.cm.
$\rho_{room\,T}$ = 14·5 μΩ.cm.
10^{-1}
10^{-2}
10
100
T °K.

FIG. 14

We may also observe that our deviations from the Reuter-Sondheimer curve appear much smaller if we make the more usual plot of (R_∞/R) versus $\sqrt{\rho}$ as employed by Chambers, for example.

We thus conclude that there is no very large discrepancy in the case of the measurements on lead as compared with that seen in niobium; however one fact of possible significance did emerge regarding the residual losses seen in the two cases. A typical value for the extraneous losses at low temperatures in the niobium measurements was about 100 kc/s. as compared with a normal state bandwidth at 9°K of about 500 kc/s., whereas the lead specimen had an extraneous loss of about 27 kc/s and a normal state bandwidth of 600 kc/s. (we should perhaps add that the value of extraneous loss for lead is based solely on a single measurement, and is therefore not very certain.) The extraneous loss for the niobium specimens has always been regarded as rather high, since estimates of the losses even at 77°K. yielded the following approximate values:

dielectric loss = 45 kc/s.

resonator loss = 65 kc/s.

i.e. a total of 110 kc/s. at 77°K., and it seems likely that these should decrease rather considerably at lower temperatures. Thus we

cannot exclude the possibility that there is an unexplained residual loss of about 75 kc/s. in the niobium measurements, and that this may be associated with a real surface loss even in the superconducting state. This could perhaps arise in an oxide layer on the surface, though there was certainly no visible deterioration of the surface even after long exposure to the air (in definite contrast to the lead specimen), as equally there was no change of the measured surface resistance with age of the specimen. It also seems rather unlikely that this could account for the somewhat sudden approach of the surface resistance to the classical value at around 40°K. (fig 12). However, in view of lack of information concerning the dielectric properties of the oxide of niobium it seems rather fruitless to speculate further along these lines, and we have preferred to consider that the effect seen is probably real, and to look for a more fundamental explanation.

To date, there seem to have been no measurements of the anomalous skin effect in normal niobium reported in the literature with which we might compare the present results, but we may note that observations for other transition metals have given rather curious values. For example, Fawcett and Griffiths (J. Phys. Chem. Solids 23, 1631 - 5, 1962) report the following values for total

Fermi surface area S deduced from R_∞ for polycrystalline tungsten and molybdenum:

	S	S'
W:	1.66 at u. = 5.93 Å^{-2}	14.5 Å^{-2}
Mo:	1.74 at u. = 6.21 Å^{-2}	24.8 Å^{-2}

Also shewn are the values S' from recent Fermi surface determinations (W: Girvan, Gold, and Phillips - J. Phys. Chem. Solids 29 1485, 1969. Mo: Leaver and Myers - Phil. Mag. 19, 465, 1969).

which are in good agreement with band-structure calculations. In view of the low purity of Fawcett & Griffiths' specimens (W: RRR - 19.8 ; Mo: 82), not much weight may be put on these results, except to say that they may be an indication of abnormally high surface resistances in these metals too.

It was also hoped that some information on any peculiarities in the non-local response of niobium might be gleaned from the microwave-ultra sonic work of Dobbs & Perz (Proc. Roy. Soc. A 296, 113-121, 1966, and Perz - thesis (unpublished)). Perz gives results for the (ql) - dependence of the normal longitinal attenuation in single crystals of various orientation as shewn in fig (15), on

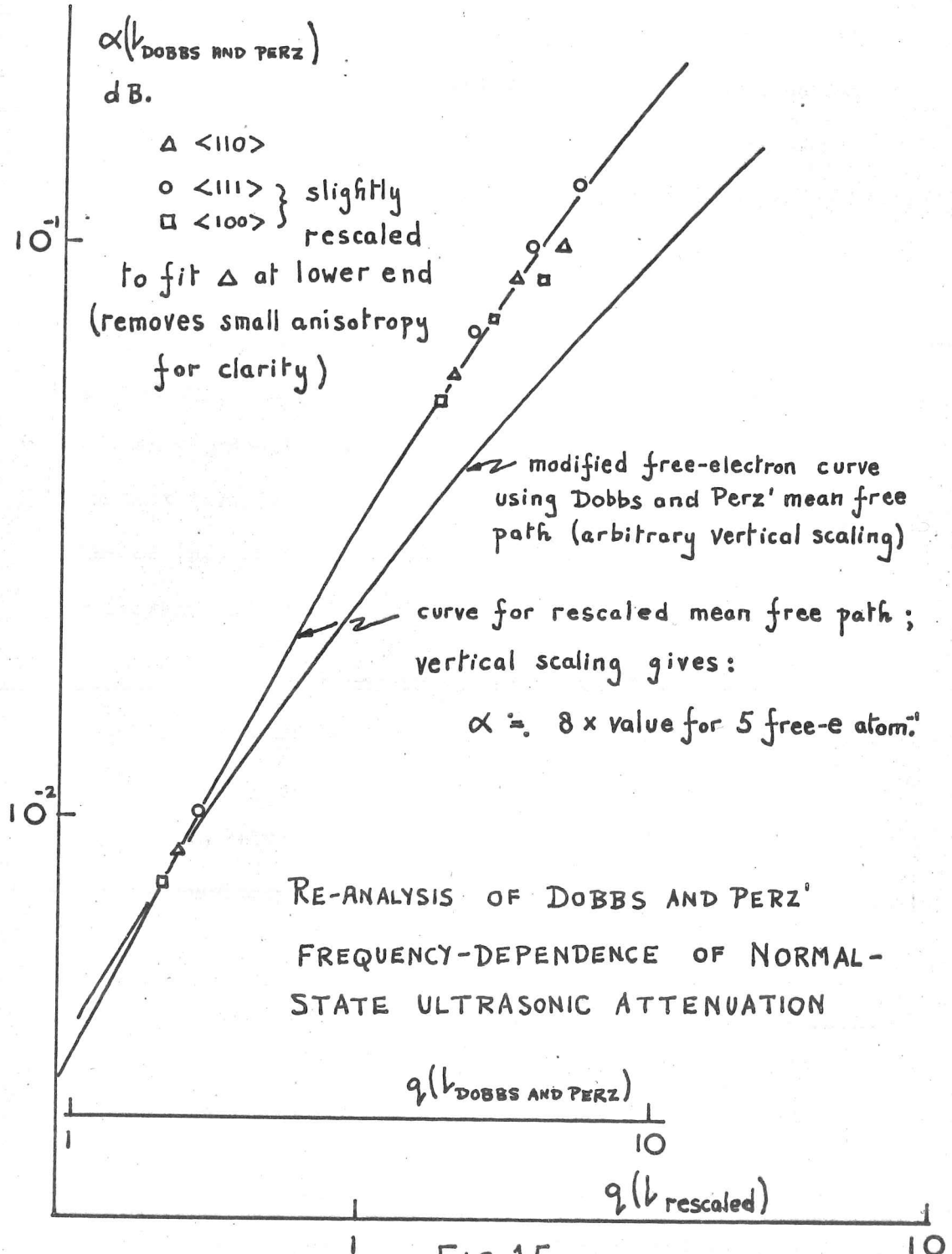
α(l DOBBS AND PERZ)
dB.
△ <110>
○ <111>
□ <100>
} slightly rescaled to fit △ at lower end (removes small anisotropy for clarity)
10^-1
10^-2
modified free-electron curve using Dobbs and Perz' mean free path (arbitrary vertical scaling)
curve for rescaled mean free path; vertical scaling gives:
α ≐ 8 x value for 5 free-e atom.
RE-ANALYSIS OF DOBBS AND PERZ' FREQUENCY-DEPENDENCE OF NORMAL-STATE ULTRASONIC ATTENUATION
q(l DOBBS AND PERZ)
1
10
q(l rescaled)
1
10

FIG. 15

which is also plotted the modified free-electron attenuation as given by Pippard (Rep. Progr. Phys. 23, 176):

$$\alpha \sim \frac{(ql)^2 \tan^{-1}(ql)}{3(ql - \tan^{-1}(ql))} - 1$$

It will be seen that the fit is very poor, and can be significantly improved by scaling down their values of (ql) by a factor of about 3.05, as represented by the second curve of fig. (15). It would seem that this discrepancy can be traced to their use of an improbable value of (pl) in calculating their mean free paths. Perz quotes the formula used as:

$$l = (0.0120 \times \text{resistance ratio})\ \mu.$$

and using the value he took for the room-temperature resistivity: $\rho = 13.9\ \mu\Omega.\text{cm.}$ gives a value of : $(pl) = 16.7 \times 10^{-12}\ \Omega\ \text{cm.}^2$
The rescaled value is: $(pl) = 5.45 \times 10^{-12}\ \Omega\ .\ \text{cm.}^2$
which is considerably closer to later, more conventional estimates:

$10^{12}(pl)\ \Omega\ \text{cm.}^2$	Source
3.27	Fischer (private communication)
3.7	Goodman & Kuhn (Journal de Physique 29, no. 2-3, 240, (1967))
3.75	French (Cryogenics 8, 301, (1968))
4.98	Maxfield and McLean (Phys. Rev. 139, A1515, (1965))
approx. 5.2	Tsuda & Suzuki (J. Phys. Chem. Solids 28, 2487)

and to values which would fit the present results at the residual scattering points. These estimates are all based on the sort of calculation of Faber and Pippard (Proc. Roy. Soc. A231, 336 (1955)) for a spherical Fermi surface, the area S of which is estimated from the electronic specific heat via:

$$\gamma = \frac{k_B^2 S \langle v_F^{-1} \rangle}{12 \pi \hbar}$$

an average Fermi-velocity being estimated from the B.C.S. expression for the coherence length:

$$\xi_0 = \frac{\hbar v_F}{\pi \epsilon_0(0)}$$

Then (pl) is given by: $(pl) = \frac{12 \pi^3 \hbar}{e^2 S} = \frac{\Lambda(0)}{\cancel{v_F}} \times v_F$

For example, Fischer obtains his value from:

$\gamma = 7.8$ mJ. mole^{-1}. °K.$^{-1}$, $\xi_0 = 430$ Å, $\epsilon_0(0) = 1.91 k_B T_c$, $T_c = 9.25$ °K.

At any rate, this error in Dobbs and Perz's calculated mean free paths implies that the maximum value of (ql) which they used was in fact only about 2.4 instead of 7.3 as they believed, or even less if one takes a slightly more realistic value of (pl) than the rescaling of their results would imply, and may go a considerable way to explaining why their apparent gap anisotropy in niobium was noticeably less than that measured by others (e.g. MacVicar and Rose - J. Appl. Phys. 39 1721 - 1727, 1968). Their slip seems traceable to the paper of Stromberg and Swenson (Phys. Rev. Lett. 9, 370) which quotes a figure for the effective number

of free electrons cm^{-3} in niobium as:

$$n = 1.72 \times 10^{23} \text{ cm.}^{-3}$$

(which gives rise to the reasonable value of $(pl) = 4.08 \times 10^{-12} \Omega.cm^2$), but is incorrectly stated to be equivalent to 18% of the density for 5 free electrons per atom.

At any rate, from the point of view of useful comparison with the present results for niobium, the value of Dobbs and Perz's data on the normal state is considerably diminished by the error in the values of (ql).

DISCUSSION OF NORMAL-STATE RESISTANCE

We shall consider 3 possible mechanisms which may have some bearing on the failure of the results given to fit the Reuter-Sondheimer theory, though we must emphasize at the outset that we shall find it difficult to come to any very positive conclusions regarding the discrepancy.

1: bulk scattering anisotropy

2: surface scattering

3: Fermi surface anisotropy

1 BULK-SCATTERING ANISOTROPY:

We observe from fig. (12) that the discrepancy persists for the $\langle 111 \rangle$ specimen up to about 40°K. where: $\rho/\rho_{N2} \sim 0.2$; assuming $(pl) \sim 5 \times 10^{-12} \Omega.cm^2$ gives a value of: $(ql) \sim \left(\frac{l}{\delta}\right) \sim 1$ at this point, so that it may be that the penetrating electric field within the skin depth δ is sampling some non-local peculiarity of the scattering within the bulk. In particular, we should like to see if there is any mechanism by which a certain ideal D.C. resistivity due to scattering off phonons is not equivalent, from the point of view of absorption of a microwave photon, to residual impurity scattering, which is presumably isotropic for point defects though may not be so for dislocations.

The Reuter-Sondheimer theory of the anomalous skin effect assumes that the scattering of the electrons is elastic and isotropic, but we know that in simple metals at low temperatures the ideal resistance contains a T^5 term due to small angle phonon scattering; in transition metals, the variation is nearer to T^3 ($T^{2.75}$ from our own results for niobium) and this is usually interpreted as arising from s-d scattering. The d-band is considered

to be much narrower in energy than the s-band, having a higher density of states and lower Fermi velocity as a consequence, and thus acting as a velocity sink for the s-band conduction electrons; in this case, s-d scattering arising from collision with a phonon is regarded as isotropic, giving rise to a T^3 variation. However, it is rather unlikely that this scattering is completely effective in destroying the current, and a more realistic model is probably scattering through a fairly wide angle whilst nevertheless being still weighted in the forward direction. Under such circumstances, it may be possible that an effect of the sort seen by Gantmakher and Sharvin (in J.E.T.P. 21, 720 (1965)) in the tilted-field cyclotron resonance in tin can occur, where the effective mean free path for scattering off the effective zone differs from the measured D.C. mean free path.† (also see footnote at end of chapter).

Suppose we consider a metal with a spherical Fermi surface (fig. 16), and its response σ_q to a transverse electric field $E e^{iqz}$, since any shape of field penetration can always be Fourier analyzed. Then assuming that the disturbance of the Fermi distribution is $N(\theta, \phi)$, the Boltzmann equation for the response may be written:

$$\int P_{\underline{k}\underline{k}'} \left[N(\theta,\phi) - N(\theta',\phi') \right] d\Omega' = \frac{e\, \underline{E}\cdot\underline{v}}{4\pi^3 \hbar v} - i\underline{q}\cdot\underline{v}\, N$$

$$= \frac{eE}{4\pi^3 \hbar} \sin\theta \cos\phi - i q v_F \cos\theta \, N$$

to be much narrower in energy than the s-band, having a higher density of states and lower Fermi velocity as a consequence, and thus acting as a velocity sink for the s-band conduction electrons; in this case, s-d scattering arising from collision with a phonon is regarded as isotropic, giving rise to a T^3 variation. However, it is rather unlikely that this scattering is completely effective in destroying the current, and a more realistic model is probably scattering through a fairly wide angle whilst nevertheless being still weighted in the forward direction. Under such circumstances, it may be possible that an effect of the sort seen by Gantmakher and Sharvin (in J.E.T.P. 21, 720 (1965)) in the tilted-field cyclotron resonance in tin can occur, where the effective mean free path for scattering off the effective zone differs from the measured D.C. mean free path.† (also see footnote at end of chapter).

Suppose we consider a metal with a spherical Fermi surface (fig. 16), and its response σ_q to a transverse electric field $E\,e^{iqz}$, since any shape of field penetration can always be Fourier analyzed. Then assuming that the disturbance of the Fermi distribution is $N(\theta, \phi)$, the Boltzmann equation for the response may be written:

$$\int P_{\underline{k}\underline{k}'} \left[N(\theta,\phi) - N(\theta',\phi') \right] d\Omega' = \frac{e\,\underline{E}\cdot\underline{v}}{4\pi^3 \hbar v} - i\underline{q}\cdot\underline{v}\,N$$

$$= \frac{eE}{4\pi^3\hbar} \sin\theta \cos\phi - iq v_F \cos\theta\, N$$

SPHERICAL FERMI SURFACE

SCATTERING GEOMETRY

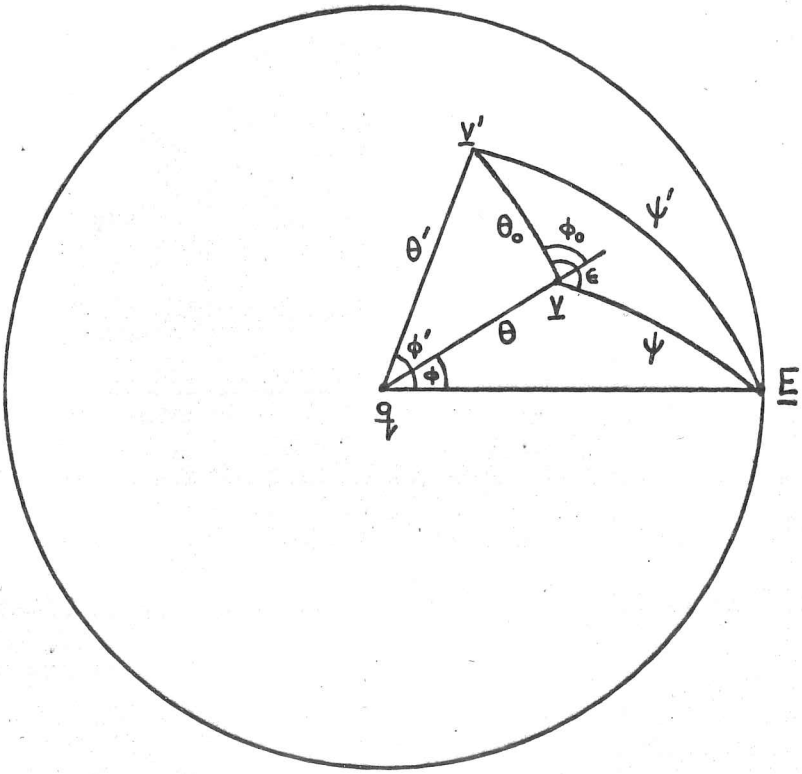

FIG. 16

where: $P_{\underline{k}\underline{k}'} = P_{\underline{k}'\underline{k}}$ is the scattering probability between states $\underline{k}, \underline{k}'$. We shall take this probability to depend only on the angle θ_o between $\underline{k}, \underline{k}'$: $P_{\underline{k}\underline{k}'} = P(\theta_o)$, and we can then effect a convenient transformation of variables by setting:

$$N = \frac{eE\,l_\infty}{4\pi^3 \hbar v_F} \frac{\cos\phi}{\sin\theta} F(x)$$

where : $\begin{cases} l_\infty^{-1} = \int P(\theta_o)\, d\Omega_o \\ x = \cos\theta \end{cases}$; $d\Omega_o = 2\pi \sin\theta_o\, d\theta_o$

l_∞ may be regarded as the mean free path which would exist if the total integrated scattering were isotropic, and we shall see that it is the relevant mean free path in the limit $(ql) \longrightarrow \infty$
At any rate, it is easily shewn now that the Boltzmann equation may be rewritten:

$$(1 + i\alpha_\infty x)\, F(x) = (1-x^2) + l_\infty \frac{\sqrt{1-x^2}}{\cos\phi} \int_{-1}^{+1} \frac{F(x')}{\sqrt{1-x'^2}}\, dx' \int_0^{2\pi} P(\theta_o)\, \cos\phi'\, d\phi' \qquad (A)$$

where θ_o is given by: $\sin\theta_o = \frac{\sin\theta'}{\sin\phi_o} \sin\delta$; $\delta = (\phi' - \phi)$; $\alpha_\infty = q l_\infty$
We note that at constant θ' and x', θ_o is even in δ , since both δ and ϕ_o are odd in δ . In view of this fact, it is

convenient to express the integral over ϕ' as:

$$\int_{-\pi}^{+\pi} P(\theta_o)\ \cos.(\delta+\phi)\, d\delta = \cos.\phi \int_{-\pi}^{+\pi} P(\theta_o)\cos.\delta\, d\delta - \sin.\phi \int_{-\pi}^{+\pi} P(\theta_o)\sin.\delta\, d\delta$$

The last integral vanishes for the symmetry reason that θ_o, and thus P, is even in δ, leaving:

$$(1+i\alpha_\infty x)\, F(x) = (1-x^2) + l_\infty \sqrt{1-x^2} \int_{-1}^{+1} \frac{F(x')dx'}{\sqrt{1-x'^2}} \int_0^{2\pi} P(\theta_o)\cos.\delta\, d\delta \qquad (B)$$

We see that, as expected, the back-scattering integral vanishes for isotropic scattering, leaving us with:

$$F(x) = \frac{1-x^2}{1+i\alpha_\infty x}$$

which is the usual Reuter-Sondheimer result for a mean free path l_∞; in fact, this result is always true for $(ql) \gg \theta_s$, where θ_s is the scattering angle representing the structure in $P(\theta_o)$ (fig. 17); since for a narrow enough effective zone, the scattering integral, which represents persistence of velocity in the electron gas, is negligibly small. This is of course not the case for truly infinitesimal scattering angles considered by Pippard (Proc. Roy. Soc. A305, 291-318 (1968)).

In the D.C. limit $\alpha = o$, the appropriate transport mean free path is no longer l_∞, and it is easiest to return to equation (A) in this limit, and transform the integral to one over θ_o, (fig. 16).

Noting that: $\cos\psi' = \sin\theta'\cos\phi' = \cos\psi\cos\theta_0 + \sin\psi\sin\theta_0\cos\epsilon$

and writing: $F(x) = k(1-x^2) = k\sin^2\theta$ the scattering integral becomes:

$$kL_\infty \frac{\sin\theta}{\cos\phi}\int_0^\pi P(\theta_0)\sin\theta_0\,d\theta_0\int_0^{2\pi}(\cos\psi\cos\theta_0 + \sin\psi\sin\theta_0\cos\epsilon)\,d\epsilon$$

$$= kL_\infty(1-x^2)\int P(\theta_0)\cos\theta_0\,d\Omega_0$$

Thus: $$k = \left(1 - L_\infty\int P(\theta_0)\cos\theta_0\,d\Omega_0\right)^{-1}$$

and: $$F(x) = \frac{L_0}{L_\infty}(1-x^2)$$

or: $$N = \frac{eEL_0}{4\pi^3\hbar v_F}\sin\theta\cos\phi$$

where: $$L_0^{-1} = \int P(\theta_0)(1-\cos\theta_0)\,d\Omega_0$$

This well-known result for the D.C. mean free path L_0 demonstrates directly the effect of velocity-persistence inherent in the scattering integral.

Returning to form (B) of the Boltzmann equation, there are some simple solutions possible in the following cases (fig. 17)

1. small angle scattering: $P \sim \frac{\delta(\theta_0)}{\sin\theta_0}$

2. wide angle scattering: $P(\theta_0) = P(1+\beta\cos\theta_0)$

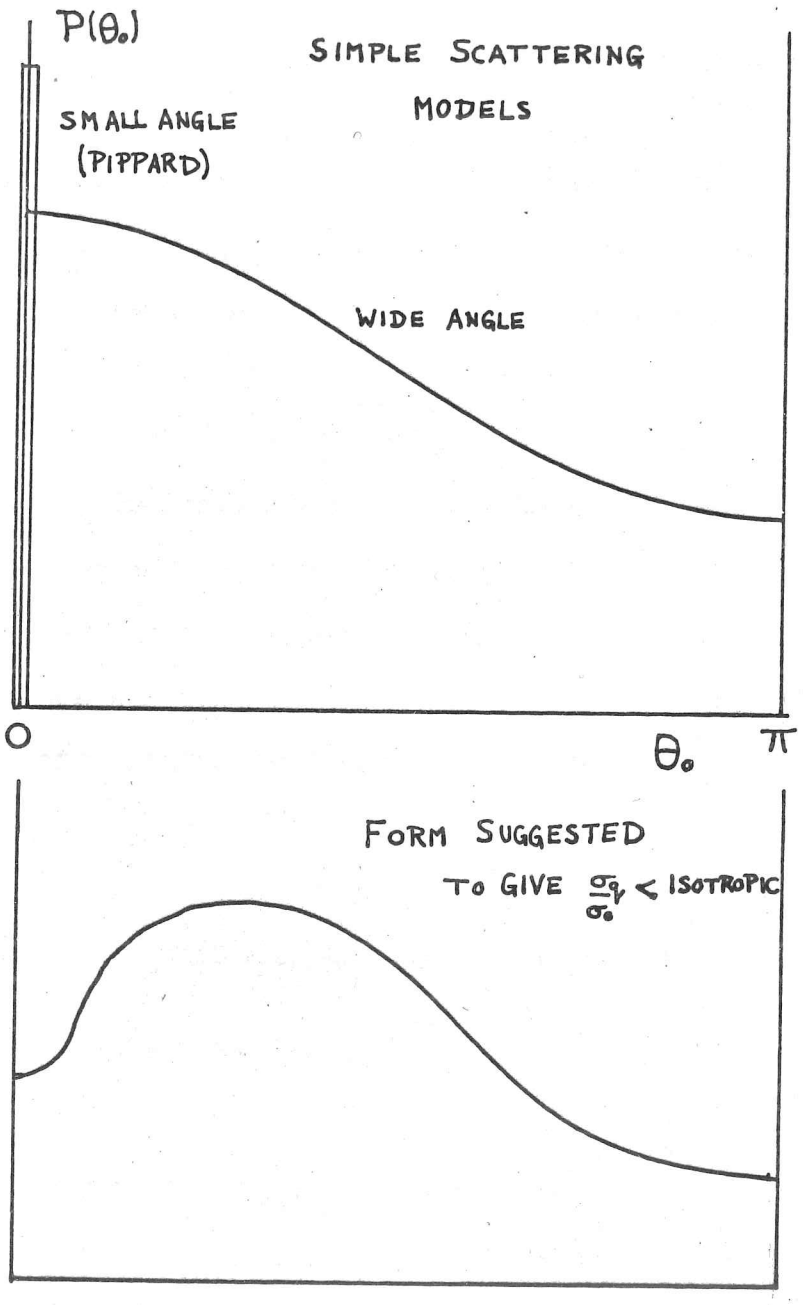
P(θ₀)
SIMPLE SCATTERING
MODELS
SMALL ANGLE
(PIPPARD)
WIDE ANGLE
0
θ₀
π
FORM SUGGESTED
TO GIVE σq/σ₀ < ISOTROPIC

FIG. 17

Case 1. has been considered by Pippard, and it is easy to show that:

$$\frac{l_\infty}{l_0} = \frac{\theta_s^2}{2}$$

which represents diffusive motion with a total m.f.p. l_∞ and diffusion constant given by $l_0 \cdot l_\infty$ is allowed to tend to zero as θ_s^2, and by expanding F(x') as a Taylor series, it can be shown that:

$$F'' + 2 - \frac{2i\alpha_0 x}{1-x^2} F = 0$$

Pippard has shown that this gives a distribution more like a Gaussian than a Lorentzian in the large α limit which is both lower and broader than in the isotropic case. The conductivity σ_q/σ_0 normalised to the D.C. value, σ_0, is shown in fig. (18) as a function of α_0, being equal to the isotropic value at large α_0:

$$\underset{\alpha_0 \to \infty}{Lt.} \left(\sigma_q/\sigma_0\right) = \frac{3}{4}\pi\alpha_0^{-1}$$

but being larger than that for isotropic scattering at intermediate (q/l_0), though nowhere differing by more than about 20%.

In case 2, it is easily shown that:

$$\begin{cases} l_0^{-1} = 4\pi P\left(1 - \frac{1}{3}\beta\right) \\ l_\infty^{-1} = 4\pi P \end{cases}$$

so that $l_0 > l_\infty$ for $\beta > 0$ as expected.

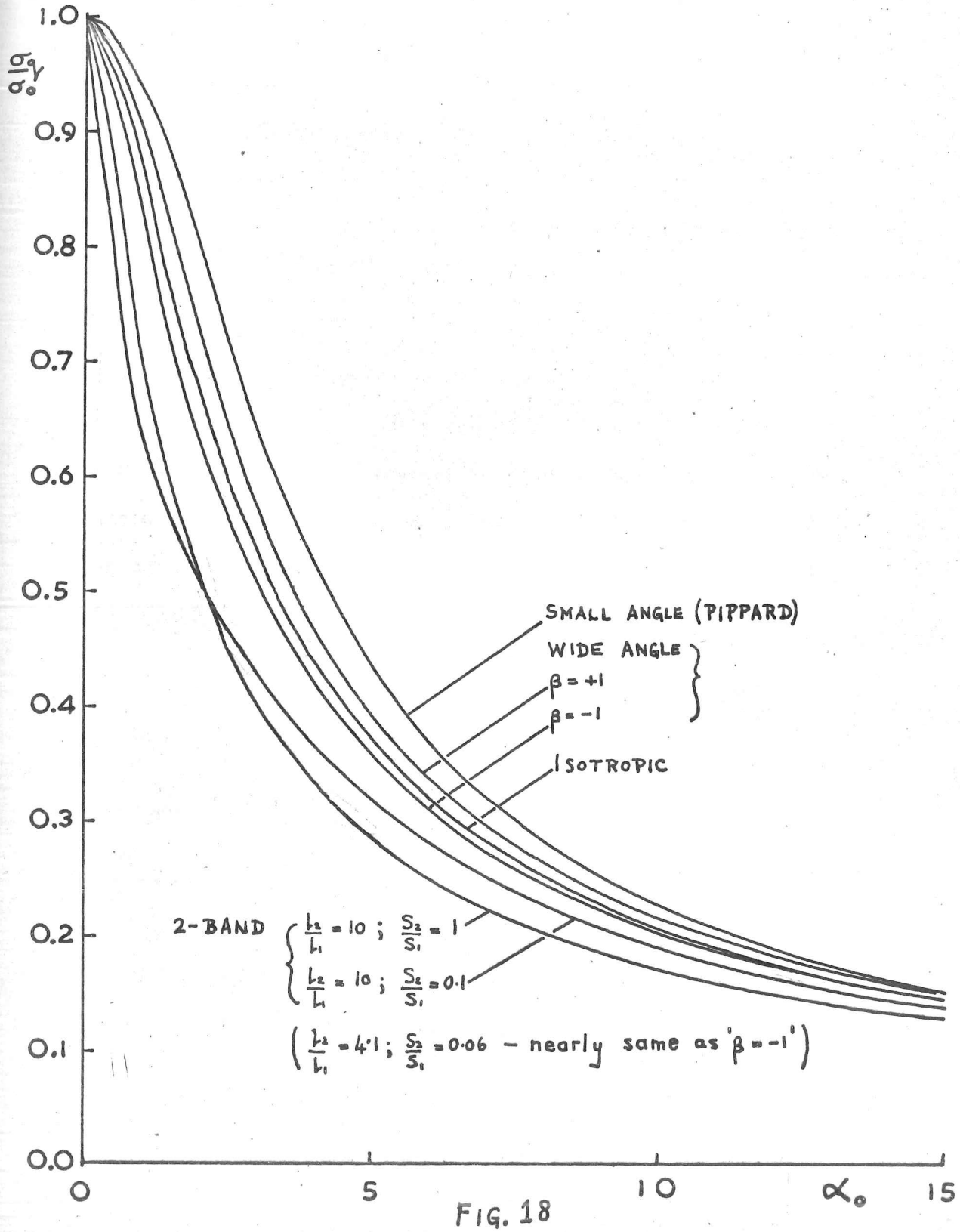
1.0
$\frac{\sigma_\theta}{\sigma_0}$
0.9
0.8
0.7
0.6
0.5
0.4
0.3
0.2
0.1
0.0
0
5
10
15
α_0
SMALL ANGLE (PIPPARD)
WIDE ANGLE
$\beta = +1$
$\beta = -1$
ISOTROPIC
2-BAND
$\frac{k_2}{k_1} = 10$; $\frac{S_2}{S_1} = 1$
$\frac{k_2}{k_1} = 10$; $\frac{S_2}{S_1} = 0.1$
$\left(\frac{k_2}{k_1} = 4.1$; $\frac{S_2}{S_1} = 0.06$ – nearly same as '$\beta = -1$'$\right)$

FIG. 18

Now since: $\cos\theta_0 = \cos\theta\cos\theta' + \sin\theta\sin\theta'\cos\delta$

the integral over δ in (B) is:

$$\int_0^{2\pi} P(\theta_0)\cos\delta\, d\delta\Big|_{\theta,\theta' \text{ const.}} = P\left(1+\beta\cos\theta\cos\theta'\right)\int_0^{2\pi}\cos\delta\, d\delta + \beta P\sin\theta\sin\theta'\int_0^{2\pi}\cos^2\delta\, d\delta$$

$$= \beta\pi P\sin\theta\sin\theta'$$

So equation (B) becomes:

$$\left(1+i\alpha_\infty x\right)F(x) = \left(1-x^2\right)\left[1+\tfrac{1}{4}\beta\int_{-1}^{+1}F(x')\,dx'\right]$$

Note that for a more general scattering function $P(\theta_0)$, the x-dependence of the scattering integral will be more complicated than the simple dependence on $(1 - x^2)$ found here. At any rate, this equation has the exact solution:

$$F(x) = \frac{\left(1-x^2\right)\left(1+\frac{1}{4}\beta I\right)}{1+i\alpha_\infty x}$$

where: $$I = \int_{-1}^{+1}F(x)\,dx = \left(1+\tfrac{1}{4}\beta I\right)J$$

and: $$J = \int_{-1}^{+1}\frac{1-x^2}{1+i\alpha_\infty x}\,dx = 2\alpha_\infty^{-1}\left\{\left(1+\alpha_\infty^{-2}\right)\tan^{-1}\alpha_\infty - \alpha_\infty^{-1}\right\}$$

It is easily shown that the conductivity is given by:

$$\frac{\sigma_\infty}{\sigma_0} = \frac{3}{4}I\left(\frac{l_\infty}{l_0}\right) = \frac{\frac{3}{4}J}{1-\frac{1}{4}\beta J}\left(\frac{l_\infty}{l_0}\right)$$

with: $$\sigma_0 = \frac{k_F^2 e^2}{3\pi^2\hbar}\,l_0$$

on direct integration of the number of displaced electrons $N \times v_F \sin\theta\cos\phi$.

In the high q limit, this yields: $\frac{\sigma_\infty}{\sigma_0} = \frac{3}{4}\pi\alpha_\infty^{-1}\left(\frac{l_\infty}{l_0}\right) = \frac{3}{4}\pi\alpha_0^{-1}$ and so, considered as a function of α_0, tends to the same value as for isotropic scattering. This feature is quite general of any scattering model at: $(ql) \gg \theta_s$, 1. (Azbel and Kaner J.E.T.P. 2, 749 (1956)). The detailed dependence on α_0 is displayed in fig. (18) for the extreme possible values $\beta = \pm 1$, and it is seen that the deviation from the isotropic response is less than for small angle scattering, being nowhere greater than about 7% in σ_q/σ_0 . Moreover, for the physically reasonable case of $\beta > 0$, the response is increased over that for isotropic scattering as in the small angle situation. Despite the smallness of the percentage correction to the value of σ_q/σ_0 at a given (ql), considered as a correction to (ql) at given σ_q/σ_0 the correction is not all that small, and we shall see later that the change in surface resistance can be quite appreciable.

We finally consider, in rather general terms, whether any sort of scattering is capable of giving a reduction in σ_q/σ_0 as a function of α_0. Our expression for the wide angle scattering model may be expressed at large q as:

$$\frac{\sigma_q}{\sigma_0} = \frac{3}{4}\pi\left(\frac{l_\infty}{l_0}\right)\alpha_\infty^{-1}\left\{1 + \left(\frac{\pi}{4}\beta - \frac{4}{\pi}\right)\alpha_\infty^{-1} + O\left(\alpha_\infty^{-2}\right)\right\}$$

$$= \frac{3}{4}\alpha_0^{-1}\left\{\pi + \left[\frac{\frac{\pi^2}{4} - \frac{4}{3}}{1 - \frac{1}{3}\beta}\beta - 4\right]\alpha_0^{-1} + O\left(\alpha_0^{-2}\right)\right\}$$

$$\because \frac{l_\infty}{l_0} = 1 - \frac{1}{3}\beta$$

so that the correction term to the Reuter-Sondheimer result is positive for: $0 < \beta < 1$ as seen earlier. If now we consider a more general scattering model, and regard a value of β as being defined by : $\frac{l_\infty}{l_0} = 1 - \frac{1}{3}\beta$ then β will represent the effect of velocity persistence for D.C. processes with appreciable contributions from over the whole Fermi surface. This will be related to that obtaining in the high (ql) limit of course, though not necessarily in the same way as for our previous model. In general, we may expect:

$$\frac{\sigma_q}{\sigma_0} = \frac{3}{4}\ \alpha_0^{-1}\left\{\pi + \left(\gamma\beta - 4\right)\alpha_\infty^{-1} + O\left(\alpha_\infty^{-2}\right)\right\}$$

γ being a factor dependent on the model. In this case:

$$\frac{\sigma_q}{\sigma_0} = \frac{3}{4}\,\alpha_0^{-1}\left\{\pi + \left[\frac{\gamma - \frac{4}{3}}{1 - \frac{1}{3}\beta}\,\beta - 4\right]\alpha_0^{-1} + O\left(\alpha_0^{-2}\right)\right\}$$

and it is no longer evident that the correction is necessarily positive. Intuitively, one can imagine that for the sort of scattering suggested in fig. (17) γ could well be rather small since the effective zone of width α_∞^{-1} may, as its width increases, sense considerably less velocity persistence than is evident in the D.C. case; though it is hard to be sure without a detailed calculation. Such a form of scattering may not be

totally improbable as a representation of that occurring between orthogonal arms of the 'jungle-gym' hole surface in niobium.

2. SURFACE SCATTERING:

Any field-penetration can, of course, be Fourier analyzed, and to this extent it is σ_q which determines the response of the metal to the microwave field. But so far, the exact relation between this and the surface impedance has been skated around, and we shall see that though according to the previous section the effect of any scattering anisotropy on σ_q is probably rather small this may not be so of the surface resistance.

For isotropic scattering and spherical Fermi surface we have the following well-known expressions for the skin depth δ :

diffuse surface scattering p = 0: $$\delta = \pi i \left\{ \int_0^\infty dq_y \, \log_e \left(1 + \frac{i\omega\sigma_q}{q^2}\right)\right\}^{-1} \quad (C)$$

specular surface scattering p = 1: $$\delta = \frac{2i}{\pi} \left\{ \int_0^\infty dq \left(q^2 + i\omega\sigma_q \right)^{-1} \right\} \quad (D)$$

where σ_q is expressed in R.M.K.S. Now the expression for p = 1 is obtained quite straightforwardly by replacing the physical case

of the semi-infinite metal conceptually by an infinite medium of response σ_q in which the fields are set up by a thin current sheet J_s parallel to the surface (fig. 19(a)). In this case:

$$\begin{cases} E_x(x,y,z) = E_x(x,y,-z) \\ B_y(x,y,z) = -B_y(x,y,-z) \end{cases}$$

so that the distribution of electrons crossing the plane $z = 0$ is a correct representation of the specular reflection at the surface of electrons from $z > 0$. This is true even for the sort of scattering process depicted in fig. (19(a)) which is indeed a process contributing to σ_q ; in physical terms this is represented by the process in fig. (19(b)). The probability of such a process for the electrons on the effective zone is much enhanced in the case of small angle scattering over that expected for isotropic scattering. So we conclude that the expression for the impedance is still correctly given by (D) even for anisotropic scattering when the surface reflexion is specular.

However, for diffuse surface scattering, the situation is more difficult. Expression (C) is calculated for isotropic

SURFACE SCATTERING

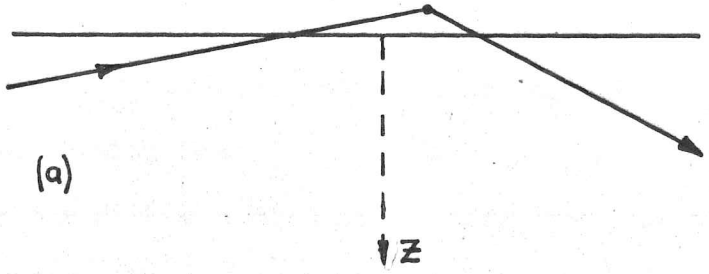

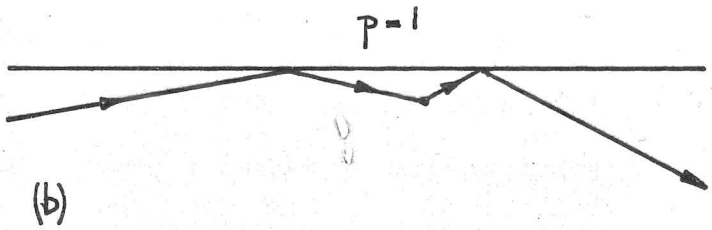

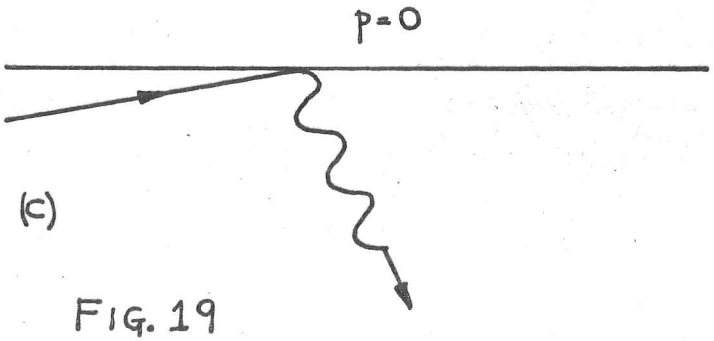

FIG. 19

scattering by replacing the semi-infinite metal by an infinite medium of response σ_ν , and such sources as render the region $z < 0$ field-free; thus for isotropic scattering, the distribution of electrons coming from $z < 0$ is isotropic, and correctly represents the diffuse scattering of electrons from $z > 0$ at the surface. This is no longer true for anisotropic scattering, since the sort of process considered previously in fig. (19(a)) carries bogus momentum back into the metal. In the absence of a detailed theory of this effect, it is very difficult to say what the result will be, or even to predict whether the surface resistance will be increased or decreased by it, since a correct analysis would clearly involve a self-consistent calculation of the alteration to the field distribution. Perhaps we may conjecture that the effective value of σ to be used in (C) under such circumstances would in fact be less than that in the absence of surface-scattering owing to the destruction of momentum at the surface, giving rise to an increase in the surface resistance. It seems quite possible, too, that the change could be much more dramatic than the changes in σ discussed in section 1 would imply even in the extreme anomalous region.

3 FERMI SURFACE ANISOTROPY

Under this heading, we also include anisotropy of the mean free path around the Fermi surface. Both Fermi surface and mean free path anisotropy can produce a variation in the width of the effective zone around the Fermi surface, and both imply that deviations from the Reuter-Sondheimer theory are possible at intermediate values of (ql). There seems to be little literature concerning the effect of Fermi surface anisotropy, since most anomalous skin effect work is done in the extreme anomalous limit where the resistance is related in a simple way to the mean curvature on the effective zone (Pippard - Proc. Roy. Soc. A 224, 273 (1954)). One might expect that at low (ql) the resistance would be related to some sort of average (σ/l) while at high (ql) to an average around the effective zone in the appropriate cross-section of the Fermi surface. Our rather limited results for niobium do not seem to show any very strong anisotropy with crystal direction, though it should be remembered that our resonator geometry averages over all effective zones passing through the axis of the specimen, giving something like a $\cos^2$ averaging over the Fermi surface. An examination of the Fermi surface of niobium proposed by the band-structure calculations

3 FERMI SURFACE ANISOTROPY

Under this heading, we also include anisotropy of the mean free path around the Fermi surface. Both Fermi surface and mean free path anisotropy can produce a variation in the width of the effective zone around the Fermi surface, and both imply that deviations from the Reuter-Sondheimer theory are possible at intermediate values of (ql). There seems to be little literature concerning the effect of Fermi surface anisotropy, since most anomalous skin effect work is done in the extreme anomalous limit where the resistance is related in a simple way to the mean curvature on the effective zone (Pippard - Proc. Roy. Soc. A 224, 273 (1954)). One might expect that at low (ql) the resistance would be related to some sort of average (σ/l) while at high (ql) to an average around the effective zone in the appropriate cross-section of the Fermi surface. Our rather limited results for niobium do not seem to show any very strong anisotropy with crystal direction, though it should be remembered that our resonator geometry averages over all effective zones passing through the axis of the specimen, giving something like a $\cos^2$ averaging over the Fermi surface. An examination of the Fermi surface of niobium proposed by the band-structure calculations

of Mattheiss (P.R. 139, A1893 (1965)) (in fig. (20)), whose features have been experimentally confirmed by the de Haas van Alphen measurements of Scott et al. (Phys. Lett 27A, 655 (1968)) and by the galvanomagnetic measurements of Reed and Soden (P.R. 173, 677 (1968)) apart from the inner hole jack at Γ shows that there are various saddle points where for decreasing (ql) the effective zone may become peculiarly broad. This might give an effect of the sort considered by Glasser (P.R. 176, 1110 (1968)) where a section of Fermi surface of low curvature can contribute to the conductivity as:

$$\sigma_{\omega} \sim q^{-2}$$

or even higher powers, rather than the more usual q^{-1}. Under such conditions, the Pippard expression for the surface resistance in terms of the curvature around the effective zone becomes invalid, and the resistance develops an odd frequency dependence.

As previously remarked, mean free path anisotropy around the Fermi surface can also produce a corresponding variation in the width of the effective zone; perhaps a model for this might be taken of a constant relaxation time and a highly anisotropic Fermi velocity. This is not unreasonable for a transition metal where

MATTHEISS' BAND STRUCTURE

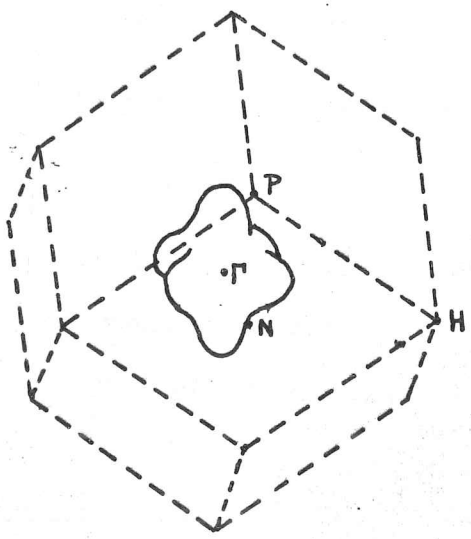

HOLE JACK

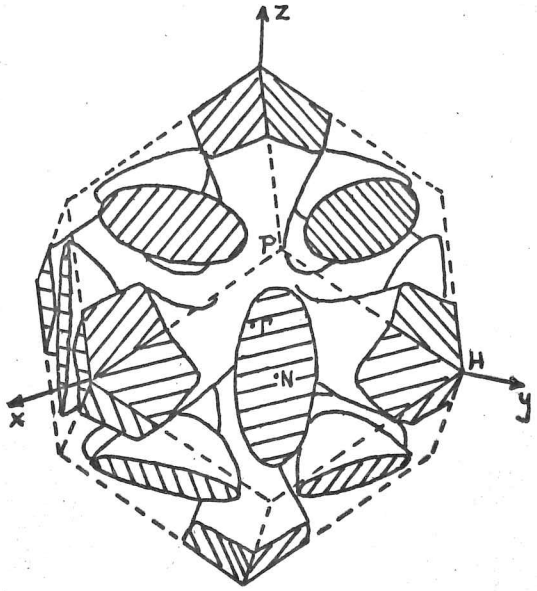

JUNGLE-GYM
AND
ELLIPSOIDAL POCKETS

JACK AND JUNGLE-GYM TOUCH IN (100) AND (110) PLANES
IF L.S COUPLING NEGLECTED

FIG. 20

the d-bands have high density of states and low Fermi velocity. For example, if we denote (σ/l) by S which is a measure of the Fermi surface area, then a simple 2-band model consisting in 2 spherical surfaces would have a D.C. conductivity:

$$\sigma_0 = (S_1 l_1 + S_2 l_2)$$

and an extreme anomalous value:

$$\sigma_\infty = \frac{3}{4}\pi\, q^{-1} (S_1 + S_2)$$

where the scattering is regarded as isotropic and may contain interband scattering.

Thus at general (ql):

$$\frac{\sigma_q}{\sigma_0} = \frac{3}{4} q^{-1} \frac{S_1 J_1 + S_2 J_2}{S_1 l_1 + S_2 l_2}$$

where : $J_1 = 2\left\{ (1+\alpha_1^{-2}) \tan^{-1}\alpha_1 - \alpha_1^{-1} \right\}$; $\alpha_1 = q l_1 = q \tau v_{F_1}$

and similarly for J_2. It is evident that this expression can only differ from that of Reuter and Sondheimer if $l_1 \neq l_2$, and some examples of its behaviour are shown in fig. (18) as a function of an average mean free path defined by:

$$\bar{\alpha} = q\bar{l} = q \frac{S l_1 + S_2 l_2}{S_1 + S_2}$$

so that: $\frac{\sigma_\infty}{\sigma_0} = \frac{3}{4}\pi\, \bar{\alpha}^{-1}$

i.e. the mean free path which would be calculated from the D.C. conductivity σ_0 and a total value of:

$$\left(\frac{\sigma}{l}\right) = S_1 + S_2$$

We see that, for example, there is an appreciable correction to (σ_q/σ_0) if 1/10th of the Fermi surface has a mean free path 10 times longer than that on the remainder, the correction amounting to about 33% at $\bar{\alpha} \sim 1$. Now the results of Sung and Shen (Phys. Lett 19, 101 (1965)) on the specific heat of superconducting niobium give a value for the relative densities of states in the s- and d- bands as:

$$N_s/N_d = 1.5 \times 10^{-2}$$

† If we assume, for an order of magnitude estimate, that the bands are parabolic at the Fermi surface, then since the Fermi energy:

$$E_F = \frac{\hbar^2 k_F^2}{2m^*} = \frac{1}{2} m^* v_F^2$$

is the same for both bands,

$$\frac{S_s}{S_d} = \left(\frac{k_{Fs}}{k_{Fd}}\right)^2 = \frac{m_s^*}{m_d^*} = \left(\frac{v_d}{v_s}\right)^2$$

and:

$$\frac{N_s}{N_d} = \frac{v_s^{-1} S_s}{v_d^{-1} S_d} = \left(\frac{v_d}{v_s}\right)^3 = 1.5 \times 10^{-2}$$

so:

$$\frac{v_s}{v_d} = 4.1 \quad \text{and} \quad \frac{S_s}{S_d} = 0.06$$

Assuming τ is constant over the Fermi surface: $l_s/l_d = 4.1$

and these values give the curve also shown in fig. (18), whose deviation from the single-band curve is again not very large, being about 7% at maximum. However, it is difficult to place much confidence in this simple calculation, and it is quite conceivable

† assuming the bands have the same zero of energy, as a purely ad hoc model

that the deviation is rather larger; in particular, we may note that our value for $\frac{m_s^*}{m_d^*} = \left(\frac{v_d}{v_s}\right)^2 \simeq 0.06$ differs appreciably from that deduced by Radhakrishnan (Phys. Stat. Solidi 20 783 (1967)) on the basis of a two-band calculation of the penetration depth in niobium fitted to the results of Maxfield and McLean (Phys. Rev. 139 A1515 (1965)). However, this last value is itself in doubt, since Radhakrishnan appears to have erroneously fitted his calculation not to the experimental results of Maxfield and McLean, but to their calculation of the penetration depth expected on the basis of the energy-bap temperature dependence given by Dobbs & Perz (see fig. 6 of Maxfield & McLean's paper) which is presumably a highly unreliable procedure.

4 To summarize our results for the various possible amendments to the conductivity, we note that in the extreme anomalous limit we may expand in a series:

$$\frac{\sigma_q}{\sigma_0} = \frac{3}{4}\alpha^{-1}\left\{\pi + (\Delta - 4)\alpha^{-1} + O(\alpha^{-2})\right\}$$

where the correction Δ has the following values:

Model	Δ
small angle scattering	+ 2.66 (private communication - Pippard)
wide angle ($\cos.\theta_o$) scattering	$\frac{\frac{\pi^2}{4}-\frac{4}{3}}{1-\frac{1}{3}\beta}\beta$ $\begin{cases} = +1.70 & \text{for } \beta=+1 \\ = -0.85 & \text{for } \beta=-1 \end{cases}$
2 band model	$\frac{-4\left(\sqrt{\frac{l_1}{l_2}}-\sqrt{\frac{l_2}{l_1}}\right)^2\frac{S_2}{S_1}}{\left(1+\frac{S_2}{S_1}\right)^2}$ $\begin{cases} = -0.50\,;\ \frac{l_2}{l_1}=4.1\,,\ \frac{S_2}{S_1}=0.06 \\ = -2.66\,;\ \frac{l_2}{l_1}=10\,,\ \frac{S_2}{S_1}=0.1 \end{cases}$

Putting aside the problem of diffuse surface scattering, and considering only the specular case, we see that these corrections to σ_q produce quite important corrections to the skin depth δ, since the leading term in the expansion of σ gives only the extreme anomalous value δ_∞. The rate at which the departure from this limit takes place as a function of the D.C. resistivity ρ is entirely determined by the 2nd order term, the correction to which is not small. In fig. (21) are shewn the results of a computation of $\delta(\rho)$ for niobium based on the figures:

$$p=1: \begin{cases} \delta_\infty = 0.0536\,\mu. \text{ at } 10\,Gc/s. \\ \delta_{N_2} = 0.402\,\mu. \\ (\rho l) = 5\times10^{-12}\,\Omega cm.^2 \end{cases}$$

where simply the lst 2 terms in the expansion of σ_q have been

SURFACE IMPEDANCE NEAR EXTREME

ANOMALOUS LIMIT

(SPECULAR SURFACE SCATTERING)

(a) 2-BAND : $\frac{l_2}{l_1} = 10$, $\frac{S_2}{S_1} = 0.1$

(b) WIDE-ANGLE : $\beta = -1$

(c) 2-BAND : $\frac{l_2}{l_1} = 4.1$, $\frac{S_2}{S_1} = 0.06$

(d) WIDE-ANGLE : $\beta = +1$

(e) SMALL-ANGLE (PIPPARD)

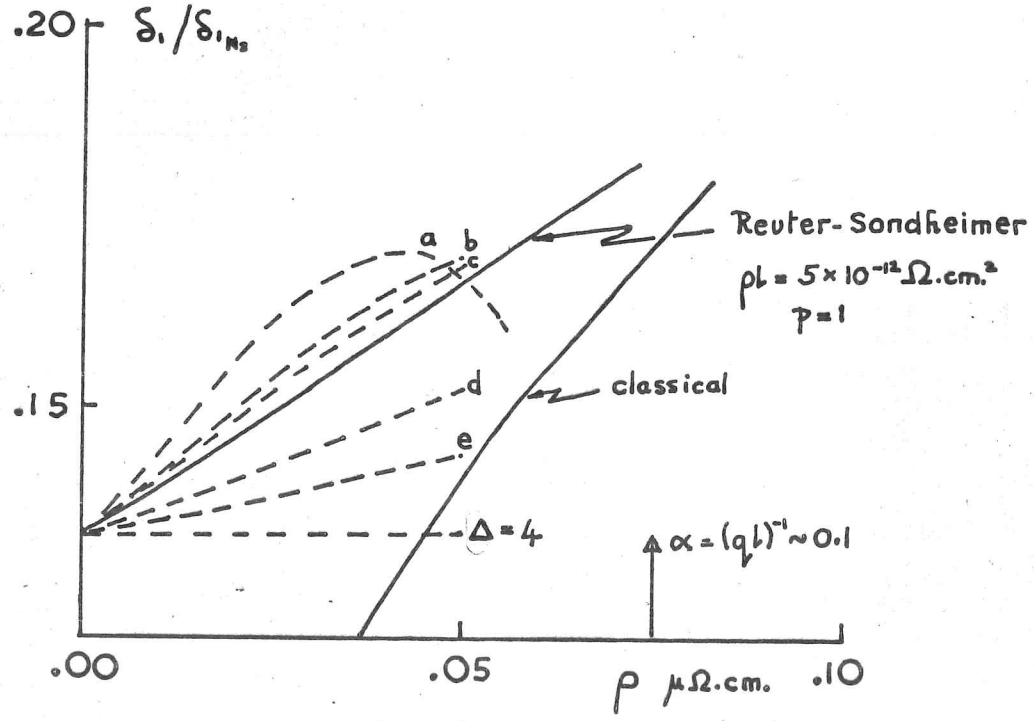

FIG. 21

retained. This at any rate should give the correct gradient at $p = o$, and the corrections to Reuter-Sondheimer are appreciable. Thus we cannot agree with Pippard's conclusion (Proc. Roy. Soc. A305, 291, (1968) that the anomalous skin effect is rather insensitive to the nature of the electron scattering, though in practice the separation of its effects from those of surface scattering and Fermi surface anisotropy would be difficult.

† footnote on section 1:

The same T^3 (rather than T^5) dependence of effective mean free path has now been seen in indium also:

Krylov & Yantmakher JETP 24, 492 (1969)

Chapter 4 The Superconducting-State in Zero Field

In this chapter we present measurements of the temperature variation of surface impedance for 7 single crystal specimens, the accumulated results of which are shown in fig. (22). The low temperature surface resistance is plotted against Pippard's empirical function:

$$f(t) = t^4(1-t^2)/(1-t^4)^2$$

and the reactance against the Gorter-Casimir function:

$$y(t) = 1/\sqrt{1-t^4}$$

It will be observed that the function f(t) is no longer a particularly good fit to the surface resistance, at any rate in the purer specimens, the graphs being rather curved, and that the reactances look generally rather more linear in y(t) at low t than they ought to according to B.C.S. This latter feature has been noted many times before in other superconductors (e.g. Waldram (5)), and, in particular, for niobium by Maxfield and McLean (2), by Finnemore et al. (53), and by French (3). However, specimens $\langle 100 \rangle$ 1 and $\langle 110 \rangle$ 1 appear to show a small upward kink in the reactance at low y(t) which is only just discernible within the experimental accuracy.

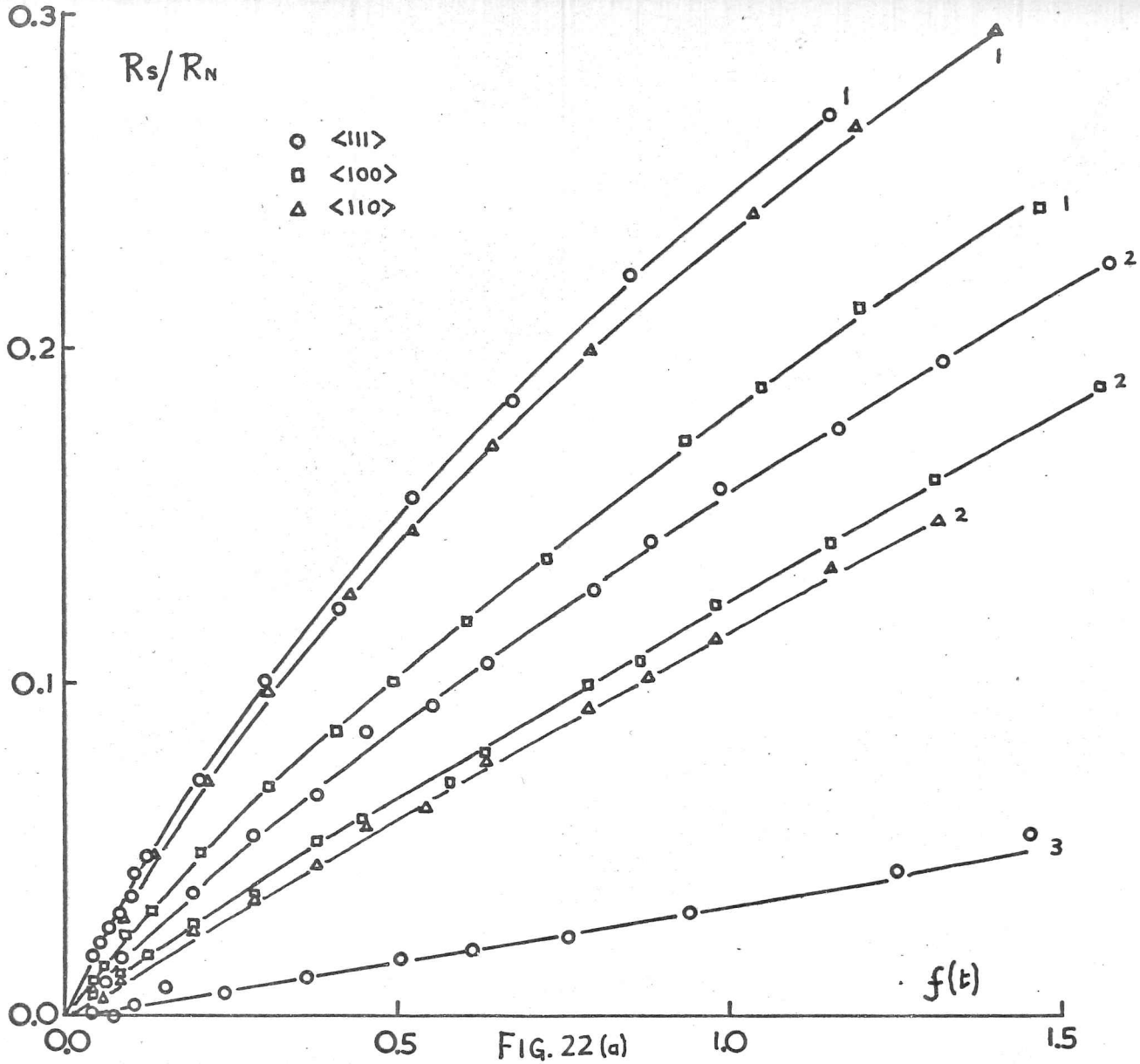

FIG. 22 (a)

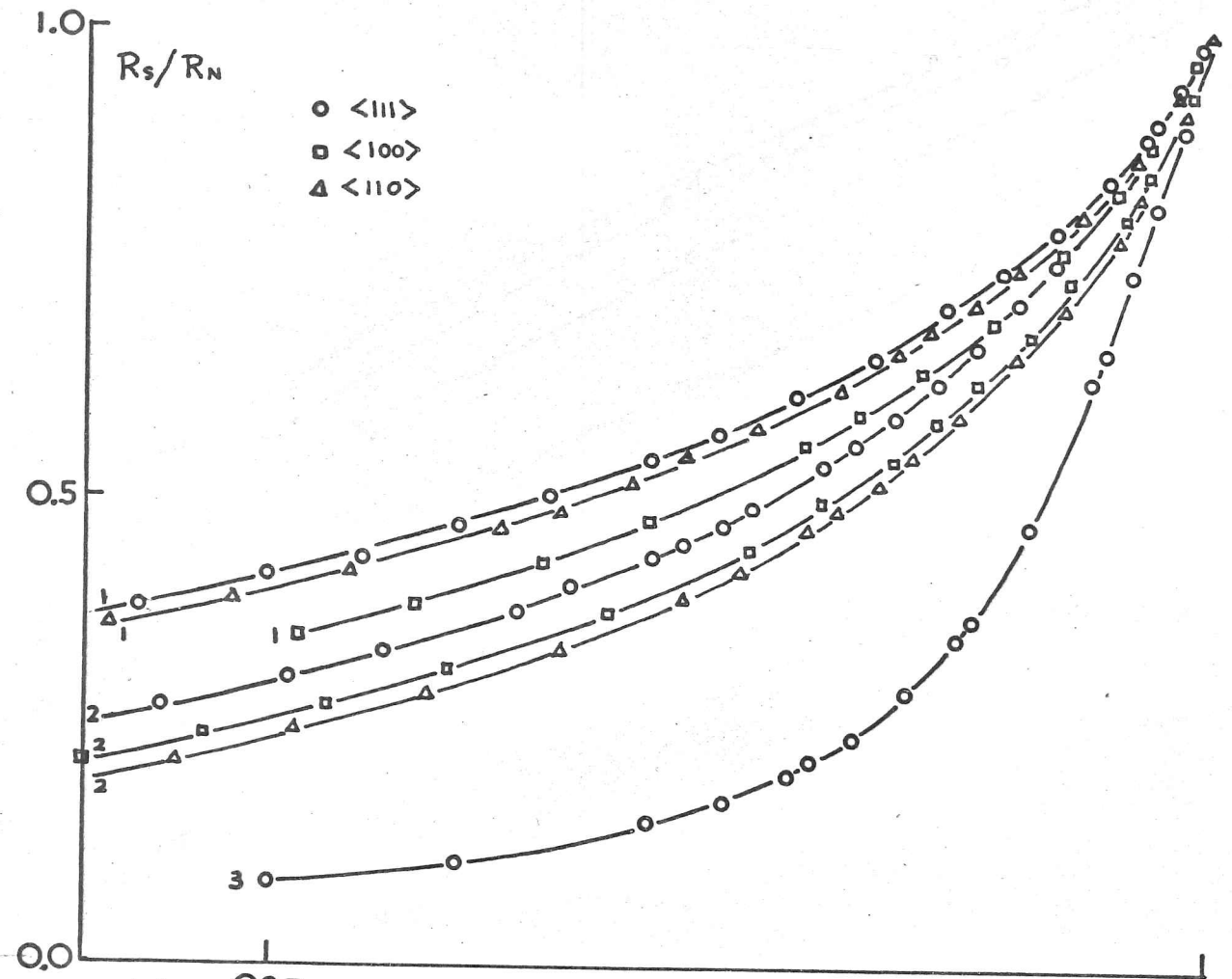

FIG. 22 (b)

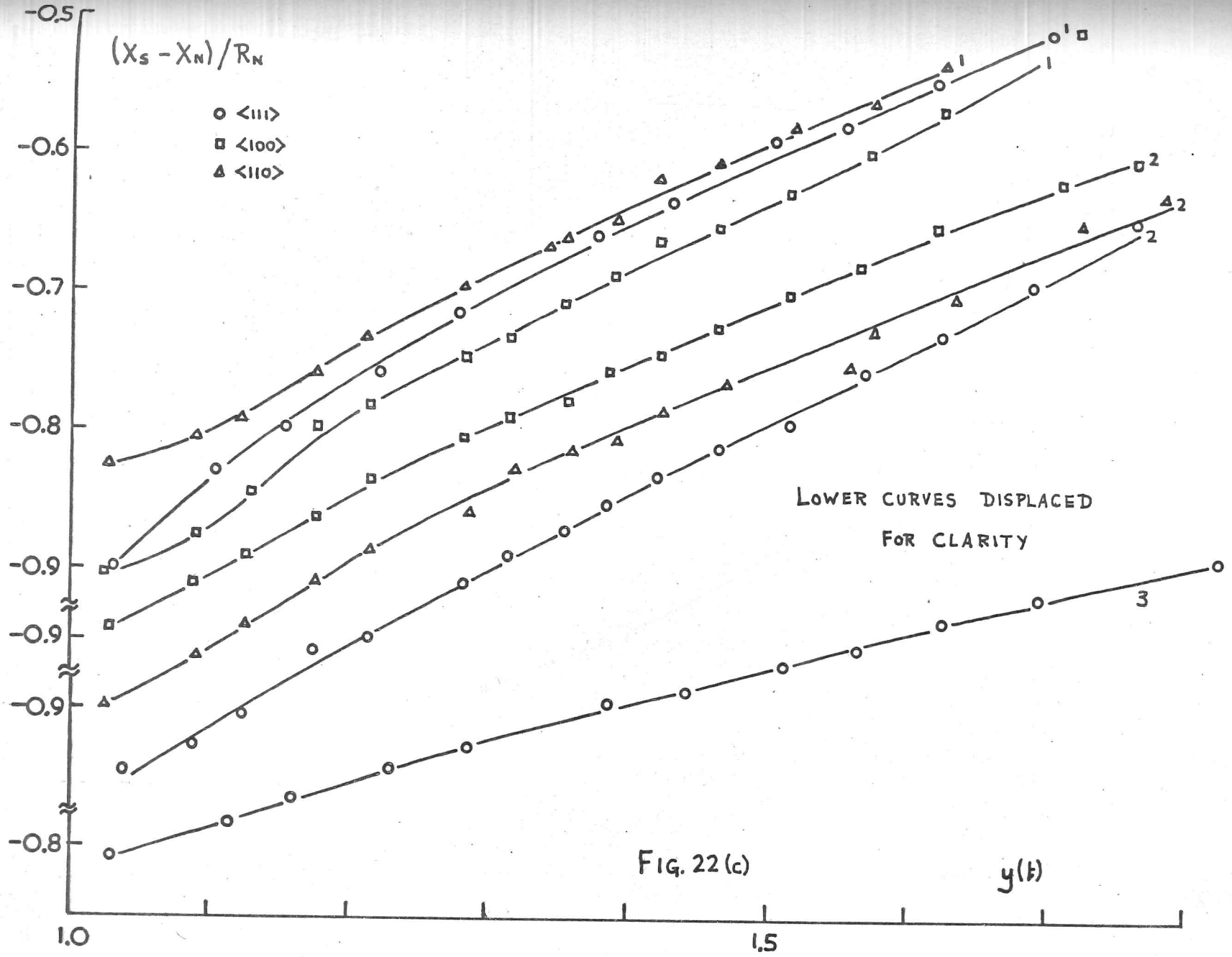
-0.5
$(X_S - X_N)/R_N$
○ <111>
□ <100>
△ <110>
-0.6
-0.7
-0.8
-0.9
-0.9
-0.9
-0.8
1
1
1'
2
2
2
3
LOWER CURVES DISPLACED
FOR CLARITY
1.0
1.5
y(t)

FIG. 22 (c)

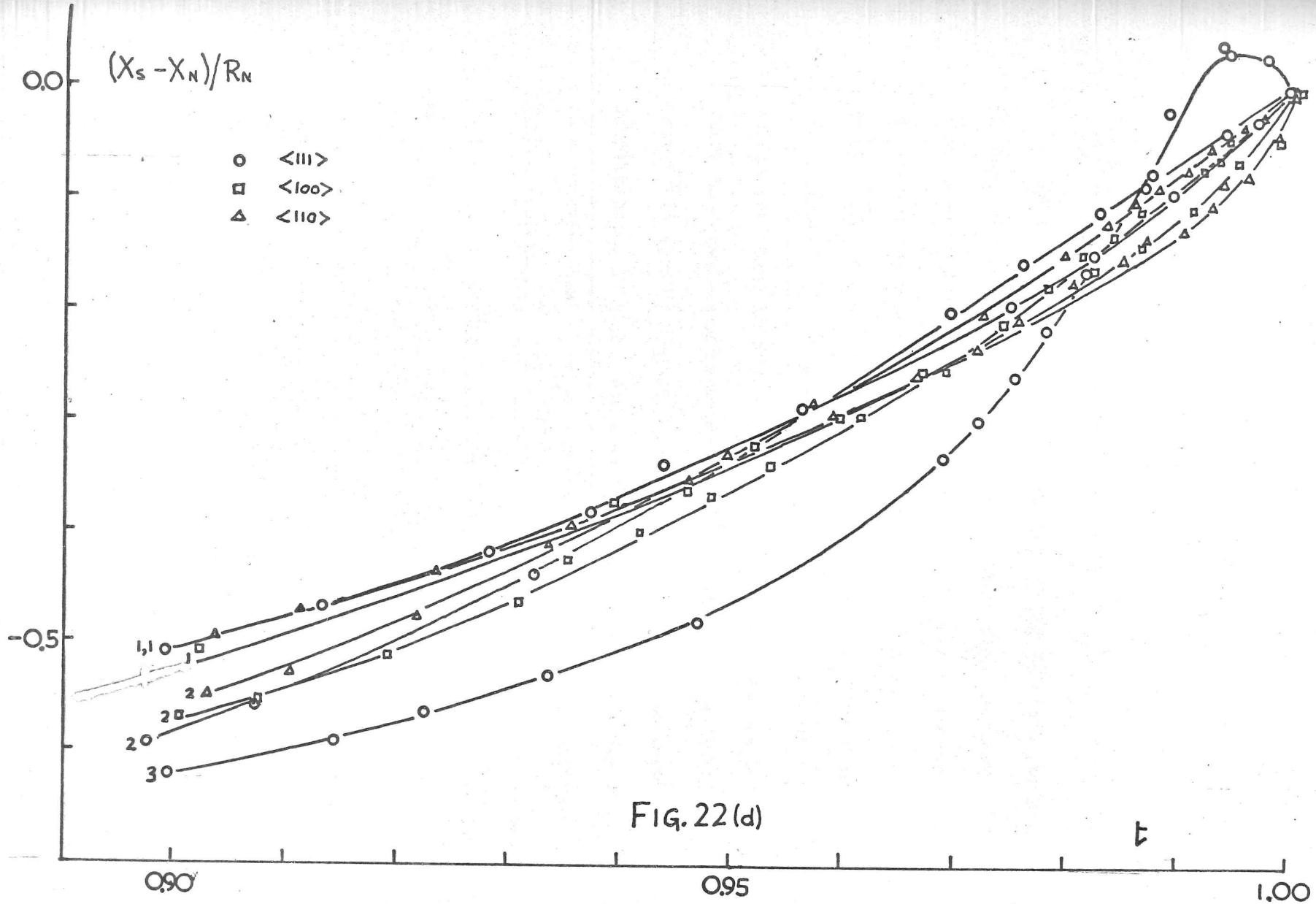

FIG. 22(d)

1. Normal State Parameters

In attempting to fit our results to the Mattis & Bardeen theory, we must, of course, try to estimate from the normal-state measurements already presented in Chapter 3 reasonable values for the electron mean free path l and for the skin depth δ_∞ in the extreme anomalous limit. We have taken the standpoint that our plots of $R(\rho)$ extrapolate to the 'correct' values according to the Reuter-Sondheimer theory at the points where the scattering is totally residual since it is then likely that it is also isotropic, and also should lead to no 2-band complications if we assume that residual scattering gives rise to a constant mean free path around the Fermi surface unlike phonon scattering. This procedure is clearly rather unsure, but it is the best we can do for the moment, and leads to the following values:

specimen	R.R.R.	ρ_0 $\mu\Omega$.cm.	ρ_{T_c} $\mu\Omega$.cm.	l_∞ μ.	l_{T_c} μ.	δ_∞ μ.	(ρl) $\Omega.cm.^2 \times 10^{10}$	%	$\left(\frac{X_N}{R_N}\right)$
<111> 1	1180	0.0126	0.0185	3.79	2.59	0.059	0.048	5	1.761
<111> 2	225	0.064	0.074	0.67	0.58	0.057	0.043	$2\frac{1}{2}$	1.491
<111> 3	15.4	1.01	1.01	(0.046	0.046	0.058	0.046	0	1.040)
<100> 1	442	0.0338	0.0408	1.60	1.26	0.061	0.051	$2\frac{1}{2}$	1.622
<100> 2	177	0.082	0.089	0.42	0.39	0.053	0.035	1	1.397
<110> 1	802	0.0185	0.0248	3.92	2.92	0.068	0.073	$3\frac{1}{2}$	1.761
<110> 2	126	0.119	0.126	0.82	0.77	0.075	0.097	1	1.474
				(0.61	0.58	0.068	0.073	-	1.427)

ρ_0 and ρ_{Tc} are the measured residual resistivity, and that at Tc, respectively; the values of δ_∞ and (ρl) shewn are those chosen to fit the Reuter-Sondheimer theory for diffuse scattering at the residual points ρ_0 obtained by extrapolation. In passing, we must observe that the values obtained in the above table are somewhat sensitive to the assumptions made concerning the effect of retardation which we neglected in Chapter 3; the quantity determining the importance of this is $\frac{\omega\tau}{\gamma l} \sim \frac{\omega\delta}{v_F}$ Taking $v_F \sim 3 \times 10^7$ cm. sec.$^{-1}$ (see section 2), we find $\frac{\omega\delta}{v_F} \sim 0.013$ for $<111>$ 1, $\sim$ 0.052 for $<111>$ 3 so that retardation is beginning to become important under our conditions and in deducing the values given we have used Dingle's tables (75) to estimate the retardation correction. In practice, the correction is at its worst for the purest specimens, where it is of order

$$\begin{cases} +17\% \text{ in } (\rho l) \\ +\ 6\% \text{ in } \delta_\infty \\ +10\% \text{ in } \left(\frac{X_N}{R_N}\right) \end{cases}$$

Now the effect of retardation is calculated in the Reuter-Sondheimer theory from the change in the area of the effective zone on a spherical Fermi surface when displaced sideways through

$k_F\left(\frac{\omega\delta}{v_F}\right)$ in k-space, and is unlikely to be a very good description of so highly anisotropic a metal as niobium. This potential uncertainty is particularly unfortunate as regards the values of X_N/R_N for the purer specimens as it limits the accuracy with which our measured frequency shifts can yield figures for the penetration depth $\lambda(0)$ of the superconducting state.

It will be seen from the table that the values of (ρl) derived though hardly very consistent lie more or less within the range of estimates due to other authors presented in Chapter 2, but more than that is difficult to say; there seems to be some evidence that (ρl) is higher in the $<110>$ orientation. The figures in the '%' column indicate the percentage by which the measured surface resistance at Tc exceeds that predicted by the Reuter-Sondheimer theory based on the fitting to the residual point. It will be as well to remember that there is inevitably an uncertainty of at least this order of magnitude in the extent to which the Mattis & Bardeen theory can be expected to fit the results for the superconducting state. The values of mean free path l_0 and l_{Tc} are to be regarded as effective mean free paths

for the normal current, not being uniquely related to the residual resistance ratio by a single value of (ρl) common to all the specimens. It is, of course, questionable whether this is really the appropriate mean free path for the supercurrent which is averaged over a different effective zone from the normal current, being of width in k-space $\sim k_F \delta \left(l^{-1} + \xi_0^{-1} \right)$ in the former case and $\sim k_F \delta l^{-1}$ in the latter. However, except for specimen <111> 3 for which $l_0 \sim \xi_0$ the supercurrent is not very sensitive to the exact value of mean free path employed in practice.

The bracketed entries in the table are estimates based not on fitting the experimental resistances, but on what seems a reasonable value of (ρl). In the case of specimen <111> 3 which is so dirty as to lie almost completely within the classical regime, a value of 0.046 has been taken as a reasonable mean for that orientation. For specimen <110> 2, direct fitting to the residual point gives a rather high value of (ρl) even considering the fact that <110> 1 also gives a value higher than the average and may thus represent a true anistropy; for this reason, we have also given values of mean free path based on the value of (ρl) obtained for the latter specimen. The calculated value for the

surface resistance is then 4% less than the measured value, which is possibly within experimental error; and in any case, the fitting of a specimen so far removed from the extreme anomalous region is bound to be rather suspect without a detailed understanding of the normal-state behaviour.

Finally, we note that if we take naively as a mean value of (ρl) a figure:

$$\rho l \sim 5 \times 10^{-12}\ \Omega.\text{cm.}^2 \simeq 5.6 \times 10^{-24}\ \text{e.s.u.}$$

as representing the results of our anomalous skin effect measurements, then combining this with a value for the electronic specific heat of the normal state:

$$\gamma = 7.8\ \text{mJ. mole.}^{-1}\ ^\circ\text{K.}^{-2} = 7200\ \text{erg. cm.}^{-3}\ ^\circ\text{K.}^{-2}$$

(76); (77) we can deduce a value for the Fermi velocity from the Faber & Pippard formulae:

$$\gamma = \frac{k_B^2 S}{12\pi \hbar v_F} \quad ; \quad S = \frac{12\pi^3 \hbar}{e^2(\rho l)}$$

This yields:

$$\begin{cases} S = 3.1 \times 10^{17}\ \text{cm.}^{-2} \\ v_F = 2.2 \times 10^{7}\ \text{cm. sec.}^{-1} \end{cases}$$

which are reasonably consistent with the estimates from magnetisation measurements (see section 2). P.95 This yields an effective mass:

$$m^* = \frac{\hbar k_F}{v_F} = \frac{\hbar}{v_F}\sqrt{\frac{S}{4\pi}} \simeq 7.6 \times 10^{-27}\ \text{gm.}$$

$$\simeq 8 \times \text{free electron mass}$$

Such a high value is, of course, what is normally expected for the d-bands of a transition metal, though presumably contains a phonon enhancement factor $\sim$ 1.82 as already discussed in Chapter 1. This result, we believe, is in direct contradiction to the speculation of Wong & Sung (78) that the deviation of the measured H_{c2} in niobium from more conventional theoretical predictions could be explained on the basis of the two band model without the necessity for a high d-band effective mass, the observed London behaviour deriving from the supposition that H_{c2} is dominated by the s-band which has much smaller effective mass. We shall comment further on this point in the following section.

2. Superconducting-state Parameters

To date, several estimates of the coherence length and penetration depths of niobium have been reported in the literature, and we show a summary below together with those for the Fermi-velocity, energy-gap, and Ginzburg-Landau parameter: $\kappa = 0.96\,\lambda_L(0)/\xi_0$

source	$\lambda(o)$ Å	$\lambda L(o)$ Å	ξ_o Å	$10^{-7} VF$ cm.sec.$^{-1}$	$\bar{\epsilon}_o(0) / \epsilon_{o_{BCS}}(0)$	Tc °K	κ
1. Maxfield & McLean (2)	470	390	380	2.6	1.00	9.19	
2. Turneaure & Weissman (21)	-	350	410	2.9	1.06	9.25	
3. French (3)	397	333	390	2.67	1.02	9.30	0.815
4. Finnemore et al. (53)	410	350	430	3.0	1.04	9.25	0.78
5. Ikushima & Mizusaki (79)	390	370	450	3.3	1.10	9.23	0.80
	(390	320	380	2.8			0.81)
6. Ohtsuka & Takano (77)		385					0.84
							or 0.92

Of these, 1 & 2 are surface-impedance measurements, whereas the remainder are based on magnetisation measurements. In 5, the observed $\lambda(o)$ was fitted values of $\lambda L(o)$ and ξ_o based on the B.C.S. relation for specular surface scattering; we have chosen to adopt the practise used in 1, 3, 4, 6 and assume diffuse surface scattering. With this assumption, we have recalculated Ikushima & Mizusaki's results and obtain the values shewn in brackets for entry 5; it will be seen that this introduces significant changes in $\lambda L(o)$ and ξ_o, but that κ is little altered.

There are several criticisms of these values which it seems appropriate to make. Firstly, Maxfield & McLean in calculating their data assumed a value of $\kappa = 1.0$ based on the rather early magnetothermal measurements of McConville & Serin (80). In view of the subsequent and much more thorough investigations listed above, it seems desirable that this value should be revised. We have made no attempt to recalculate their results using a more realistic value of κ, but we can make the general observation that since the seminal quantity which they deduce is $\lambda L(o)$ estimated from:

$$\begin{cases} \left.\frac{d\lambda_L}{dy}\right|_{y \geq 2.5} = \frac{\lambda_L(0)}{0.213B} \simeq \left.\frac{d\lambda}{dy}\right|_{y \geq 2.5} & \text{for } \kappa \sim 1 \\ \epsilon_o(T) = B\sqrt{1-t}\, k_B T_c & \text{with } B = 3.9 \text{ (cf. 3.03 - B.C.S.)} \\ B - \text{estimated from Waldram's self-consistent analysis of } \lambda_L(t) & (5) \end{cases}$$

then the effect of using a lower value for κ would be to increase their estimates of ξ_0 and $\lambda(0)$, probably bringing ξ_0 at any rate into rather closer agreement with the magnetisation measurements. Without going through their self-consistent analysis again, if we take their $\lambda L(0) = 390$ Å, and assume a value of $\kappa_L = 0.83$, we would obtain:

$$\xi_0 = 460 \text{ Å} \quad , \quad \lambda(0) = 470 \text{ Å}$$

where $\lambda(0)$ is now the value obtained from the B.C.S. curve for $t = 0$ rather than that deduced from the high-temperature behaviour.

Secondly, we wish to comment on the values deduced from the magnetisation measurements. The procedure adopted by the authors mentioned is generally as follows:

1. from the observed temperature dependence of the magnetisation characteristic near H_{c2}, the Maki parameters:

$$\begin{cases} \kappa_1(t) = H_{c2} / \sqrt{2}\, H_c \\ \kappa_2(t) = \sqrt{\frac{1}{2}\left\{1 + 1/4\pi \times 1.16 \left.\frac{dM}{dH}\right|_{Hc2}\right\}} \end{cases}$$

may be deduced and extrapolated to $t = 1$ to give the Ginzburg-Landau parameter:

$$\kappa = 0.96\, \lambda_L(0) / \xi_0 = \kappa_1(1) = \kappa_2(1)$$

2. the penetration depth $\lambda(T)$, and in particular $\lambda(o)$, is deduced from the relation due to Abrikosov (81) and Tinkham (82):

$$H_{c_2}(t) = 4\pi \lambda^2(t)\, H_c^2(t) / \phi_o$$

3. the penetration depth so determined can be used to determine the London penetration depth $\lambda L(o)$ via the B.C.S. relation for $\lambda/\lambda L$ as a function of $\xi_o/\lambda L$, and hence ξ_o. The Fermi velocity may then be deduced from the B.C.S. expression for ξ_o :

$$\xi_o = \frac{\hbar v_F}{\pi \bar{\epsilon}_c(o)}$$

We believe that the procedure outlined in step 2 is subject to considerable doubt on account of its neglect of the effects of non-locality. Tinkham's argument appears to be based on writing down an expression of the Ginzburg-Landau type for the free energy near H_{c2} in terms of an order parameter which is subsequently determined by a variational method. Now it is true that since the transition to the mixed-state is second-order at H_{c2} in the sense that the order parameter nucleates continuously from zero, then the electrodynamics involved is indeed of the local London type sufficiently near to H_{c2} as the magnetic field there is uniform. However, it is the way in which the magnitude

of the order parameter under such conditions is then related to the zero-field penetration depth $\lambda(t)$ and to the bulk critical field $Hc(t)$ which seems to be valid only in the London limit. Indeed such a conclusion seems inescapable in view of the treatment of $Hc2(t)$ based on the Gorkov theory given by Helfand & Werthamer (83); ( ) and by Hohenberg & Werthamer (65) in which specific account is taken of non-locality, at any rate to first order; for a metal with an isotropic electronic structure, this theory gives results negligibly different from that in which non-locality is neglected as by Eilenberger (84), but Hohenberg & Werthamer show that crystalline anisotropy of $Hc2$ can only arise in an anisotropic metal of cubic symmetry when non-locality is taken into account. According to Farrell et al. (85) this theory is in at least qualitative agreement with the measured anisotropy in single crystals, and according to French (3) may go some way to explaining the large discrepancy noted by many workers between the measured value of $k_1(t)/k$ for a polycrystal and that predicted by the isotropic theory. For example, French's value for $k_1(0)/k$ is 1.68 as compared with the prediction of 1.26.

For these reasons we are inclined to believe that the parameters estimated from the magnetisation measurements are

subject to doubt, though it is rather hard to estimate by how much since the behaviour of $H_{c2}(t)$ in niobium still lacks a detailed explanation. In particular, we are inclined to doubt the temperature variations $\lambda(t)$ deduced by Finnemore et al. and by French, and to think that French's use of Waldram's inversion technique to obtain $\epsilon_0(t)$ therefrom is probably rather meaningless (see Chapter I for graph) particularly in view of the fact (see Chapter I) that the analogous inversion of $H_c(t)$ using the method suggested by Finnemore & Mapother (55) would yield an energy gap deviating negligibly from that of B.C.S. The authors mentioned are unfortunately not completely explicit about the way in which they have used Tinkham's relation; it would seem that the best procedure would be to take for $\lambda(o)$ the value estimated from the value of $\frac{d\lambda}{dy}$ near Tc where the electrodynamics is more nearly local, rather than that deduced directly for t=o. There is some suggestion that this is in fact what Ikushima & Mizusaki did, some doubt as to what French did, and a definite indication that Finnemore et al. took the value directly calculated from Tinkham's formula at t=o.

We feel that the quantity which can most reliably be deduced from the magnetisation measurements is in fact the value of the

Ginzburg-Landau parameter κ . Despite the fact that there is as yet no detailed explanation of the temperature-dependence of Hc2, and therefore of κ_1 & κ_2 , in the extrapolation to t = 1 there would seem to be little real doubt that the local Ginzburg-Landau equations will be a good description since in any case niobium is not vastly removed from the London region. Accordingly, we take as a 'best' estimate for an average over all crystal orientations of:

$$\kappa = 0.80 \qquad \text{or:} \quad \kappa_L = \lambda_L(0)/\xi_0 = 0.83$$

It should still be realised that this value is subject to uncertainty on the following grounds:

1. Strong-coupling

Various treatments have been given of the effects of strong coupling on Hc2 (York & Bardasis (64); Werthamer & McMillan (63); Eilenberger & Ambegaokar (62) and on Hc (56). However, it is by no means transparent to the author what implications this has for κ . Werthamer & McMillan unfortunately do not give the detailed results of their computation, being content with the statements that the temperature dependence is identical (to within 2%) to that obtaining in the weak-coupling limit and that the overall scaling of Hc2 is substantially modified

by the Fermi-velocity renormalisation factor Z; they do not say whether this is caused simply by the modification to Hc, or includes one to κ also. In contrast, York & Bardasis say that the slope: $H_{c2}^{-1} \left.\frac{\partial H_{c2}}{\partial t}\right|_{t=1}$ is modified by the effects of strong coupling, but seem to make no comments on the absolute value of Hc2. However, it would seem to the author that equation (18) of York & Bardasis's paper indicates that the Ginzburg-Landau parameter κ does correspond to a London-parameter renormalised by a factor Z. Perhaps the best we can do is to express the hope that the London-parameter appropriate to the high-field local electrodynamics is in fact that also relevant to the low-field non-local behaviour.

2. Two-Band Effects:

An analysis of the Ginzburg-Landau equations for an isotropic two-band superconductor has given Hc2 for pure material after Tilley (36) and Geylikman (32) and for impure material after Kon (37) and Chow (40); ~~( )~~. The latter work considers the effect of the s-band on Hc2 in the intraband phonon coupling limit (which is probably the case for niobium where the interband interaction

is estimated to be small and repulsive - see Chapter 1) for the case:

$$N_s \ll N_d$$

as for niobium, and where the d-band is in the dirty limit $l_d / \xi_{0d} \ll 1$; it is found that the s-band plays the rôle of a small perturbation on the value of Hc2 given by the d-band, depressing it near Tc and enhancing it near T = o by an amount which is small if the s-band is Pippard-like and larger if London-like. This prediction is in qualitative contradiction, we feel, to the speculation by Wong & Sung (78) that in a pure 2-band superconductor Hc2 is dominated by the S-band near Tc on account of the much smaller effective mass of this band. As we have already mentioned in section 1, they claim to explain the peculiar temperature dependence of Hc2 in niobium on this basis together with the supposition that the effective mass of the d-band is not particularly large, unfortunately without giving any detailed quantitative requirements; this latter assumption appears to be in contradiction with the effective mass deduced from our own measurements of the anomalous skin effect together with the measured specific heat value. By their own admission, the thermodynamics of niobium should be dominated by the d-band and there seems little reason to believe

that the s-like area of the Fermi surface is very large compared with the d- which should therefore also dominate the anomalous skin effect, and we feel that their argument probably does not stand up on this ground at least. However, we must preserve the mental reservation thatthe value of κ deduced from Hc2 by extrapolation to Tc may be substantially in error if their interpretation is correct.

Armed with this value of $\kappa_L = 0.83$, we are now in a position to turn first to a discussion of the dirty specimens $<111>3$ for which the complications of the purer specimens seem largely not to arise; of these, we shall have more to say later.

3. Specimen <111> 3

It is regrettable that this is the only dirty specimen ($\frac{l}{\xi_0} \sim 1$) we have available with an at all tolerable D.C. transition; we have made measurements on several other specimens of comparable dirtiness, but do not present the results here on account of the very poor transitions of these crystals. We should point out that even for this specimen, the D.C. transition was not ideal being broadened by about 40 m°K. and this is a fact we must remember in attempting to fit the transition region; it should be emphasised here that the same objection cannot be levelled at the results for the purer specimens to be presented later - these all showed excellent D.C. transitions.

It is convenient to analyse the low-temperature impedance of this specimen by means of the 'σ-plot' described by Waldram (5) from the point of view of obtaining a value for $\epsilon_0(0)$ and for correcting any possible zero-errors in the experimental values of the frequency shifts. Waldram's analysis shews that in the dirty limit with a supercurrent penetration not deviating too greatly from that obtaining in the London regime then to order $(\frac{l}{\lambda})$ a plot of:

$$\left[\frac{R_S}{R_N} \frac{\sigma_N}{\sigma_1} \Big/ \left(1 - \frac{3l}{8\lambda} \right) \right]^{1/3} \text{ vs. } (X_S - X_N)/R_N$$

3. Specimen <111> 3

It is regrettable that this is the only dirty specimen ($\frac{l}{\bar{\ell}_0} \sim 1$) we have available with an at all tolerable D.C. transition; we have made measurements on several other specimens of comparable dirtiness, but do not present the results here on account of the very poor transitions of these crystals. We should point out that even for this specimen, the D.C. transition was not ideal being broadened by about 40 m°K. and this is a fact we must remember in attempting to fit the transition region; it should be emphasised here that the same objection cannot be levelled at the results for the purer specimens to be presented later - these all showed excellent D.C. transitions.

It is convenient to analyse the low-temperature impedance of this specimen by means of the 'σ-plot' described by Waldram (5) from the point of view of obtaining a value for $\epsilon_0(0)$ and for correcting any possible zero-errors in the experimental values of the frequency shifts. Waldram's analysis shews that in the dirty limit with a supercurrent penetration not deviating too greatly from that obtaining in the London regime then to order $(\frac{\ell}{\lambda})$ a plot of:

$$\left[\frac{R_S}{R_N} \frac{\sigma_N}{\sigma_1} \Big/ \left(1 - \frac{3l}{8\lambda} \right) \right]^{1/3} \text{ vs. } (X_S - X_N)/R_N$$

should be linear and of slope - 0.5. In fig. (23), such a plot is made for various gap scalings $\epsilon_o(t)/\epsilon_{o_{B.C.S.}}(t)$. As nearly as one can tell, the best fit is obtained for a B.C.S. gap in fact; the slope of the graph obtained is about -0.54, the difference of this value from -0.5 presumably indicating deviations of the actual field penetration from the simple form used by Waldram. The graph extrapolates to a value of $X_N/R_N \simeq 1.032$ compared with the value of 1.040 estimated for this specimen when due allowance is made for retardation (section 1) using values:

$$(\rho l) \simeq 4{\cdot}6 \times 10^{-12}\,\Omega.cm.^2 \quad , \quad v_F \sim 3 \times 10^7\, cm.sec.^{-1}$$

the figure for (ρl) being a suitable average of our values for the $<111>$ orientation given previously. This close agreement is very satisfactory, though this may be due to the fact that the retardation correction to X_N/R_N is only about 1% anyway and there is therefore little of the uncertainty which attaches to the purer specimens as regards this correction. We have not considered it worthwhile to correct for the small zero error which the σ-plot would indicate on account of the uncertainty over the precise value of X_N/R_N , and have simply fitted the uncorrected value of $\lambda(o)$ using the figure of $\kappa_L = 0.83$;

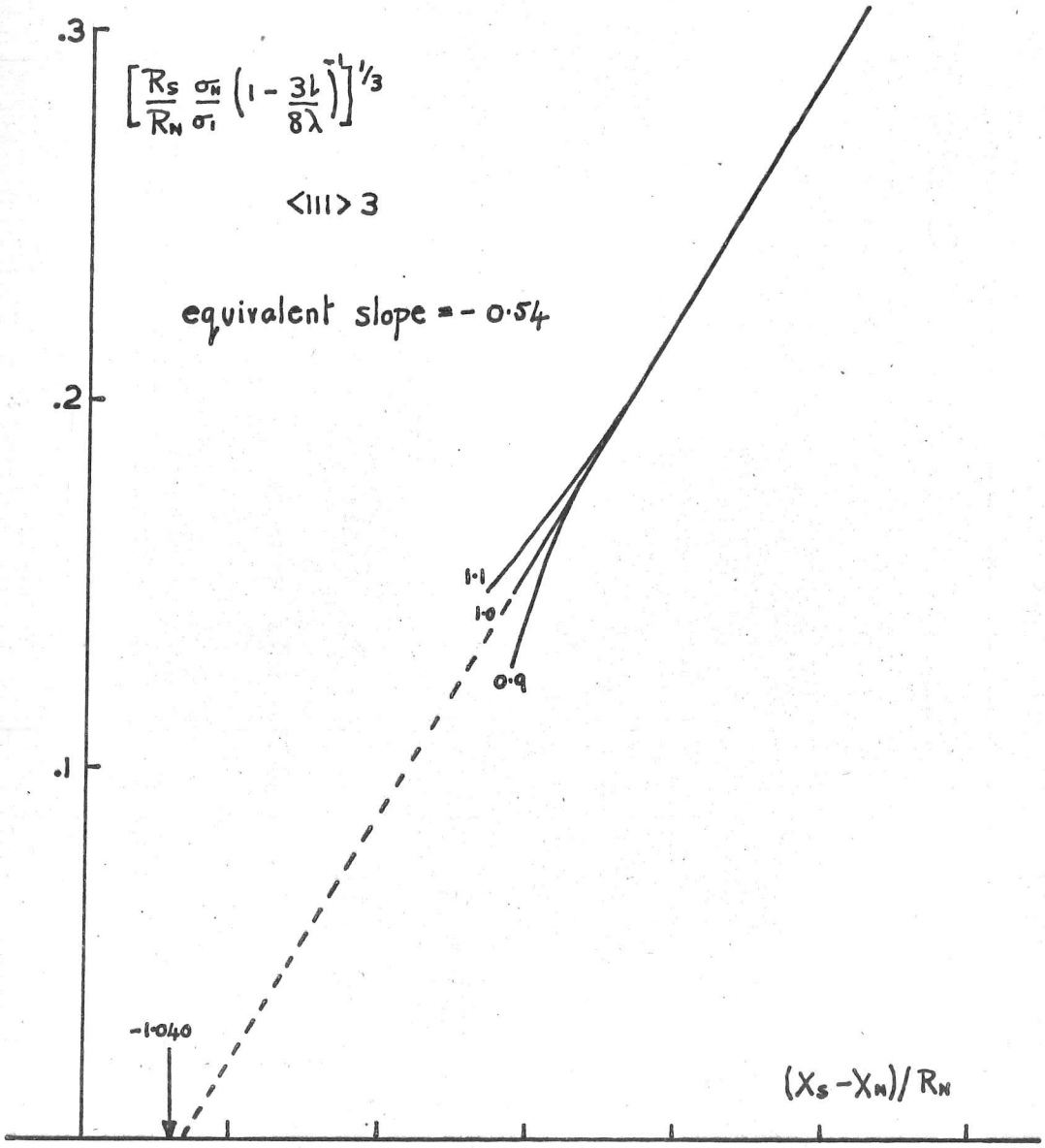
.3
.2
.1
$\left[\frac{R_S}{R_N}\frac{\sigma_N}{\sigma_1}\left(1-\frac{3l}{8\lambda}\right)^{-1}\right]^{1/3}$
<111> 3
equivalent slope = - 0.54
1·1
1·0
0·9
-1·040
$(X_S - X_N)/R_N$
-1.0
-0.5

FIG.23 (a)

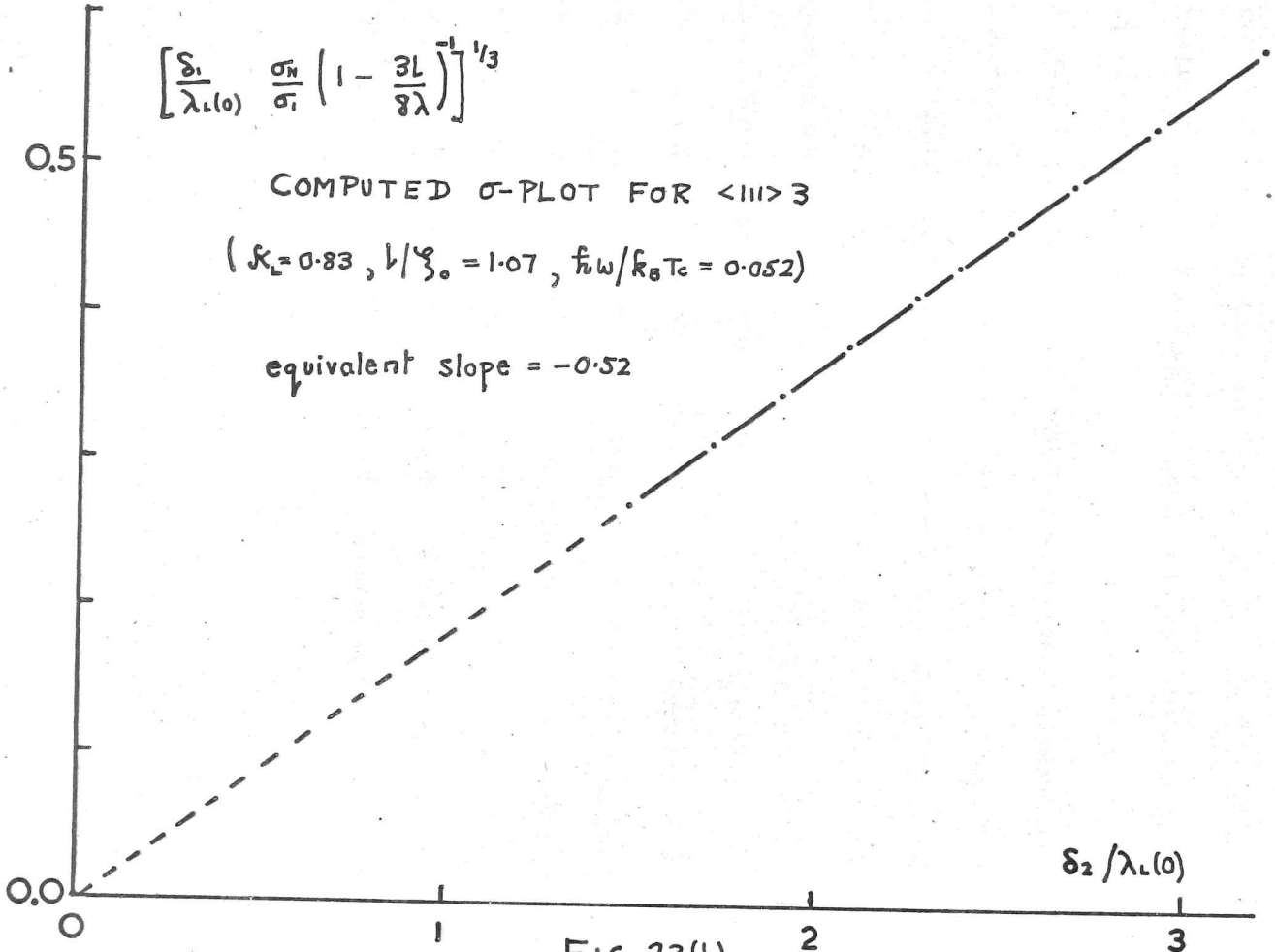
$\left[\frac{\delta_1}{\lambda_L(0)}\ \frac{\sigma_N}{\sigma_1}\left(1-\frac{3L}{8\lambda}\right)^{-1}\right]^{1/3}$
0.5
COMPUTED σ-PLOT FOR <111> 3
(κ_L = 0.83 , l/ξ_0 = 1.07 , $\hbar\omega/k_B T_c$ = 0.052)
equivalent slope = −0.52
0.0
0
1
2
3
$\delta_2/\lambda_L(0)$

FIG. 23(b)

this can be done with a value of $l/\xi_0 = 1.07$ and a B.C.S. energy gap, and we show in fig. (24) the results of the detailed computation for these values where we have included Argand plots of the impedance also for the low- and high-temperature regions. As will be seen, the fit obtained with these parameters is very satisfactory, at any rate up to t = 0.97, and it is evident that, in particular, the penetration depth in this specimen can be fitted quite simply with a B.C.S. energy gap in contrast to the conclusions of Maxfield & McLean, and French, for purer niobium. The predicted penetration depth is certainly correct to within the experimental error as regards its slope against y(t) and absolute value, and the low-temperature surface resistance is well fitted too though here the scatter of the experimental data precludes great accuracy. We have included in the figures computations for an energy gap of 0.8 B.C.S., and also curves for $l/\xi_0 = 0.90$ and 1.24 for comparison.

If we take the figures of $\kappa_L = 0.83$ and $l/\xi_0 = 1.07$ as representing the best fit to the results, then using our mean value of $(\rho l) = 4.6 \times 10^{-12} \Omega.\text{cm.}^2$ for this specimen we arrive

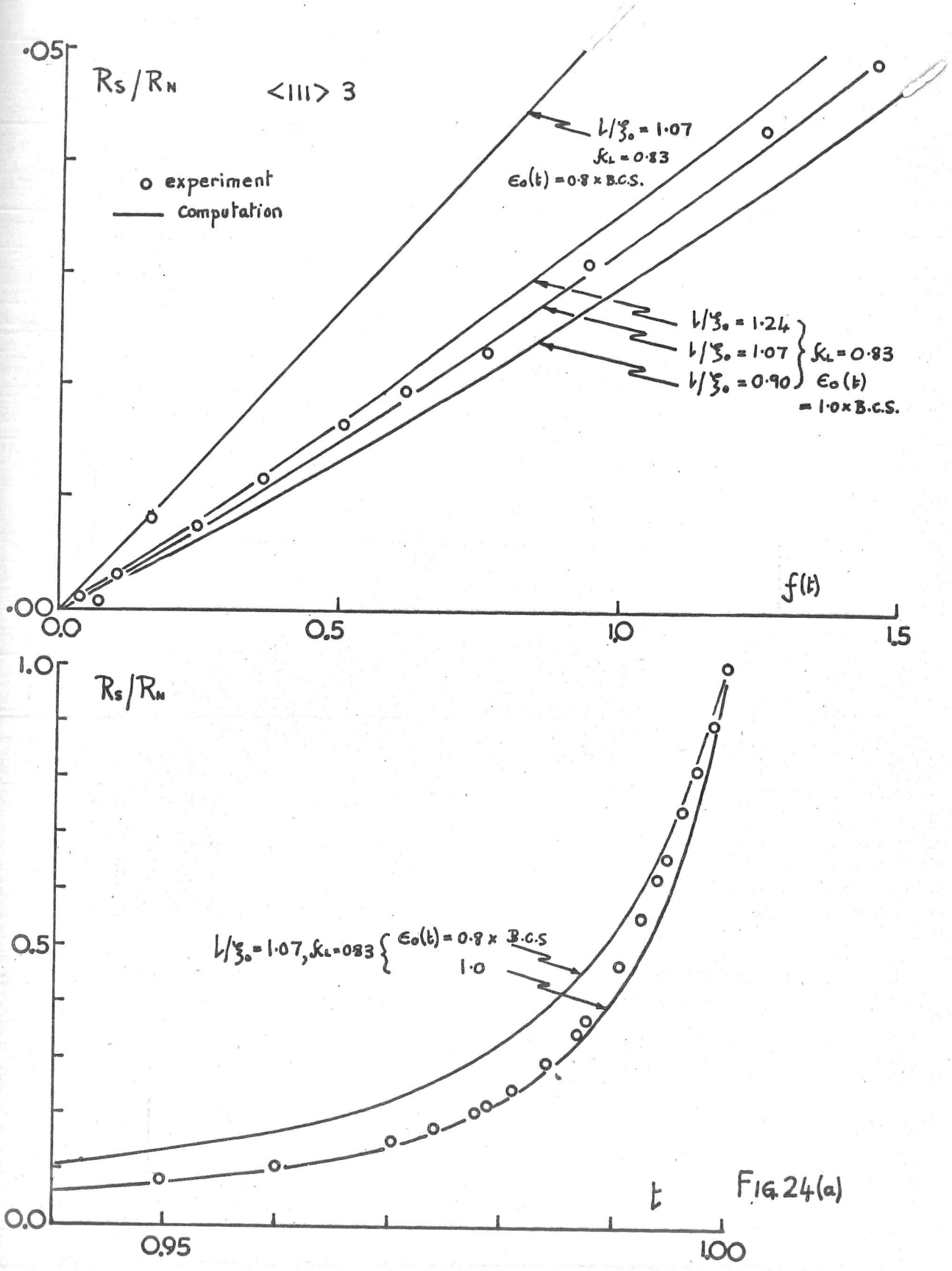
·05
·00
R_S/R_N
<111> 3
o experiment
— computation
$l/\xi_0 = 1.07$
$f_L = 0.83$
$\epsilon_0(t) = 0.8 \times$ B.C.S.
$l/\xi_0 = 1.24$
$l/\xi_0 = 1.07$
$l/\xi_0 = 0.90$
$f_L = 0.83$
$\epsilon_0(t) = 1.0 \times$ B.C.S.
$f(t)$
0.0
0.5
1.0
1.5
1.0
0.5
0.0
R_S/R_N
$l/\xi_0 = 1.07, f_L = 083$
$\epsilon_0(t) = 0.8 \times$ B.C.S
1.0
t
0.95
1.00

FIG. 24(a)

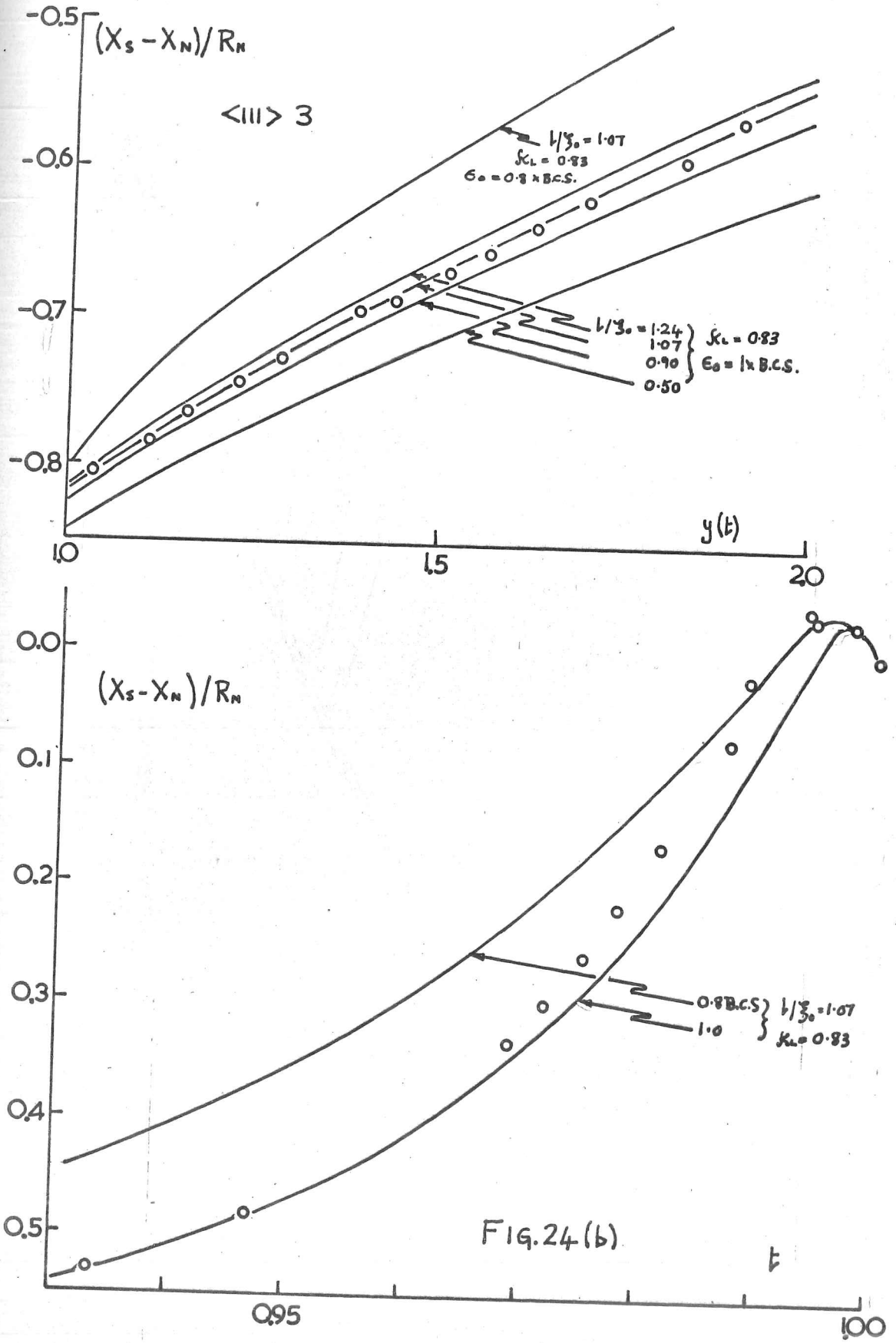
-0.5
$(X_s - X_N)/R_N$
<111> 3
-0.6
$l/\xi_0 = 1.07$
$\kappa_L = 0.83$
$\epsilon_0 = 0.8 \times$ B.C.S.
-0.7
$l/\xi_0 = 1.24$
1.07
0.90
0.50
$\kappa_L = 0.83$
$\epsilon_0 = 1 \times$ B.C.S.
-0.8
y(t)
1.0
1.5
2.0
0.0
$(X_s - X_N)/R_N$
0.1
0.2
0.3
0.4
0.5
0.8 B.C.S
1.0
$l/\xi_0 = 1.07$
$\kappa_L = 0.83$
t
0.95
1.00

FIG. 24 (b)

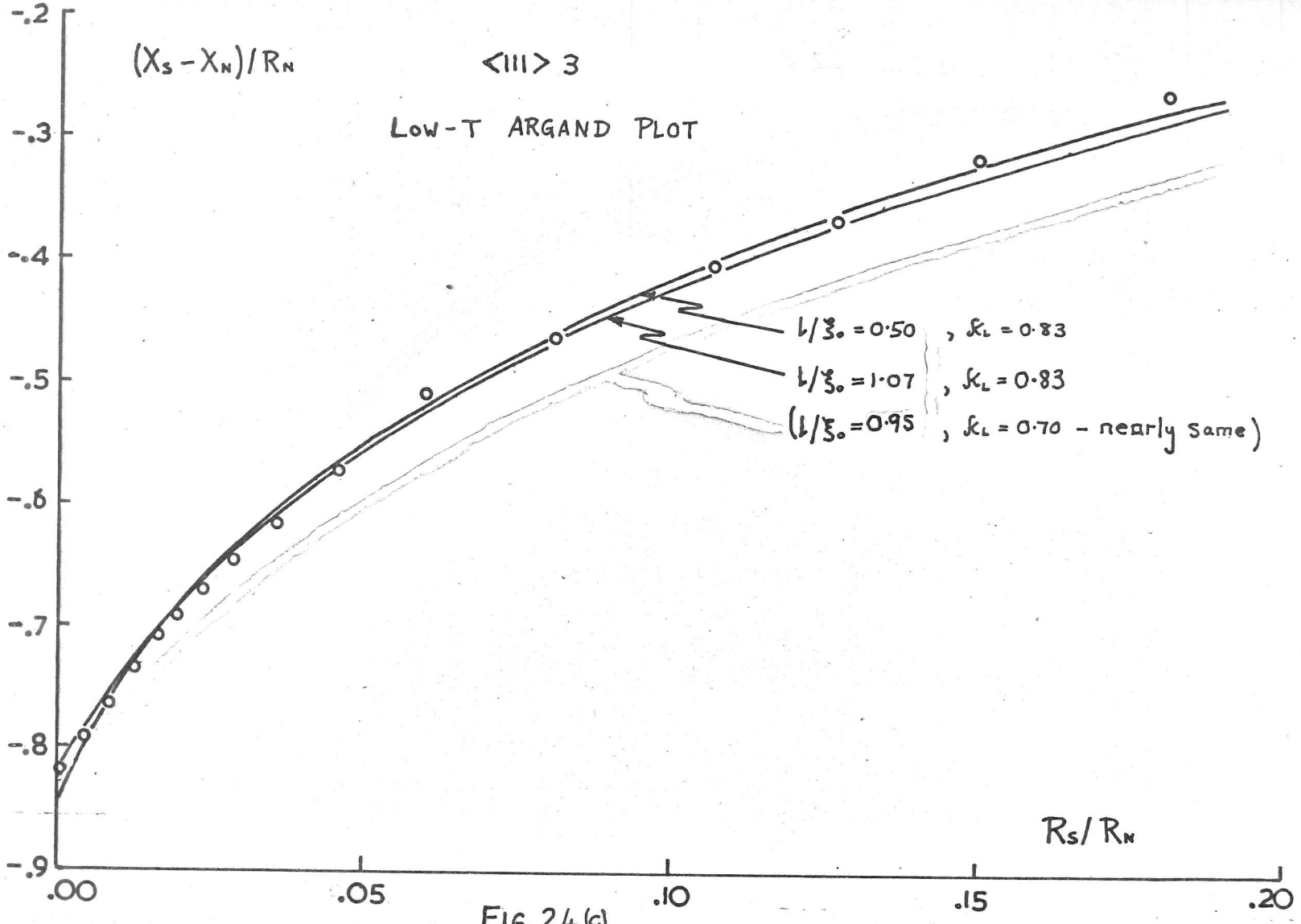
(Xs - XN)/RN
<111> 3
LOW-T ARGAND PLOT
-.2
-.3
-.4
-.5
-.6
-.7
-.8
-.9
.00
.05
.10
.15
.20
Rs/RN
l/ξ0 = 0.50 , kL = 0.83
l/ξ0 = 1.07 , kL = 0.83
(l/ξ0 = 0.95 , kL = 0.70 - nearly same)

FIG. 24 (c)

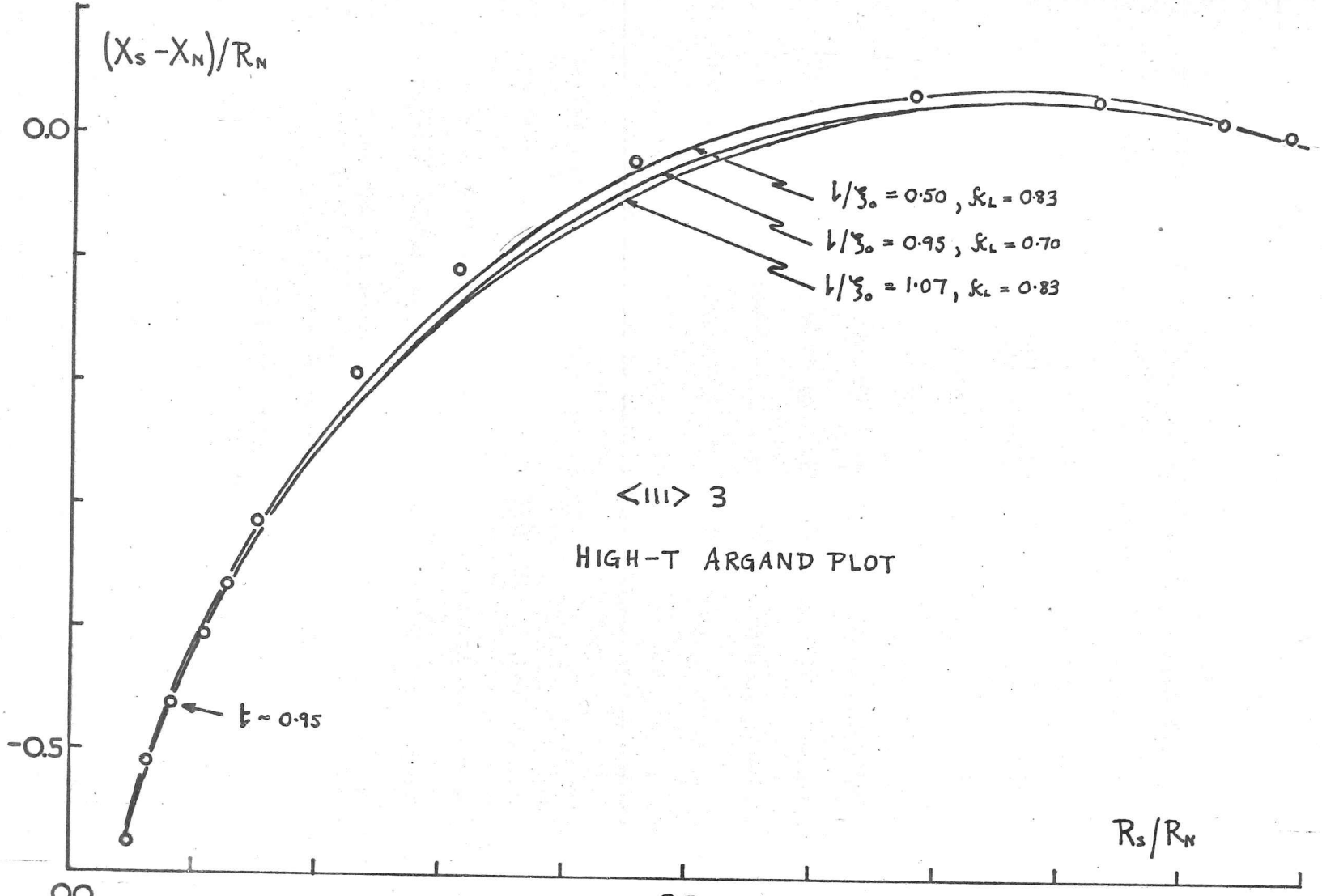

<111> 3

HIGH-T ARGAND PLOT

FIG. 24(d)

at a mean free path $l = 460\text{Å}$, and this allows us to deduce the figures:

$$\begin{cases} \xi_0 = 430\,\text{Å} \quad ; \; v_F = 2{\cdot}7 \times 10^7 \,\text{cm.sec.}^{-1} \\ \lambda_L(0) = 360\,\text{Å} \\ \lambda(0) = 435\,\text{Å} \; - \text{ pure Nb} \end{cases}$$

where, according to the ideas presented in Chapter 1, the Fermi velocity is the phonon-enhanced value. These values are in tolerable agreement with those of other authors given in section 2.

Comment must now be made on the failure of the computation to fit the transition region $0.97 \lesssim t < 1$ for this specimen. Although it seems more than likely that this fact can be dismissed on the basis of the broadening of the D.C. transition alone, in view of the similar difficulties which arise for the purer specimens where the same objection cannot be raised we feel that we should at least consider what modifications to the calculation might conceivably fit the results.

For this purpose, it is convenient to refer to the high-

temperature Argand plot where it will be seen that near the transition the computed curve based on the previously deduced parameters lies below the experimental points. A point which ought to be made is that this is not really what would be expected for a specimen with a blurred transition; presumably a reasonable model in such a case is one with an approximately Gaussian distribution of transition temperature, and roughly speaking one would expect that any given point on the ideal plot would receive contributions to its impedance from points on the surrounding curve within the temperature width of the blurring. The effect of this would be to shift each point of the plot roughly along the inward-pointing normal to the curve, that is in the direction of decreasing reactance; the actual deviation is opposite to this in fact, so that perhaps we should not be too glib about the effects of transition-blurring. A further point to be made concerning the experimental points is that in the case of such a dirty specimen where the surface resistance drops very rapidly below Tc our ability to make the heating correction accurately (about 70 $m^{\circ}K$ for this specimen) is severely taxed.

The most significant remark to be made about the deviation is that it appears that no simple change in the energy-gap is capable of fitting it; to be sure, either part of the impedance could be fitted by a temperature-dependent scaling down of the gap for $t > 0.97$ (see fig. (24a,b)), but the effect on the Argand plot is indiscernible - for example near Tc the computation shews the same Argand plot for 0.8 x B.C.S. gap as for 1.0 x B.C.S. gap, differences between the plots setting in only at the lowest temperatures. This is presumably because over a considerable temperature range the current response of the superconductor in our sort of frequency range is dominated by its dependence on the ratio ($k_B T/\epsilon_0(T)$) rather than on ($\hbar\omega/\epsilon_0(T)$); thus although the temperature scaling along the impedance plot can be modified significantly, its shape cannot and there is no evidence for a non-B.C.S. gap in this specimen, at any rate. This concept is one which will be found of even more relevance in the discussion of the purer specimens in section 4.

Another possibility to be considered is that the London-Pippard character of the superconductor is different near Tc as compared with its low-temperature behaviour, that is that the

normal- and super-currents are scaled differently here. This could be effected in two ways:

1. a change in the effective coherence length near Tc:

$$\xi_0 \longrightarrow \xi_0' \quad , \quad 1/\xi_0 \longrightarrow 1/\xi_0'$$

thus changing the range of the supercurrent, but not changing κ_L.

2. a change in the effective coherence length in which κ_L is also allowed to change in such a way as to maintain (ρl) constant.

Both these methods of scaling the supercurrent are similar to that discussed by Waldram in obtaining a value for the effective coherence length near Tc in his impure tin specimens but we should note that his use of $\xi_0' = 0{\cdot}75\,\xi_0$ is the B.C.S. value for the effective range of the supercurrent near Tc and is therefore already included in our computation. Using either of these rather arbitrary scalings, it is found difficult to fit the experimental points without somewhat unreasonable changes in the parameters (for example, see the Argand plot fig. (24d) in which are shown computations for the values: $\kappa_L = 0{\cdot}83$, $1/\xi_0 = 0{\cdot}50$ and $\kappa_L = 0{\cdot}70$, $1/\xi_0 = 0{\cdot}95$ corresponding to the two types of scaling). Using the dirty limit of the two-band

model discussed later in section 4 in which the response kernel is given by:

$$K = K_d + \frac{i\hbar\omega}{\pi \lambda_{LS}^2(0)\, \epsilon_{0S}(0)} \left(\frac{l}{\xi_{0S}}\right) \left(\frac{\sigma_S}{\sigma_N}\right)_S$$

we have also found it difficult to fit the experimental points using the parameters discussed in section 4; the deviation from the single band calculation is nowhere more than about 0.5%. In any case, it is hard to know how valid such an estimate is for this dirty specimen since the calculations of Sung & Wong (28) indicate that the s-d anisotropy should be washed out at our sort of R.R.R. (~ 15), while the specific heat measurements of Shen et al (23) indicate its presence in a specimen of R.R.R. ~ 24.

The final imponderable in our interpretation is the effect of strong-coupling, and it is possible that some sort of temperature-dependent scaling of the effective coherence length could arise on this score, but there is little we can do by way of a detailed discussion.

Summary

We conclude that this specimen for which $l/\xi_0 \simeq .1$ is well-fitted over nearly the whole temperature range by the single-band, weak-coupling B.C.S. theory using parameters already given which appear reasonable on the basis of the results of others; the deviations which do occur near Tc can probably be dismissed as due to transition broadening in this specimen. We now pass to a consideration of the purer specimens.

4 PURE SPECIMENS:

Before we proceed to a detailed discussion of the results for the pure specimens, a point of experimental uncertainty must be made; in chapter 3 we indicated that the 'extraneous' losses for our pure niobium specimens tended to be unusually high, and in the following table we give these losses together with the normal-state bandwidths for comparison:

specimen	R.R.R.	extraneous loss Re kc./s.	R_N/T_c kc/s.	R_e/R_N
<111> 1	1180	136	413	0.33
<111> 2	225	138	500	0.28
<111> 3	15.4	29	1389	0.02
<100> 1	442	156	665	0.23
<100> 2	177	117	550	0.21
<110> 1	802	145	415	0.35
<110> 2	126	85	685	0.12

These estimates of extraneous loss were obtained in the 'usual' way for surface impedance measurements, namely by plotting the low temperature bandwidths against f(t) and extrapolating to t = o; unfortunately, our measurements only extended down to T = 4.2°K. and in retrospect it would have been better to have pumped down to 1.2°K. at any rate to check for any possible low

temperature anomalies. All the measurements were made with the same dielectric specimen holder, though some uncertainty always arises over the contribution of the distrene cement used to hold the specimen in position. The estimates of extraneous loss are also subject to the accuracy with which the coupling losses can be subtracted out; in most cases, we did not actually made a coupling extrapolation at helium temperatures, being content to calculate the coupling losses by assuming that the low-temperature padding attenuators retained the same value as deduced in the nitrogen-temperature extrapolation. Where checks were made, this assumption appeared to be justified to better than 1%. With these provisos in mind, we see from the table that there is a suspicion of a correlation between the extraneous losses and specimen purity - certainly the loss for specimen <111> 3 is markedly less than that for the purer specimens and is much more nearly equal to that obtained for the lead specimen (27 kc./s.) to which we referred in Chapter 3. In view of the arguments to be presented later concerning possible two-band effects in our results, we are unable to exclude the possibility that these apparently extraneous losses, even at $t \sim 0.45$, are in fact large real losses in the superconductor.

Such an eventuality does not appear to be a result of the simple calculations which we shall give later, nor does it appear to agree with the results of Turneaure & Weissmann (21) who seem to have been able to fit their measurements of low temperature surface resistance to the single-band model, at any rate between $\sim 2^{\circ}$K. & 4.2°K., though they have made no measurements at higher temperatures. Also it may be noted that if the extraneous losses were truly real, our measurements of normal-state surface resistance would tend to be even more incomprehensible than they are at present, the failure of the $\delta(\rho)$ plots to 'join up' for specimens of different purity becoming yet more severe. Therefore, for the moment, we tentatively assume that we can neglect this possibility while recognizing that a reanalysis of our results might have to take it into account.

We now attempt to analyse our measurements of low temperature impedance using Waldram's σ-plot for the pure regime, namely:

$$\left(\frac{R_S}{R_N}\frac{\sigma_N}{\sigma_1}\right)^{1/4} \text{ vs. } (X_S - X_N)/R_N$$

None of our specimens is sufficiently pure to be completely within this regime, but nevertheless our surface-impedance computation

shows that this plot should be a reasonable approximation even for specimen <100> 2, say. In fig. (25) is shown the plot of:

$$\left(\frac{\delta_1}{\lambda_L(0)}\,\frac{\sigma_N}{\sigma_1}\right)^{1/4} \quad \text{vs.} \quad \frac{\delta_2}{\lambda_L(0)}$$

for the mean free path which we have estimated for this specimen (~ 4000Å) using the computed values of $\delta_{1,2}$ for a B.C.S. gap. The plot is satisfactorily linear, but does not quite pass through the origin; this effect reduces for longer mean free paths representing the correction necessary for finite mean free path and is about 3% of the normal state resistance in the shift intercept for <100> 2. We have in all cases computed this correction for our experimental shifts, and it is shown on the subsequent σ-plots. Also shown in fig. (25) is the computed σ-plot in which the cube root is taken (as in the dirty limit) for comparison.

In fig. (26) are shown the experimental σ-plots for our specimens, together with the computed mean free path corrections, and the values of λ_N/R_N already calculated in section 1. All the plots can be straightened for an energy gap near to 1.1 x B.C.S.

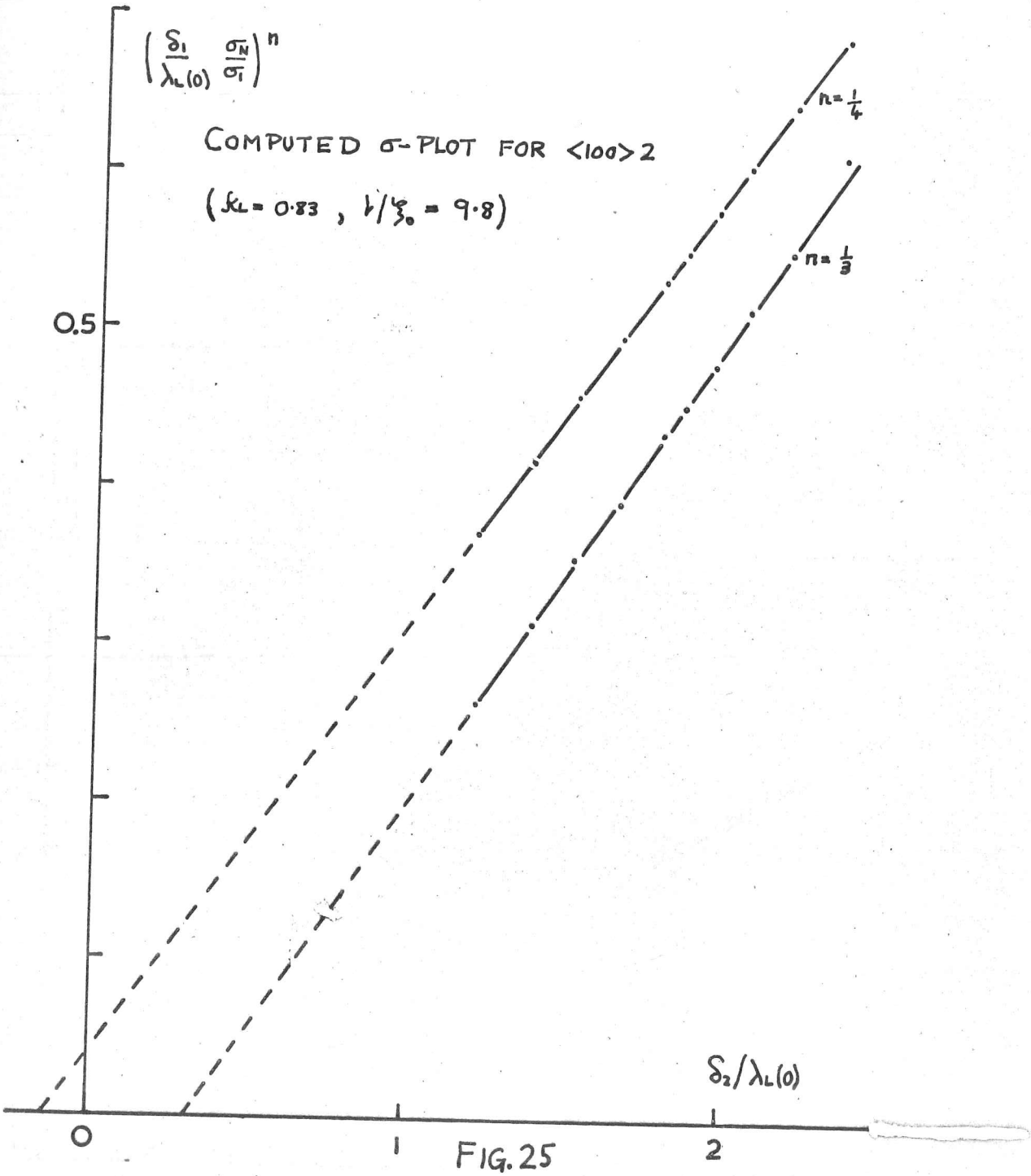
$\left(\frac{\delta_1}{\lambda_L(0)}\,\frac{\sigma_N}{\sigma_1}\right)^n$
COMPUTED σ-PLOT FOR <100>2
($k_L = 0.83$, $b/\xi_0 = 9.8$)
$n = \frac{1}{4}$
$n = \frac{1}{3}$
0.5
0
1
2
$\delta_2/\lambda_L(0)$

FIG. 25

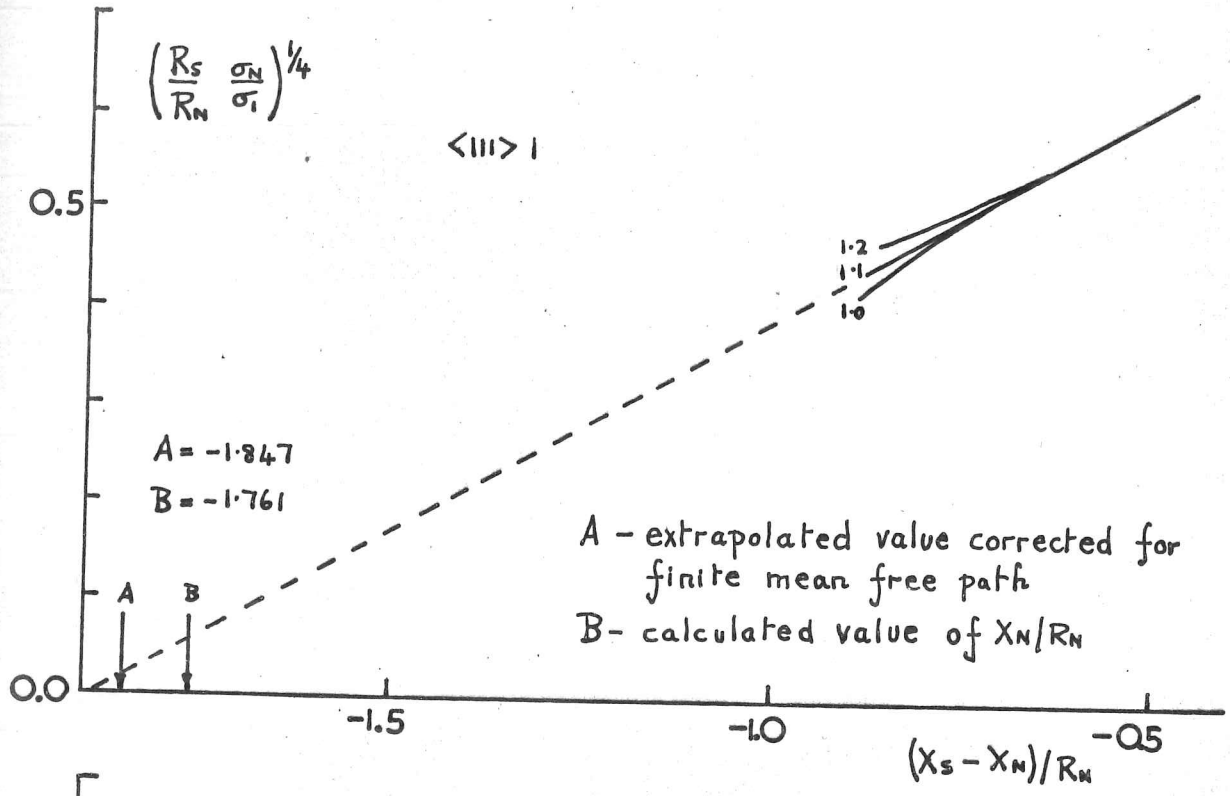
$\left(\frac{R_S}{R_N}\frac{\sigma_N}{\sigma_i}\right)^{1/4}$
<111> I
0.5
0.0
1·2
1·1
1·0
A = -1·847
B = -1·761
A
B
A - extrapolated value corrected for finite mean free path
B - calculated value of X_N/R_N
-1.5
-1.0
-0.5
$(X_S - X_N)/R_N$

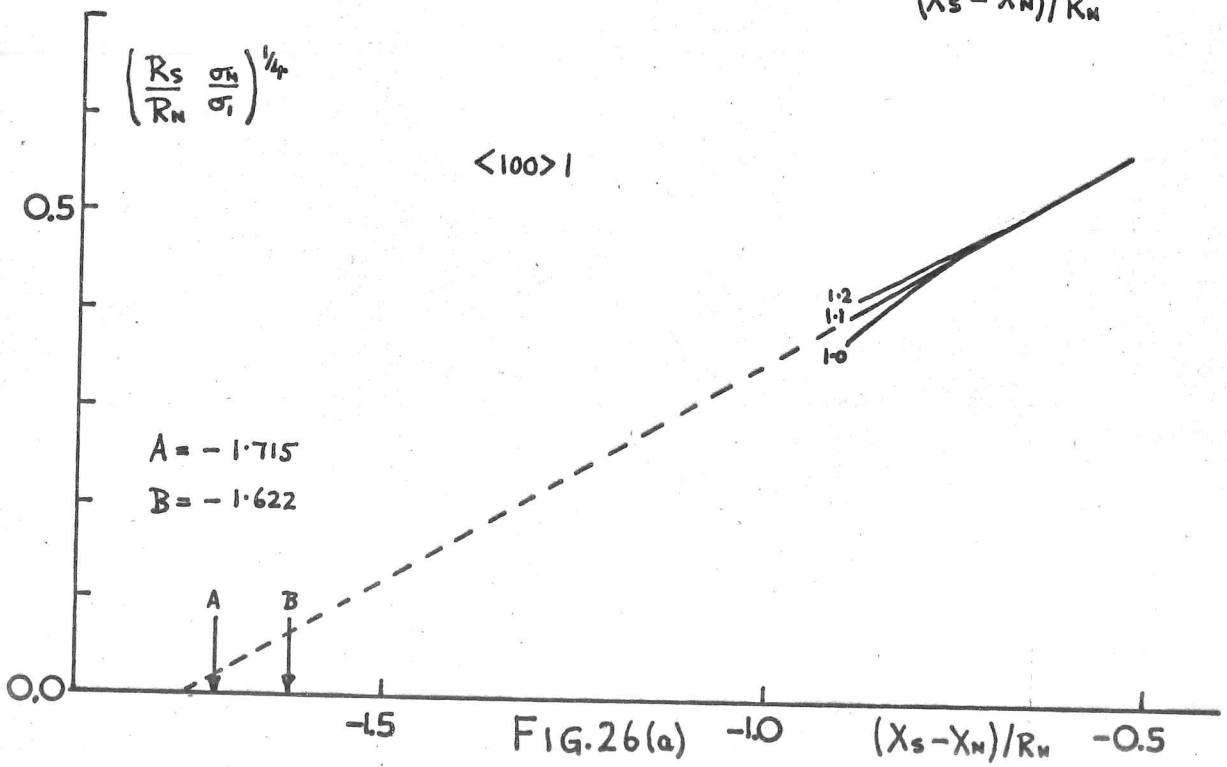
$\left(\frac{R_S}{R_N}\frac{\sigma_N}{\sigma_i}\right)^{1/4}$
<100> I
0.5
0.0
1·2
1·1
1·0
A = - 1·715
B = - 1·622
A
B
-1.5
-1.0
-0.5
$(X_S - X_N)/R_N$

FIG.26(a)

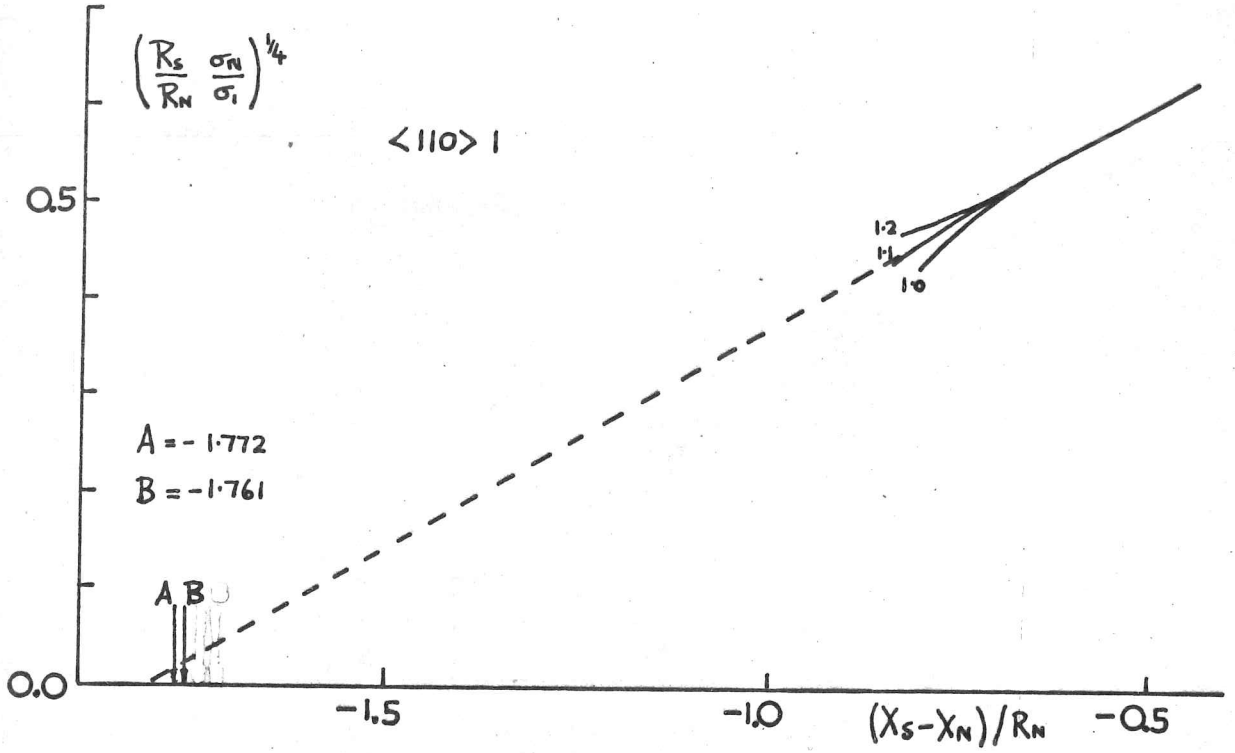
$\left(\frac{R_S}{R_N}\frac{\sigma_N}{\sigma_i}\right)^{1/4}$
<110> 1
0.5
0.0
1·2
1·1
1·0
A = - 1·772
B = - 1·761
A B
-1.5
-1.0
$(X_S - X_N)/R_N$
-0.5

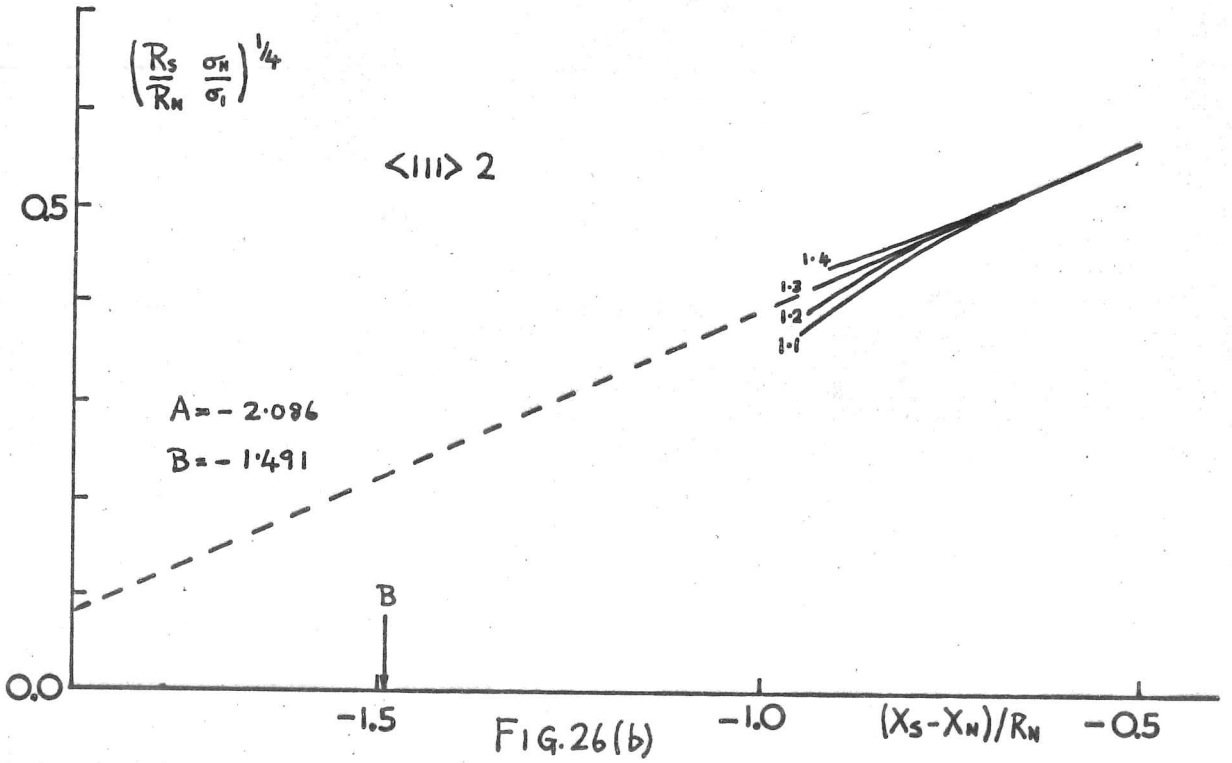
$\left(\frac{R_S}{R_N}\frac{\sigma_N}{\sigma_i}\right)^{1/4}$
<111> 2
0.5
0.0
1·4
1·3
1·2
1·1
A = - 2·086
B = - 1·491
B
-1.5
-1.0
$(X_S - X_N)/R_N$
-0.5

FIG. 26(b)

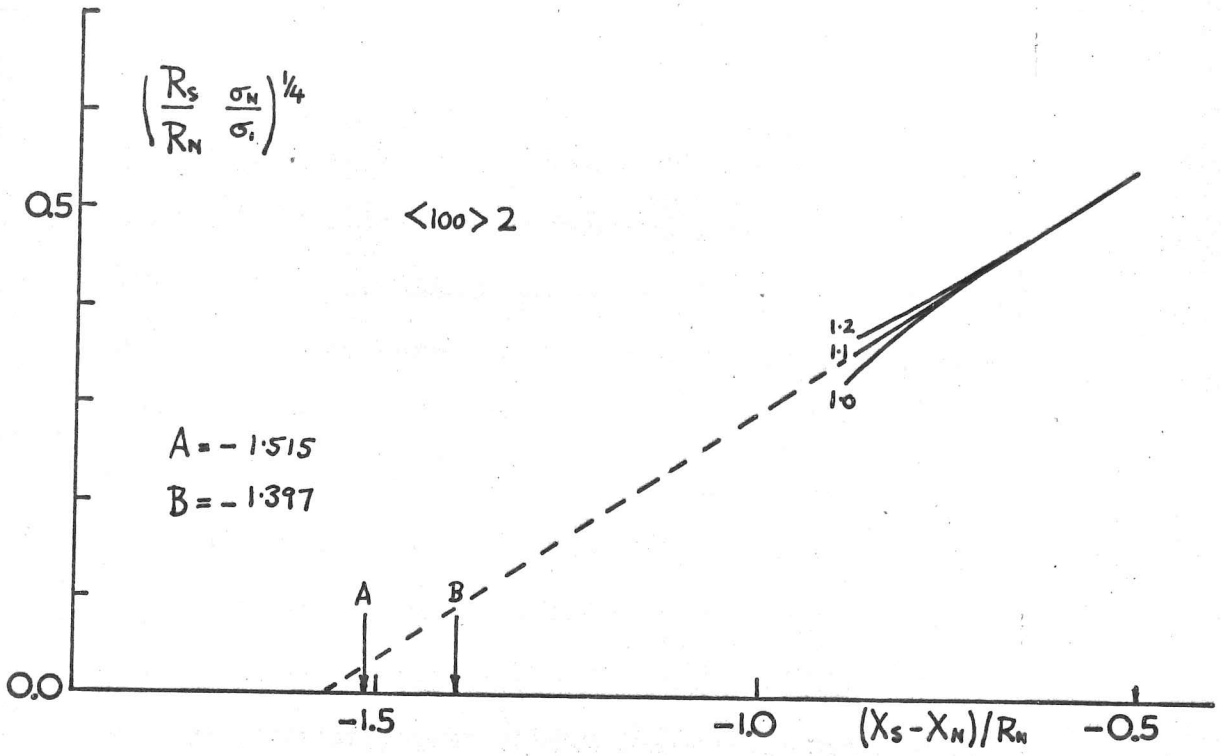
$\left(\frac{R_S}{R_N}\ \frac{\sigma_N}{\sigma_i}\right)^{1/4}$
0.5
<100>2
1·2
1·1
1·0
A = − 1·515
B = − 1·397
A
B
0.0
−1.5
−1.0
$(X_S - X_N)/R_N$
−0.5

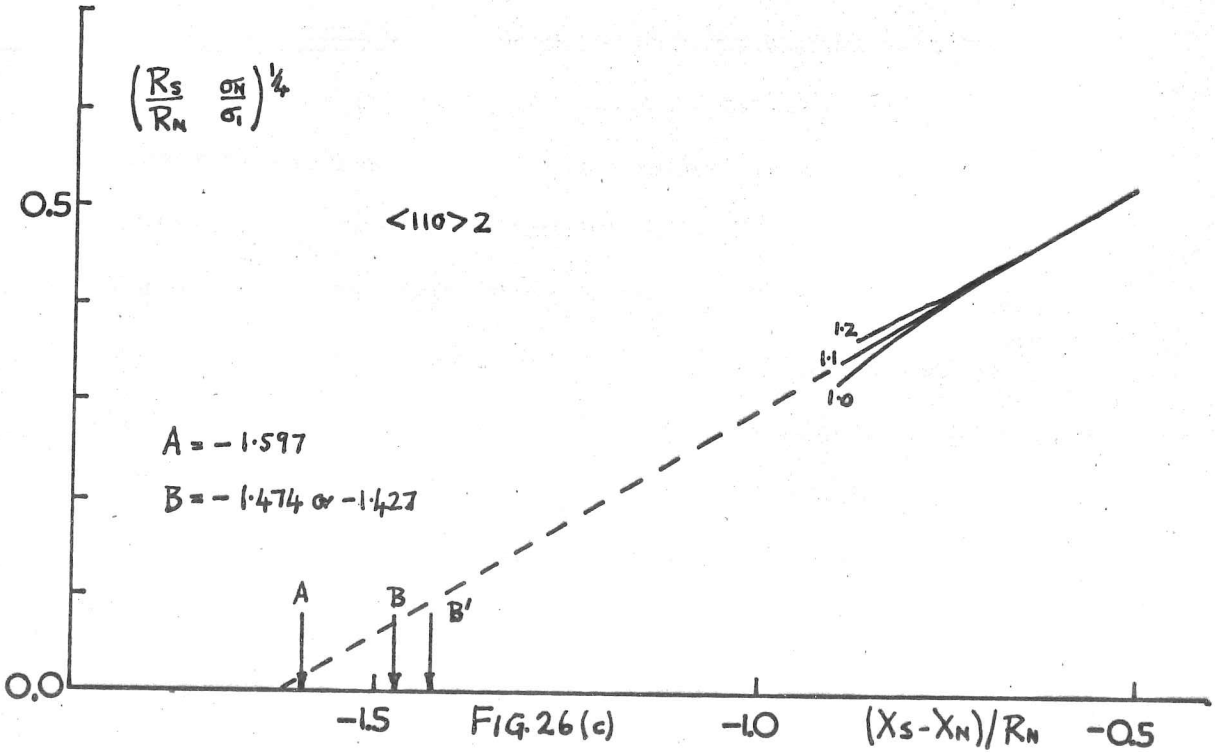
$\left(\frac{R_S}{R_N}\ \frac{\sigma_N}{\sigma_i}\right)^{1/4}$
0.5
<110>2
1·2
1·1
1·0
A = − 1·597
B = − 1·474 or −1·427
A
B
B'
0.0
−1.5
−1.0
$(X_S - X_N)/R_N$
−0.5

FIG. 26(c)

except that for $\langle 111 \rangle$ 2 which would indicate near to 1.3 x B.C.S. ; this latter value is curiously high and must serve to cast some doubt upon the validity of the σ-plot for this specimen at least, particularly in view of the more reasonable value for $\langle 111 \rangle$ 1. An unfortunately consistent feature of all these plots is that they tend to indicate a zero error such as would decrease all the measured shifts and thus increase all the calculated penetration depths; we shall see later that we shall have enough difficulty in explaining the largeness of even the uncorrected penetration depths. It seems odd that the zero error should have the same sign for all 6 specimens since if it were due to the effects of skewness or line reflections, it would be expected to be random; we note that in fact all our curves of measured shifts join up remarkably well at $t \sim 0.95$ which is approximately the point below which shift measurements are made by taking alternate frequency readings at a given level in the normal & superconducting states, and above which they are made by noting power transmissions at a given frequency. This would tend to indicate that we have made the skewness correction to the low temperature shifts rather well, and the

only remaining source of zero error should be that produced by a differential distortion of the shifts such as might arise from line reflections, or thermal expansion of the specimen in the cases where temperature switching to the normal-state was used. As remarked line reflections should almost certainly be highly frequency dependent, and would thus be expected to be random from one specimen to another, unlike thermal expansion which would give a zero error of consistent sign. This latter effect would serve to decrease the apparent shift as the σ-plot would suggest, but an order of magnitude estimate shows it to be utterly improbable as an appreciable source of error since:

$$\alpha|_{Nb,\,10°K.} \sim 4\times10^{-8}\ °K.^{-1} \qquad (86)$$

giving: $\delta\nu \sim 10^{10}\times 4\times10^{-8}\times 5$ c./s. ~ 2 kc./s.

Equally, it is difficult to envisage slight changes in coupling with temperature as being sufficient to account for the shift in zero.

A further source of uncertainty which has already been mentioned is the retardation correction to the value of X_N/R_N; since we have already had difficulty in understanding the normal-

state surface resistance, it would not be altogether surprising if the reactance behaved anomalously too and in retrospect it might have been useful to have made shift measurements in the normal-state also. For these reasons, we have preferred not to regard the σ-plots as giving very reliable estimates of any putative zero errors in our measured shifts for pure niobium particularly since the whole basis of the plot is open to question in a two-band superconductor as we shall see later. Under the circumstances, it seems more reliable to take the experimental shifts as being probably free of any very large errors and to deduce values of penetration depth from these using the previously estimated values of X_N/R_N.

Accordingly, we have used the uncorrected shifts to calculate values of the penetration depth $\lambda(o)$ (applying a small correction for finite mean free path from the results of Miller); it is then possible self-consistently to fit these penetration depths using the measured values of (ρl) and regarding the coherence length (and therefore Fermi velocity) as an adjustable parameter. The relations:

$$\Lambda(0) = \frac{\rho l}{v_F} \quad ; \quad \xi_o = \frac{\hbar v_F}{\pi \epsilon_0(0)}$$

and the B.C.S. relationship for $\lambda/\lambda L$ as a function of ξ_o/λ_L yield the following values on taking $\epsilon_o(o) = 1.10 \times$ B.C.S. for our specimens:

specimen	$\lambda(o)$ Å	$\lambda L(o)$ Å	ξ_o Å	$10^{-7} v_F$ cm.sec^{-1}	κ_L
<111> 1	570	530	185	1.4	2.9
<111> 2	430	360	350	2.6	1.03
<100> 1	520	470	250	1.9	1.87
<100> 2	410	350	310	2.3	1.15
<110> 1	690	640	195	1.4	3.3
<110> 2	600	520	390	2.9	1.34
	(550	480	340	2.5	1.43)

In calculating the values of $\lambda(o)$, we have ignored the small kinks in the shifts at low y(t) for <100> 1, <110> 1, and extrapolated back the upper portion of the shift curves; such kinks certainly cannot be fitted to the B.C.S. theory, though we believe they may be real.

These figures immediately pose some problems. It would seem that in each case, the less pure specimen of each orientation has a more nearly reasonable value of $\lambda(o)$ and derived parameters than the purer ; <111> 2 & <100> 2 are really quite reasonable, though $\lambda(o)$ for <110> 2 is rather high even if we take the modified

value of (ρl) as in section 1 (shown in brackets). However, we have seen from our normal-state measurements that (ρl) is high for this orientation, and this may represent a true anisotropy in the effective area of the Fermi surface, the values for the Fermi velocity and coherence length still being comparable with the other orientations. In fig. (27) we plot $\lambda(o)$ as a function of mean free path l/ξ_o together with the B.C.S. prediction for $\kappa_L = 0.83$. If we take these penetration depths seriously, the increasing divergence in the pure specimens for each orientation at long mean free paths is most remarkable and quite inconsistent with the usual mean free path dependence of penetration depth in a superconductor, where there is always a monotonic decrease in $\lambda(o)$ with increasing l. We believe that this behaviour may have a plausible explanation in terms of the two-band properties of niobium, but defer discussion of this until later.

It is important first that any sources of experimental error should be examined in regard to these results. Firstly we note that had we used the σ-plots to correct the values of shift, the penetration depths derived would have been uniformly even

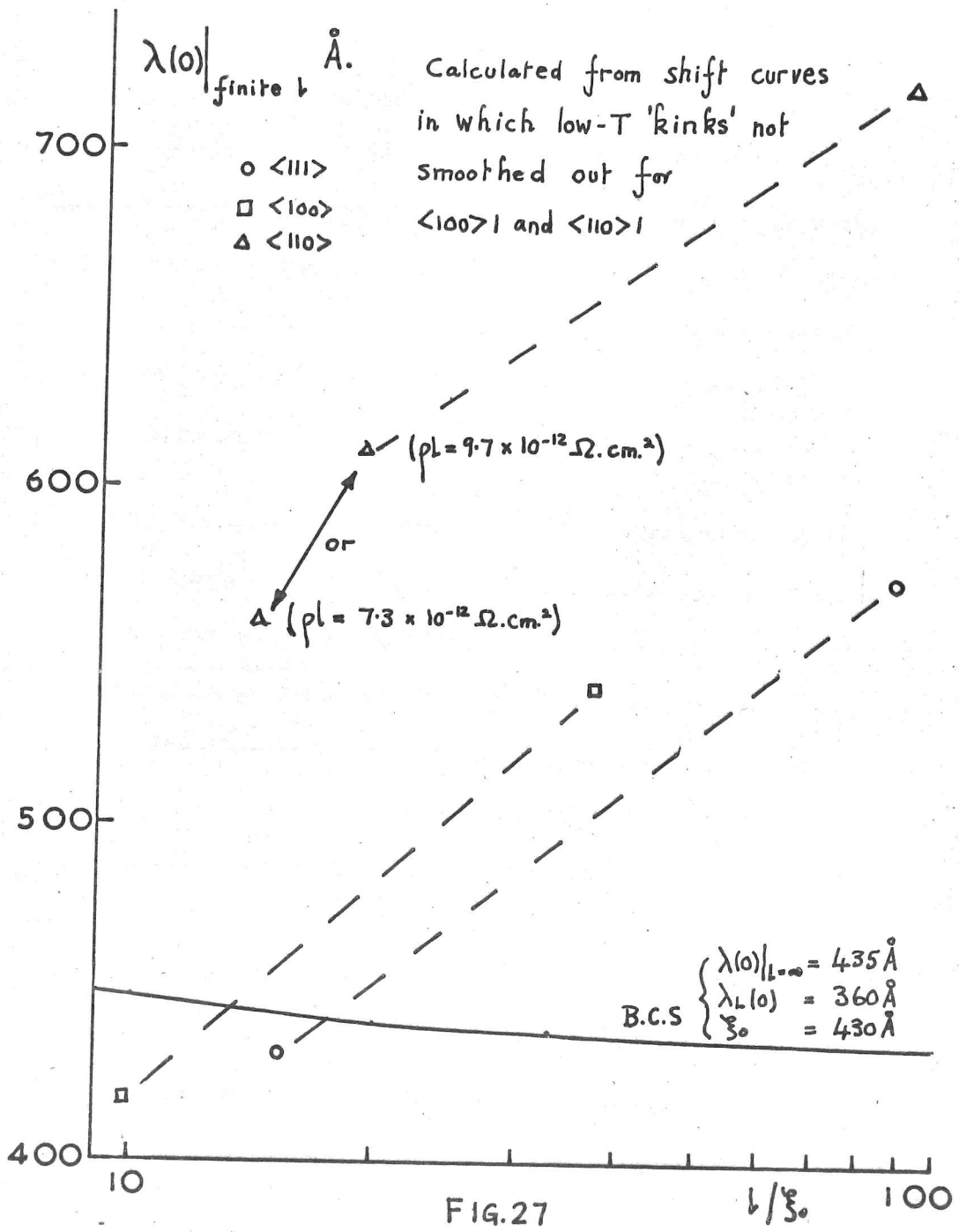
λ(0)|finite l Å.
Calculated from shift curves in which low-T 'kinks' not smoothed out for <100>1 and <110>1
o <111>
□ <100>
Δ <110>
700
600
500
400
Δ (ρl = 9·7 × 10⁻¹² Ω.cm.²)
or
Δ (ρl = 7·3 × 10⁻¹² Ω.cm.²)
B.C.S
λ(0)|l=∞ = 435 Å
λL(0) = 360 Å
ξ0 = 430 Å
10
100
l/ξ0

FIG. 27

larger and more inexplicable. Secondly, as regards the large extraneous losses, if these are real losses then the usual assumption that the reactive microwave skin depth correctly extrapolates to the D.C. penetration depth $\lambda(o)$ at $y = 1$ may be incorrect if there is any considerable structure below $y = 1.02$ (corresponding to $T = 4.2^{o}K$); again, this is a possibility which cannot be totally eliminated.

We now examine to what extent the experimental impedances can be reconciled with the penetration depths and coherence lengths which we have tentatively deduced. Our fitting of the peculiarly large penetration depths was based on regarding the area of Fermi surface as fixed by the measured value of (ρl) for each specimen, and on the Fermi velocity & coherence length as adjustable parameters; the largeness of the penetration depth forced us to use rather low values of V_F & ξ_o in order to increase the London penetration depth, thus making the superconductor more London-like than would be expected from magnetisation measurements particularly for the purest specimens. The large correction found necessary to the Fermi velocity for these latter

specimens particularly in fact renders the calculation no longer self-consistent, since the normal metal now becomes significantly more retarded. This implies that our estimated value of (pl) should be increased, and the value of χ_N/ρ_N is also significantly increased thereby resulting in an increase in the estimate of the penetration depth calculated from the measured frequency shifts. The iterative calculation which is required to fit the purest specimens '1' actually appears to diverge slowly, but not before it has reached quite ridiculous values of κ_L , and we have in fact found it impossible to obtain a strict fit to the penetration depths.

Accordingly, we have been compelled to adopt a rather arbitrary procedure for the specimens '1' in order to make any sort of attempt to explain the measured penetration depths on the simple theory; this has been achieved by retaining a scaling for the normal-current consistent with our estimates for specimen <111> 3 i.e. taking $\kappa_L = 0.83$, $\xi_0 = 430\text{Å}$, and regarding the supercurrent scaling as adjustable. This can be done by varying:

1. London-Pippard character i.e. κ_L
2. the supercurrent energy gap
3. the supercurrent mean free path

It may be noted that any of these methods can be made reasonable as an approximate description of Fermi-surface-, energy gap-, and scattering- anisotropies since, as observed in Chapter 1, the effective zones for the normal- and super-currents are of markedly different widths representing their differing degrees of non-locality; it is scarcely as reasonable to have to adopt an assumption of a consistent scaling-down of the supercurrent for all our three crystallographic orientations, however. We have chosen simply to scale $\mathcal{K}_L$; the largest scaling necessary is for $\langle 110 \rangle$ 1, the supercurrent being taken as about 57% of its predicted value.

In fig. (28) we show Argand plots of our measured impedances, together with computed curves based on $\mathcal{K}_L = 0.83$, $\xi_o = 430\text{Å}$ and curves in which we have attempted to fit the measured shift; for the less pure specimens '2' we have simply given the computation for our previous 'self-consistent' parameters, though as pointed out they are not in fact self-consistent because of the decrease in Fermi velocity and this accounts for the small discrepancies in the shift at R = o - we have not considered it worthwhile carrying the iteration further because of the already

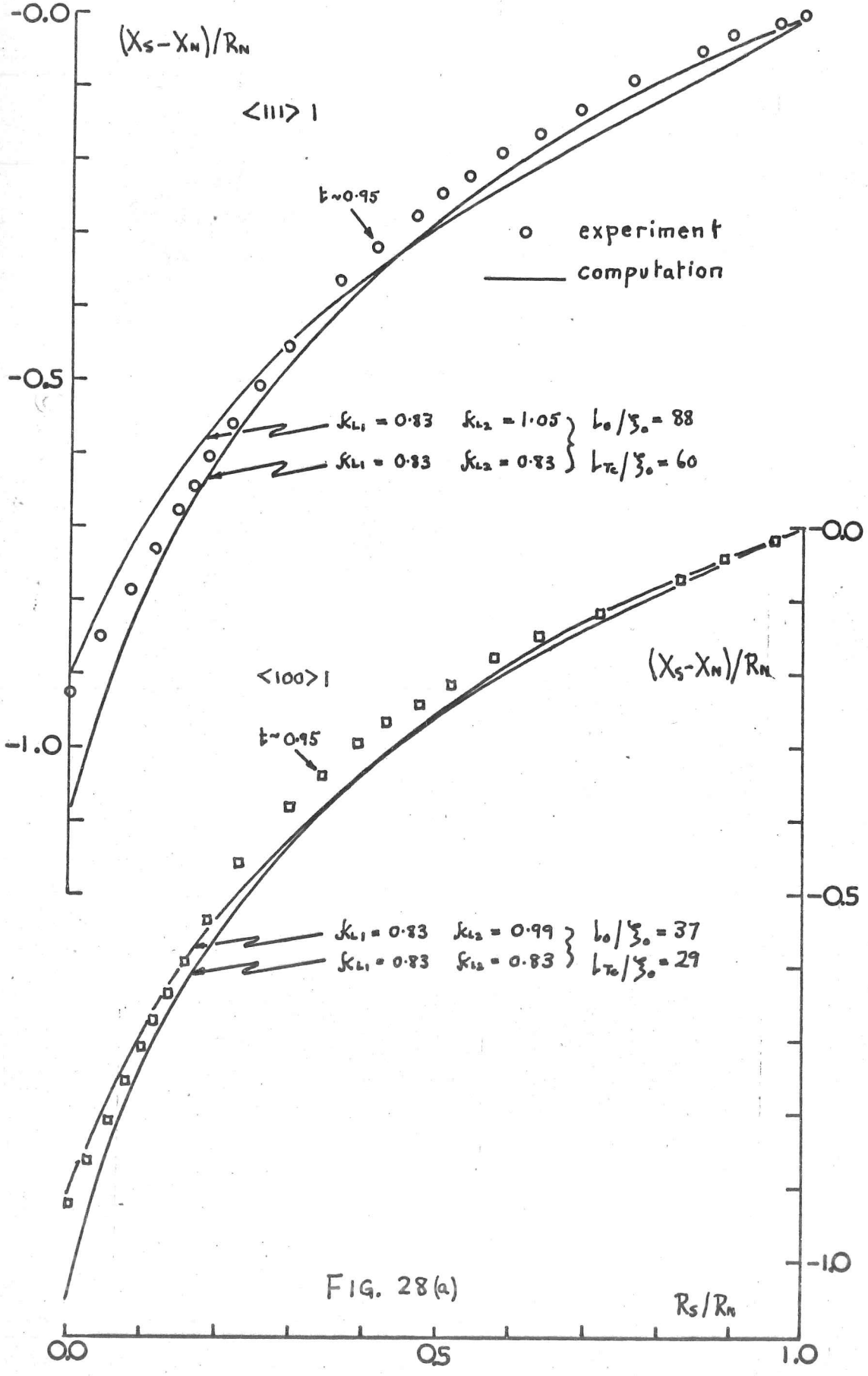
-0.0
(Xs-XN)/RN
<111> I
t~0.95
o experiment
computation
-0.5
kL1 = 0.83 kL2 = 1.05 } L0/ξ0 = 88
kL1 = 0.83 kL2 = 0.83 } LTc/ξ0 = 60
-1.0
<100> I
t~0.95
(Xs-XN)/RN
kL1 = 0.83 kL2 = 0.99 } L0/ξ0 = 37
kL1 = 0.83 kL2 = 0.83 } LTc/ξ0 = 29
0.0
0.5
1.0
Rs/RN

FIG. 28(a)

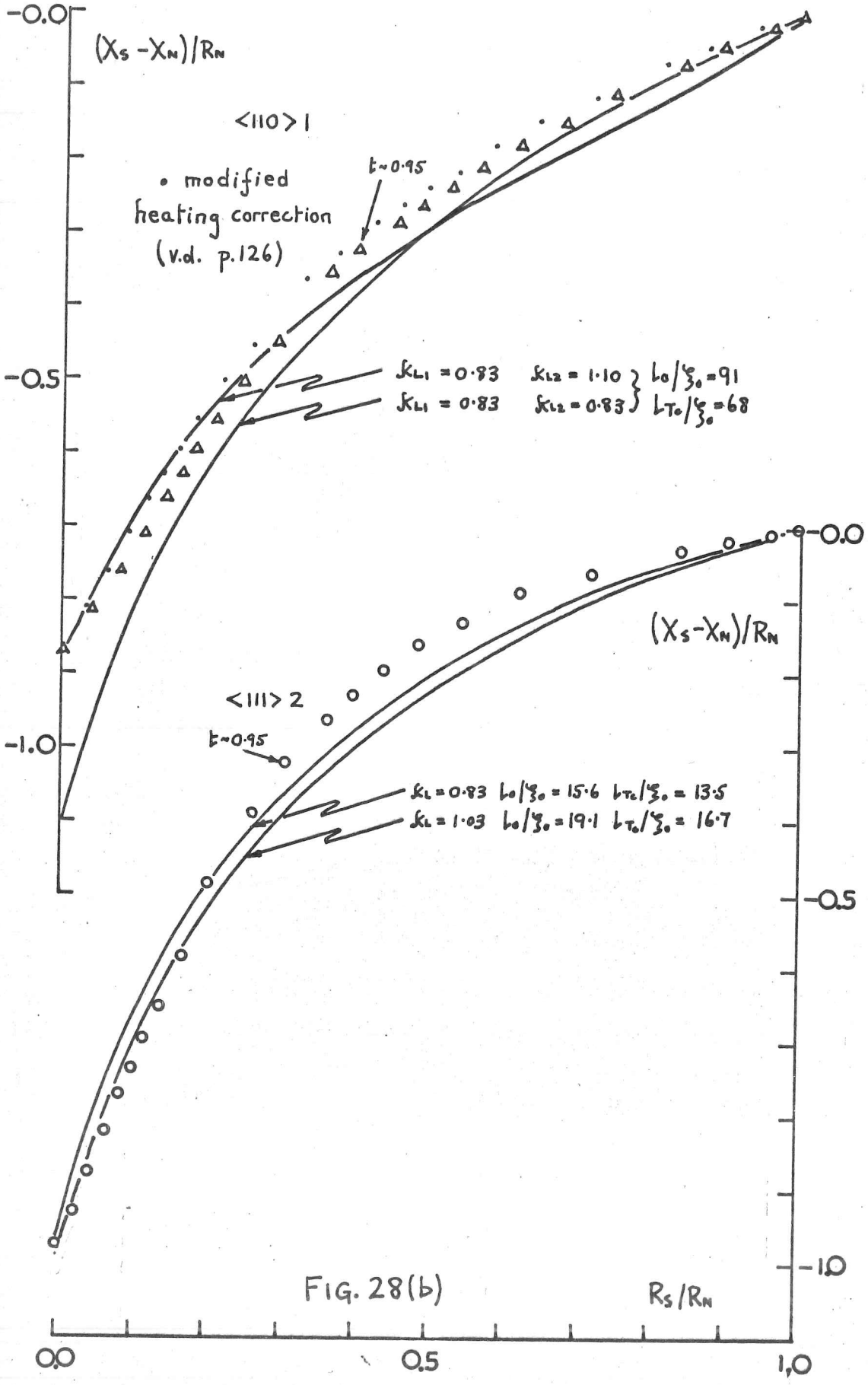
-0.0
$(X_S - X_N)/R_N$
<110> 1
• modified heating correction (v.d. p.126)
t~0.95
$k_{L1} = 0.83$ $k_{L2} = 1.10$ $L_0/\xi_0 = 91$
$k_{L1} = 0.83$ $k_{L2} = 0.83$ $L_{T_0}/\xi_0 = 68$
-0.5
-1.0
-0.0
$(X_S - X_N)/R_N$
<111> 2
t~0.95
$k_L = 0.83$ $L_0/\xi_0 = 15.6$ $L_{T_0}/\xi_0 = 13.5$
$k_L = 1.03$ $L_0/\xi_0 = 19.1$ $L_{T_0}/\xi_0 = 16.7$
-0.5
-1.0
0.0
0.5
1.0
R_S/R_N

FIG. 28(b)

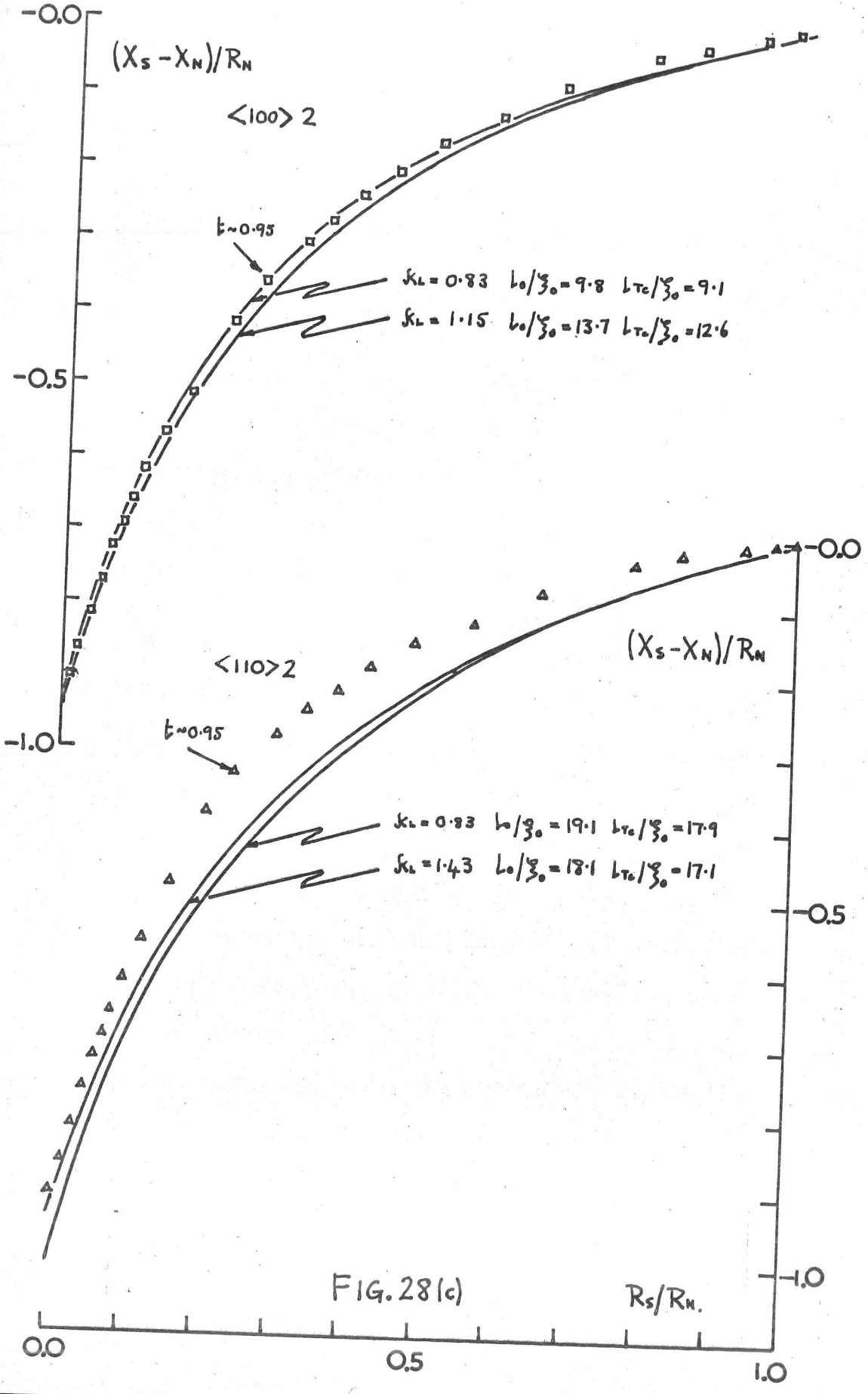
-0.0
$(X_S - X_N)/R_N$
<100> 2
t~0.95
$\kappa_L = 0.83$ $L_0/\xi_0 = 9.8$ $L_{Tc}/\xi_0 = 9.1$
$\kappa_L = 1.15$ $L_0/\xi_0 = 13.7$ $L_{Tc}/\xi_0 = 12.6$
-0.5
-1.0
<110>2
t~0.95
$\kappa_L = 0.83$ $L_0/\xi_0 = 19.1$ $L_{Tc}/\xi_0 = 17.9$
$\kappa_L = 1.43$ $L_0/\xi_0 = 18.1$ $L_{Tc}/\xi_0 = 17.1$
-0.0
$(X_S - X_N)/R_N$
-0.5
-1.0
0.0
0.5
1.0
R_S/R_N.

FIG. 28(c)

very apparent discrepancies, except for <100> 2 which seems quite well fitted. For the purer specimens '1', we give the curves computed for the appropriate supercurrent scaling. We also show individual plots of the temperature dependence of the resistance and reactance for various parameters in fig. (29). The temperature dependence of mean free path has been allowed for in these calculations using a T^3 interpolation, though the results are not very sensitive to it.

Experimentally, the useful feature of the Argand diagrams is that they are quite independent of the temperature calibration, depending solely on one's ability to make the heating correction with accuracy; we should warn the reader that they tend to overemphasise the importance of the transition region and minimise that of the low-temperature regime, and we show on all the plots the point at which t = 0.95 where most of the resistive transition has been accomplished. For specimen <110> 1, we demonstrate the sort of discrepancy which might derive from uncertainties in the heating correction, where the upper points are those calculated on the assumption that effective specimen heating might arise from that produced in the 'extraneous' losses. Such a correction is

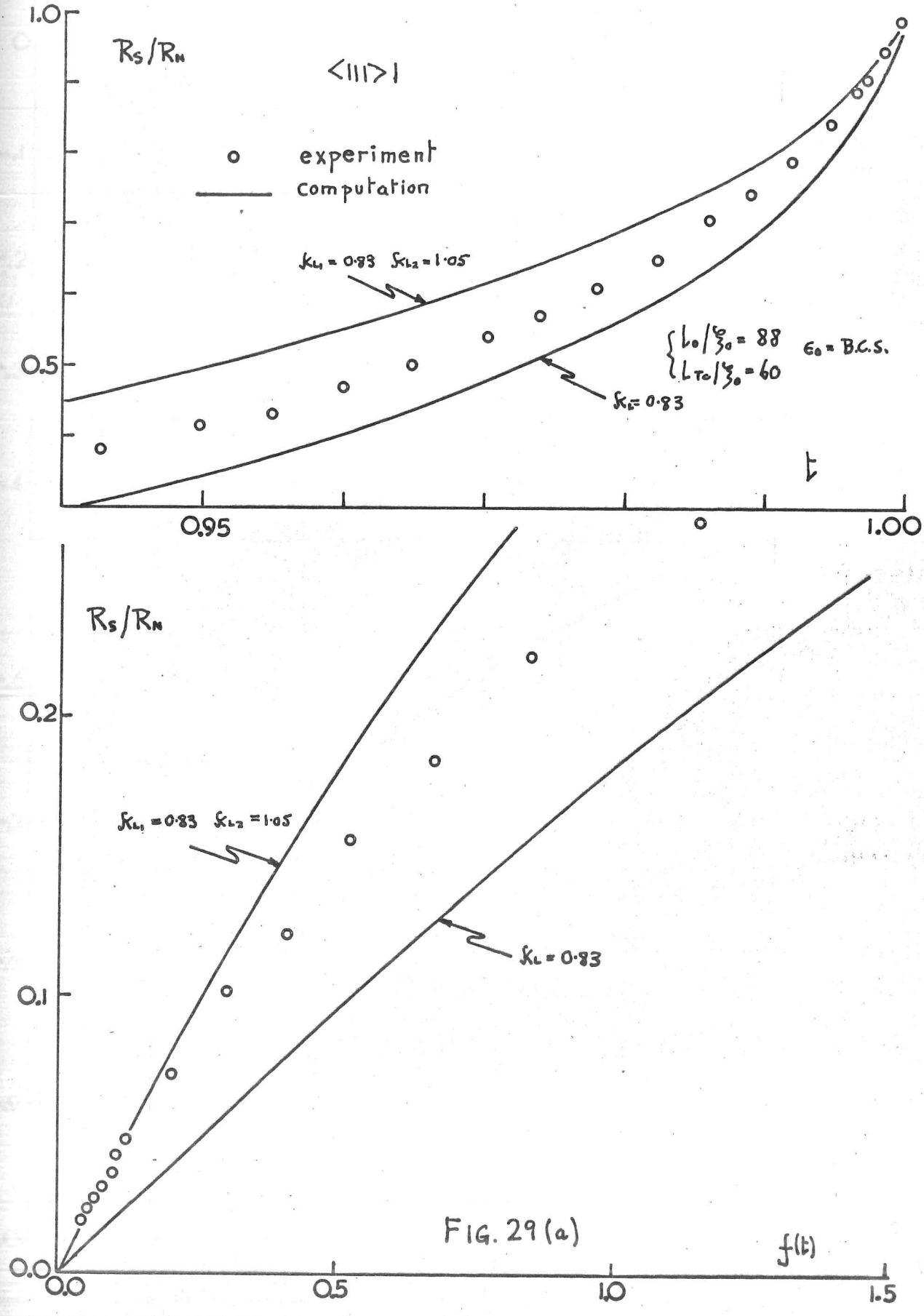
1.0
R_S/R_N
<111>
experiment
computation
$f_{L_1} = 0.83$ $f_{L_2} = 1.05$
$\{L_0/\xi_0 = 88$ ϵ_0 = B.C.S.
$L_{TC}/\xi_0 = 60$
$f_L = 0.83$
0.5
t
0.95
1.00
R_S/R_N
0.2
$f_{L_1} = 0.83$ $f_{L_2} = 1.05$
$f_L = 0.83$
0.1
0.0
0.0
0.5
1.0
1.5
f(t)

FIG. 29 (a)

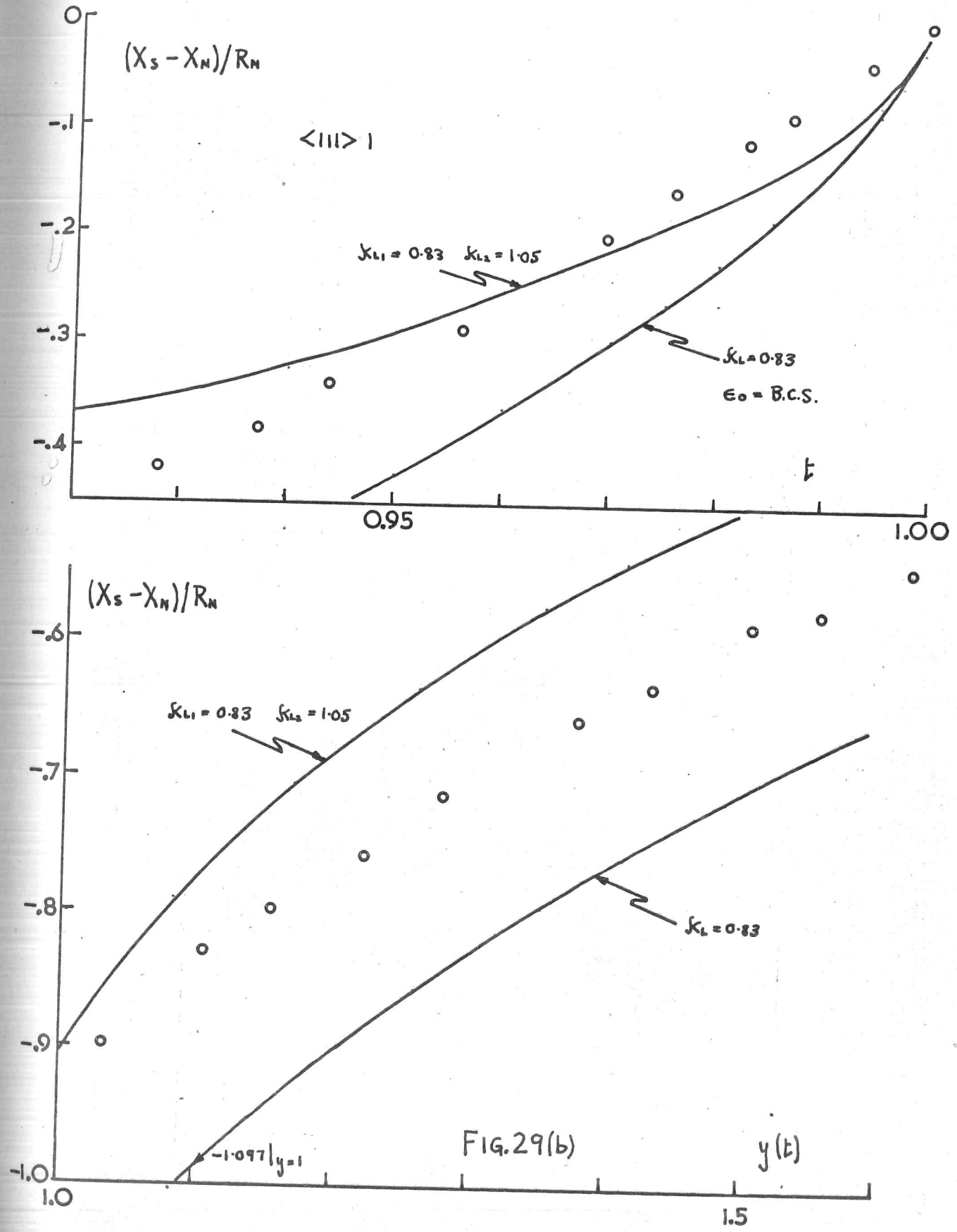
$(X_S - X_N)/R_N$
0
-.1
-.2
-.3
-.4
<111> 1
$\gamma_{L1} = 0.83$ $\gamma_{L2} = 1.05$
$\gamma_L = 0.83$
ϵ_0 = B.C.S.
t
0.95
1.00
$(X_S - X_N)/R_N$
-.6
-.7
-.8
-.9
-1.0
$\gamma_{L1} = 0.83$ $\gamma_{L2} = 1.05$
$\gamma_L = 0.83$
$-1.097|_{y=1}$
1.0
1.5
y(t)

FIG. 29(b)

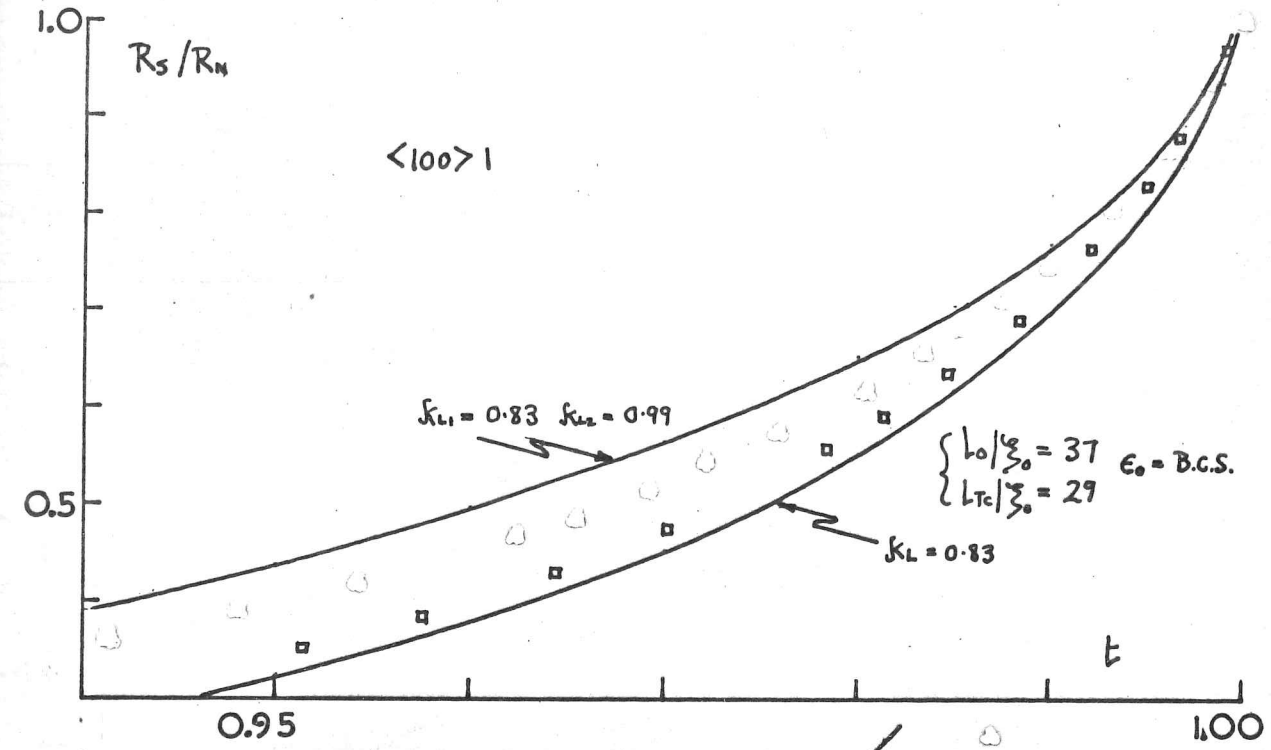
1.0
R_S/R_N
<100>1
$f_{L1} = 0.83$ $f_{L2} = 0.99$
$f_L = 0.83$
$\begin{cases} L_0/\xi_0 = 37 \\ L_{Tc}/\xi_0 = 29 \end{cases}$ ϵ_0 = B.C.S.
0.5
t
0.95
1.00

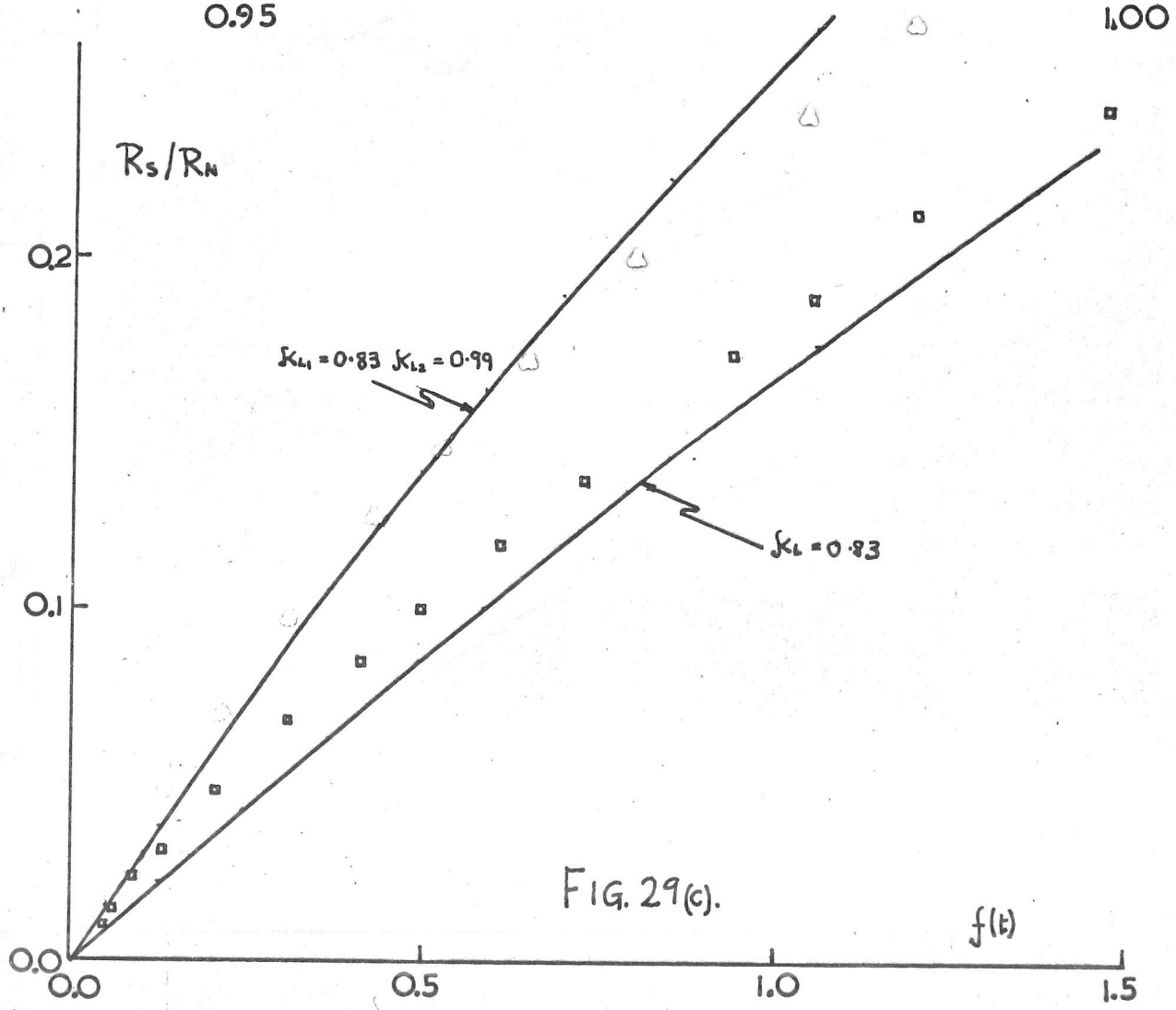
R_S/R_N
0.2
$f_{L1} = 0.83$ $f_{L2} = 0.99$
$f_L = 0.83$
0.1
0.0
0.0
0.5
1.0
1.5
f(t)

FIG. 29(c).

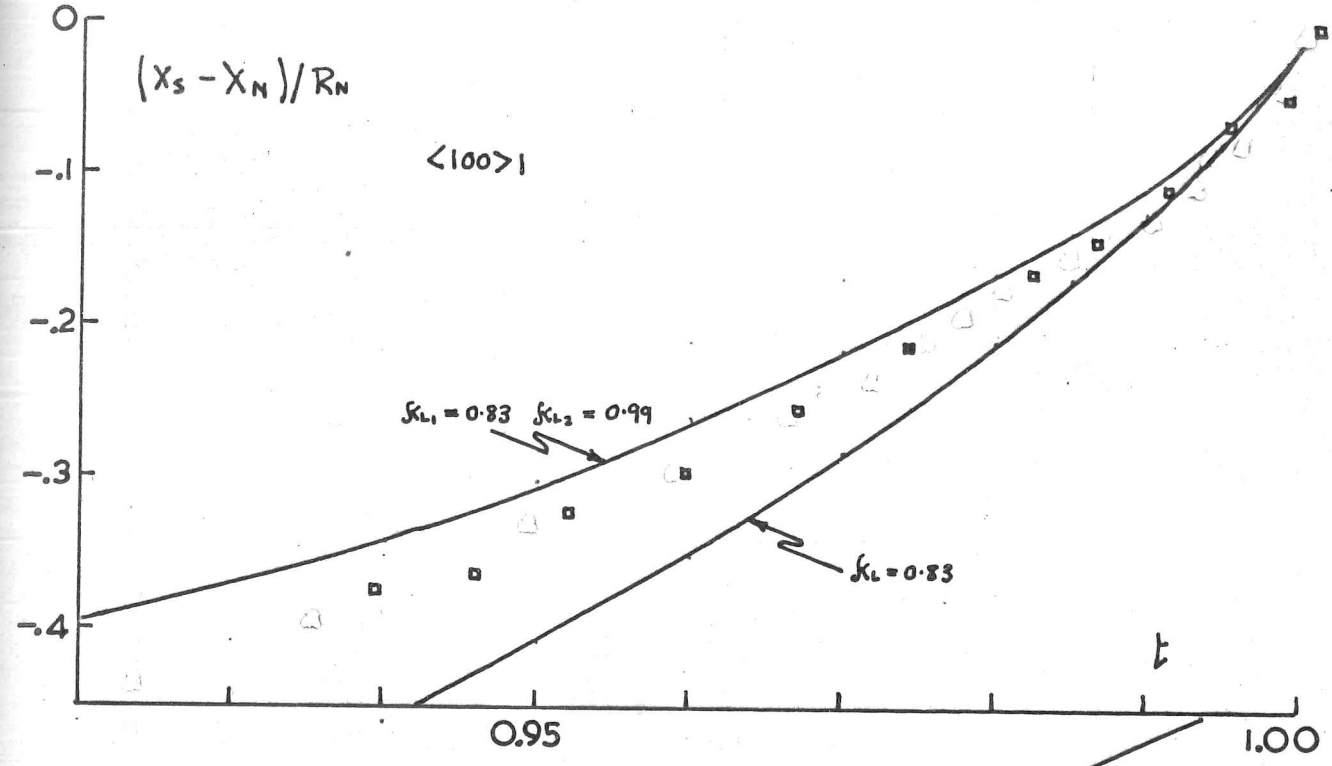
0
$(X_S - X_N)/R_N$
<100>1
-.1
-.2
-.3
-.4
$k_{L_1} = 0.83$ $k_{L_2} = 0.99$
$k_L = 0.83$
t
0.95
1.00

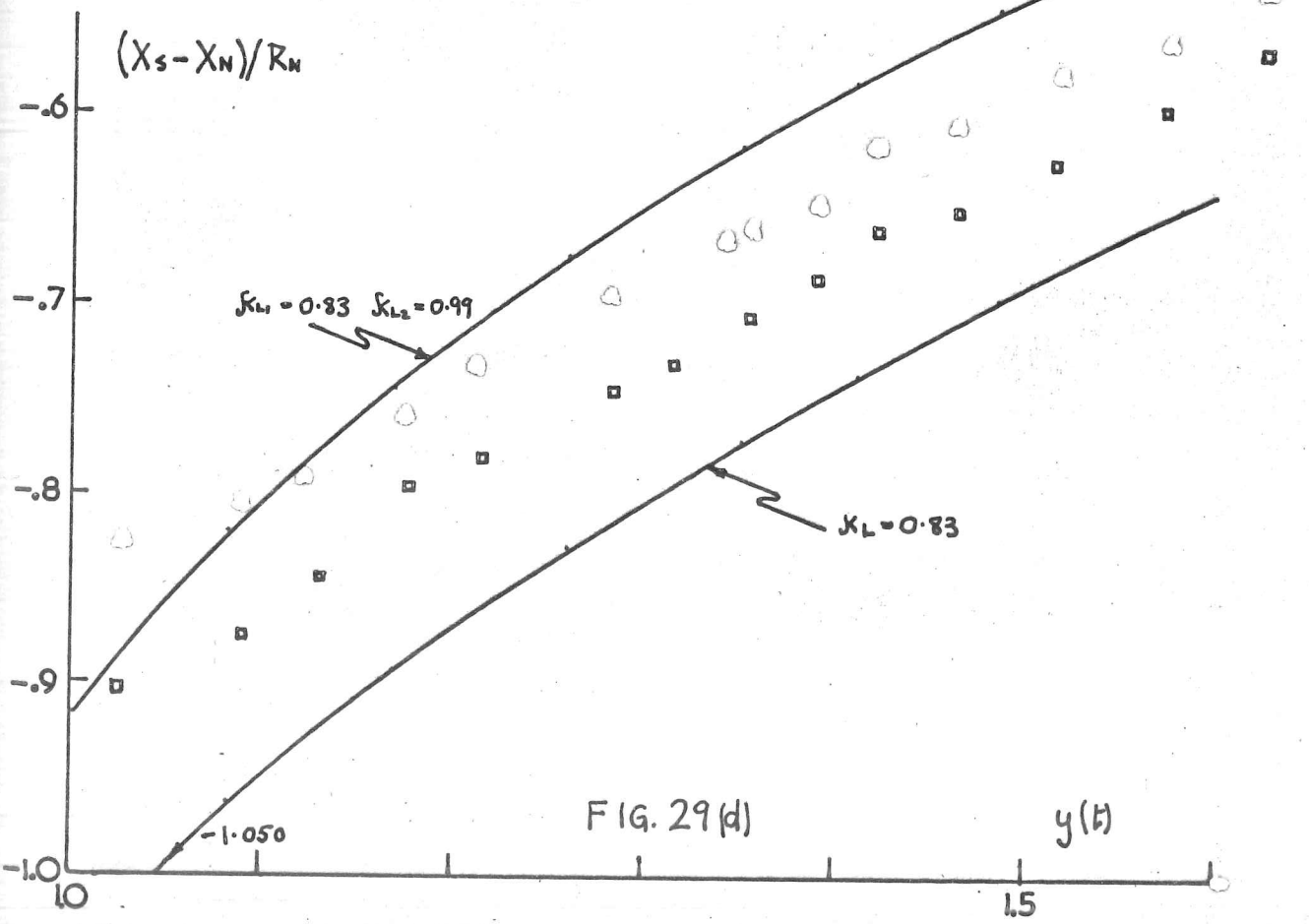
$(X_S - X_N)/R_N$
-.6
-.7
-.8
-.9
-1.0
$k_{L_1} = 0.83$ $k_{L_2} = 0.99$
$k_L = 0.83$
-1.050
1.0
1.5
y(t)

FIG. 29(d)

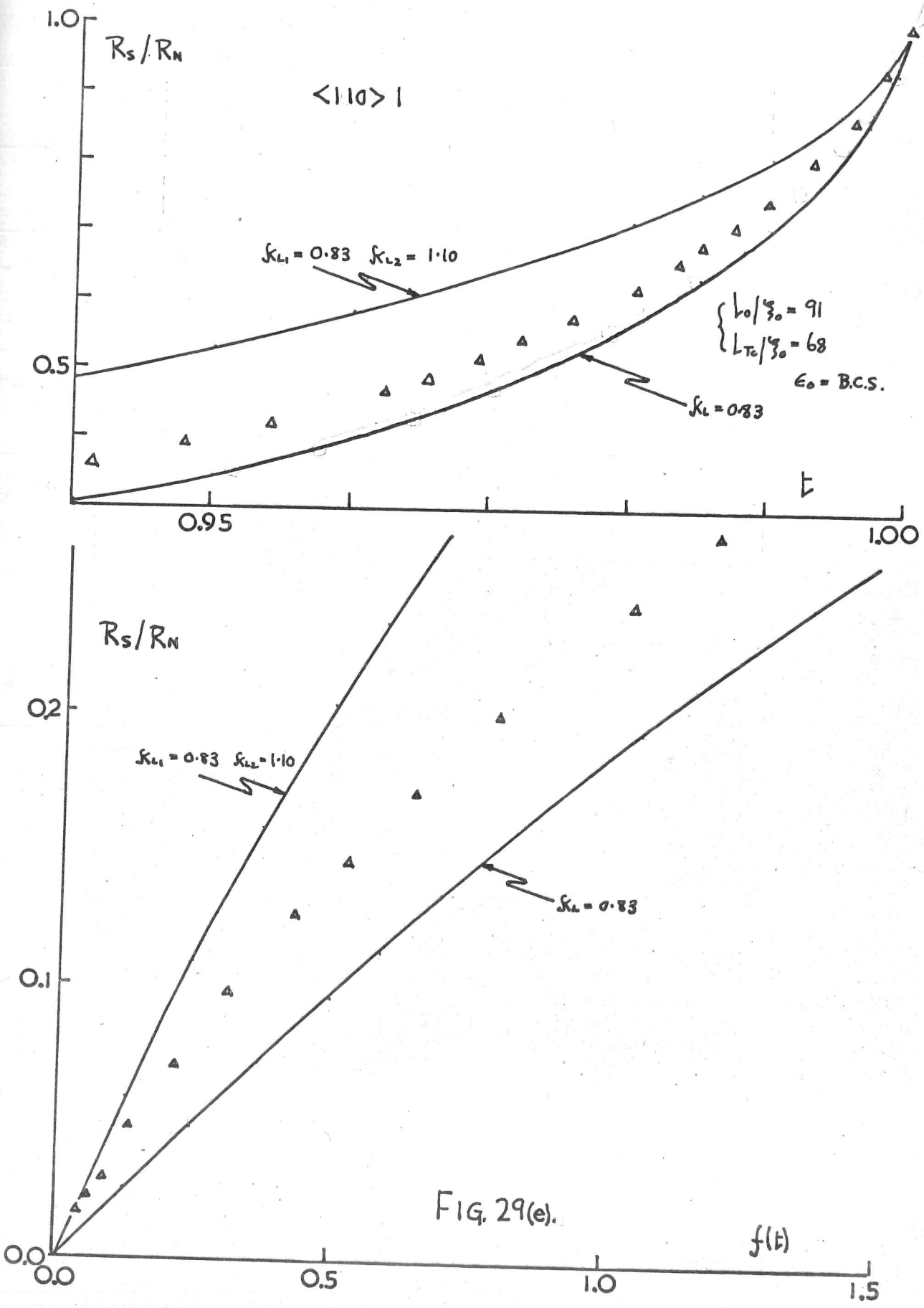
1.0
R_S/R_N
<110> I
$\kappa_{L_1} = 0.83$ $\kappa_{L_2} = 1.10$
$\{ l_0/\xi_0 = 91$
$l_{T_c}/\xi_0 = 68$
ϵ_0 = B.C.S.
$\kappa_L = 0.83$
0.5
t
0.95
1.00
R_S/R_N
0.2
$\kappa_{L_1} = 0.83$ $\kappa_{L_2} = 1.10$
$\kappa_L = 0.83$
0.1
0.0
0.0
0.5
1.0
1.5
f(t)

FIG. 29(e).

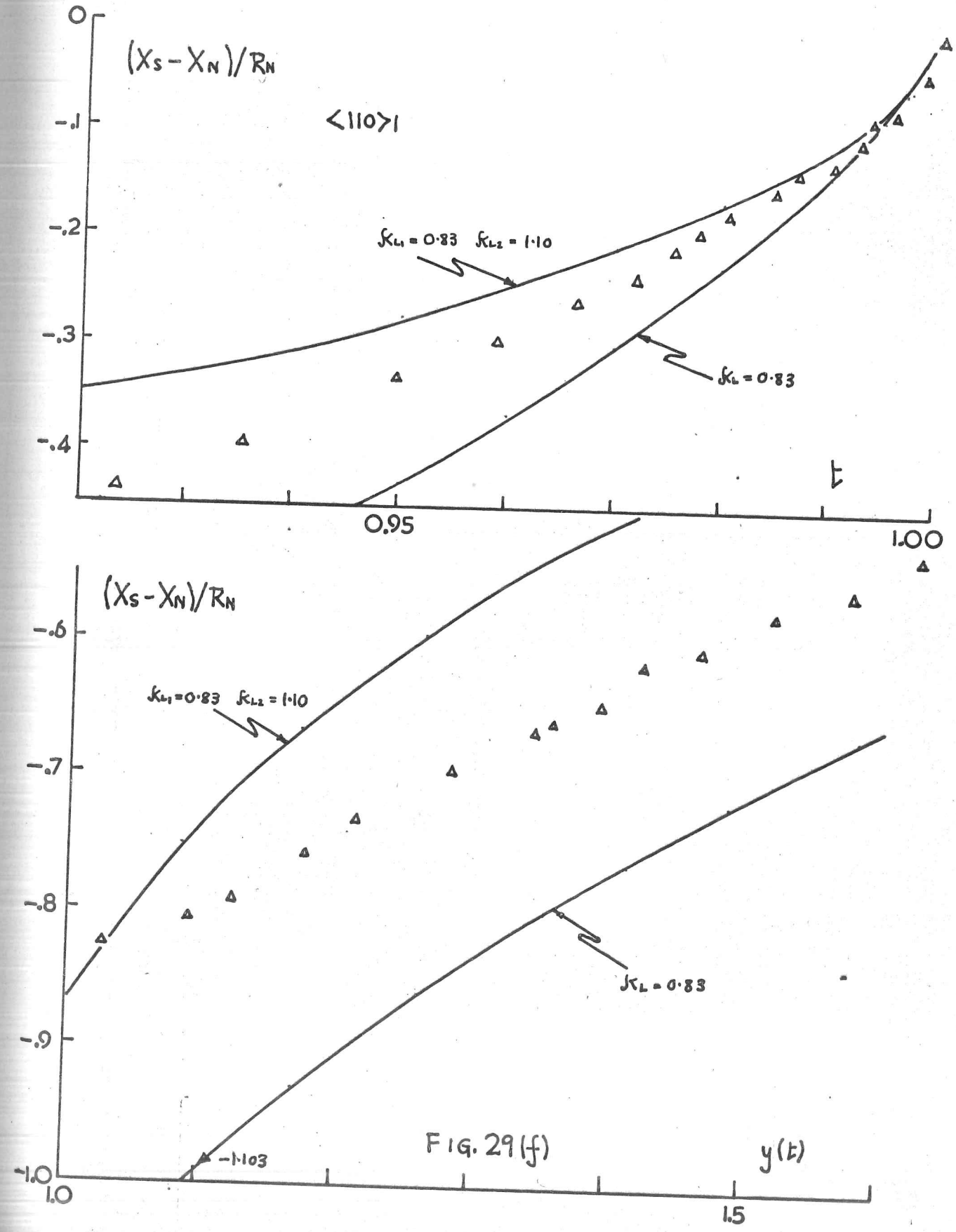
0
-.1
-.2
-.3
-.4
$(X_S - X_N)/R_N$
<110>1
$\kappa_{L1} = 0.83$ $\kappa_{L2} = 1.10$
$\kappa_L = 0.83$
t
0.95
1.00
-.6
-.7
-.8
-.9
-1.0
$(X_S - X_N)/R_N$
$\kappa_{L1} = 0.83$ $\kappa_{L2} = 1.10$
$\kappa_L = 0.83$
-1.103
1.0
1.5
y(t)

FIG. 29 (f)

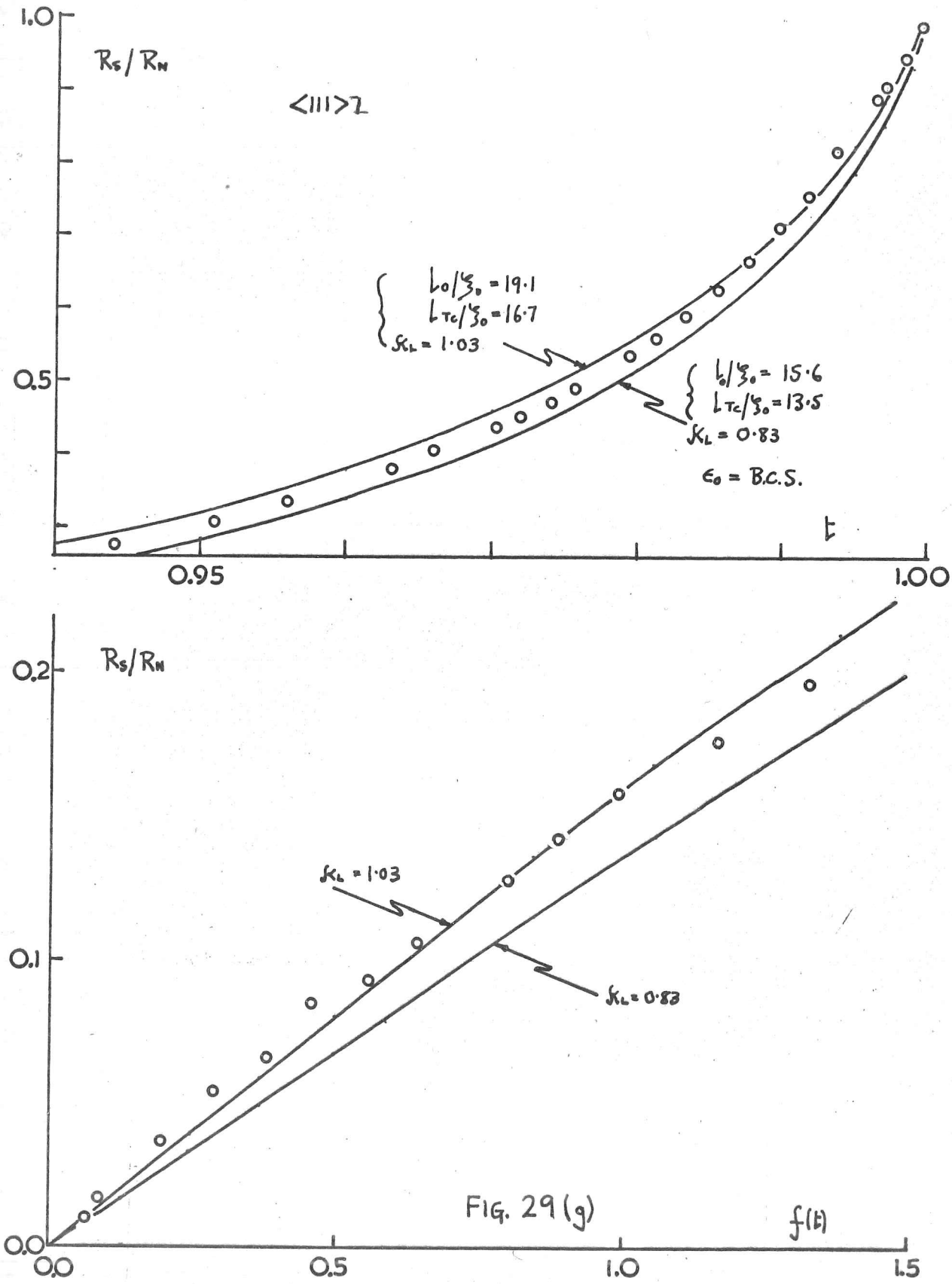
1.0
R_S/R_N
<111>Z
$l_0/\xi_0 = 19.1$
$l_{Tc}/\xi_0 = 16.7$
$\kappa_L = 1.03$
$l_0/\xi_0 = 15.6$
$l_{Tc}/\xi_0 = 13.5$
$\kappa_L = 0.83$
ϵ_0 = B.C.S.
t
0.5
0.95
1.00
0.2
R_S/R_N
$\kappa_L = 1.03$
$\kappa_L = 0.83$
0.1
0.0
0.0
0.5
1.0
1.5
f(t)

FIG. 29 (g)

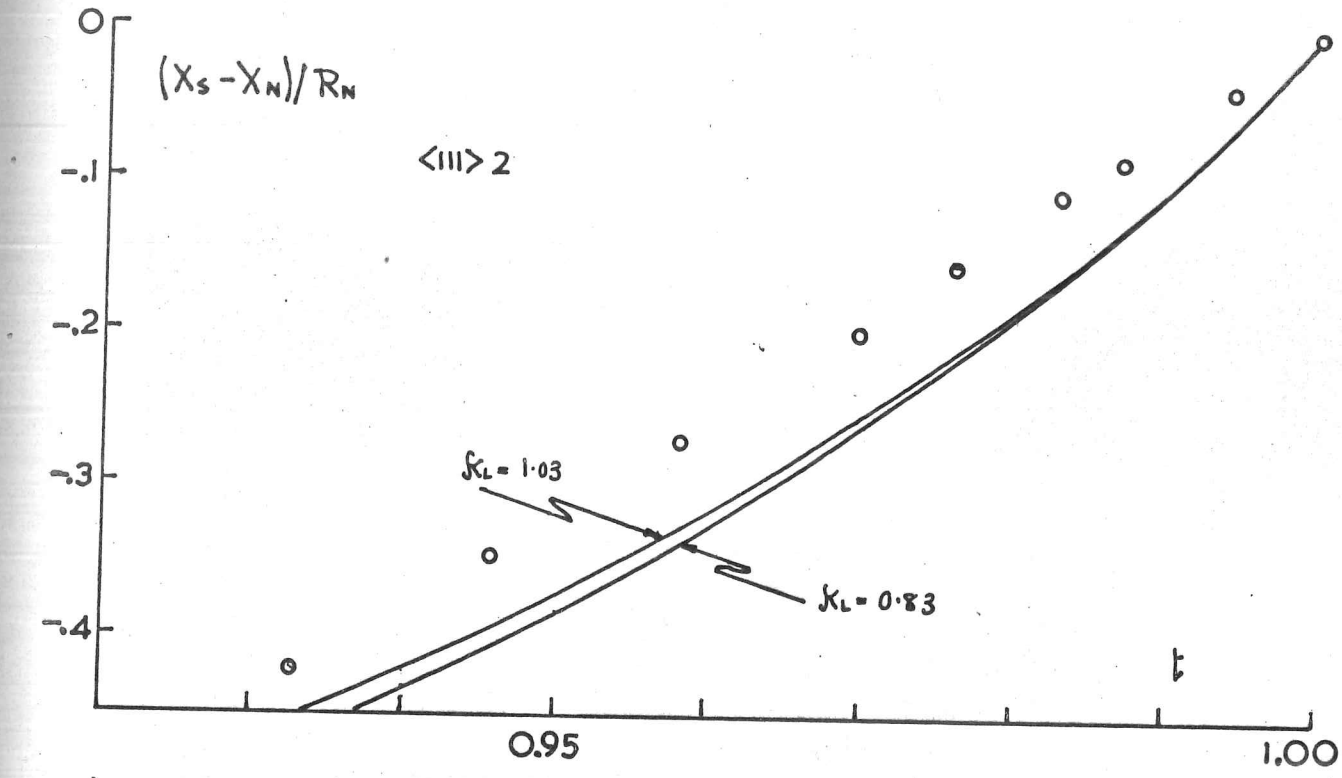
0
-.1
-.2
-.3
-.4
$(X_S - X_N)/R_N$
<111> 2
$K_L = 1.03$
$K_L = 0.83$
t
0.95
1.00

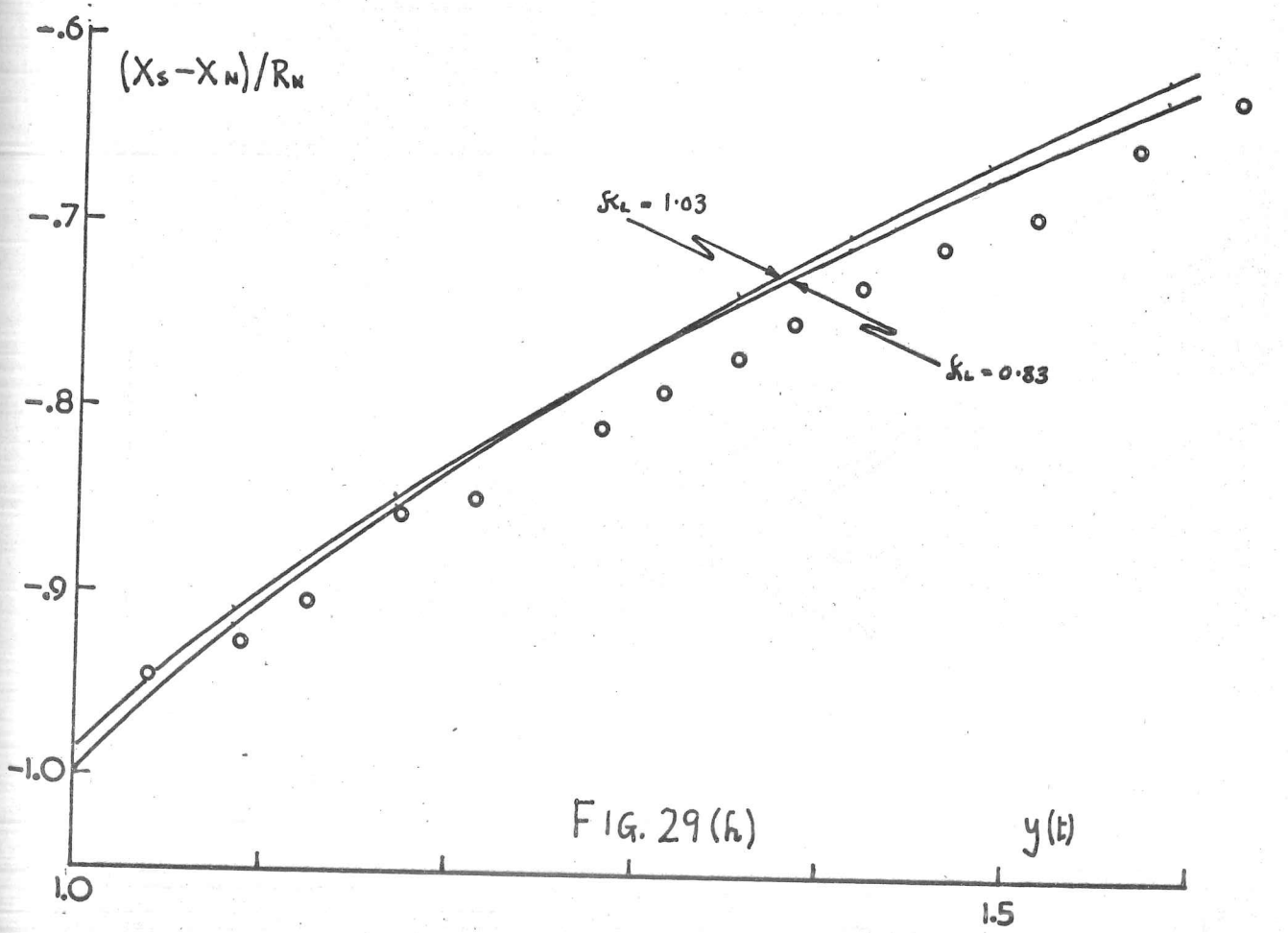
-.6
-.7
-.8
-.9
-1.0
$(X_S - X_N)/R_N$
$K_L = 1.03$
$K_L = 0.83$
1.0
1.5
y(t)

FIG. 29(h)

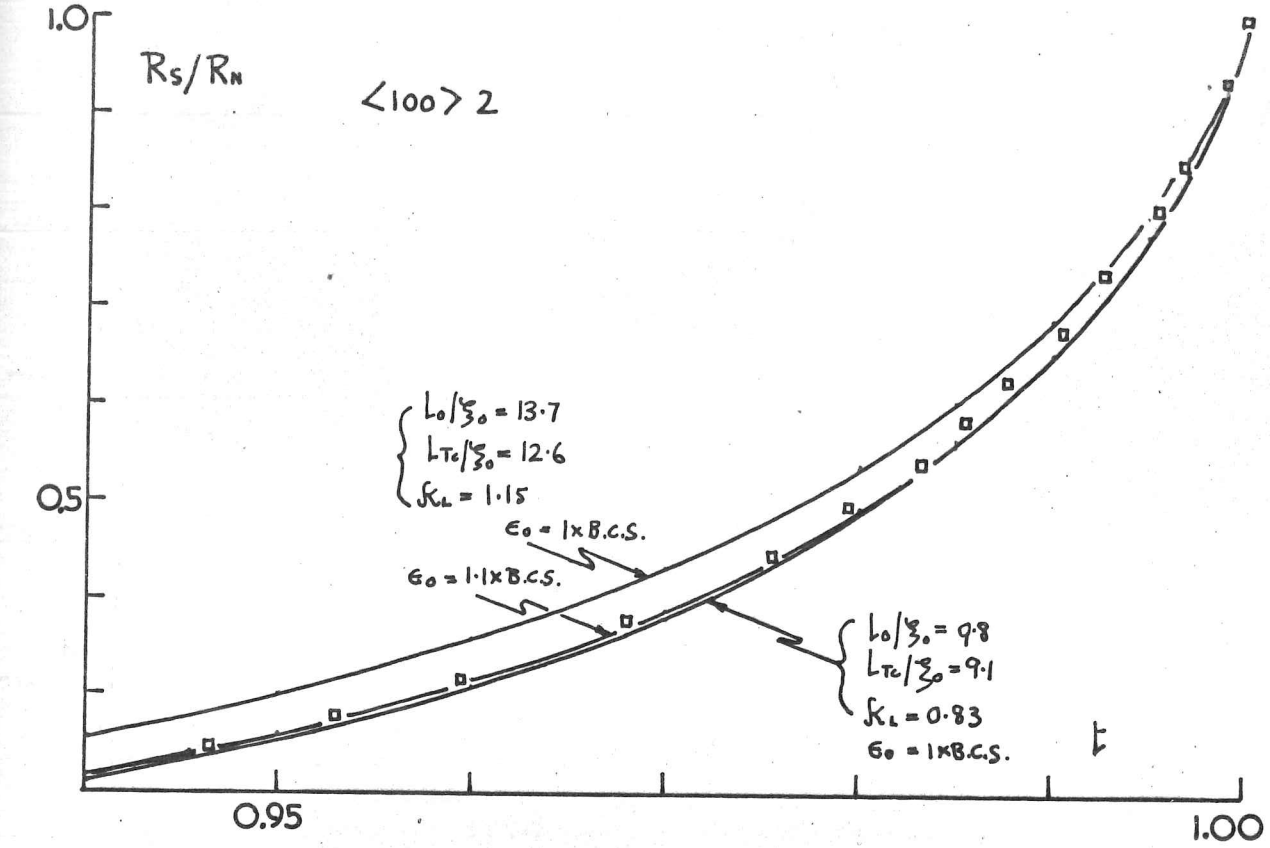
1.0
R_S/R_N
<100> 2
0.5
$L_0/\xi_0 = 13.7$
$L_{Tc}/\xi_0 = 12.6$
$f_{KL} = 1.15$
$\epsilon_0 = 1 \times B.C.S.$
$\epsilon_0 = 1.1 \times B.C.S.$
$L_0/\xi_0 = 9.8$
$L_{Tc}/\xi_0 = 9.1$
$f_{KL} = 0.83$
$\epsilon_0 = 1 \times B.C.S.$
t
0.95
1.00

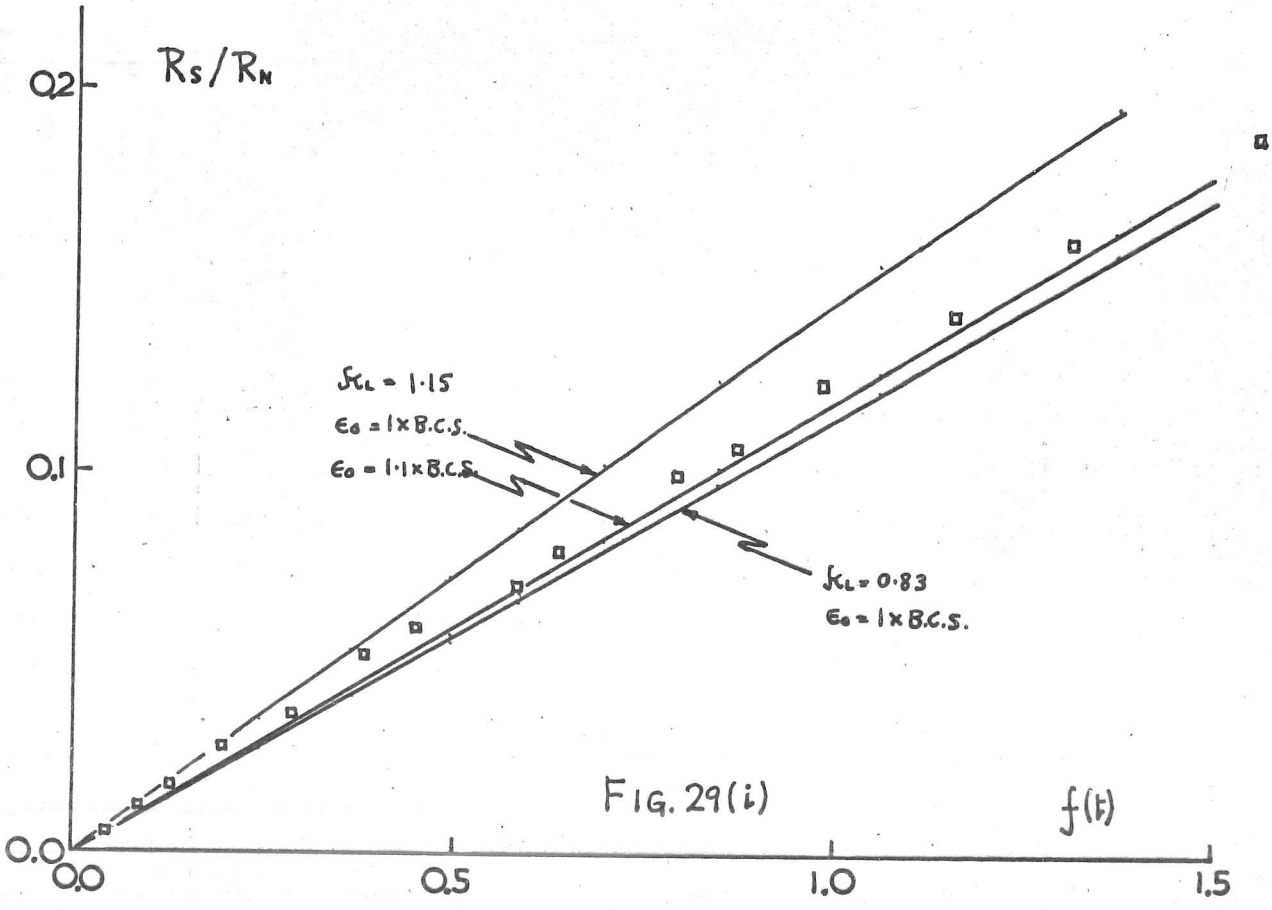
0.2
R_S/R_N
0.1
$f_{KL} = 1.15$
$\epsilon_0 = 1 \times B.C.S.$
$\epsilon_0 = 1.1 \times B.C.S.$
$f_{KL} = 0.83$
$\epsilon_0 = 1 \times B.C.S.$
0.0
0.0
0.5
1.0
1.5
f(t)

FIG. 29(i)

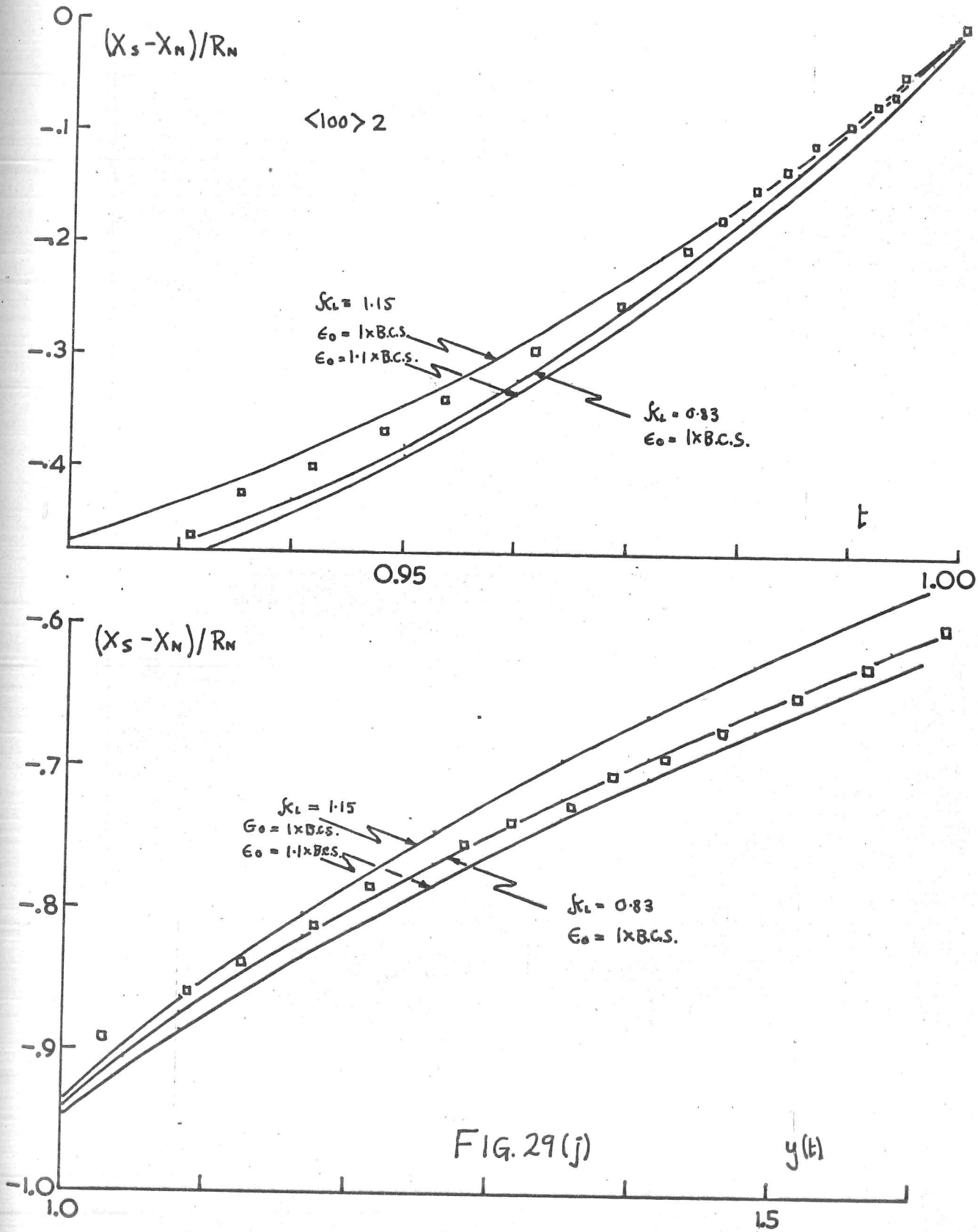
0
-.1
-.2
-.3
-.4
$(X_S - X_N)/R_N$
<100> 2
$\mathcal{K}_L$ = 1.15
ϵ_0 = 1×B.C.S.
ϵ_0 = 1.1×B.C.S.
$\mathcal{K}_L$ = 0.83
ϵ_0 = 1×B.C.S.
t
0.95
1.00
-.6
-.7
-.8
-.9
-1.0
$(X_S - X_N)/R_N$
$\mathcal{K}_L$ = 1.15
ϵ_0 = 1×B.C.S.
ϵ_0 = 1.1×B.C.S.
$\mathcal{K}_L$ = 0.83
ϵ_0 = 1×B.C.S.
1.0
1.5
y(t)

FIG. 29(j)

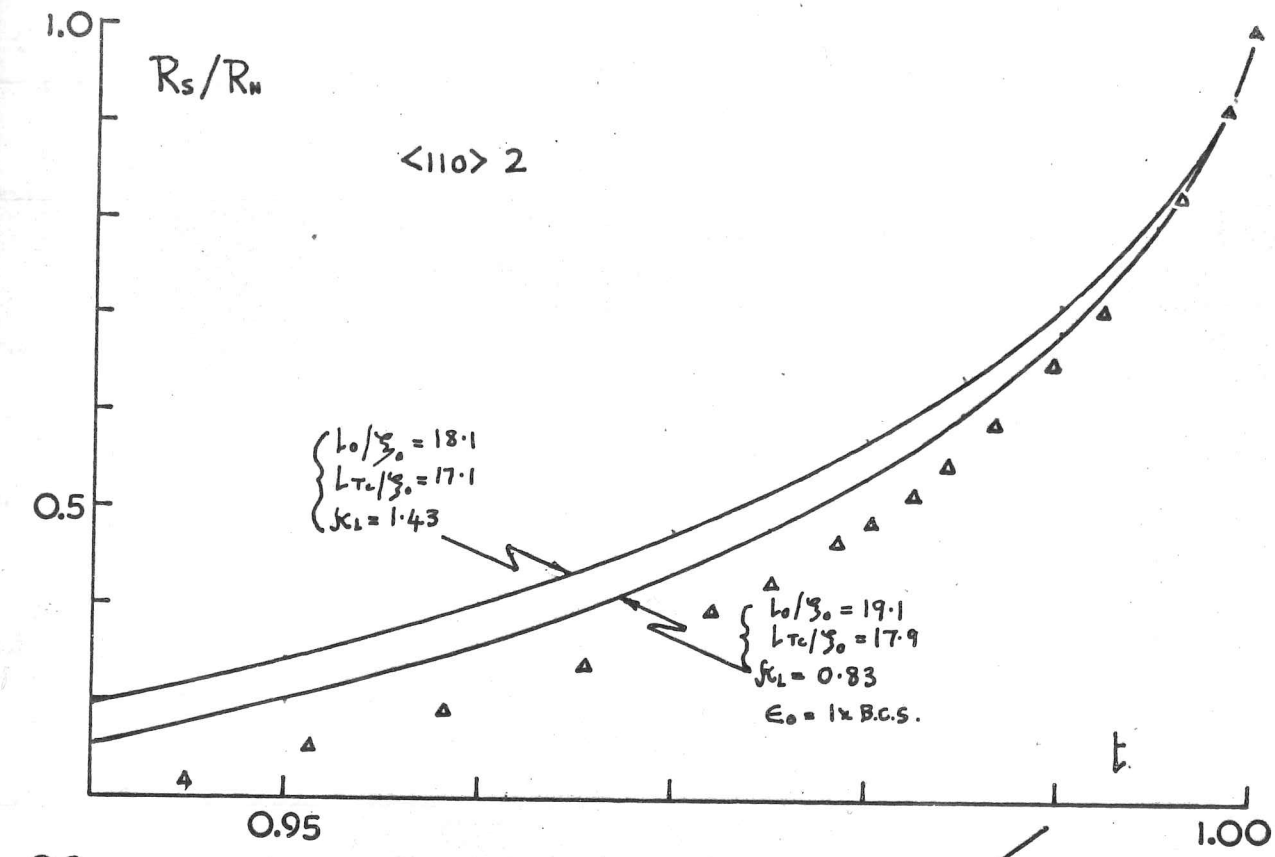
1.0
R_S/R_N
<110> 2
0.5
$l_0/\xi_0 = 18{\cdot}1$
$l_{Tc}/\xi_0 = 17{\cdot}1$
$\kappa_L = 1{\cdot}43$
$l_0/\xi_0 = 19{\cdot}1$
$l_{Tc}/\xi_0 = 17{\cdot}9$
$\kappa_L = 0{\cdot}83$
ϵ_0 = 1x B.C.S.
t
0.95
1.00

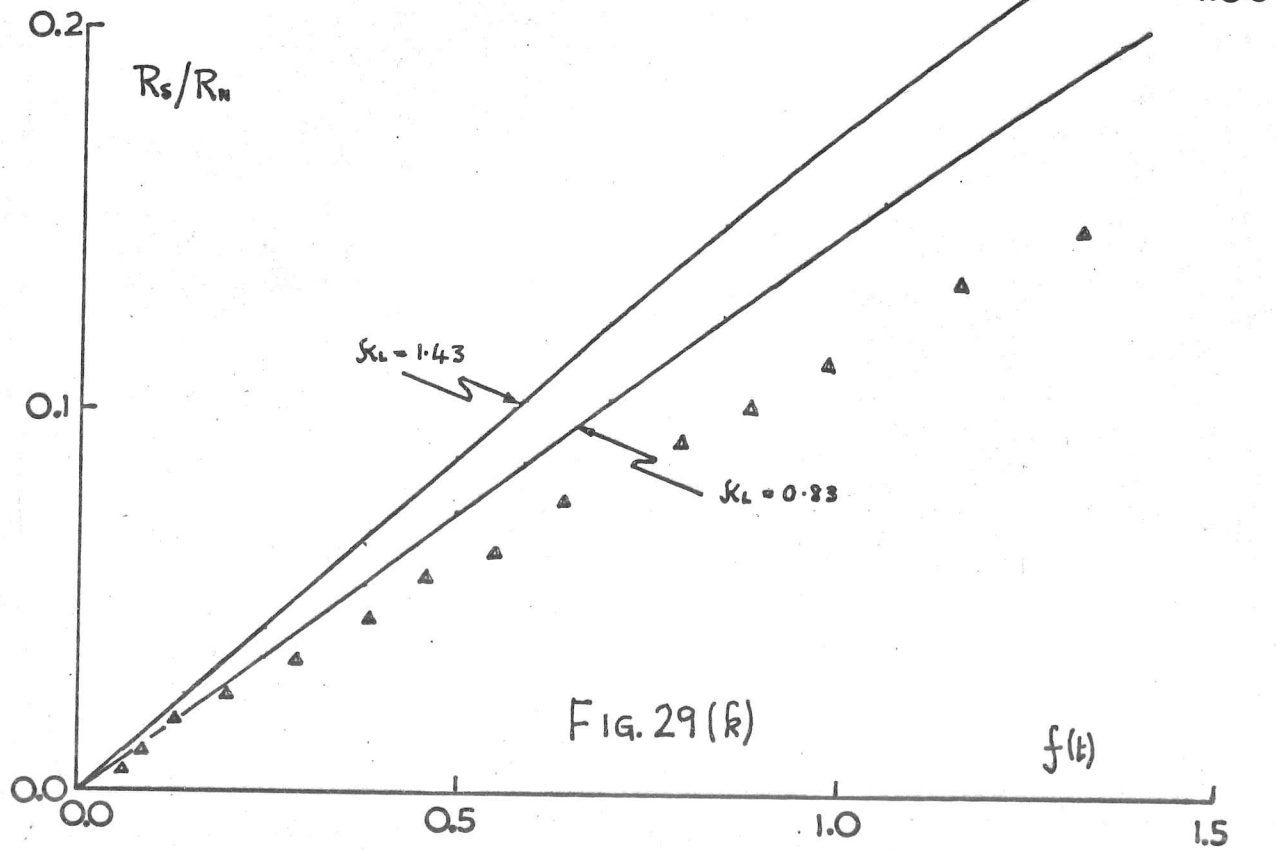
0.2
R_S/R_N
$\kappa_L = 1{\cdot}43$
0.1
$\kappa_L = 0{\cdot}83$
0.0
0.0
0.5
1.0
1.5
f(t)

FIG. 29 (k)

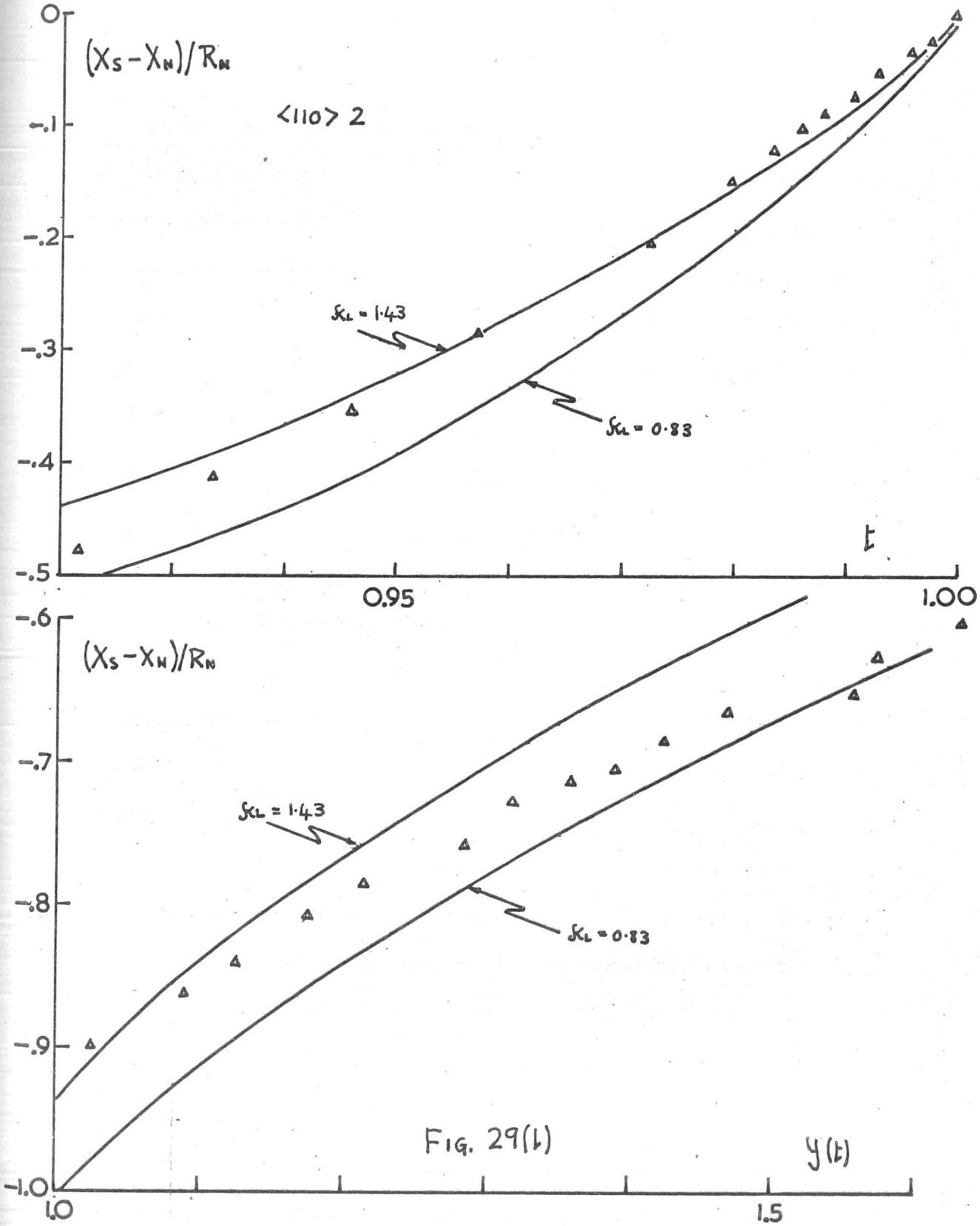
0
$(X_S - X_N)/R_N$
<110> 2
-.1
-.2
-.3
-.4
-.5
$k_L = 1.43$
$k_L = 0.83$
t
0.95
1.00
-.6
$(X_S - X_N)/R_N$
-.7
-.8
-.9
-1.0
$k_L = 1.43$
$k_L = 0.83$
1.0
1.5
y(t)

FIG. 29(b)

indeed significant, but would appear to be unlikely as a possible explanation for the form of the deviation between the experimental and computed plots. In our defence as regards this point, it should be said that it is much more difficult to allow for the heating correction in the pure London limit than in the Pippard, since the low-temperature-dependence of the resistance is about an order of magnitude higher (for $\kappa_L \sim 0.8$).

We believe that the discrepancies evident in the Argand plots are probably outside the range of experimental error, and at any rate it would appear that the qualitative form of the impedance predicted by the Mattis & Bardeen theory is significantly incorrect; extensive efforts to fit the Argand plots have all proved unsuccessful, but we will not confuse the reader by including all these trials. A most important point to be made about these plots is that the detailed computation shows that while changing the energy gap, by up to say 30% changes the individual temperature-dependences of resistance and reactance, the shape of the Argand diagram is remarkably insensitive to this except at the lowest temperatures; as remarked in section 3, this is presumably because the impedance depends much more strongly on

($k_B T / \epsilon_0(T)$) than on ($\hbar\omega / \epsilon_0(T)$). This fact argues the futility of attempting to fit the present results using the Waldram inversion procedure for the London penetration depth, since it is apparent that while either part of the impedance can be fitted with a non-B.C.S. temperature dependence of the energy gap, simultaneous reconciliation is impossible. Again, use of the σ-plots to 'correct' the measured shifts would seem universally to raise the lower ends of the Argand plots in such a way as to make their explanation yet more remote.

DISCUSSION:

One of the most imponderable of effects which could be of importance in the present results is that of strong coupling; as indicated in Chapter 1, the calculation of McMillan suggests that the normally deduced values of the electronic specific heat, London parameter, and coherence length already contain an appreciable renormalisation factor:

$$Z(0) \simeq 1{\cdot}82$$

of the Fermi velocity due to the electron-phonon and Coulomb interactions. We can therefore feel little confidence that the current response kernels can validly be approximated by taking the weak-coupling form and simply renormalising the values of V_F and $\Lambda(0)$ which appear there. As far as we are aware, no calculation of Nam's results has yet been made for either low frequencies or the London limit which would allow us to assess the corrections involved, but it seems unlikely that here would lie any explanation of the increasingly large penetration depths which we seem to observe in the purer specimens.

However, the work of Sung and Wong (28) on the two-band model does seem to provide a possible explanation. Their calculation

suggests that the s-band energy gap is rather sensitive to the scattering present, and, in Anderson fashion, should start to become washed out at impurity levels where the effect on the degree of electrodynamic coherence is little affected directly; as already pointed out, the specific heat measurements tend to show the persistence of this anisotropy to very low resistance ratios, but this measurement is subject to fair experimental uncertainty according to Sung & Wong.

Now on any reasonable sort of estimate, the s-band energy gap would appear to be considerably more Pippard-like than the usual d-gap; for example, on the simple two parabolic band model discussed in Chapter 3, we would obtain:

$$\frac{\epsilon_{os}}{\epsilon_{od}} = 0.1 \; ; \; \frac{N_s}{N_d} \simeq 0.015 \; ; \; \frac{v_s}{v_d} \simeq 4.1 \; ; \; \frac{m_s^*}{m_d^*} = 0.06 = \frac{S_s}{S_d}$$

so that:

$$\frac{\lambda_{Ls}}{\lambda_{Ld}} = \sqrt{\frac{S_d v_d}{S_s v_s}} \simeq 2 \; ; \; \frac{\xi_{os}}{\xi_{od}} = \frac{v_s}{v_d}\frac{\epsilon_{od}}{\epsilon_{os}} \simeq 40$$

and:

$$\frac{\kappa_s}{\kappa_d} \simeq 0.05$$

As previously mentioned in connection with the ratio of effective masses, these estimates can only be very approximate, but the general

conclusion would appear to be correct. If this interpretation is anywhere near the mark, this would imply that niobium should become increasingly more Pippard-like as it becomes purer at rather low impurity levels. Thus its penetration depth should increase, as we observe, and what is more, the slope of the impedance plot at the transition $\frac{\partial X_s}{\partial R_s}\Big|_{T_c}$ should become less steep in accordance with the ideas of Waldram (5). This behaviour seems to be in qualitative agreement with our Argand plots, and contrasts with the single-band calculations given where it was necessary to make the superconductor more London-like in order to increase the penetration depth, thereby increasing the gradient at Tc and taking it further from the experimental plot. Equally, this model would seem to offer an explanation of the decreased experimental slope at T = o compared with the single-band model on account of the increased absorption expected at a given penetration depth from a contribution from a small energy gap. On this basis, it may be that the suggestion of a slight kink in the penetration depth at low temperatures noted earlier for specimens $\langle 100 \rangle$ 1 and $\langle 110 \rangle$ 1 is in fact real; perhaps it represents the relatively sudden onset of increasingly Pippard character associated with an anomalously increasing energy gap

at around 4.2°K.

All this is, of course, highly speculative, but we feel it would be foolish to ignore the evidence from the specific heat and tunnelling measurements that there probably is a rather small second gap in niobium, and to consider what peculiarities this might generate in the electrodynamics. Accordingly, we have attempted to make a simple two-band calculation of the surface impedance of a superconductor with such a combination of London and Pippard character, and have approximated the response with a kernel:

$$K(q\ell) = \frac{S_d}{S_s+S_d} K_d(q\ell) + \frac{S_s}{S_s+S_d} K_s(q\ell)$$

where: $K_s(q\ell) = \frac{3i\hbar\omega}{4\pi\lambda_{Ls}^2(0)\epsilon_{0s}(0)} \left(\frac{\sigma_s}{\sigma_N}\right)_s (q\ell_{0s})^{-1}$ is the Pippard current.

and: K_d is the single band contribution previously calculated.

The weighting according to Fermi surface area strictly leaves the normal-state impedance unaltered only in the extreme anomalous limit, of course, but there is no point in trying to be too precise here; the detailed computation given later for $<110>$ 1 shows this effect to be negligible in that case, anyway. Also, we neglect

any interband scattering complications as being far too much of a nicety at this stage since we have only a very crude approximation to the excitation spectrum anyway. We have taken as a rough representation of the s-gap:

$$\epsilon_{os}(t) = 0{\cdot}1\ \epsilon_{oB.C.S.}(t)$$

and the estimates of the other parameters as given previously, and show the results of the calculation for specimen $\langle 110 \rangle$ 1 on an Argand plot in fig. (30). It will be seen that at $\sim 4.2^{\circ}K.$, the predicted surface resistance is very small arguing against the possibility that our 'extraneous' losses might be real on this model at any rate, but that the Pippard supercurrent estimated is too small to account for the observed penetration depth. Accordingly, we also show calculations in which the supercurrent has been arbitrarily scaled up by a factor 5. This is still insufficient to explain the measured penetration depth, but in view of our very crude model of the second energy gap, there is little point in trying to do better. We are still not at all near to a respectable fit over the whole temperature range, and the best we can claim for our simple calculation is that it qualitatively verifies the intuitive ideas given previously. Until

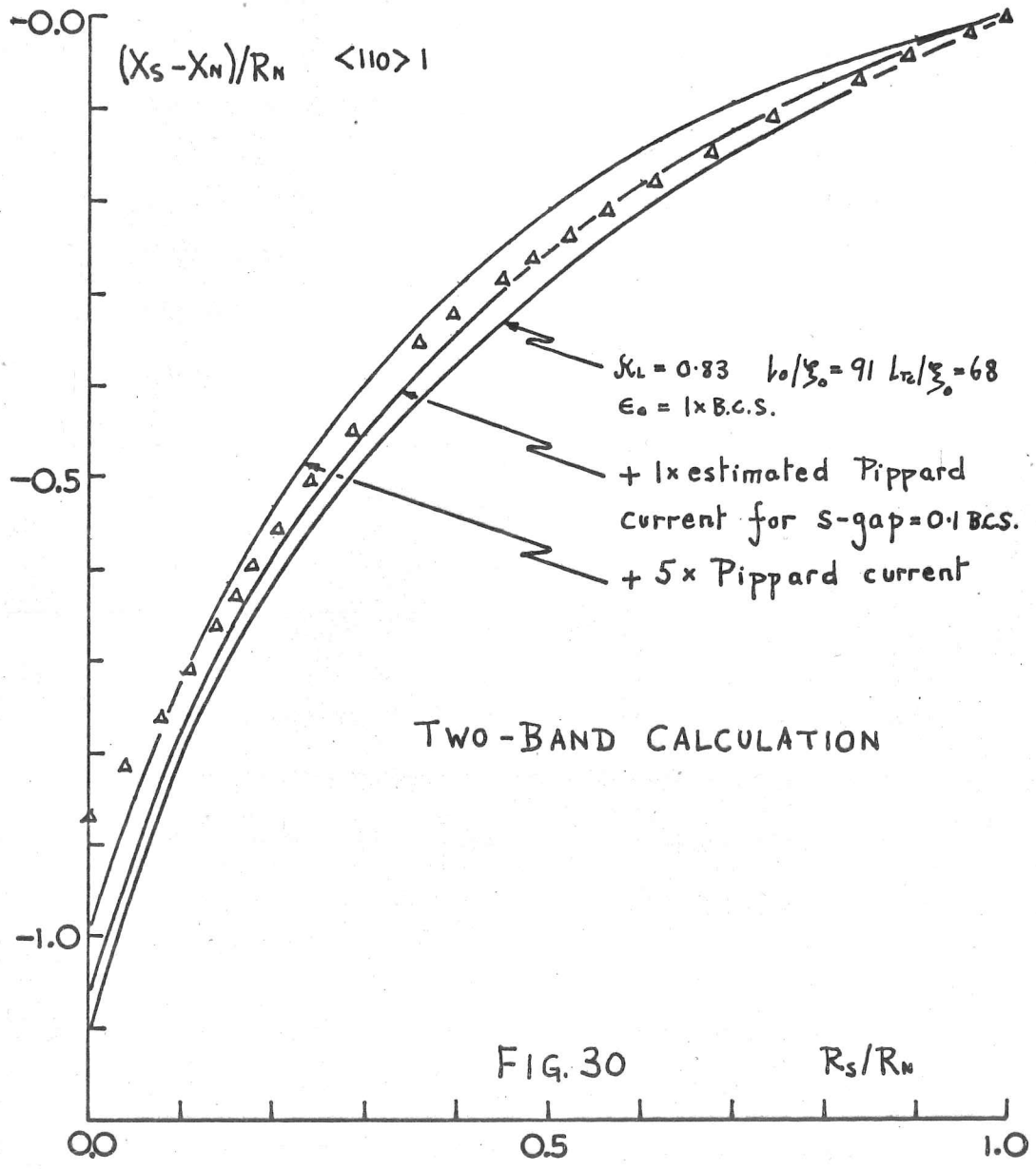
-0.0
$(X_S - X_N)/R_N$ <110> 1
$\kappa_L = 0.83$ $l_0/\xi_0 = 91$ $l_{tr}/\xi_0 = 68$
ϵ_0 = 1× B.C.S.
+ 1× estimated Pippard current for s-gap = 0.1 BCS.
+ 5× Pippard current
-0.5
TWO-BAND CALCULATION
-1.0
R_S/R_N
0.0
0.5
1.0

FIG. 30

a reliable explanation of the low temperature impedance can be given, we feel that the σ-plot of Waldram must be interpreted with some caution for niobium.

If this interpretation of the results is correct, there is perhaps a faint glimmer of hope that such measurements could be made to yield the temperature dependence of the s-gap, together perhaps with relative values for the Fermi velocities (or, equivalently, the effective masses) of the two bands which determines the relative scaling of the Pippard current - information which would be of considerable value. Such an analysis would hardly seem to be feasible at present, however.

Lastly, it is necessary to consider whether such an interpretation is consistent with the measurements of penetration depth reported by other authors. For reasons already given, the only results in which we feel great confidence are those of Maxfield & McLean; unfortunately, however, their niobium specimen had a resistance ratio of only 115 and is therefore comparable only with our specimens '2' for which no large anomaly in $\lambda(o)$ has been observed. It is perhaps significant that they were able

to fit their results with a value of $\kappa = 1.0$ rather than 0.83 as indicated by the magnetisation measurements, therefore deviating in the same direction as our results suggest for a single-band fit. It is thus possible that their inference that the non-B.C.S. temperature dependence of the energy gap deduced by Waldram 's inversion procedure for the non-B.C.S. form of $\lambda(t)$ observed could be replaced by an explanation based on two-band properties, as suggested by Radhakrishnan. As regards the measurements of Turneaure & Weissman, they unfortunately have no results for the penetration depth, but the increased absorption seen by them at less than $1.8^{\circ}K$. can possibly be interpreted as evidence for the second gap; they do not appear to give figures for the resistance ratios of their niobium, but made their computation for a mean free path of 10^{-4}cm. corresponding to R.R.R. $\sim$ 300. Finally, we have the magnetisation measurements, the most recent of which have been carried out on specimens of R.R.R. $\sim$ 1000, so the effects we have been considering should be important. This may serve to add some weight to the explanation offered by Wong & Sung (78) for the discrepant Hc2 of niobium in terms of two-band properties, although, as already pointed out, our results are not concordant with their assumptions of a low effective mass for the d-band.

CHAPTER 5 - THE MAGNETIC-FIELD DEPENDENCE OF THE SURFACE IMPEDANCE.

We have made measurements of the effect of the application of a steady magnetic field on the surface impedance of our specimens; the orientation of the field was in all cases parallel to the specimen axis, that is parallel to the microwave current and transverse to the microwave magnetic field. The field-dependence may conveniently be divided into two regions:

1. the Meissner region below H_{c1} - low field behaviour
2. the mixed state and surface sheath regimes - high field behaviour.

These two regions will be considered separately.

1. LOW-FIELD BEHAVIOUR:

The complete investigation of the field- and temperature -dependence of surface impedance for a series of specimens is a major task in itself, and time has only allowed a rather cursory set of measurements to be made. However, in figure (31) we shew the results of measurements on 6 specimens made at 4.2°K., together with graphs at higher temperatures for specimens $\langle 111 \rangle$ 3, $\langle 100 \rangle$ 1, and $\langle 110 \rangle$ 2 only. The measurements were made by the

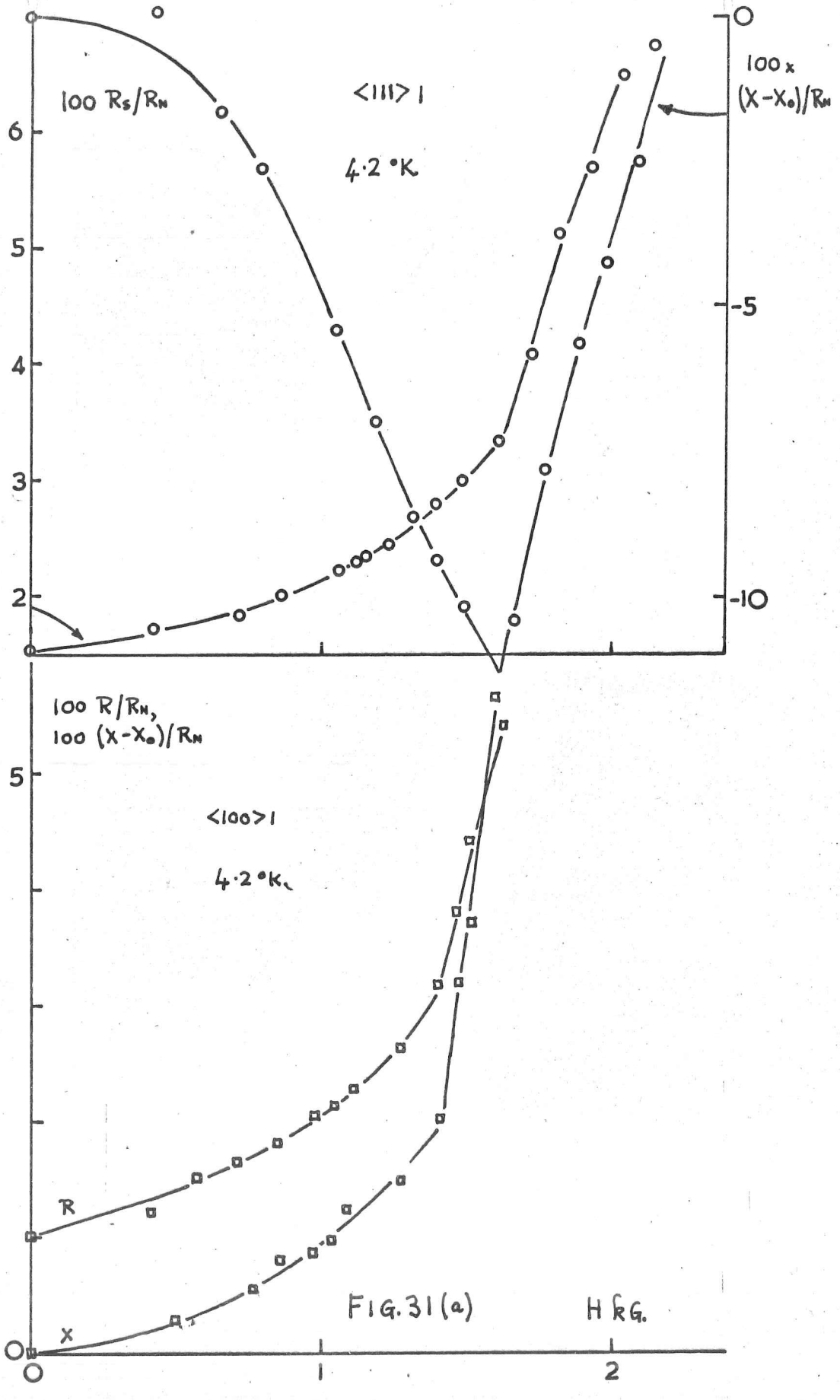
100 Rs/RN
<111>1
4·2 °K
100 x
(X-Xo)/RN
6
5
4
3
2
0
-5
-10
100 R/RN,
100 (X-Xo)/RN
<100>1
4·2 °K.
5
R
X
0
1
2
H kG.

FIG. 31 (a)

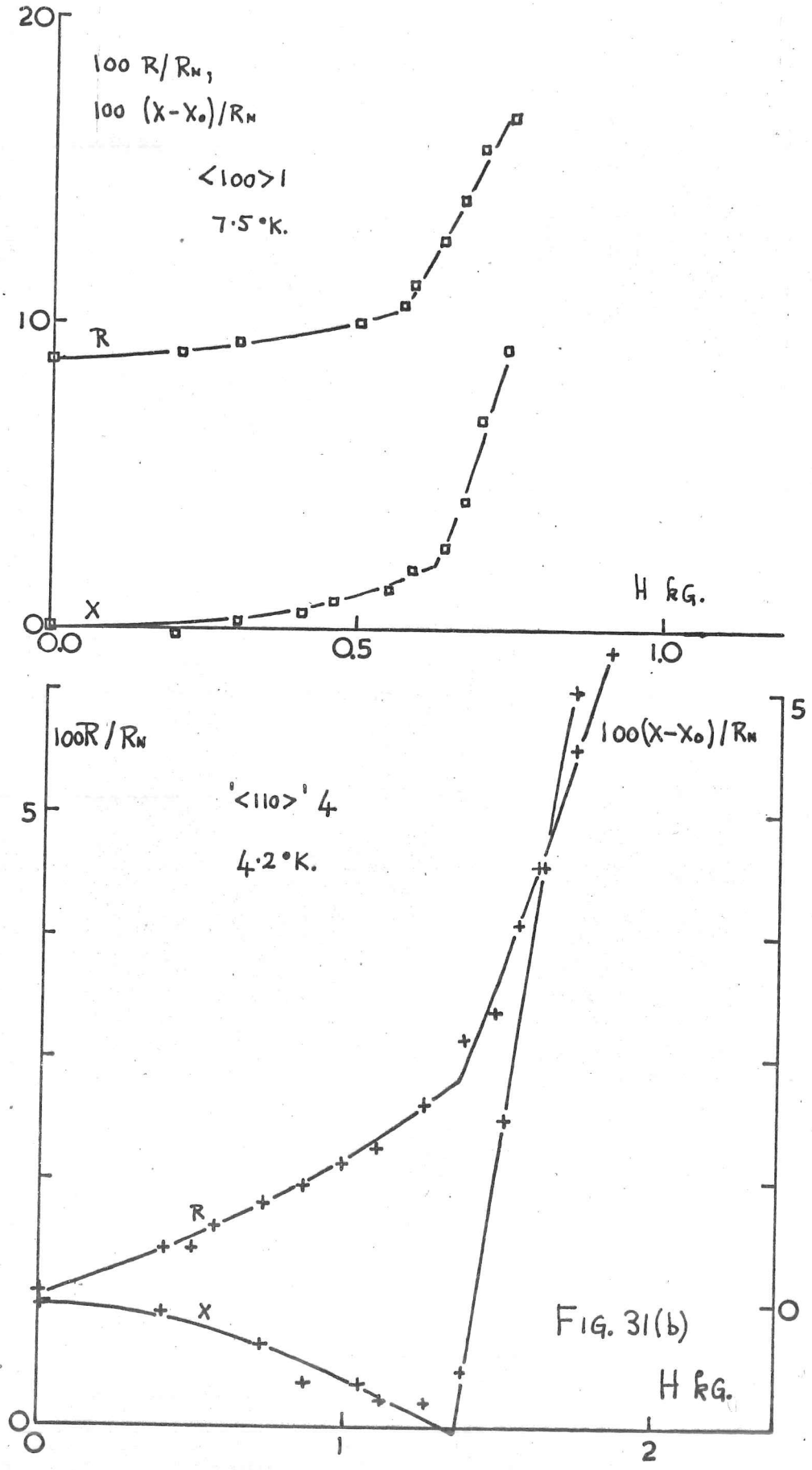
20
100 R/R_N,
100 (X-X_o)/R_N
<100>1
7·5 °K.
10
R
X
0
0.0
0.5
1.0
H kG.
100R/R_N
5
'<110>' 4
4·2 °K.
100(X-X_o)/R_N
5
R
X
0
0
1
2
H kG.

FIG. 31(b)

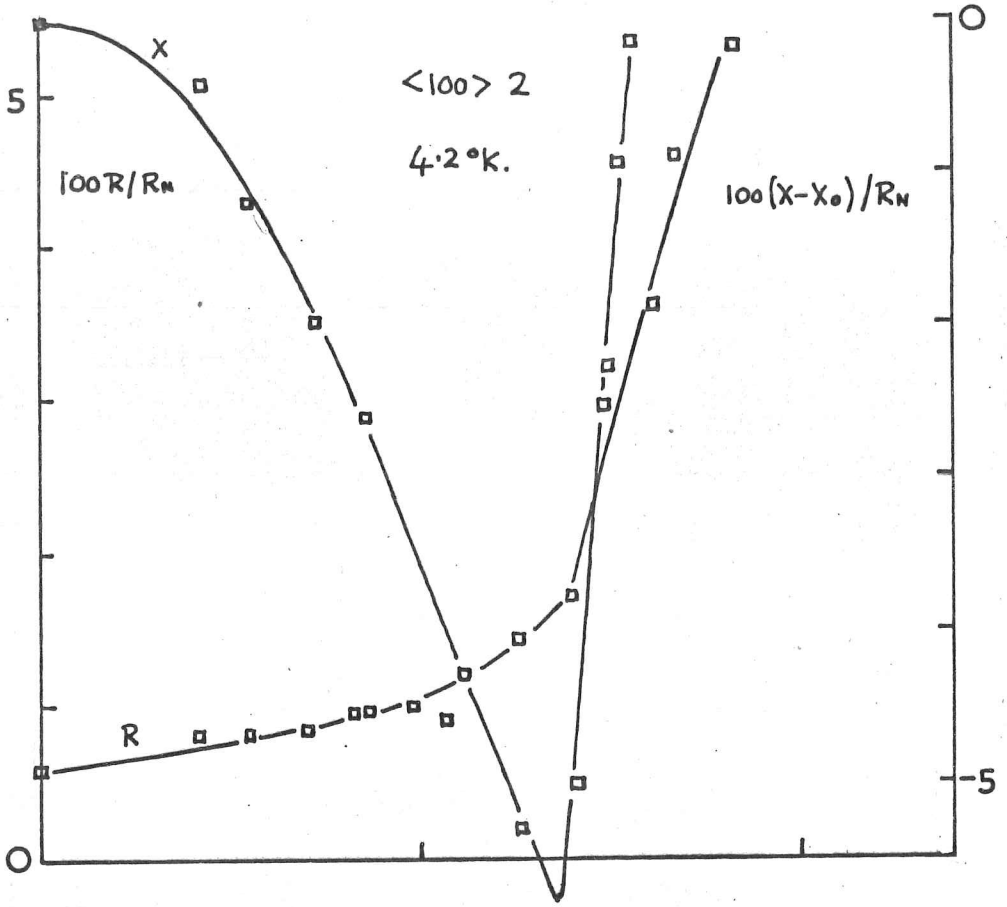
X
<100> 2
4·2°K.
100R/RN
100(X-X0)/RN
R
5
0
-5

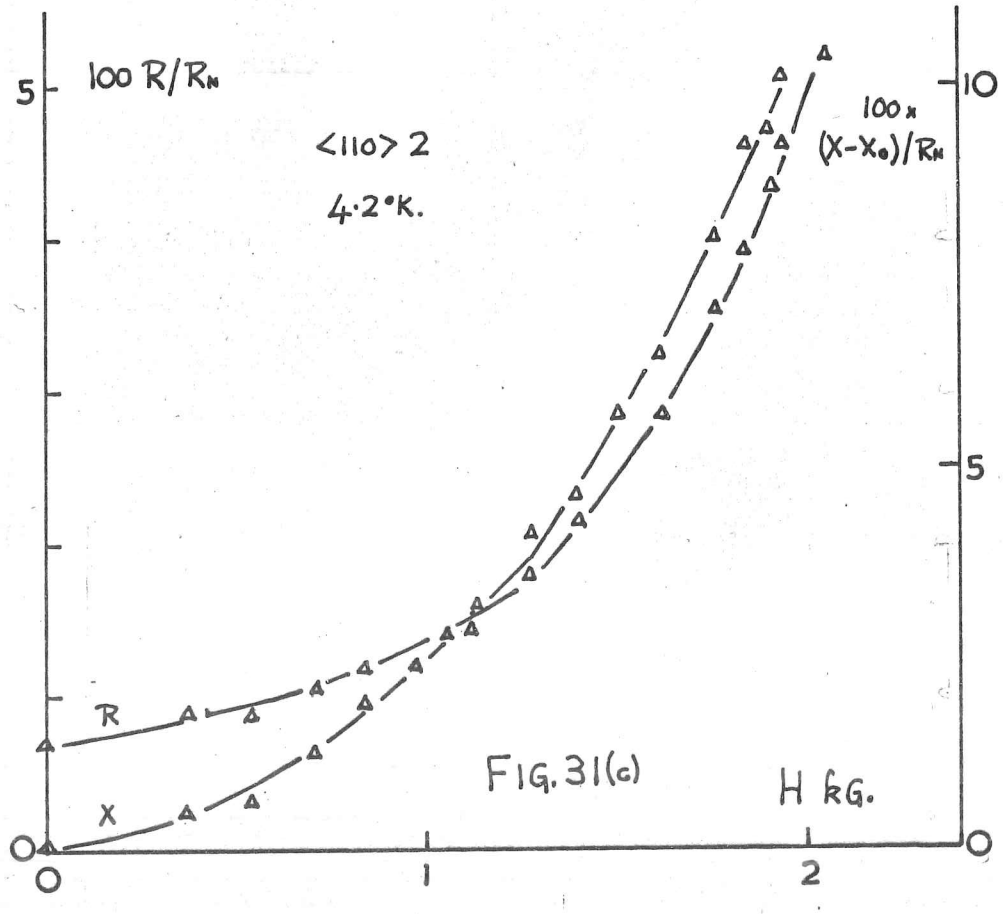
100 R/RN
<110> 2
4·2°K.
100 x
(X-X0)/RN
R
X
5
10
0
1
2
H kG.

FIG. 31(c)

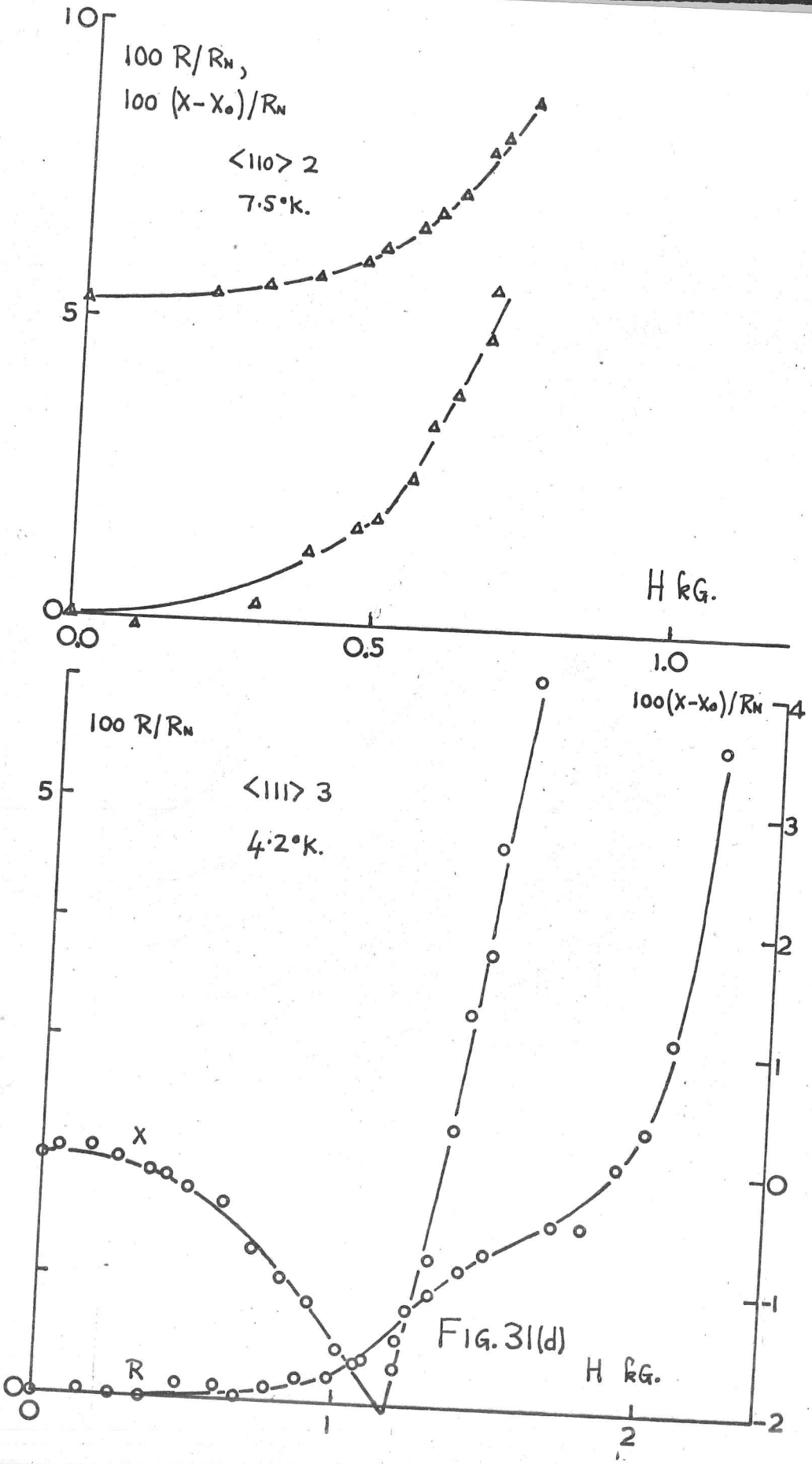
10
100 R/R_N,
100 (X-X_0)/R_N
<110> 2
7.5°K.
5
0
0.0
0.5
1.0
H kG.
100 R/R_N
5
<111> 3
4.2°K.
100(X-X_0)/R_N
4
3
2
1
0
-1
-2
X
R
0
1
2
H kG.

FIG. 31(d)

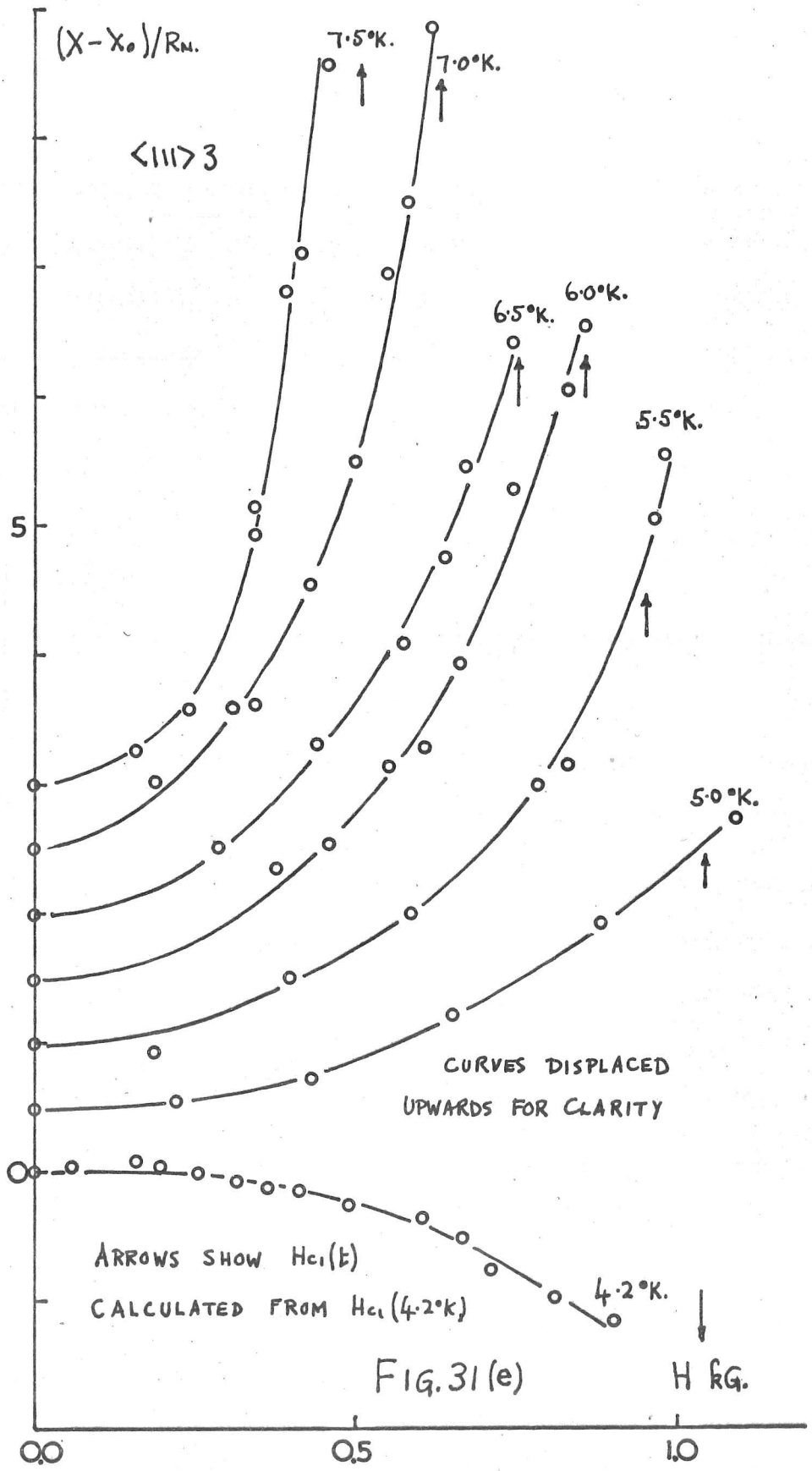
(X-X₀)/Rɴ.
<111>3
7·5°K.
7·0°K.
6·5°K.
6·0°K.
5·5°K.
5·0°K.
5
CURVES DISPLACED
UPWARDS FOR CLARITY
ARROWS SHOW Hc1(t)
CALCULATED FROM Hc1(4·2°K)
4·2°K.
H kG.
0·0
0·5
1·0

FIG. 31 (e)

usual technique of noting the power transmissions of the cavity whilst alternately switching on and off a given magnetic field in order to eliminate the effects of frequency drift. The shifts have been corrected for the spurious skewness as a function of field occasioned by the effect of the stray field of the magnet on the klystron frequency. The value of the magnetic field used was swept down from above + H_{cl} through zero to - H_{cl}, no hysteresis being observable below H_{cl}.

Several general features of the field-dependence may at once be noted:

1. the location of H_{cl} is easily seen in both resistance and reactance, particularly at the lowest temperatures.

2. there is some indication that in the pure specimens at low temperature, particularly $<110>4$, the surface resistance tends to H = 0 with a finite non-zero slope, R(H) showing a non-analytic cusp there. A similar effect has been observed at 170 Mc/s. in the reactance X(H) of tin near T_c by Josephson (thesis - unpublished) and has been commented on theoretically by Garfunkel (88). We have in most cases, unfortunately, insufficient points in the neighbourhood of the origin to be certain that R(H) is indeed truly non-analytic there, but the slope of the dependence is suggestive of this.

3. the reactance shews the more conventional approximately parabolic dependence $\sim H^2$, but has the interesting feature that at sufficiently low temperatures ($4.2^{\circ}K$) for certain specimens, namely: $<111>$ 1 and 3, $<100>$ 2, and $<110>$ 4, there is a decrease with increasing field up to H_{c1}; for $<111>$ 3, the decrease changes to an increase above about $5^{\circ}K$. and remains so up to $7.5^{\circ}K$. at any rate. This behaviour has been seen in several other superconductors (see Josephson - thesis, and Garfunkel (88) for a review), but does not appear to be an incontrovertible result of Garfunkel's theory.

In view of the peculiarities noted in 2 and 3 above, it is a pity that more time was not available to investigate the behaviour of the impedance closer to T_c; in particular, it would have been interesting to know whether or not the decrease in reactance at $4.2^{\circ}K$. for $<111>$ 1, and $<100>$ 2, and $<110>$ 4 showed the same reversion to an increase at higher temperatures as exhibited by $<111>$ 3, and whether sufficiently near to T_c all the specimens then again reverted to a decrease as predicted by Garfunkel.

Also, we should have liked to have looked for any further evidence of non-analytic behaviour in this region in view of Josephson's results for the case of the transverse field orientation, and to have extended our observations to the parallel field configuration. We feel too that further investigation would have been desirable of the crystal-orientation dependence of the reactance decrease; it seems curious that both <111>specimens should agree in shewing the decrease at 4.2°K, while the two <100> specimens disagree:

<100> 1 - increase

<100> 2 - decrease

Of course it may be that there is some as yet unknown dependence on specimen purity or surface condition, though the two <111> samples were of widely differing mean free paths. We must draw attention to the fact that the two <110> specimens also disagree in this respect:

<110> 2 - increase

<110> 4 - decrease

though this discrepancy should be taken less seriously since the latter specimen is known to be poorly oriented being about 8° off axis.

2. HIGH-FIELD BEHAVIOUR

We have made no systematic attempt to investigate the behaviour of the surface impedance in fields higher than H_{c1}, but we shew in fig. (32) the results of measurements of surface resistance for a few specimens up to H_{c3} at 4.2°K. These were obtained, as in the low-field measurements, with a D.C. magnetic field parallel to the specimen axis, and therefore to the microwave current. The changes in slope of R(H) at H_{c2} and H_{c3} are in most cases clearly visible, though we have unfortunately too few points near H_{c2} to make a very accurate determination of this field possible. None of the specimens investigated seemed to shew any very considerable hysteresis in R(H), at any rate to within the experimental accuracy, and the curves shown are averages taken in increasing and decreasing field. In the following table, we give estimates of the critical fields from our curves, together with values of H_{c1} from the low-field measurements:

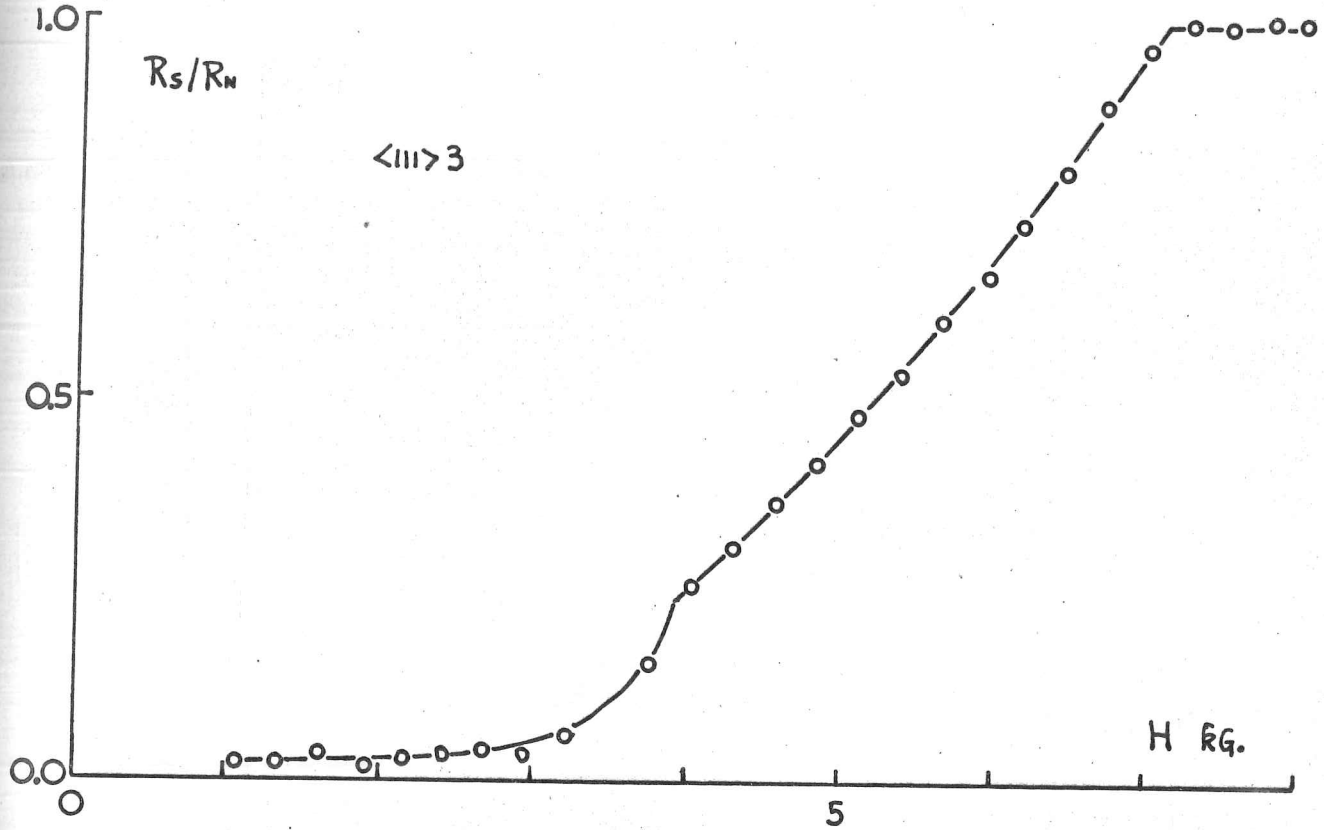

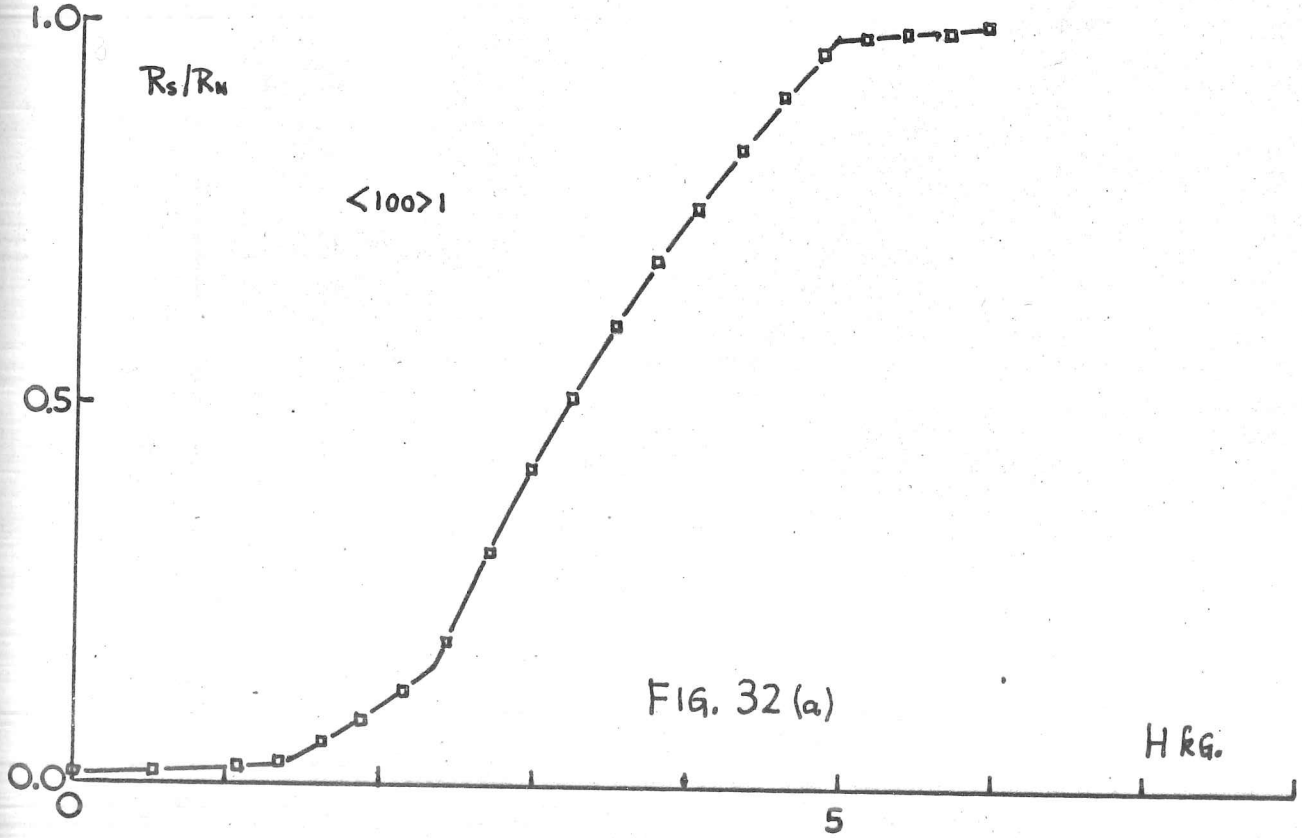

FIG. 32 (a)

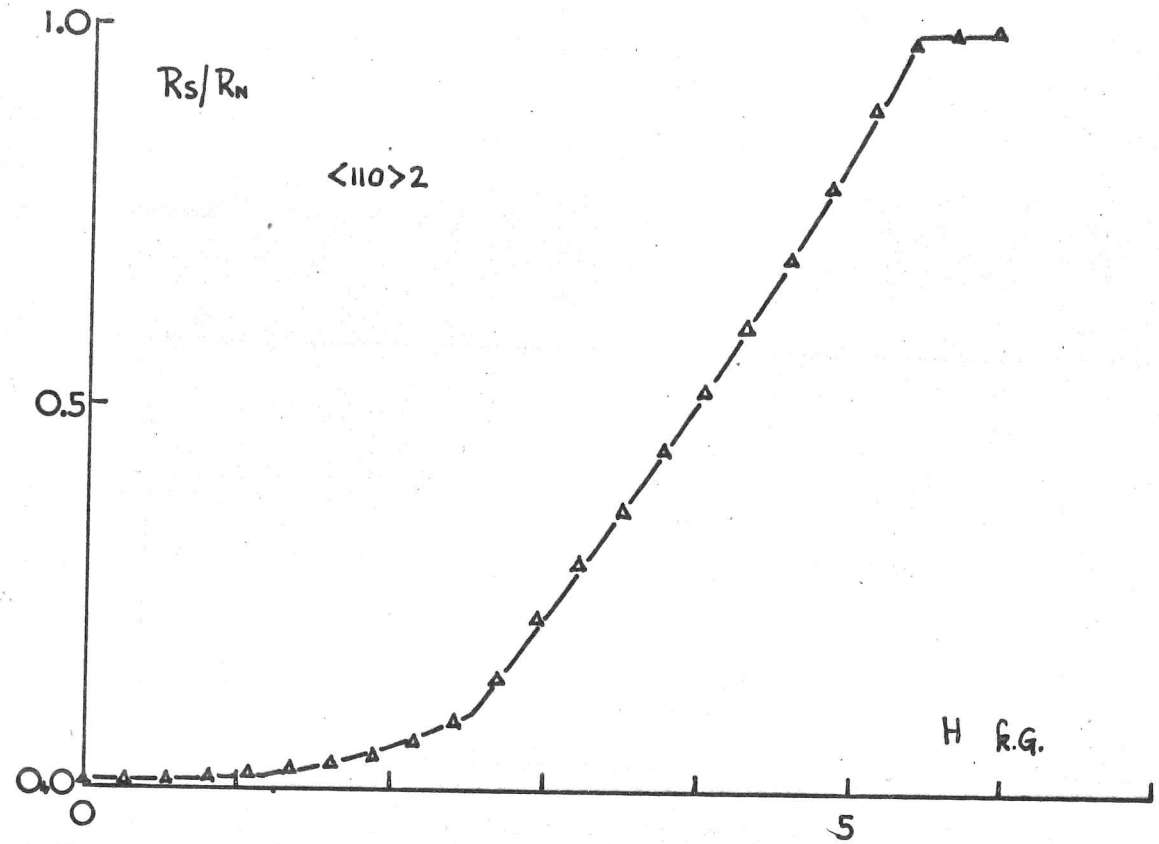

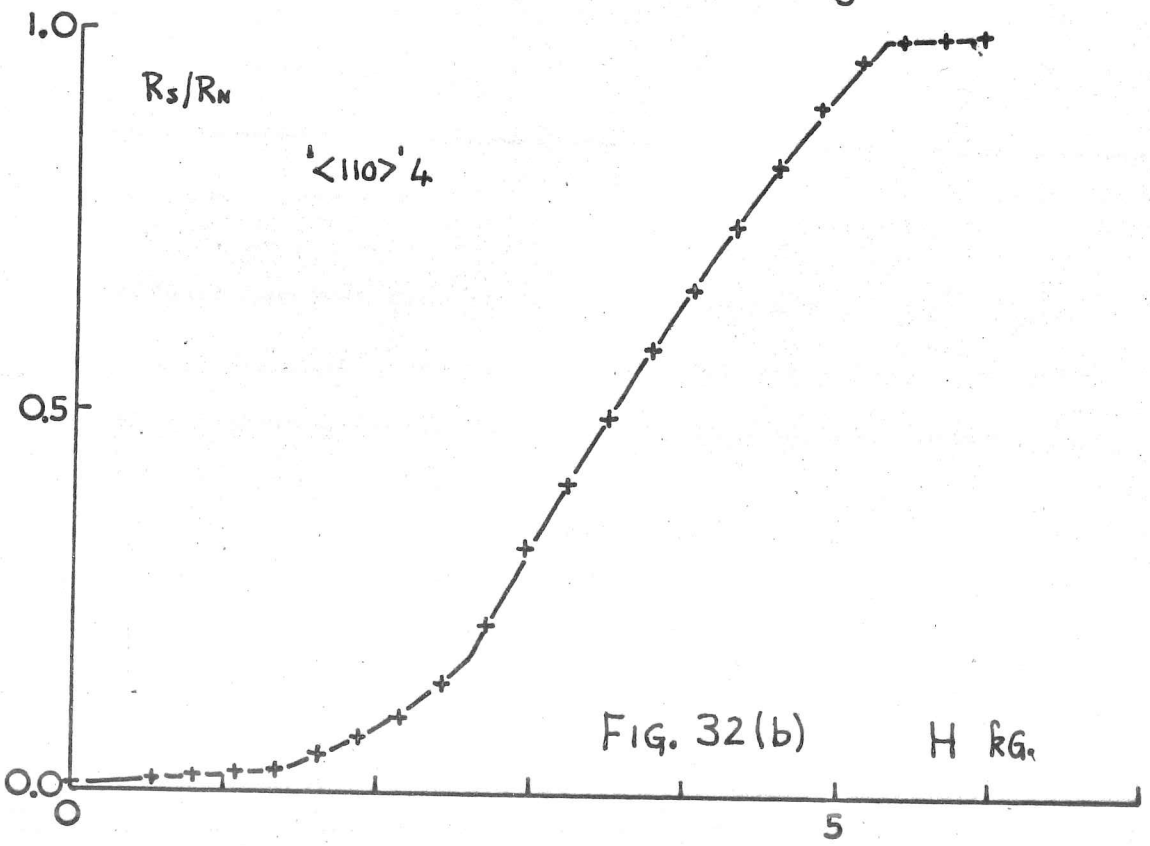

FIG. 32(b)

specimen	ρo	H_{c1}/4.2°K	H_{c2}	H_{c3}	H_{c3}/H_{c2}
	μΩ. cm.	kG.			
<111> 1	0.0126	1.61			
<111> 3	1.01	1.10	3.92	7.12	1.82
<100> 1	0.0338	1.40	2.37	4.91	2.07
<100> 2	0.082	1.35			
<110> 2	0.119	1.28	2.53	5.39	2.13
<110>* 4	0.0302	1.36	2.58	5.26	2.04

* - poorly oriented.

No attempt has been made to correct the above results for H_{c1} for the demagnetisation factor of the specimen which is estimated from the tables given by Stoner (Phil. Mag. 36, 803 (1945)) to be:

$$4\pi N \sim 0.18$$

for an ellipsoid of semiaxes ~ 0.05 cm. and 0.6 cm.. The effect of this correction would presumably be to increase our estimate of H_{c1}.

The work of Cape & Zimmerman (90) shews that the effect of non-zero N is to modify the slopes of the magnetisation characteristic in the Meissner region to:

$$\frac{dM}{dH} = -1/4\pi(1-N)$$

and near H_{c2} to:

$$\frac{dM}{dH} = 1/4\pi\left[1{\cdot}16(2\kappa_2^2-1)+N\right]$$

At H_{c1} no detailed calculation appears to have been made, but empirically the results of Aston et al. (91) show that at any rate in the materials which they investigated, having fairly high κ , the field at which flux first starts to penetrate is given approximately by:

$$H^* = H_{c1}/(1-N)$$

This would imply that our values of H_{c1} should be increased by about 1½%.

For comparison, we show in the following table some relevant information adduced from other authors:

source	ρ_o $\mu\Omega$.cm.		H_{c1}/4.2°K. kG.	H_{c2}	H_{c3}	H_{c3}/H_{c2}
Finnemore et al. (53)	0.01		1.37	2.60	-	-
French (3)	0.01		1.41	2.66	-	-
Webb (92)	0.001		-	-	-	1.87
Ostenson & Finnemore (93)	0.01		-	-	-	1.85
Tsuda & Suzuki (10)	0.018	<110>	-	2.74	-	-
	0.036		-	2.78	-	-
	0.073		-	2.97	-	-
	0.15		-	3.76	-	-
	0.018	<111>	-	2.74	-	-
	0.024		-	2.77	-	-
	0.058		-	2.87	-	-
Ikushima & Mizusaki (79) (Nb-Ta alloys)	0.016			2.63		
	0.219			3.00		
	0.373			3.04		
	0.843			3.55		
	1.29			3.78		
	2.56			5.30		

We see from this table that the mean-free-path dependences of H_{c2} obtained by Tsuda & Suzuki and by Ikushima & Mizusaki do not seem to agree very well with each other, but this is no doubt due to the fact that the principal impurity in the case of the former authors was probably oxygen, whereas the latter used controlled additions of T_a. At any rate, our specimen <111> 3 would appear to fit fairly well with Ikushima & Mizusaki's results in regard to its value of H_{c2}, which is a little higher than theirs at a comparable resistance ratio. Their results also would show a depression in T_c of about $0.7^{\circ}K$ for this specimen, our observed depression being $0.70^{\circ}K$.

There is little more we can do in detail to analyse the purity-dependence of our critical fields; as regards anisotropy, there is perhaps some indication from our results that:

$$H_{c2} \ \langle 110 \rangle \ > \ H_{c2} \ \langle 100 \rangle$$

in agreement with the findings of Reed et al. (94), Farrell et al. (85), and Williamson (95).

Our values of H_{c3}/H_{c2} seem a little higher than that reported by Webb (92), which is probably the most reliable measurement to date. This may perhaps indicate the effect of strain or differential

impurity diffusion at the surface of our samples, though values as high as 2.6 have been reported by Catterall et al. (96) in specimens having: $\rho_o \sim 0.5\ \mu\Omega$.cm. which would be inconsistent with our value of 1.82 for specimen <111> 3, $\rho_o \sim 1.01\ \mu\Omega$.cm. We have unfortunately made no measurements of H_{c3}/H_{c2} at higher temperatures for any of our pure specimens which would enable us to cast any light on the interesting discrepancy near T_c between the results of Webb and Ostenson & Finnemore. Webb finds the temperature-dependence of the ratio to be given by:

$$\frac{H_{c3}}{H_{c2}} = \begin{cases} (1.89 \pm 0.03) & \text{at } t=0 \\ 1.67 + 0.8(1-t) & \text{for } 0.85 < t < 1.0 \end{cases}$$

the temperature dependence near T_c being close to that predicted for a pure type II superconductor by Ebneth & Tewordt (97). Ostenson & Finnemore find good agreement with Webb's results up to about t = 0.85, but find that at higher temperatures, the ratio drops dramatically, probably to unity at t=1. They speculate that this is due to the breakdown of the Ginzburg - Landau theory sufficiently near to T_c owing to spontaneous fluctuations in the order parameter with an associated breakdown in the uniformity of the 'molecular field' on which the Ginzburg-Landau theory is based;

for type I superconductors, this occurs only within about $1m^{o}K$ of T_c, but for the gapless regime in the surface-sheath state of a type II superconductor such fluctuations may be effective over a much larger temperature range.

DISCUSSION OF HIGH-FIELD SURFACE-RESISTANCE:

The field orientation which we have used, namely parallel D.C. magnetic field and microwave current, is the easiest to treat theoretically, since none of the problems inherent in the perpendicular case arise where collective oscillations of the order parameter are known to give additional loss - flux-line motion below H_{c2} as discussed by Caroli & Maki (98), and depairing effects in the gapless superconducting sheath regime below H_{c3} by Fischer & Klein (99), Fink & Kessinger (100), and Maki (101). Even so, a detailed analysis of R(H) is still scarcely possible. The surface-sheath regime in the dirty limit has been considered by Rothwarf et al. (102) on the basis of a two-fluid model with an order-parameter at the surface of amplitude and thickness estimated from the work of Fink & Kessinger (103); while Fischer & Maki (104) have extended the theory to enable the determination of $f_1(t)$ and $f_2(t)$ from microwave measurements in this field orientation,

together with an estimate of the effective sheath thickness.

They give the following expressions for the slope discontinuities at H_{c3} and H_{c2}:

$$S_3 = \left.\frac{\partial\left(\frac{R}{R_N}\right)}{\partial\left(\frac{H}{H_{c3}}\right)}\right|_{H_{c3}} = 2\pi\sqrt{\frac{B_{c_2}(t)\,\delta_{d.}^2}{\phi_0}}\left[2\,k_2^2(t) - 0.334\right]^{-1}$$

$$S_2 = \left.\frac{\partial\left(\frac{R}{R_N}\right)}{\partial\left(\frac{H}{H_{c_2}}\right)}\right|_{H_{c_2}-0} - \left|_{H_{c_2}+0}\right. = r\left[1 - r + r\sqrt{\frac{2}{r} - 1}\right]\left(\frac{B_{c_2}(t)\,\delta_{d.}^2}{\phi_0}\right)\left\{2.32\left(2k_2^2 - 1\right)\right\}^{-1}$$

where: ϕ_0 = flux quantum = 2.07×10^{-7} G.cm.$^{-2}$

$r \equiv \frac{R}{R_N}$; $\delta_{d.}$ = classical skin depth in normal-state.

and for the ratio of the sheath-thickness at H_{c2} to that at H_{c3} they obtain:

$$\alpha(t) = \frac{\sqrt{\frac{2}{r} - 1} - 1}{S_3(t)}\left(\frac{H_{c3}}{H_{c3} - H_{c2}}\right)$$

The relations for S_3 & α appear to be valid in the dirty, local regime $l \sim \xi_0$, and provided:

$$\delta_{d.} >> \sqrt{\frac{\phi_0}{B_{c_2}(t)}} = \sqrt{2\pi}\,\xi(t)\ ;\ \xi\text{- sheath thickness}$$

whereas that for S_2 is derived on the basis of a simple superposition of the vortex-state and the sheath-state right up to the

surface; as Fischer & Maki point out, this rather implausible assumption appears to yield poor values for $\kappa_1(t)$ for their measurements on Pb Bi and Pb In alloys, and so the expression for S_2 is probably of little use.

None of our specimens is really sufficiently local for the theory to be directly applicable; for example $<111>$ 3 has $\frac{l}{\xi_0} \sim 1$ compared with $\sim$ 0.2 for Fischer & Maki's alloys which, however, have comparable or larger values of $\kappa(\sim 3\text{-}4)$. Anyway, supposing we put in figures for specimen $<111>$ 3, we get at 4.2°K:

$S_3 = 1.98$ (from graph), $B_{c2} = 3.92$kG., & $\delta_{el.} = 0.503\ \mu$.

gives: $\kappa_2|_{4.2°K.} = 3.37$

This figure looks rather unreasonably high compared with the figure which we would estimate for this specimen by comparison with the data of Ikushima & Mizusaki, viz:

$$\kappa_2|_{4.2°K.} = 2.1$$

c.f. their figure for pure Nb of 1.53. In the absence of any detailed knowledge of the impurity content of the specimen or of its actual magnetisation characteristic, it is difficult to throw any further light on this discrepancy beyond saying that our specimen is probably insufficiently local electrodynamically for

the Fischer-Maki theory to apply very closely.

Finally, taking:

$H_{c3} = 7.12$ kG. and $t|_{H_{c2}} = 0.235$ (from graph)

we obtained the reduced sheath thickness at H_{c2} of:

$$\alpha|_{4.2°K.} = 1.96$$

as compared with that at T_c estimated from Fink & Kessinger's calculation for $\kappa = 1.5$,

$$\text{i.e.} \quad \alpha/T_c = 1.63$$

The increased value at low temperatures is in agreement with the trend of Fischer & Maki's results, and is of comparable magnitude.

Regarding the behaviour of the purer specimens, there is little we can do in the way of quantitative analysis beyond remarking that as expected the screening exerted by the surface sheath at H_{c2} is even more substantial than for $<111>3$; for example, the normal-state skin depth for $<100>1 \sim 700$Å compared with a sheath thickness at 4.2°K of presumably 400-500Å.

CHAPTER 6 - SUMMARY

We are conscious of having been able to make only a rather incomplete analysis of the results of our measurements on niobium, but are certainly unable to agree with the opinion voiced by Maxfield and McLean that - 'there appear to be no anomalies in the electrodynamic behaviour of (niobium).....'. Our results show peculiarities in both the normal- and superconducting-states; regarding the former, we have been able to arrive at no very firm conclusions, save that there may well be the effects of scattering- and Fermi-surface-anisotropies in operation perhaps in rather complicated combination. Equally, neither does the superconducting state appear to be very well described by the simple Mattis & Bardeen theory for the purest specimens, though it must be admitted that the evidence here is rather slender; there is clearly a need for a much more extensive investigation to be made of the mean free path dependence of penetration depth in rather pure samples involving preferably known additions of both non-magnetic and magnetic impurities. It would be interesting to extend the measurements, using a He^3 apparatus, to vanadium and tantalum in which anomalies in the specific heat similar to those

in niobium have also been reported. Lastly, we feel that there is a distinct need for rather thorough tunnelling measurements to be made of the temperature- and purity- dependence of the second gap in niobium, since any less than a direct measurement of the gap is fraught with many difficulties of interpretation.

APPENDIX A: Effect of Line Reflexions:

As pointed out in (5), the most serious effect of small mismatches in the input and output waveguides is on the measured values of frequency shift, and we have extended the analysis given there to shew these effects in detail. Unfortunately, the actual procedure for correcting the shifts is very tedious in practice and was not used during routine measurements; however, it was thought fit to include a description of it as it could prove useful if at any time an absolute value of shift should be required.

We may take as a suitable equivalent circuit that shewn in fig. 33(a), in which the microwave resonator is represented by a series resonant circuit, of impedance:

$$Z = R\left[1 + 2i\left(\frac{\omega - \omega_0}{\omega_B}\right)\right]$$

the resistance R being related to the bandwidth ω_B by the resonator constant γ : $R = \gamma \frac{\omega_B}{\omega_0}$

The coupling to the external circuits is represented by M, the klystron as a voltage source 2V feeding through the characteristic impedance of the line Z_0, and the output detector by a matched

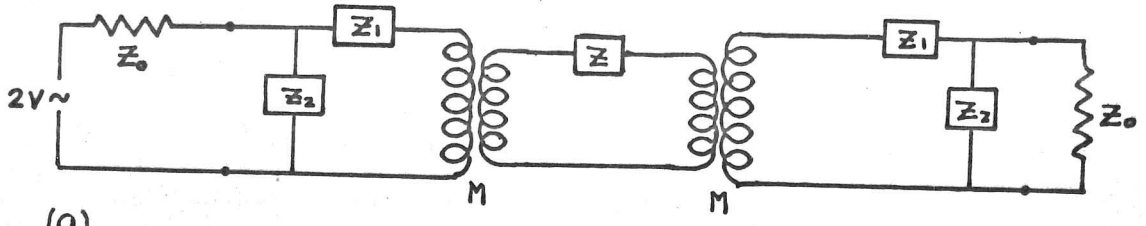

(a)

EQUIVALENT CIRCUIT

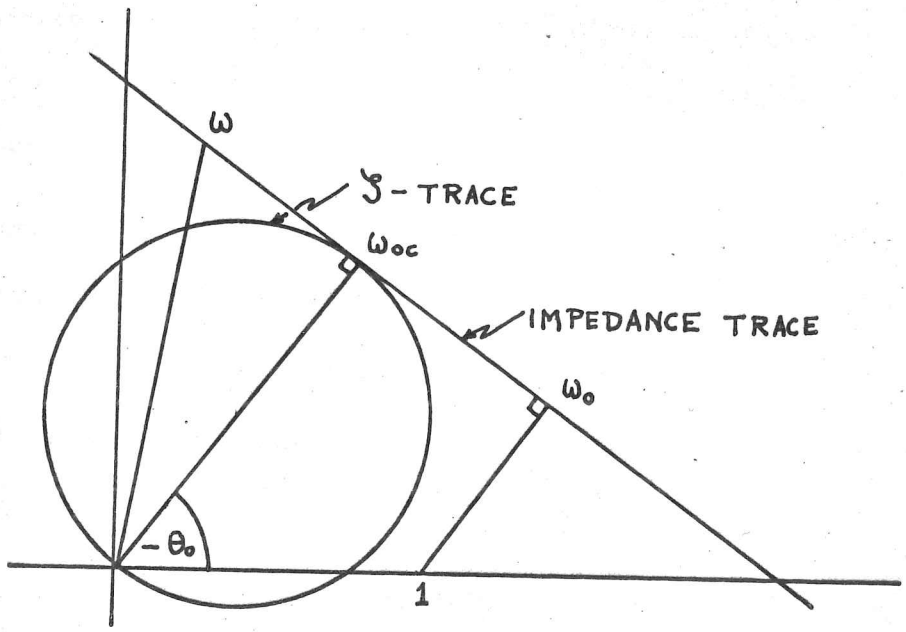

(b)

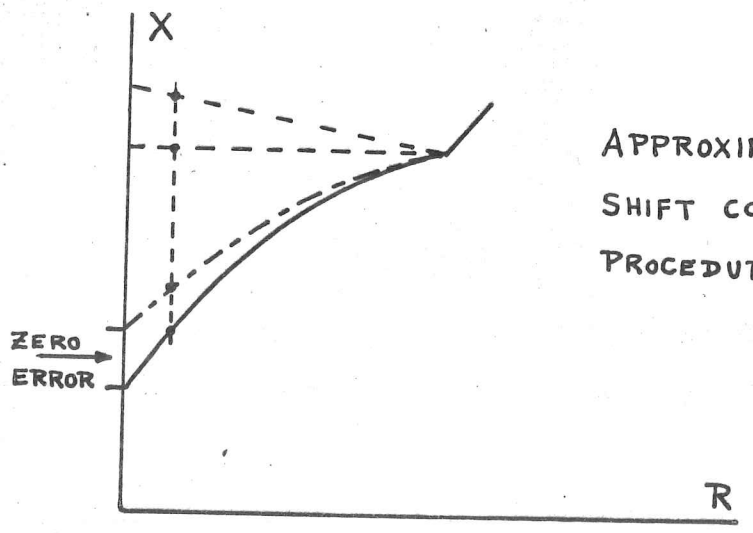

(c)

APPROXIMATE
SHIFT CORRECTION
PROCEDURE

FIG. 33

load Z_o. Impedances Z_1 and Z_2 represent the effect of reflexions, which can be envisaged as of two sorts:

1. reflexions at the coupling probes themselves, which are virtually frequency-independent within a typical bandwidth.
2. more distant reflexions in the line, which may well be quite frequency-dependent owing to the large number of wavelengths separation from the resonator.

A straightforward circuit analysis yields the voltage transmission coefficient as:

$$\mathcal{J} = 1 \Big/ \left(\frac{Z}{Z_c}+1\right)\left(\frac{2\omega^2 M^2}{Z_c Z_o}\right)\left(1+\frac{Z_o}{Z_2}\right)^2$$

where the coupling impedance: $Z_c = \dfrac{2\omega^2 M^2}{Z_1 + \dfrac{1}{\frac{1}{Z_o}+\frac{1}{Z_2}}}$

Note that for no reflexions $Z_1=0$, $Z_2=\infty$, we have:

$\mathcal{J} = 1 \Big/ \left(\frac{Z}{Z_c}+1\right)$ and: $Z_c = \dfrac{2\omega^2 M^2}{Z_o}$ — the real coupling losses.

We shall assume that Z_1 is the frequency-independent reflexion, and that $Z_2 \gg Z_o$ and has a small frequency dependence.

First, we note that if $A_2 = \frac{1}{Z_2} = 0$ then:

$$Z_c \equiv Z_{co} = \frac{2\omega_o^2 M^2}{Z_o(1+Z_1/Z_o)} \equiv |Z_{co}|\, e^{i\theta_o}$$

where the non-zero phase θ_o arises from the frequency-independent reflexion at the probes; this has the effect (compare (5)) of changing the phase of Z by $-\theta_o$ in terms of the effect on $\mathcal{J}$ and so the whole impedance plot is swung round on the Argand diagram (fig. 33 (b)). The resonance remains Lorentzian and there is a change in resonant frequency which depends on coupling, but not on ω_B , since $\omega_B \propto R$:

$$\frac{\omega_{oc} - \omega_o}{\omega_B} = -\frac{1}{2}\,\frac{|Z_{co}|}{R}\,\sin\theta_o$$

and a trivial change in voltage transmission at infinite coupling from 1 to:

$$\mathcal{J}_o = 1 \Big/ \cos\theta_o \left|1+\frac{Z_1}{Z_o}\right| \leqslant 1$$

equality occurring when Z_1 is purely reactive; this merely represents the dissipation of power in a lossy coupling structure.

The effect on the resonance is so far trivial, since there are other effects contributing large coupling-dependent frequency shifts, such as the variation of the capacitance between the coupling probes and the end of the specimen; the important point is that there is no change in shift with bandwidth at a fixed coupling.

Now we consider the effect of introducing a small shunt admittance $A_2 = 1/Z_2$ with, as first approximation, a linear frequency-dependence. This means that the coupling impedance may now be written:

$$Z_c = Z_{co}\left[1 + \frac{\mu}{Q_o}\left(\frac{\omega-\omega_o}{\omega_B}\right)\right]$$

where: $Q_o = \frac{\omega_o}{\omega_B}$ and μ is the small complex coefficient:

$$\mu = \frac{\omega_o}{Z_c}\left.\frac{dZ_c}{d\omega}\right|_{\omega_o} = Z_o\,\omega_o\left.\frac{dA_2}{d\omega}\right|_{\omega_o}\left(1+\frac{Z_1}{Z_o}\right)^{-1}$$

In this case, the voltage transmission is given by:

$$\mathcal{J}^{-1} = \left\{\frac{Z}{|Z_{co}|}\,e^{-i\theta_o} + \left[1+\frac{\mu}{Q_o}\left(\frac{\omega-\omega_o}{\omega_B}\right)\right]\right\}$$

$$\times\left\{\frac{\left|1+\frac{Z_1}{Z_o}\right|e^{-i\theta_o}}{\left[1+\frac{\mu}{Q_o}\left(\frac{\omega-\omega_o}{\omega_B}\right)\right]^2}\right\}\times\left\{1+Z_o A_2\left[1+\frac{q}{Q_o}\left(\frac{\omega-\omega_o}{\omega_B}\right)\right]\right\}^2$$

where: $q = \frac{\omega_o}{A_2}\left.\frac{dA_2}{d\omega}\right|_{\omega_o} \propto \mu$

The 1st bracket gives a (renormalised) Lorentzian resonance and is the most interesting, while the 2nd 2 give renormalisation of $\mathcal{J}$ and skewness of the resonance.

We observe that the 1st bracket can be rewritten as a Lorentz resonance of frequency ω_{oc}' and coupled bandwidth ω_{Bc}'

$$e^{-i\theta_o'}\left\{\left(\frac{R}{|Z_{co}|}+\cos.\theta_o'\right)\left[1+2i\left(\frac{\omega-\omega_{oc}'}{\omega_{Bc}'}\right)\right]\right\}$$

where:

$$\begin{cases}\left(\dfrac{\omega_{oc}'-\omega_o}{\omega_B}\right) \simeq -\dfrac{1}{2}\dfrac{|Z_{co}|}{R}\left\{\sin.\theta_o+\dfrac{1}{2}\dfrac{\mu_r}{Q_o}+\dfrac{1}{2}\dfrac{|Z_{co}|}{R}\,Re\left(\dfrac{\mu}{Q_o}e^{i\theta_o}\right)\right\}\\ \dfrac{\omega_B}{\omega_{Bc}'} \simeq \dfrac{1+\frac{1}{2}\frac{\mu_i}{Q_o}\frac{|Z_{co}|}{R}}{1+\frac{|Z_{co}|}{R}\left(\cos.\theta_o-\frac{1}{2}\frac{\mu_r}{Q_o}\frac{|Z_{co}|}{R}\sin.\theta_o\right)}\end{cases}\qquad (A)$$

and:

$$\begin{cases}(\theta_o'-\theta_o) \simeq \dfrac{1}{2}\dfrac{\mu_r}{Q_o}\dfrac{|Z_{co}|}{R}\\ \mu_r \equiv Re.(\mu)\\ \mu_i \equiv Im.(\mu)\end{cases}$$

We now see that the frequency of the shifted resonance ω_{oc}' contains a term proportional to the bandwidth; given two resonances of different bandwidths ω_{B1} and ω_{B2}, we have,

$$(\omega_{oc_1}'-\omega_{oc_2}')-(\omega_{o1}-\omega_{o2}) = -\frac{1}{4}\alpha(\omega_{B1}-\omega_{B2})$$

where: $\alpha = \dfrac{\mu_r}{Q_o}\dfrac{|Z_{co}|}{R}$ — independent of bandwidth

$$\simeq \frac{\mu_r}{Q_o}\left(\frac{\omega_{Bc}'}{\omega_B}-1\right) = \mu_r \sec.\theta_o\left(\frac{\Omega_B}{\omega_o}\right)$$

where: $\Omega_B = (\omega_{Bc}'-\omega_B)$ is the coupling loss.

so that:

$$\Delta\omega_{oc}'-\Delta\omega_o = -\frac{1}{4}\mu_r \sec.\theta_o\left(\frac{\Omega_B}{\omega_o}\right)\Delta\omega_B$$

This result implies that it should be possible to obtain the frequency shift $\Delta\omega_o$ between the 2 resonances free of the effect of reflexions by masking a coupling-extrapolation of the measured shifts $\Delta\omega_{oc}'$ against the coupling losses Ω_B, in rather the same spirit as the extrapolation of bandwidths to zero coupling. The shifts for all other bandwidths could in principle then be calculated. In practice, the difficulty is that the frequency shifts must also be corrected for skewness of the resonance, and this is also coupling-dependent; we defer discussion of this till later, and pause to note that to the order of approximation we are now considering, the coupling extrapolation of bandwidths is no longer linear for $\mu_r \neq 0$ owing to the coupling-dependence of θ_o'.

In order to cast equation (A) into a form related to the voltage transmission, a detailed calculation of the normalisation brackets occurring in the expression for $\mathcal{J}$ must first be made, taking account of the fact that the factors expressing the skewness of the resonance should be centred on ω_{oc}' rather than on ω_o, and after some tedious algebra, we arrive at:

$$\left(\frac{\omega_B}{\omega_{Bc'}}\right) = 1 - \frac{|\varphi_{res.}|}{|\varphi_o'|} + \left[\sin\theta_o \, R_e\left(\frac{\mu}{Q_o}\frac{Z_1}{Z_o}\right) + \frac{1}{2}\frac{\mu_r}{Q_o}\cos\theta_o \tan\theta_o\right]\left(\frac{1-2\frac{|\varphi_{res.}|}{|\varphi_o'|}}{1-\frac{|\varphi_{res.}|}{|\varphi_o'|}}\right)\left(\frac{|\varphi_{res.}|}{|\varphi_o'|}\right)^2$$

where: $$|\mathcal{S}_o'|^{-1} = \cos\theta_o \left|1+\frac{Z_1}{Z_0}\right| \left|1+2\frac{Z_0}{Z_2}\right| \left(1-\frac{1}{2}\frac{\mu_i}{Q_0}\sec\theta_o\right)$$

and $|\mathcal{S}_{res.}|$ is the voltage transmission at resonance

to be compared with the usual expression: $\left(\frac{\omega_B}{\omega_{BC}}\right) = 1-|\mathcal{S}_{res.}|$

We see that:

1 the bandwidths still extrapolate to the correct value ω_B at $|\mathcal{S}_{res.}|=0$, as they must physically, apart from the effects of direct coupling between input and output.

2 at higher couplings, there is a non-linear correction term $\propto \omega_B$ which vanishes at $\frac{|\mathcal{S}_{res.}|}{|\mathcal{S}_o|} = \frac{1}{2}$, and diverges at 1, where our expansions fail anyway.

3 the normalised response $|\mathcal{S}_o'|$ (extrapolated from the low behaviour) now has a non-trivial dependence on ω_B.

Estimate of Effect of Reflexions on Present Measurements:

Supposing Z_2 can be represented by a small shunt susceptance Y situated at phase ϕ from the resonator, and seen through an

attenuation constant α, it is easy to shew that:

$$|\mu| \sim \frac{Z_0 Y}{\left|1+\frac{Z_1}{Z_0}\right|} e^{-2\alpha} \left(\frac{\lambda_g}{\lambda_0}\right)^2 \phi \quad ; \quad \lambda_g \text{ - guide wavelength.}$$

So for a voltage reflection factor $\sim$ 0.1 situated 25 wavelengths away, and seen through an attenuation of 15dB.,

$$|\mu| \sim 0.1 \times 10^{-1.5} \times 2\pi \times 25 \sim 1$$

Now: $Q_0 \gtrsim 10^4$ for typical normal state bandwidth,

so error in shift $\sim \frac{\mu}{Q_0} \omega_B \sim 10^{-4} \times 1$ Mc/s. ~ 0.1 kc/s.

Even if the attenuation was absent, error should only be a few kc/s.

APPROXIMATE CORRECTION PROCEDURE FOR SHIFTS:

We have seen that the first order effect of line reflexions on the coupled bandwidths is to introduce a non-linear correction to the coupling-dependence which itself depends on the uncoupled bandwidth. Thus although the bandwidths extrapolate to the correct value, the usual procedure in which a fixed quantity is subtracted from the measured bandwidth as representing the coupling losses is strictly incorrect, and the resistances would in principle require correction for this effect. As an approximation, however, we neglect this (our coupling extrapolations have, in practice, always been linear to within the experimental error) and consider only the correction to the measured shifts. As we have seen, at given coupling, this is proportional to the difference in bandwidths between the normal and superconducting resonances, and the appropriate correction to the reactance is obtained by the construction indicated in fig. (33c); this is an Argand plot of the impedance, and the reactance X is remeasured relative to the shifted base-line shown. This procedure may be used to correct the shifts for the zero-error as determined experimentally from the 'σ-plot' of low temperature impedance described by Waldram (5).

APPENDIX B: Skewness of the Resonance, and Shift Measurements:

Generally, there are 3 sources of resonance-skewness:

1 direct-coupling between input and output

2 frequency-dependence of klystron output, and detector response.

3 line reflexions.

In principle, the effects of 2 may be allowed for by direct measurement of throughput on the assumption that there is no coherent interaction between them, although this is not always convenient in practice, and was only used in the case of the bandwidth extrapolation.

As discussed in (5), the effect of 1 is to modify ζ to a form:

$$\zeta^{1-1} = \left(\frac{Z'}{R_c} + 1\right)\left(1 - i\alpha\frac{Z}{R_c}\right) + O(\alpha^2)$$

where α is the small direct-coupling coefficient, and Z' contains a small coupling-dependent frequency shift: $\left(\frac{\omega_0' - \omega_0}{\omega_B}\right) = \frac{1}{2}\alpha\frac{R_c}{R}$

It is easy to shew that this has roots:

$$2\left(\frac{\omega - \omega_0'}{\omega_{BC}}\right) = \pm\sqrt{\frac{P_{res.}}{P} - 1} - \alpha\frac{R}{R_c}\frac{\omega_{BC}}{\omega_B}\left(\frac{P_{res.}}{P}\right) + O(\alpha^2)$$

where: $\frac{\omega_{BC}}{\omega_B} = \frac{\frac{R}{R_c} + 1}{\frac{R}{R_c}} = \left(1 - |\zeta_{res.}|\right)^{-1}$ — coupling extrapolation

and: $P_{res.}$ is the power transmitted at resonance.

So to 1st order, we still have a resonance of Lorentzian width:

$$\left(\frac{\omega_1 - \omega_2}{\omega_{Bc}}\right) = \sqrt{\frac{P_{res.}}{P} - 1}$$

but with a skew-central frequency $\propto \frac{1}{P}$, P being the power level of measurement:

$$\frac{1}{2}\left(\omega_1 + \omega_2\right) = -\frac{1}{2}\alpha\omega_B \frac{R_c}{R}\left(\frac{P_0}{P}\right) \quad ; \quad P_0 = |S_0|^2$$

which is independent of ω_B , since $\omega_B \propto R$.

We may now add that the effects of 2, 3 are (as we have seen previously) to introduce factors into the power transmission of the form:

$$\left[1 + \beta\left(\frac{\omega - \omega_0}{\omega_0}\right)\right]$$

β being a small skewness coefficient independent of ω_B , but depending on the bandwidths of the klystron and the detector, and on the value of 'μ' for line reflexions.

So the overall skewness is given by:

$$\frac{1}{2}\left(\omega_1 + \omega_2\right) = -\frac{1}{8}\left[\left(4\alpha\frac{\omega_B}{R}\right)R_c + \left(\beta\frac{\omega_B^2}{\omega_0 R^2}\right)R_c^{\cdot 2}\right]\left(\frac{P_0}{P}\right)$$

which is again ω_B -independent.

So we have:

direct coupling skewness α (coupling losses)

remainder of skewness α (coupling losses)^2

It is this rather unpleasant behaviour which makes the coupling extrapolation of shifts so tiresome in practice, since the skewness has to be separately measured at each coupling - if the 2nd term were absent, the correction to the shifts if measurements were made at given $\frac{P_0}{P}$ (which could itself be difficult in practice) would be linear in the coupling losses, and could be absorbed into the real central frequency-shift of the resonance caused by line-reflexions, as discussed previously.

Usually, however, shift measurements were merely made at fixed coupling, and at any rate for the low temperature shifts it was found most convenient to make the measurements between fixed levels P in the normal and superconducting states, so that the skewness correction should be constant for all the measurements and should not distort the temperature-variation of the shifts even if not allowed for at all.

In practice, the most satisfactory method of measuring the skewness correction was found to be to use the method employed for measuring shifts i.e. for a given resonance, to switch alternately between the level P and some reference level (say $^3/_4$

of the peak) making shift measurements in the usual way to allow for drift.

A typical plot of shift vs. $1/P$ is shown in fig. (34), the skewness correction between typical practical levels of measurement being about 10kc/s. i.e. about 2% of the normal-state bandwidth, and a measurable to somewhat better than 1kc/s. In fact, it was usually found unnecessary to make the full plot against 1/P, a single direct measurement of the shift between the 2 measuring levels sufficing. On the few occasions where switching to the normal-state was accomplished by magnetic field rather than by heating above the transition, it was also found necessary to correct for the rather large shift caused by the effect of the stray magnetic field on the klystron by measuring the apparent shift of the normal-state resonance above T_c in a magnetic field (partly owing to a real magnetoreactance of course); this usually amounted to about 25 kc/s.

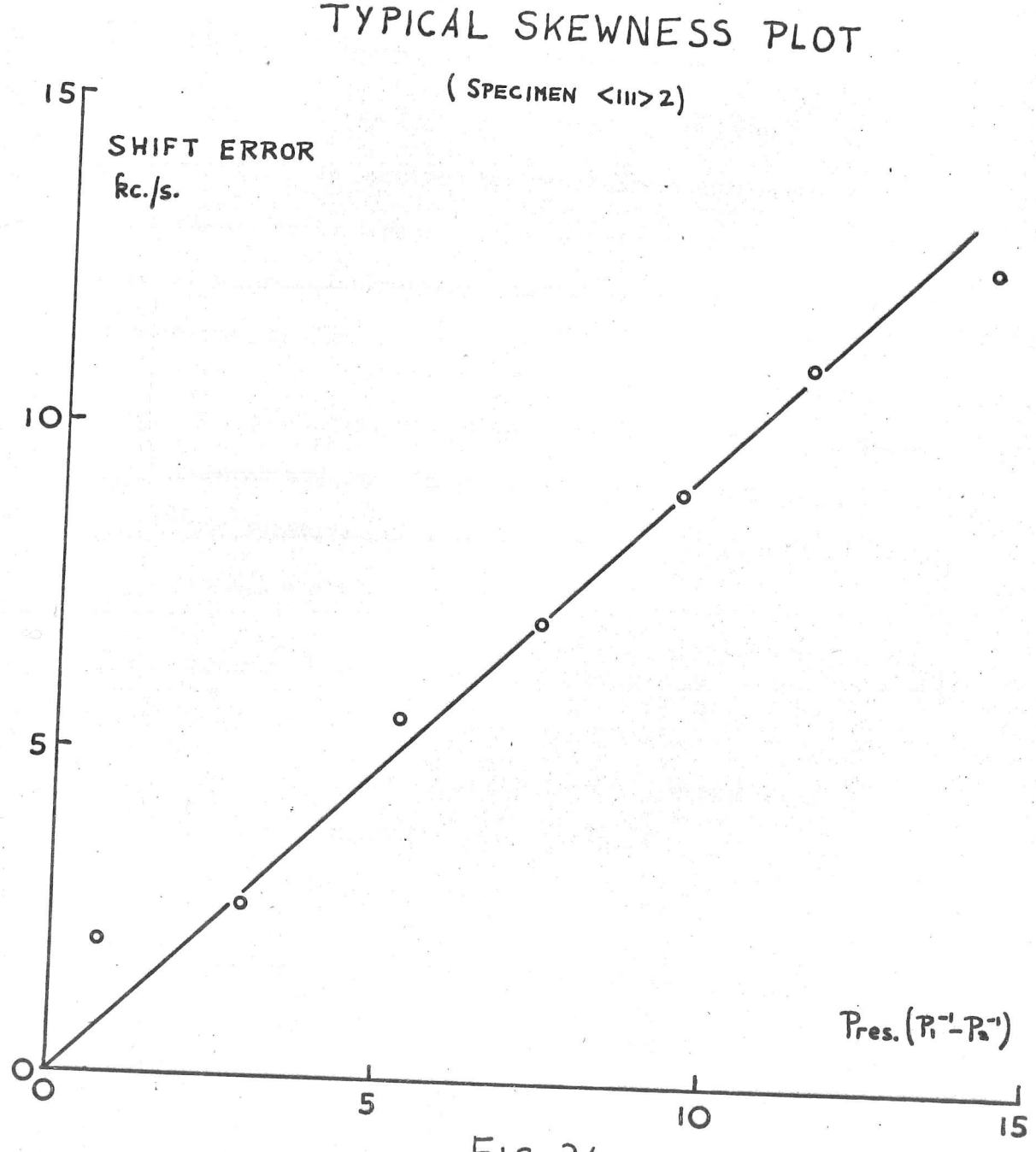
TYPICAL SKEWNESS PLOT
(SPECIMEN <111> 2)
15
SHIFT ERROR
kc./s.
10
5
0
0
5
10
15
Pres. (P1^-1 - P2^-1)

FIG. 34

APPENDIX C: Specimen Heating Correction

As pointed out by Pippard (Thesis) and Waldram (5), the heating of the specimen by the incident microwaves produces a noticeable distortion of the measured impedances near to Tc; this effect was particularly a nuisance during the present set of measurements for:

1. the least pure specimens, where the heating correction, though not very large, was certainly comparable with the relative width of the transition (owing to the high normal state resistance)

2. the purest specimens, where, on account of the low normal state resistance, it was not possible to reduce the coupling sufficiently to prevent distortion of the apparent transition-shape by the bandwidth-dependence of the heating correction (see later).

A short calculation shews that the thermal resistance between the specimen of radius a, length l, through exchange gas of conductivity k to the outer can of the resonater, radius b, is:

$$2\pi k l / \log.(b/a)$$

Now at 9°K., the exchange gas (not in the Knudsen region) has k = 0.13 mW $^{\circ}K^{-1}$. cm^{-1}. (White - Experimental techniques in low-T physics 2nd ed. p.82 Oxford), and taking l = 1·2cm., $2b$ = 1·5cm., $2a$ = 1mm. gives a thermal resistance of about 0.35 mW.$^{\circ}K^{-1}$. Assuming that the crystal detector receives 1μW. of microwave power, and allowing for the padding atten uation of 15dB., the power dissipated in the specimen is about 32μW. at a voltage transmission of 0.5 (see later) ; the resulting temperature rise is then about 100 m°K. In practice, the rises observed are from 30 to 80 m°K. These are somewhat larger than might have been desired, mainly because the specimens are rather small, and the padding attenuator might, in retrospect, have been reduced a little too. The alternative would have been to use a galvanometer amplifier in the detection system and operate at lower signal levels, though this would have required some care in the reduction of thermal e.m.f.'s and noise.

In view of the size of these heating corrections, a method of analysis was devised to allow for the non-linearity of the R(T) curve within a range of about 100 m°K.

A simple circuit analysis shows that the power dissipated in the specimen is:

$$\frac{P_o}{\left|1+\frac{Z+R_e}{R_c}\right|^2}\cdot\frac{R}{R_c} = P_o|S|^2\frac{R}{R_c} = P(\omega,T)\frac{R(T)}{R_c}$$; $P(\omega,T)$-power transmitted from the resonator

assuming that all the heating in the specimen arises from the dissipation in its own resistance R(T), and none from that in the extraneous loss Re (might not be completely true of the dielectric loss). This power may be equated to $k\delta$

where: $\begin{cases} k - \text{thermal resistance to the specimen} \\ \delta = T - T_o = \text{temperature excess over the resonator.} \end{cases}$

If we consider the R(T) curve as measured by the transmissions at the resonance peak (fig. 35a), at given resonator temperature T_o, S and R depend on P_o; so, at a fixed resistance R' (and therefore $S'_{res.}$) we have:

$$\frac{\delta'}{\delta'-(T_o-T_o')} = \frac{P_o}{P_o'}$$

so that the correction: $$\delta' = \frac{T_o-T_o'}{1-\frac{P_o'}{P_o}}$$

But for the curve measured at input power P_o, we know that:

$$\frac{\delta'}{\delta} = \frac{P'_{res.}/P_o'}{P_{res.}/P_o}\,\frac{R'}{R}$$

HEATING CORRECTION

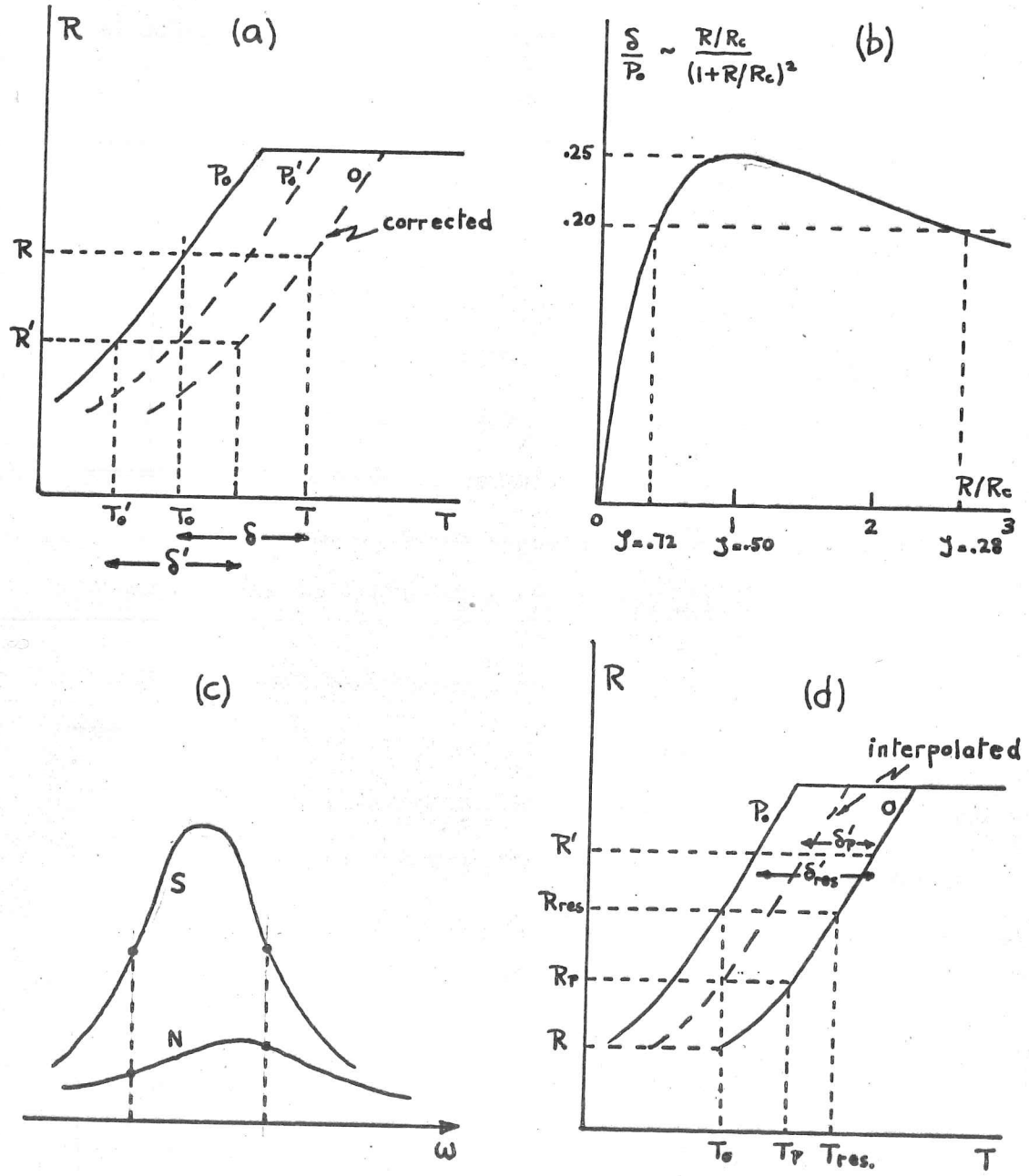

FIG. 35

So that if we adopt the technique of first measuring R(T) at given input P_o, and then sitting at some convenient temperature T_o and measure how R depends on various inputs P_o', we can see that a plot of:

$$(T_o' - T_o) \quad \text{vs.} \quad -\left(1 - \frac{P_o'}{P_o}\right)\left(\frac{P_{res.}'}{P_o'}\right)\left(\frac{R'}{R_c}\right)$$

will yield a straight line, of gradient: $\delta \Big/ \left(\frac{P_{res.}}{P_o}\right)\left(\frac{R}{R_c}\right)$ see fig. (35e). T_o' being the value of T_o on the original curve at which the resistance was R'. This procedure is exact in that it does not assume δ to be small in comparison with the width of the R(T) curve, and allows δ to be calculated at all points on the original curve to within at most about 5 m^oK.

An important point to notice is that since $\delta \propto \frac{R/R_c}{(1+R/R_c)^2}$ its variation with R as one passes through the transition shews the variation in fig. (35b), and that power matching occurs at $R = R_c$; so that although the heating correction at fixed input power is actually maximised for $R_N \sim R_c$, this, or somewhat lower coupling, is the best coupling at which to work from the point of view of producing least distortion of the transition shape - the R(T) curve is simply shifted sideways by an almost constant δ except at the lowest values of R.

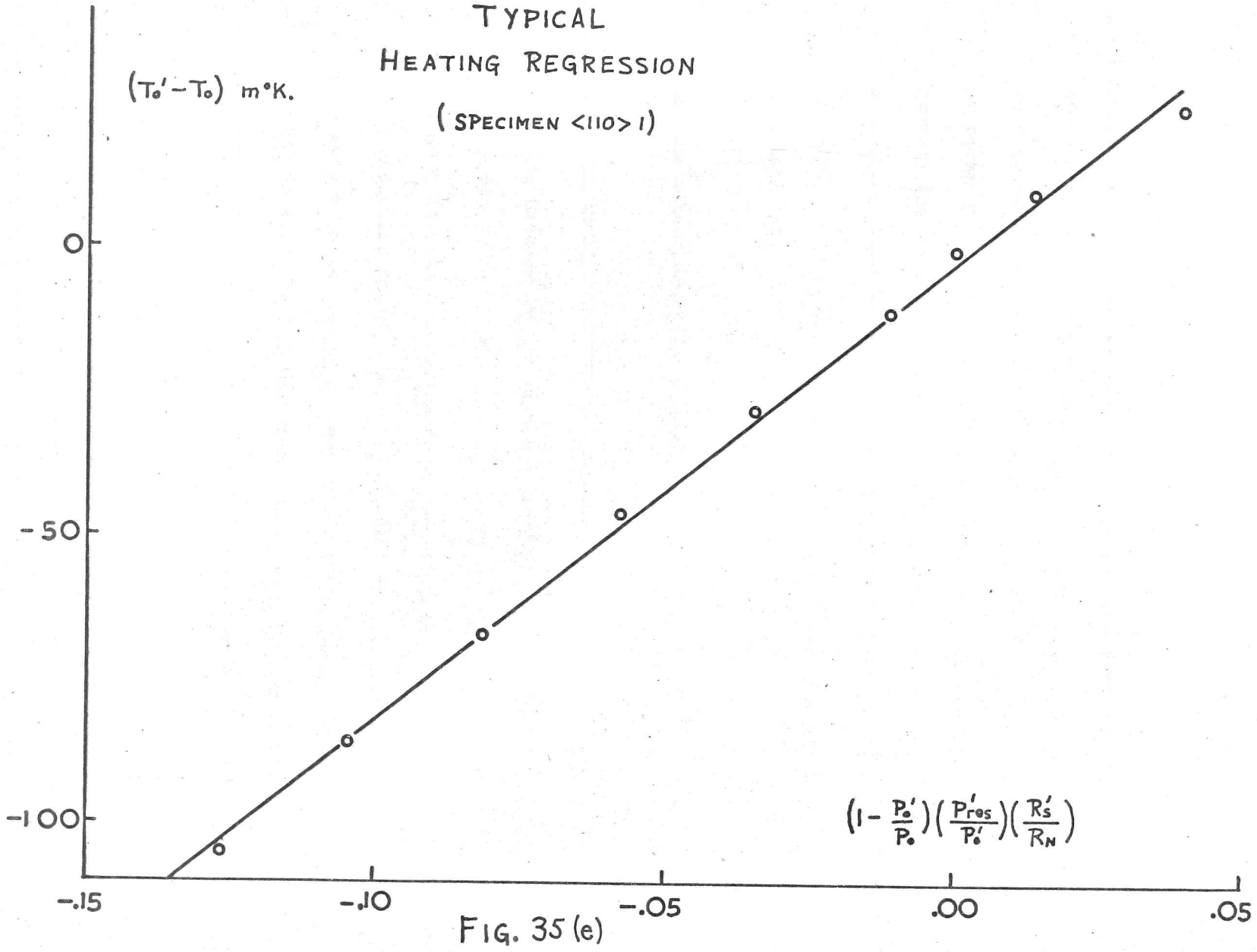
TYPICAL
HEATING REGRESSION
(SPECIMEN <110> 1)
$(T_o' - T_o)$ m°K.
0
-50
-100
-.15
-.10
-.05
.00
.05
$(1 - \frac{P_o'}{P_o})(\frac{P_{res}'}{P_o'})(\frac{R_s'}{R_N})$

FIG. 35 (e)

We now turn to the slightly more involved question of the correction of the shifts near T_c. In this region, the shifts were measured by the method described by Waldram (5) in terms of the changes in Lorentz factors: $Z = \sqrt{\frac{P_{NO.}}{P} - 1}$ on switching between the normal and superconducting states at the peaks, and at a lower level on each side of the resonance fig. (35 c). The shift is then given in terms of the coupled normal-state bandwidth by:

$$\frac{2\Delta w}{w_{BCN}} = \frac{Z_{1N} Z_{2S} - Z_{2N} Z_{1S}}{Z_{1S} + Z_{2S}}$$

and the superconducting coupled bandwidth by

$$\frac{w_{BCS}}{w_{BCN}} = \frac{Z_{1N} + Z_{2N}}{Z_{1S} + Z_{2S}} \qquad (A)$$

Since the heating in the superconducting state depends on the power level P, it is most convenient to arrange the measurements on either side of the resonance to be at equal powers in the superconducting state, i.e. $Z_{1S} = Z_{2S}$ and the difference in levels then occurs on switching to the normal state, where the heating is unimportant. In this way the shifts only involve a single heating correction δ_P, though the peak is still heated by δ. So having already made the correction to the peaks, we are now in a position to interpolate to find δ_P (fig. 35 d). A family of curves of R(T) corresponding to given levels P are constructed

by taking: $\delta_P' = \frac{P'}{P_{res}'}\,\delta'$ at a given R' i.e. linear horizontal interpolation, which is exact for any shape of R(T). Thus at any given resonator temperature T_o, tuning through the resonance gives: $R \longrightarrow R_P \longrightarrow R_{res} \longrightarrow R_p \longrightarrow R$ and similarly: $T_o \longrightarrow T_P \longrightarrow T_{res} \longrightarrow T_p \longrightarrow T_o$. Hence vertical (nonlinear) interpolation at the appropriate value of T_o to the level P enables the corrected temperature T_P to be read off.

If it is also required to calculate the bandwidths from equation (A), the correction is a little more involved, since the corrected temperature is still T_P, but the Lorentz factors Z_s require correction for the fact that the measured peak P_{res} is determined by R_{res} rather than R_p. In fact:

$$Z_s \text{ corrected} = \sqrt{\frac{P_{res.}}{P}\left(\frac{R_{res.}+R_c+R_e}{R_P+R_c+R_e}\right)^2 - 1}$$

where: R_e - extraneous loss.

Actually, values of Z_s so corrected were also used in the calculation of the shifts, though here it is less critical than for bandwidths. At any rate, these corrected values of Z_s are those required for

calculation of the coupled bandwidth W_{BCS}, which is subsequently corrected for coupling and extraneous losses to produce a value of (R_s/R_N) appropriate to temperature T_p. This procedure differs from that outlined by Pippard (Thesis) who used the above value of Z_s to correct (R_s/R_N) directly; in practice, it produces good agreement with R(T) as measured directly from the peaks.

REFERENCES:

(1) Bardeen J., Cooper L. N., & Schrieffer J. R., Phys. Rev. 108, 1175 (1957)

(2) Maxfield B. W. & McLean W. L. Phys. Rev. 139, 1515 (1965)

(3) French R. A. Cryogenics 8, 301 (1968)

(4) Dobbs J. M. & Perz E. R. Proc. Roy. Soc. A296, 113 (1966)
Perz E. R. thesis

(5) Waldram J. R. Adv. in Phys. 13, 1 (1964)
Rev. Mod. Phys. 36, 187 (1964)

(6) Levy M. et al. Phys. Rev. 132, 2039 (1963)

(7) Weber R. Phys. Rev. 133, 1487 (1964)

(8) Ikushima A. et al. J. Phys. Chem. Solids 27, 327 (1966)

(9) Tsuda N. et al. Phys. Lett. 22, 414 (1966)

(10) Tsuda N. & Suzuki T. J. Phys. Chem. Solids 28, 2487 (1967)

(11) Deaton B. C. Phys, Rev. Lett. 16, 577 (1966)

(12) Phillips W. A. Proc. Roy. Soc. A309, 259 (1969)

(13) Kadanoff L. P. & Pippard A. B. Proc. Roy. Soc. A292, 299 (1966)

(14) Rickayzen G. 'Theory of Superconductivity' - Interscience (1964)

(15) Pippard A. B. Proc. Roy. Soc. A251, 165 (1960)

(16) MacVicar M. L. A. & Rose R. M. J. Appl. Phys. 39, 1721 (1968)

(17) Townsend P. & Sutton J. Phys. Rev. 128, 591 (1962)

(18) Sung C. C. & Shen L. Y. L. Phys. Lett. 19, 101 (1965)

(19) Cappelletti R. L. et al. Phys. Rev. 158, 340 (1967)

(20) Mendelssohn K. I.B.M. J. Res. Develop. 6, 27 (1962)

(21) Turneaure J. P. & Weissman I. J. Appl. Phys. 39, 4417 (1968)

(22) Thouless D. J. Phys. Rev. 117, 1256 (1960)

(23) Shen L. Y. L. et al. Phys. Rev. Lett. 14 1025 (1965)

(24) MacVicar M. L. A. & Rose R. M. Phys. Lett. 26A, 510 (1968)

(25) Garland J. W. Phys. Rev. Lett. 11, 111 (1963)

(26) Suhl H. Et al. Phys. Rev. Lett. 3, 552 (1959)

(27) Kondo J. Progr. Theor. Phys. 29, 1 (1963)

(28) Sung C. C. & Wong. V. K. J. Phys. Chem. Solids 28, 19633 (1967)

(29) Soda T. & Wada Y. Progr. Theor. Phys. 36, 1111 (1966)

(30) LeWpold H. A. & Boorse H. A. Phys. Rev. 134 (1964)

(31) Radhakrishnan V. Phys. Stat. Solidi 20, 783 (1967)

(32) Geylikman B. T. et al. Phys. Metals & Metallography 23 no.5, 26 (1967); Ibid. 25 no.1, 154 (1968)

(33) Falko I. I. Phys. Metals & Metallography 23 no. 3, 6 (1967)

(34) Radhakrishnan V. Nuovo Cimento X 48, 111 (1967)

(35) Brown A. et al. Phys. Rev. 92 52 (1953)

(36) Tilley D. R. Proc. Phys. Soc. 84, 573 (1964)

(37) Kon L. Z. Phys. Metals & Metallography 23 no. 2, 17 (1967)

(38) Geylikman B. T. et al. Phys. Metals & Metallography 23 no. 5, 796 (1967)

(39) Moskalenko V. A. Sov. Phys. Dokl. 12 no. 3, 256 (1967) J.E.T.P. 24 no. 4, 780 (1967)

(40) Chow W. S. Phys. Rev. 176, 525 (1968); ibid. 179, 444 (1969)

(41) Leggett A. J. Progr. Theor. Phys. 36, 901 (1966)

(42) Prange R. E. & Kadanoff L. P. Phys. Rev. 134 566 (1964)

(43) Prange R. E. & Sachs A. Phys. Rev. 158, 672 (1967)

(44) Scalapino D. J. et al. Phys. Rev. 148, 263 (1966)

(45) McMillan W. L. Phys. Rev. 167, 331 (1968)

(46) Mattis D. C. & Bardeen J. Phys. Rev. 111, 412 (1958)

(47) Nam S. B. Phys. Rev. 156, 470 (1967); ibid., 487.

(48) Nakajima S. & Watabe M. Progr. Theor. Phys. 29 341 (1963)

(49) McMillan W. L. Phys. Rev. 167, 331 (1968)

(50) Tomasch W. J. Phys. Rev. Lett. 16 16 (1966)

(51) Rowell J. M. & McMillan W. L. Phys. Rev.Lett. 16, 453 (1966)

(52) McMillan W. L. & Anderson P. W. Phys. Rev. Lett. 16, 85 (1966)

(53) Finnemore D. K. et al. Phys. Rev. 149, 231 (1966)

(54) van der Hoeven B. J. C. & Keesom P. H. Phys. Rev. 134, 1320 (1964)

(55) Finnemore D. K. & Mapother D. E. Phys. Rev. 140, 507 (1965)

(56) Wada Y. Phys. Rev. 135, 1481 (1964)

(57) Bardeen J. & Stephen M. Phys. Rev. 136, 1485 (1964)

(58) Swihart J. C. et al. Phys. Rev. Lett. 14 106 (1965)

(59) Sheahen T. P. Phys. Rev. 149, 368 (1966)

(60) Rothwarf F. Phys. Lett. 26A, 43(1967) ibid. 28A, 430 (1968)

(61) Toxen A. M. Phys. Rev. Lett. 15, 462 (1965)

(62) Eilenberger G. & Ambegaokar V. Phys. Rev. 158, 332 (1967)

(63) Werthamer N. R. & McMillan W. L. Phys. Rev. 158, 415 (1967)

(64) Yorke E. D. & Bardasis A. Phys. Rev. 159, 344 (1967)

(65) Hohenberg P. C. & Werthamer N. R. Phys. Rev. 153, 493 (1967)

(66) Miller P. B. Phys. Rev. 113, 1209 (1959) ibid. 118, 928 (1960)

(67) Ginsberg D. M. Phys. Rev. 151, 241 (1966)

(68) Halbritter J. thesis - Institut für Experimentelle Kernphysik Kernforschungszentrum, Karlsruhe, (1969)

(69) Anderson P. W. J. Phys. Chem. Solids 11, 26 (1961)

(70) Tegart W. J. McG. 'Electrolytic & Chemical Polishing of Metals' - Pergamon (1956)

(71) Chambers R. G. Proc. Roy. Soc. A215, 481 (1952)

(72) Aubrey L. E. Phil. Mag. 8, 1001 (1960)

(73) Ashcroft N. W. thesis - unpublished.

(74) Hahn H. et al. J. Appl. Phys. 39, 2606 (1968)

(75) Dingle R. B. Physica XIX, 311 (1953)

(76) Corsan J. M. & Cooke A. J. Phys. Lett. 28A, 500 (1969)

(77) Ohtsuka T. & Takano N. J. Phys. Soc. Japan 23, 983 (1967)

(78) Wong V. K. & Sung C. C. Phys. Rev. Lett. 19, 1236 (1967)

(79) Ikushima A. & Mizusaki T. J. Phys. Chern. Solids 30, 873 (1969)

(80) McConnville T. & Serin B. Phys. Rev. Lett. 13 365 (1964)

(81) Abrikosov A. A. J.E.T.P. 5, 1175 (1957)

(82) Tinkham, M. Phys. Rev. 129, 2413 (1963)

(83) Helfand E. & Werthamer N. R. Phys. Rev. Lett. 13, 686 (1964)
Phys. Rev. 147, 288 (1966)

(84) Eilenberger G. Phys. Rev. 153, 584 (1967)

(85) Farrell D. E. et al. Phys. Rev. 176, 562 (1968)

(86) Collins J. G. & White G. K. Progr. Low Temp. Phys. 4, 450 (1964)

(87) Josephson B. D. thesis - unpublished.

(88) Garfunkel M. P. Phys. Rev. 173, 516 (1968)

(89) Stoner E. C. Phil. Mag. 36, 803 (1945)

(90) Cape J. A. & Zimmerman J. M. Phys. Rev. 153, 416 (1967)

(91) Aston D. et al. Phys. Lett. 28A, 774 (1969)

(92) Webb G. W. Solid State Comm. 6, 33 (1968)

(93) Ostenson J. E. & Finnemore D. K. Phys. Rev. Lett. 22, 188 (1969)

(94) Reed W. A. et al. L. T. 10 IIA, 368 (1967)

(95) Williamson S. J. Phys. Lett. 28A, 665 (1969)

(96) Catterall J. A. et al. Br. J. Appl. Phys. 15, 1369 (1964)

(97) Ebneth G. & Tewordt L. Z. Phys. 185, 421 (1965)

(98) Caroli C. & Maki K. Phys. Rev. 159, 306 (1967)

(99) Fischer G. & Klein R. Phys. Rev. 165, 578 (1968)

(100) Fink H J. & Kessinger R. D. Phys. Lett. 25A, 357 (1967)

(101) Maki K. Progr. Theor. Phys. 39, 1165 (1968)

(102) Rothwarf A. et al. Phys. Rev. 155, 370 (1967)

(103) Fink H. J. & Kessinger R. D. Phys. Rev. 140, 1937 (1965)

(104) Fischer G. & Maki K. Phys. Rev. 176, 581 (1968)

(105) Shaw W. & Swihart J.C. Phys. Rev. Lett. 20, 1000 (1968)